NTNU – Trondheim
Norwegian University of
Science and Technology

Large-Scale Underground Mining in Tromsdalen

With focus on dimensioning and design of stopes and pillars

Anja Hammernes Pedersen

Geotechnology
Submission date: June 2014
Supervisor: Steinar Løve Ellefmo, IGB
Co-supervisor: Håkon Mork, Verdalskalk AS

Norwegian University of Science and Technology
Department of Geology and Mineral Resources Engineering

The Assignment

This master thesis was originally intended as a continuation of the Project "Assessment of Underground Mining in Tromsdalen", by Pedersen, 2013. However, due to recent evaluations the mining method determined in this project is no longer considered the best alternative. The aim of this thesis will be to evaluate stope dimensions and mine layout for a sublevel stoping mine. The result will be presented as a preliminary model of the future underground mine, modelled in Surpac.

Abstract

The objective of this thesis is to estimate the stope dimensions for a future underground mine in Tromsdalen, Verdal. Additionally, the most favourable orientation of the stopes and possible stope layouts will be assessed.

Initially, surface mapping was conducted and geotechnical features such as joint orientations, roughness, aperture and weathering were registered. The rock mass quality was assessed using the RMR and Q-system, and the results conclude a rock mass of fair to good quality. The surface mapping of the discontinuities in Tromsdalen founds the basis for evaluation of possible wedge failures in the stopes. The author has completed a small wedge analysis in *Unwedge*. This concludes that the largest stability issue is found in the roof of the stopes.

Various layout options are assessed against safety, criteria from Verdalskalk AS, and economic viability. It is concluded that longhole drilling or simultaneous blasting of benches are the best options. The stope dimensions were assessed with the help of numerical analyses in *Phase*^{2}. Two vertical cross-sections through the mine was analysed. The following stope dimensions are evaluated: length 100-150 m, width 30 m, height 50 m. The rib and crown pillars were tested for a thickness of 15 m, which is considered unstable. An increase in the pillar thickness is advised, and a 3D analysis of the problem is recommended to get a more accurate image of the situation. The dimension of the stopes are most likely viable, but the author cannot recommend any final dimensions due to insufficient data.

The orientation of the stopes are based on the principle of orienting the longitudinal axis of the stope in close proximity to the bisection line of the largest angle of intersection between the two major joint sets. This results in the most favourable stope orientation being approximately 298° NW. The author has also conducted a minor literature study regarding Norwegian underground mines. This was in order to gather information about their mine solutions which can be used as a basis for comparison in the authors investigation of large-scale underground mining in Tromsdalen.

In conclusion, to better assess the stability of the rock mass and decide a final design of the underground mine, stress measurements have to be conducted. The application and knowledge about rock stresses in a mining area is of great importance for the development of the mine design.

Sammendrag

Målet med denne oppgaven er å vurdere strosse dimensjoner for en fremtidig underjordsgruve i Tromsdalen, Verdal. Videre skal den beste orienteringen av strossene vurderes og mulige layout design drøftes.

Det er i første omgang gjennomført kartlegging av sprekker i dagbruddet hvor geotekniske egenskaper som sprekkeorientering, sprekkeavstand, sprekkeruhet og forvitring er registrert. Bergmassens kvalitet er vurdert opp mot RMR og Q-verdi systemet og resultatene tilsier en bergmasse av god til bra kvalitet. Sprekkekartleggingen har gitt grunnlag for vurdering av mulige kiledannelser i strossa. Til dette formålet har forfatteren foretatt en enkel analyse i *Unwedge* og kommet frem til at den største faren er i taket av strossa. Forfatteren har også utført et mindre litteraturstudie av norske underjordsgruver for å få informasjon om deres gruveløsninger, som igjen kan brukes til sammenligningsgrunnlag i forfatterens undersøkelser av storskala underjordsdrift i Tromsdalen. Ulike layout variasjoner er diskutert og vurdert opp mot sikkerhet, krav fra Verdalskalk AS, og økonomisk lønnsomhet. Det har blitt konkludert med at langhullsboring eller samtidig sprengning av paller vil være de beste alternativene.

Strosse dimensjoner er vurdert ved hjelp av numerisk analyse i $Phase^2$. Disse analysene har sett på to vertikale snitt gjennom forekomsten og den fremtidige gruva. Følgende dimensjoner er vurdert for strossene: lengde 100-150 m, bredde 30 m, høyde 50 m. Det er tatt utgangspunkt i 15 m tykke vertikale og horisontale pilarer. Ut i fra analyseresultatene kan det konkluderes med at 15 m tykke pilarer ikke er tilstrekkelig. Det bør vurderes å øke tykkelsen på pilarene, eventuelt utføre 3D analyser for å få et mer korrekt bilde av situasjonen. Dimensjonene av strossa kan høyst sannsynlig benyttes, men forfatteren kan ikke anbefale noen endelige dimensjoner i denne omgang. Orienteringen av strossene er basert på prinsippet om å orientere strossens lengdeakse nærmest mulig opp mot halveringslinjen for den største skjæringsvinkelen mellom de to viktigste sprekkesystemene. Den mest gunstige orienteringen av strossene vil være cirka 298° NV, midt mellom de to hovedsprekkesettene.

Det har blitt konkludert med at for å kunne vurdere stabiliteten til bergmassen og bestemme et endelig design av gruva bør det utføres en grundigere kartlegging av sprekkesystemer, og det må utføres spenningsmålinger i området. Måling av bergspenninger er vesentlig for den videre fremdriften av gruveplanleggingen.

Preface

This master thesis was written at the Faculty of Engineering Science and Technology, Department of Geology and Mineral Resources Engineering (NTNU) in Trondheim, Norway. The thesis work was conducted during the spring semester of 2014.

The main supervisor for this thesis was Dr. Steinar Løve Ellefmo, Associate Professor at the Department of Geology and Mineral Resources Engineering.

The thesis is conducted in collaboration with Verdalskalk AS and Håkon Mork, external supervisor.

The author would like to direct her gratitude to supervisor Steinar L. Ellefmo for his guidance and help during the semester. His academic advice and helpful contributions were of great importance. Further gratitude is directed to the external supervisor Håkon Mork for introducing this exciting topic and for helpful contributions during the writing process.

Professors Sunniva Haugen, Bjørn Nilsen, and Adjunct Associate Professor Nghia Quoc Trinh have contributed with useful knowledge within their respective fields. Gratitude is directed towards these professors. The author would also like to direct her gratitude to the geologist in Verdalskalk AS, Juan Rojas Ruiz, for important guidance regarding the carbonate deposit.

Finally, the author would like to thank her friends Brooke Norling and Oliver Deutschle for proofreading the thesis, and my family for their support. Much obliged.

Trondheim, June 16, 2014

Anja Hammernes Pedersen

Contents

List of Figures

List of Tables

Nomenclature

σ_1	Major principal stress
σ_3	Minor principal stress
σ_c/σ_{ci}	Uniaxial Compressive Strength (UCS), intact rock
E_i	Young's modulus of elasticity, intact rock
δ	Displacement
γ	Unit Weight
ν	Poissons ratio
ϕ_b	Basic friction angle
ρ	Density
ρ_s	The Rock Density
σ_t	Uniaxial Tensile Strength
σ_{cm}	Uniaxial compressive strength, rock mass
$\sigma_{H_{max}}$	Maximum Horizontal Stress
E_{rm}	Rock mass modulus of deformation
m_b	Reduced material constant, rock mass

m_i	Material constant, intact rock
S_{20}	Brittleness Value
V_p	Sonic Velocity
a	Constant, depend on the characteristics of the rock mass
AV	The Abrasion Value of tungsten carbide
AVS	The Abrasion Value of Steel Cutter
BWI	Bit Wear Index
CLI	Cutter Life Index
comp	The compaction index (from the brittleness test)
D	Disturbance Factor
DRI	Drilling Rate Index
f	Flakiness Value, intermediate ratio for mean width and thickness of grains
GSI	Geological Strength Index
JRC	Joint Roughness Coefficient
RMR	Rock Mass Rating
RQD	Rock Quality Designation
s	Constant, depend on the characteristics of the rock mass
SJ	Sievers' J-Value, mean value of the measured depth in mm/10 of 4-8 drill holes after 200 revolutions

Chapter 1

Introduction

The Thesis

This is a master thesis on large-scale underground mining in the Tromsdalen Limestone deposit, with focus on dimensioning and design of stopes. The thesis is a continuation of the Project "Assessment of underground mining in Tromsdalen", Pedersen (2013). Although this is true, the author had to make some changes as the mining method of choice from the project work was redefined before work on the master thesis began. Verdalskalk AS requested large bench heights, and this resulted in a change of mining method from room and pillar to sublevel stoping. The mining method presented in this thesis is that of sublevel stoping.

The outline of the thesis is structured in the following manner:

1. Introduction
   - Gives a brief description of what the reader can expect to find in the thesis.
2. Background
   - Information about the company, geology and stresses in the area, criteria for the mine.
3. Material
   - Description of the material. Distinguishing features, quality variations and rock mechanical properties.

4. Theory

   - General theory about stresses and stress distribution. The strength criterion used in the numerical analysis is presented, as well as an introduction to sublevel stoping and mine design. A brief literature study of Norwegian underground mines is included.

5. Methodology

   - Describes empirical and analytical methods. The procedure for surface mapping is described, and the process of the utilized software, $Phase^2$, *Unwedge* and *Surpac*, is explained and illustrated. In addition, the reader will find information about 3D numerical modelling.

6. Results

   - This chapter presents the results of the surface mapping, numerical modelling and layout suggestions.

7. Discussions

   - Discusses the results and findings from the previous chapter.

8. Conclusions

   - Contains preliminary conclusions regarding the stope design and layout, and suggestions for further work.

In this master thesis, the reader will find the necessary theoretical foundation to comprehend the scope of planning and designing an underground mine, as well as some preliminary results of stope and pillar dimensions. The field mapping founding the basis of the rock mass classification and discontinuity orientations was conducted during the fall of 2013 in connection with the project work by Pedersen (2013). Additionally, the author has referred to the deposit as a limestone deposit in this thesis, but geologically speaking it is a grey marble.

The government has restricted the area for extension of the open pit to the border seen in figures E.0.1 and E.0.3. This is in order to ensure the rest of the area as a recreation area for the residents of Verdal. For this reason, an underground mine is the only option for further exploitation of the deposit, unless new regulations are made

in the future. The area regulated for underground mining is visible in figure E.0.2 on page 162.

Limitations

As the focus of this thesis will be on the stope dimensions and layout, the author will not cover all the aspects of mine planning. Mine infrastructure such as power supply, buildings, workshops and rescue containers are not covered by this thesis. Nor is dimensioning of ventilation shafts and emergency exits, or the location of explosive magazines, fuel stores and pumphouses. The drilling pattern for the stopes have not been considered in this work. Drainage is not specified, but has been considered for road dimensioning and inclination of the drifts.

The focus of the analyses for the future underground mine will be on the south side of the open pit, see the brick-patterned area illustrated in figure 2.1.1. The shaded area in the same figure is also intended for underground mining by the company, but will not be considered in this thesis. The large open pit mine is part of the numerical modelling, however the stability of the open pit will not be analysed in this thesis.

This assignment is in reality a three-dimensional problem that requires a 3D numerical simulation. However, the author has performed a 2D numerical analysis of the situation. This is due to the substantial amount of time a 3D analysis requires.

The mining method, sublevel stoping, has been presented as the mining method of choice and basic theory regarding the method is presented in the theory chapter. Nevertheless, the author has not carried out an assessment of whether this method is suitable for the deposit in Tromsdalen or not. This method was determined by Verdalskalk AS.

Chapter 2

Background

2.1 Verdalskalk AS

Verdalskalk AS was founded in 1991 and is owned by Franzefoss Bruk AS (Franzefoss Minerals AS) (55%), Faxe Kalk AS (Lhoist) (35%) and Nordkalk OY AB, Finland (10%). Today the company consists of four different units: Tromsdalen (extraction and crushing of limestone), Hylla (burning and hydration of lime, laboratory), the Harbour (milling and shipping) and Transportation of the limestone, see map in figure 2.2.1.

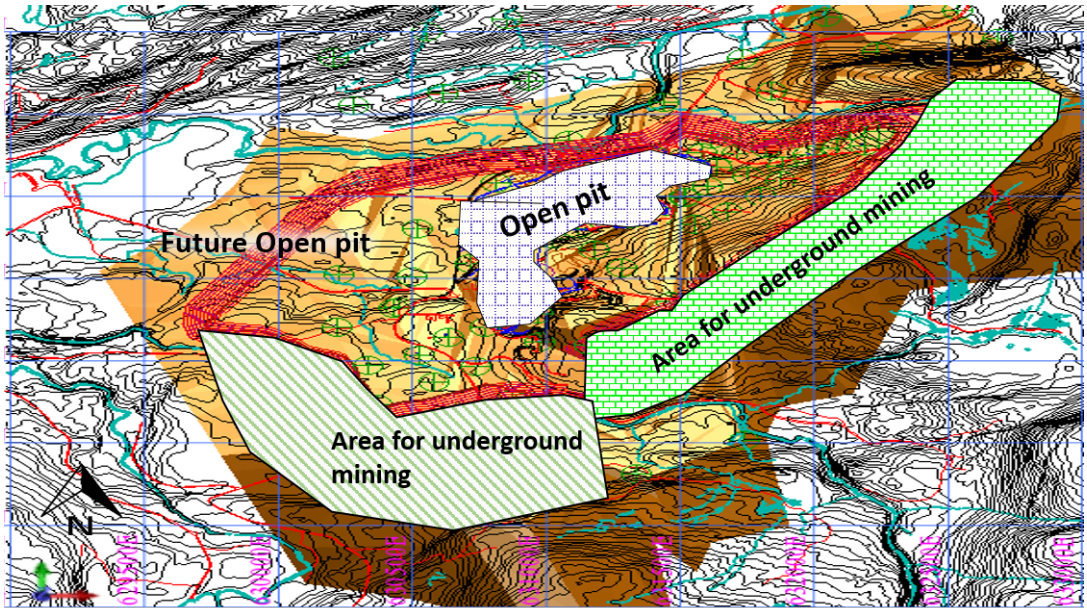

Figure 2.1.1 – Geological model of the limestone deposit in plan view. The current open pit is illustrated with a checkered pattern. 500 x 500 m grid for scale. (Map from Surpac, Geological model by courtesy of Ruiz, 2014)

People have been aware of Tromsdalen Limestone deposit for hundreds of years. A small hill on the south side of the open pit is called “Limbuåsen”, this together with findings of old kilns in Tromsdalen gives reason to believe that the limestone has been exploited since the middle age (Mork, 2014).

Since the early 1960’s, the deposit in Tromsdalen has been known as one of the largest and purest carbonate deposits ($CaCO_3$), both in Norway and in Europe. Because of its purity and structure, the limestone is utilized to make “quicklime” which is an important factor in the process of making PCC, precipitated calcium carbonate. PCC is used as a filler and coating pigment for the production of eco-friendly paper.

The limestone is used in a number of different products such as mineral fibres, cement, agricultural liming materials, water purification and more. In the industry they make use of limestone products for chemical and metallurgical processes such as slag formers and fluxing agents. The major products from Verdalskalk AS are limestone products, quicklime and hydrated lime.

Verdalskalk AS has acquired the mining rights to the deposit in Tromsdalen and currently run an open pit mine. The company has plans to expand the current open pit mine, and they are also planning an underground mine south of the open pit. This is in order to meet the markets increasing demand for mineral resources. The limestone deposit in Tromsdalen is considered to be of great economic significance due to its size and purity. According to Gautneb (2012), the deposit is assumed to be approximately 7.5 billion tonnes.

In figure 2.1.1, a rough geological model of the limestone deposit is displayed with the current open pit mine and a possible future open pit mine, as well as the areas intended for underground mining.

2.2 Geography

The limestone deposit is a more or less massive deposit located in Tromsdalen, Norway, approximately 25 km ESE of Verdal, UTM: Zone 33 V, 630952 Easting and 7068973 Northing. The area is restricted by highway 72 in NE and by the farms Buran and Sørengen in SW.

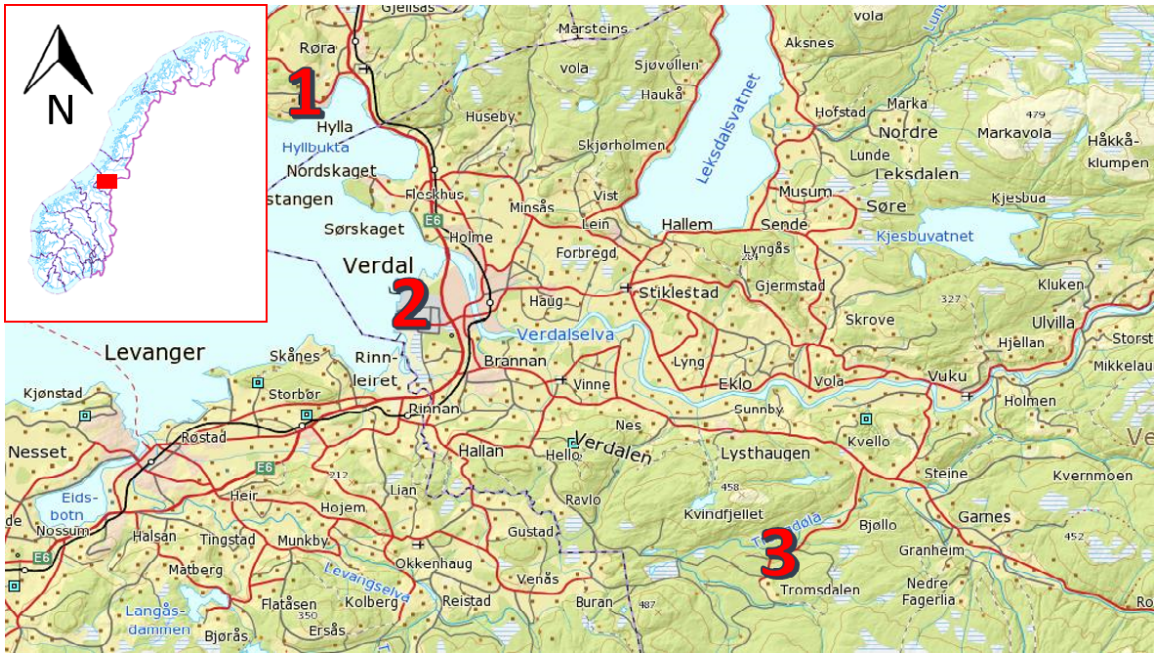

Figure 2.2.1 – Map showing the location of three of Verdalskalk's units. 1 Hylla, where the first lime plant started and now holds the kiln and hydration plant. 2 Harbour (Havna), where the company mills and ships out the products. 3 Tromsdalen, location of the current open pit mine and the crushers (Section of topographic map adapted from NGU, Trondheim, map projection WGS84 UTM zone 33).

2.3 Geology

The Carbonate Deposit

The deposit in Tromsdalen has a dip of 35-55° and a dip direction approximately SE-NW. According to Gautneb (2012); Korneliussen (2009); Ramberg et al. (2007), the deposit is a pure, low metamorphic limestone of the Ordovician Period, approximately 460 million yrs. old. The limestone is part of a quite extensive geological unit that occurs as isolated localities from Hølonda in the south to the area around Snåsa in the north. The largest coherent area of limestone is found along the lake Snåsavannet. In Verdal the limestone occurs from Levangerneset and eastwards towards Tromsdalen,

before it tapers out northeast towards Vuku (see figure 2.3.1). A branch of the same limestone formation is found at Hylla and northwest over Inderøy.

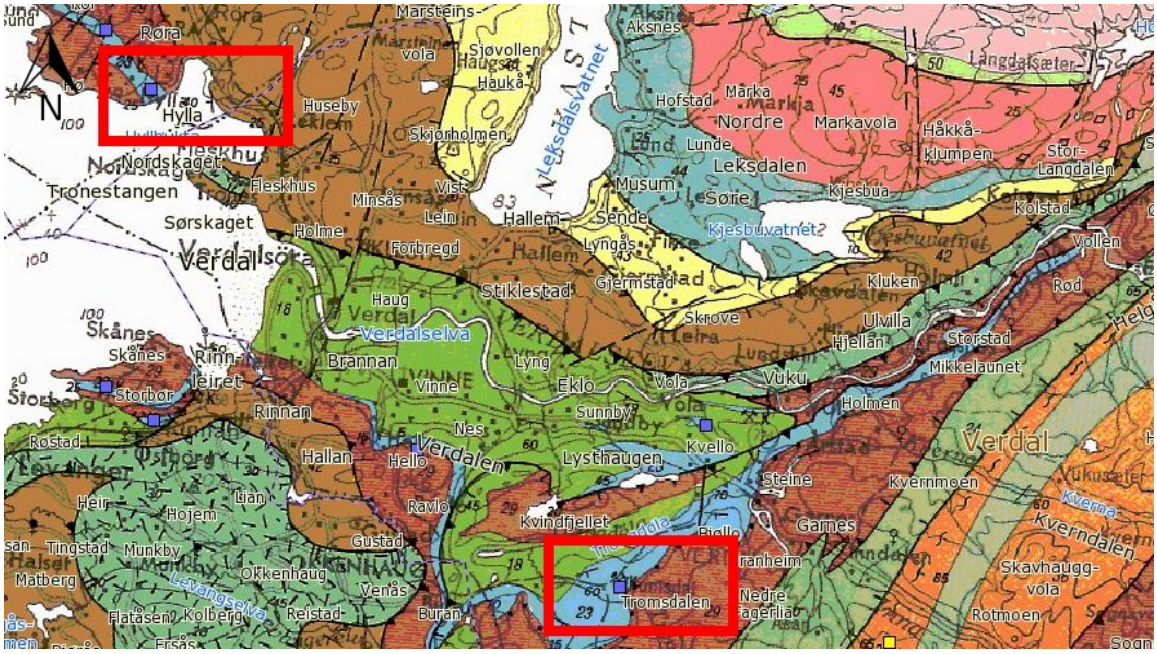

Figure 2.3.1 – Map showing the bedrock distribution in Verdal, localities Hylla and Tromsdalen are indicated on the map with a red box. Limestone = blue, phyllite = green and greenschist = brown (Section of geological map adapted from NGU, Trondheim, map projection WGS84 Zone 33).

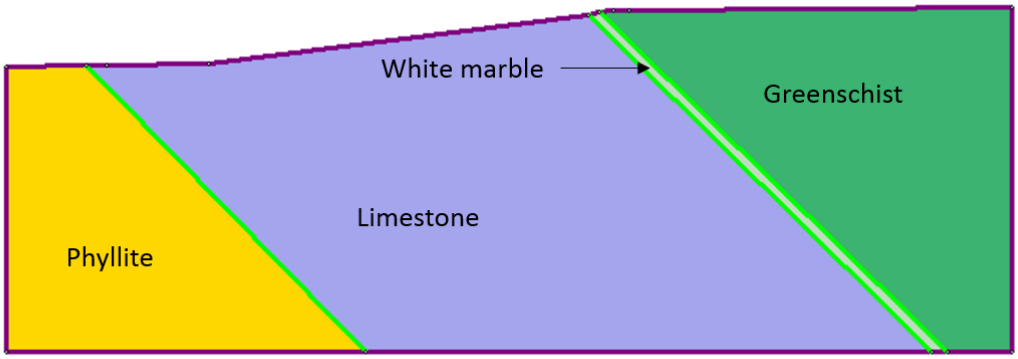

Figure 2.3.2 – Geological profile of the area, showing four lithologies. This is a rough profile of the geology based on borehole information from Tromsdalen and information from Ruiz, 2014.

A characteristic feature is that the limestone is situated between metamorphic rocks such as greenschists and phyllitic rocks. In many of the localities folding and deformation have turned this stratification upside down and this is also the case in Troms-

dalen. Here greenschists lie above the limestone and the phyllite is underneath. See figure 2.3.2 for a geological profile.

Foliation and tectonic activity such as compression and tension have given the deposit a varying dip. The foliation yields variable geochemistry that results in different impurities of the limestone. As a consequence the deposit is divided into two qualities, A and B. Quality A is suitable for production of quicklime used in the PCC process, and quality B is appropriate for all limestone products except quicklime used in production of PCC.

The use of borehole data helps in the analysis of how the quality of the deposit is oriented due to the foliation, see figure 2.3.3. The boreholes are drilled perpendicular to the dip of the deposit, and the purple lines represent the interpretation made by the geologist in Verdalskalk AS, Ruiz (2014), of how rock quality A propagate downwards. It is evident from the interpretation that the foliation makes the two qualities appear in bands or lenses.

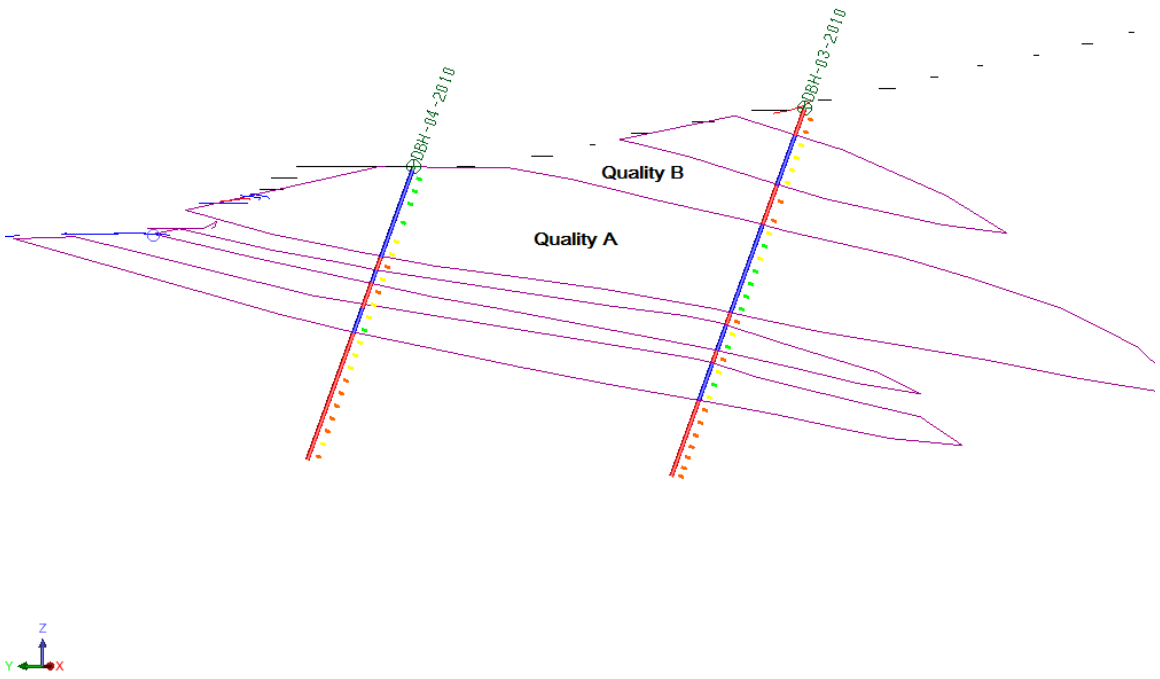

Figure 2.3.3 – Foliation in the carbonate deposit.The blue sections of the boreholes represents quality of type A and the red sections represents quality of type B. See map in figure 2.3.4 for location of the boreholes (Verdalskalk AS, 2013a; Ruiz, 2014).

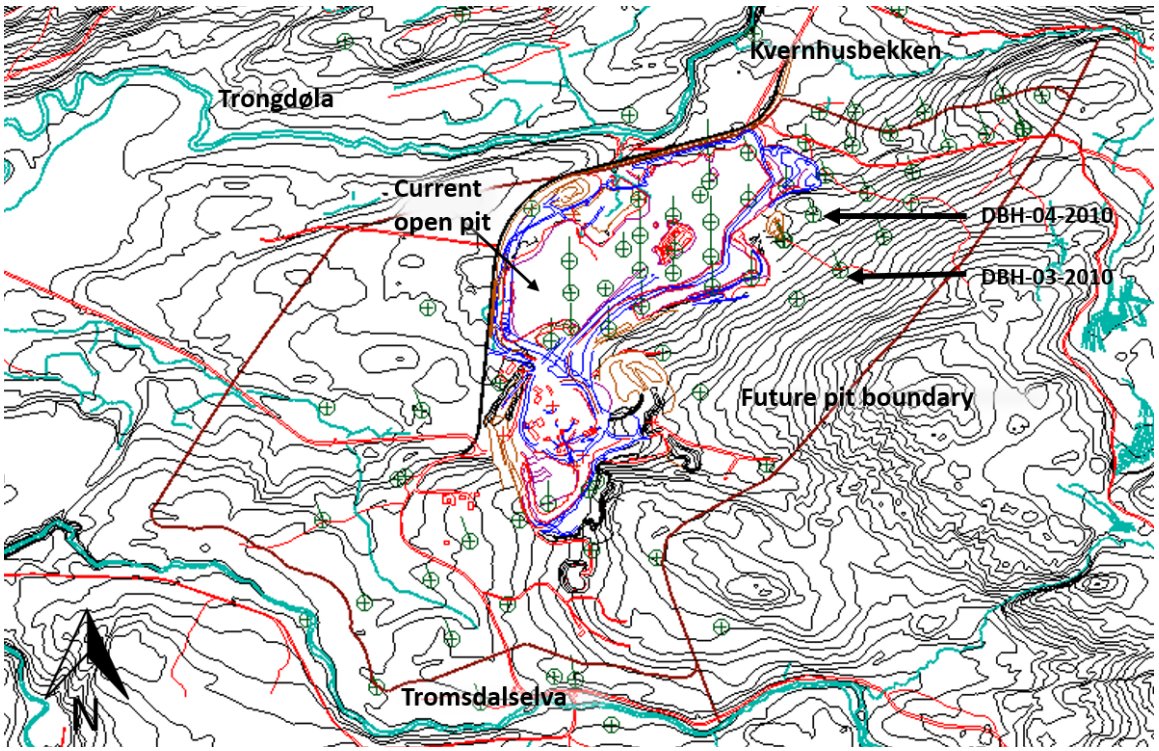

Figure 2.3.4 – Current open pit in Tromsdalen. Green circles indicates the borehole locations. The brown boundary inclosing the open pit represents the future open pit boundary. Three rivers act as limiting factors for this project, displayed on this map as "Trongdøla" north of the pit, "Kvernhusbekken" also in the north area of the open pit, and "Tromsdalselva" southwest of the open pit. (Map from Surpac, borehole data by courtesy of Ruiz, 2014)

2.4 Water Management

The open pit in Tromsdalen is surrounded by a system of rivers as seen in figure 2.3.4 above. Closest to the open pit is the river Trongdøla, located to the north across county road 155. Figure 2.4.1 displays the river in relation to the county road and the open pit. A water pool was excavated in July 2013 in order to see how much water that would find its way into the open pit. As soon as the digging commenced, water appeared and started filling up the pool. The result is visible in figure 2.4.2, a nice pool of 5 meters depth, filled with clear water. However, it is not proven that this water originates from the river, it might also come from groundwater or surface water in the surrounding area.

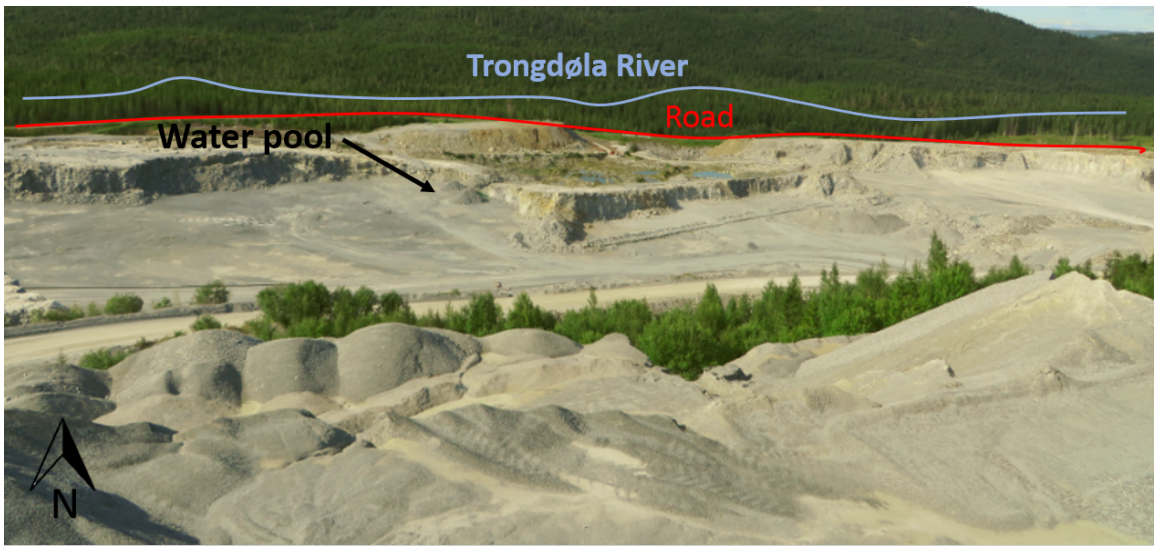

Figure 2.4.1 – Overview of the open pit, seen from south to north. The blue line represents the location of the river, the red line is county road 155. (Photo: Author).

As of May 2014, the company is about to open level 165 in the open pit, which is 18 meters below Trongdøla. They are in the progress of establishing a water sump where one or more pumps will be installed. The idea is to pump the water from the sump to a sedimentation pond located at level 185. From here, the water will be transported in pipes under the road and into a creek that ends in the river. Water samples will be collected from the water sump and in the creek. In the short run, a larger system for diverting the water southeast of the open pit will be established. This is to avoid runoff from areas at higher elevations to flow into the open pit (Mork, 2014).

Figure 2.4.2 – Water pool in the open pit at level 185. See also figure 2.4.1. (Photo: Author).

Another aspect of mining is acid mine drainage, where polluted water leaks into the surrounding rivers and creeks. Acid mine drainage can have a severe impact on fish, animals and plants. In Norway, the Norwegian Environment Agency and the county administrator have the controlling authority for the pollution problems. Mines have to report their water discharge on a yearly basis. However, acid mine drainage is not a problem in Tromsdalen. The mined limestone contains alkaline agents with the ability to neutralize acidic river systems.

In order to monitor the water quality of the open pit and the areas in close proximity, Verdalskalk have set up a monitoring program. Samples have been collected upstream of the open pit, from the open pit itself and downstream of the open pit since 2004. These samples give the basis of comparison needed for interpreting the analytical results. Large variations in nitrogen content have been found, and analyses show elevated nitrogen levels both from the quarry and upstream of the quarry. There are also evidence of reduced values of iron and aluminium from the samples collected in the open pit.

The nitrogen from the open pit originates from uncombusted explosives, but the nitrogen upstream is from agricultural activity. Three surveys of electrical fishing and benthic fauna investigations have been carried out, the latest in 2011, and they have all concluded that the river is virtually in its natural state. This means that the operations in Tromsdalen pose no danger to the river. The discharge from the open pit mainly consists of pure water with slightly elevated nitrogen content (Mork, 2014).

2.5 Rock Stresses in the Area

The stress situation in the area has not yet been measured or investigated. However, Roberts and Myrvang (2004) have performed in situ rock stress measurements and observed contemporary stress orientation structures at diverse sites in the Trøndelag area that are fairly close to the deposit in Tromsdalen, see figure 2.5.1.

In general, early investigations measuring in-situ stress in Scandinavian bedrock have showed that horizontal stresses almost always exceed the theoretical horizontal stress that is due to overburden (Hast, 1958). Later measurements show that this trend also is evident in many locations in Norway, and that the major principal stress is in fact horizontal. Measured vertical stresses on the other hand normally corresponds well with the theoretical stress calculated from the thickness of overburden, at least down to depths of approximately 500 m (Roberts and Myrvang, 2004).

Roberts and Myrvang (2004) found that in most locations the horizontal stress field is anisotropic, i.e. one of the horizontal components dominates: $\sigma_{H_{max}}$. Evidence show that in practical tunnelling and underground excavations, high horizontal stresses normal to the tunnel axis tend to generate severe technical problems. High stress concentrations in the roof and floor of tunnels and excavations causes a phenomenon called spalling or rock burst: a violent shear failure of the rock. Stress-related prob-

lems of this kind require comprehensive and extensive rock support measures. Nevertheless, not all stresses should be considered a problem. A favourable magnitude of the horizontal in-locked (residual) stresses makes the mine roof more stable and reduce the number of necessary pillars in a mine (Dahle et al., 2006).

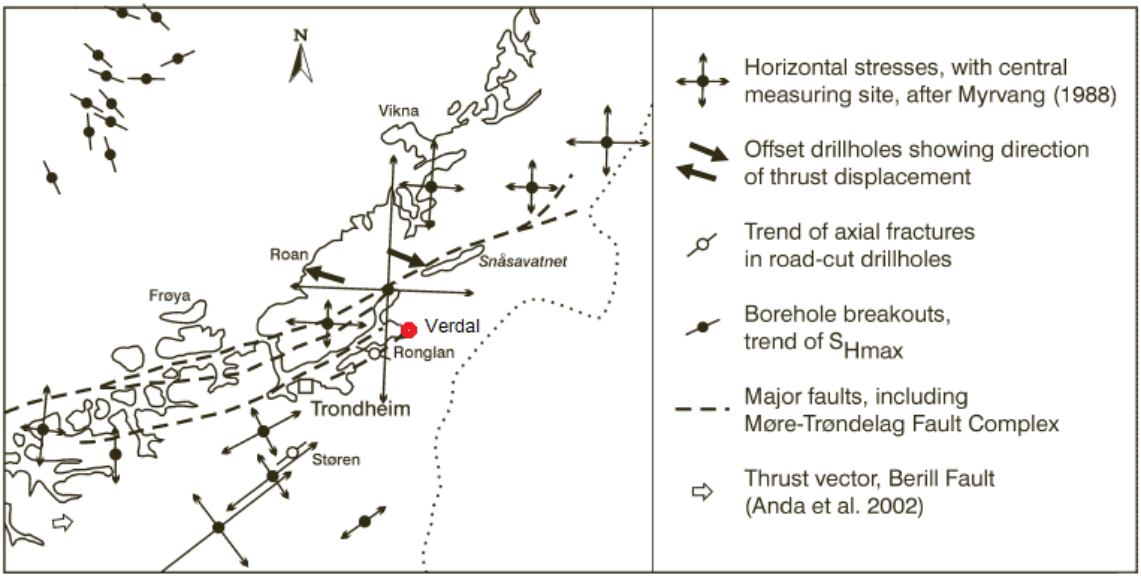

Figure 2.5.1 – Outline map showing the diverse rock-stress orientation data from central Norway and the Trøndelag Platform, adapted from Roberts and Myrvang (2004).

An indication of high in-situ stresses in the earth's crust is often recognized as core disking. Field evidence suggests that core disking in vertical boreholes is the direct result of high horizontal stresses. Investigation of cores from Tromsdalen show little to no indication of core disking (Ruiz, 2014), coincident with low horizontal stresses. However, there are no measurement to support this theory. Based on horizontal stresses found in similar limestone, Myrvang (2013) estimates the maximum horizontal stress in Tromsdalen to be ~1-2 times the vertical stress.

2.6 Mine Criteria

Verdalskalk AS have chosen a mining method believed to give less pressure on the surface, sublevel stoping. It is of great importance to keep the subsidence on the surface as low as possible to ensure the site as a recreation area for the residents of Verdal. The maps in figures E.0.1, E.0.2, and E.0.3 gives an overview of the regulated areas for mining. Section 4.2.2 on page 30 provides supplementary reading about sublevel stoping.

Verdalskalk AS (Mork, 2014) further lists these criteria for the underground mine:

- The underground design should, if possible, be dimensioned so that the same equipment can be utilized both over and underground.
- A flexible system giving access to multiple drifts of different quality at all times.
- A cost efficient and rational operation.
- Highest possible ore recovery.
- Good stability and little long-term rock support for underground infrastructure/stopes left after completion of production. Possibly locate the adit below the water level of the water established at the bottom of the open pit.
- Possibilities for automated operations.
- Lowest possible amount of fines (-35 mm).
- Selective mining, if possible.

2.7 Previous Work

The table below lists previous work concerning the carbonate deposit in Tromsdalen.

Table 2.7.1 – Previous work

Author	Report Description
Skjerlie and Gausdal (1961)	Exploration diamond drilling in Tromsdalen limestone deposit. Geological Survey of Norway (NGU), report 300a.
Skjerlie and Tan (1961)	Geological investigations of the Limestone deposit in Tromsdalen. NGU report 300b.
Sverdrup (1966)	Geological investigations in Tromsdalen, Northern Trøndelag county, NGU report 725.
Svinndal and Vassbotn (1969)	Technical report of diamond drill holes from the limestone site in Tromsdalen, Verdal.
Sellæg (2005)	Engineering geological issues with the establishment of a transport tunnel, Tromsdal - Ørin.
Sellæg (2006)	Feasibility study for tunnel transport Ørin - Tromsdalen.
Thomas-Lepine (2012)	Rock bolts - Improved design and possibilities.
Møller (2013)	Regulated maps of Tromsdalen, both underground and surface excavation.
Halvorsen and Tuttle (2013)	Impact study of the future open pit mine in Tromsdalen with focus on groundwater.
Verdalskalk AS (2013b)	Mapping of the contact between marble and phyllite and tracing of major joints.
Pedersen et al. (2013)	Results from testing in laboratory in subject TGB4505 Engineering Geological Laboratory Methods.
Pedersen (2013)	Assesment of underground mining in Tromsdalen, with focus on rock mechanical properties.

Chapter 3

Material

3.1 Material Description

In this chapter, the reader will find some general information about carbonate rocks in addition to specific data about the Tromsdalen Limestone.

3.1.1 Carbonates

Carbonate rocks make up a class of sedimentary rocks whose primary components are the carbonate minerals calcite ($CaCO_3$), magnesite ($MgCO_3$) and dolomite($CaMg(CO_3)_2$). These minerals form the two major types of carbonate rocks, limestone and dolomite also known as dolostone (Deer et al., 1992).

Table 3.1.1 – This table gives the general mineral content of the Tromsdal Limestone adapted from XRF analyses performed by Verdalskalk AS. In addition to these minerals, the limestone also contains trace elements.

Mineral	$\mathbf{Fe_2O_3}$	$\mathbf{Al_2O_3}$	$\mathbf{K_2O}$	**MgO**	**MnO**	$\boldsymbol{Na_2O}$	$\mathbf{SO_3}$	$\mathbf{SiO_2}$	$\mathbf{TiO_2}$	$\mathbf{CaCO_3}$
%	0.05	0.1	0.02	0.4	0.004	0.01	0.02	0.2	0.01	> 98

Limestone makes up nearly 10% of the total volume of all sedimentary rocks and is composed of more than 50% carbonate minerals, where calcite and aragonite [1] are the dominating minerals. If the limestone is exposed to high pressure and temperature over time (metamorphose), it will recrystallize and transform into a marble or calciferous marble (Marshak, 2008). The limestone in Tromsdalen is slightly metamorphosed which makes it a type of marble.

[1] Aragonite is a different crystal form of calcium carbonate ($CaCO_3$)

Pure limestone contains more than 95% calcite. The XRF analysis of the Tromsdal Limestone seen in table 3.1.1 shows a calcite content of more than 98%. Therefore, it is among the purest limestones in Norway. This is also evident from the triangular diagram in figure 3.1.1, where the Tromsdalen Limestone is plotted in the far right corner as a high-calcium limestone.

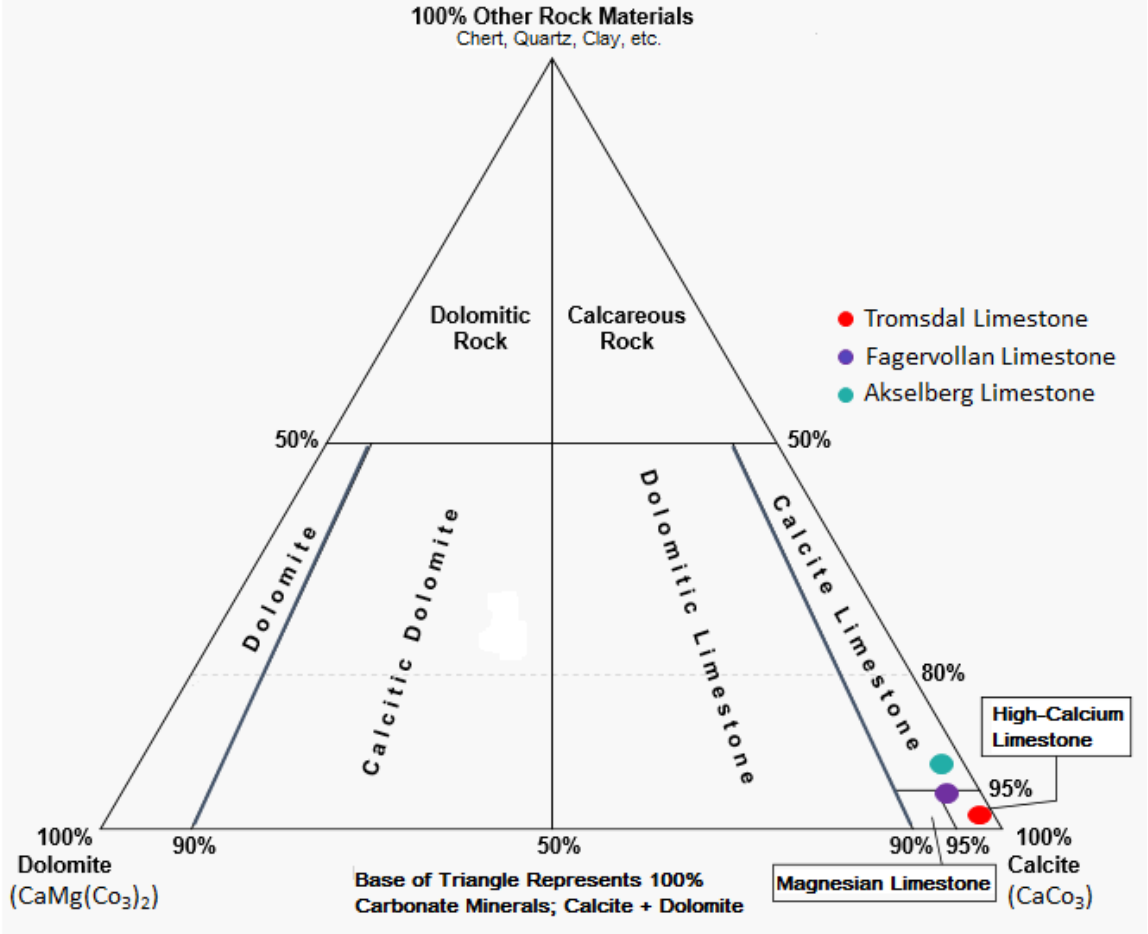

Figure 3.1.1 – Triangular diagram of limestones in Norway. Modified from Nixon and Pauley (2014).

3.1.2 Distinguishing features

The limestone may be recognized as a rhombohedral carbonate due to the rhombohedral structure and cleavage of calcite, its main constituent (see figure 3.1.2c). Furthermore, the Tromsdal Limestone is found to have two distinct joint sets. A primary joint set that is parallel to the direction of the foliation, and a secondary joint set that is almost perpendicular to the primary joint set. For photo illustrations, see figure 3.1.2. In the top left photo, the reader may see joints from a drilled core of the Tromsdal Limestone. To the top right, the two main joint sets are shown as they appear in the outcrop.

A number of joints and discontinuities in the Tromsdal Limestone contains a white mineral infill. This soft, paper-like infill is no more than 3 mm thick and is most likely the result of mineral rich water seeping through cracks and joints in the rock. See figure 3.1.2d for illustration.

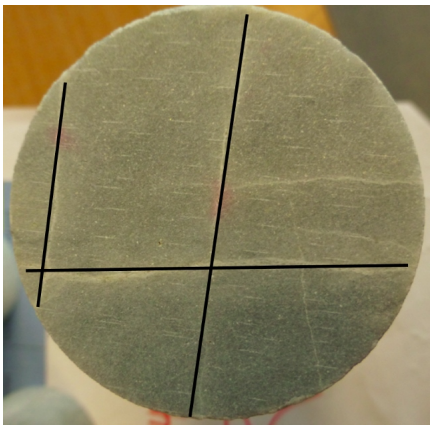

(a) Visible joint sets and random joints in a drilled core, $D = 50mm$.

(b) The two main joint sets as seen in the outcrop in Tromsdalen. Note GPS for scale: 2m.

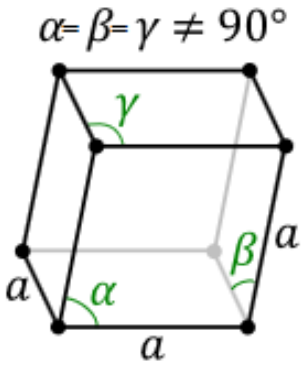

(c) The crystal structure of calcite, Rhombohedral shape (Wiktionary, 2013).

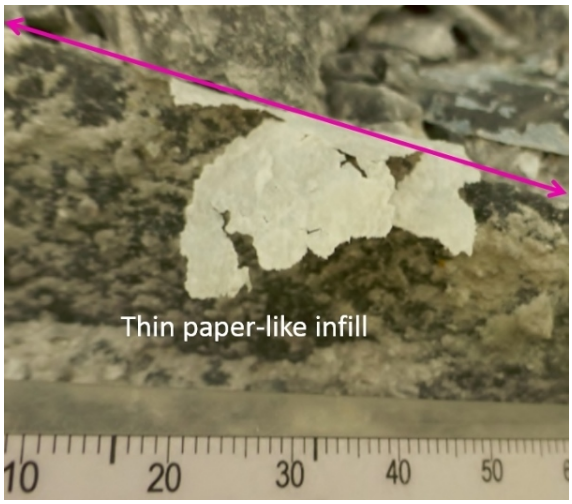

(d) White mineral infill in joint.

Figure 3.1.2 – Distinguishing features of the Tromsdal Limestone (Photos: Pedersen, 2013).

3.1.3 Quality Variations

The limestone in Tromsdalen has been divided into six different types based on their purity and mineral content (Ruiz, 2014):

1. Light grey, pure crystalline marble (limestone) of quality A.

2. Dark grey, pure crystalline marble (limestone) with some evidence of graphitic layers, quality A.

3. Dark marble (limestone) with impurities of white marble and phyllite layers, iron oxides, greenschist and green minerals such as chlorite and epidote, quality B.

4. Discoloured pale marble (limestone) with impurities. The impurities are caused by high concentrations of Fe, Si, Mn, Al and SO_3. The discolouring is due to Fe and Mn oxides, quality B.

5. Extremely dark marble (limestone), normally chemically pure. In the terrain this is normally indicated by a sharp contact. It also shows graphitic layering, quality A.

6. White marble with large crystal structure. Often impure, with visible pyrite grains and green minerals (chlorite, epidote). Yellow discolouring may occur due to the presence of iron oxides, and pink discolouring is related to the manganese oxides. Observations made from borehole logging suggests that the white marble mainly is found in contact zones, at depths in the contact with phyllite and at the surface in contact with greenschist.

3.2 Rock Mechanical Properties

In table 3.2.1 the general rock mechanical properties of the Tromsdal Limestone is presented. These are the results of laboratory testing executed by Group 1 and 2 [2] in the subject TGB4505 Engineering Geological Laboratory Methods at NTNU (Pedersen et al., 2013).

Table 3.2.1 – Lab results from tests performed on the Tromsdal Limestone, modified after Pedersen et al. (2013).

Parameter	Unit	Mean (Gr 1)	St.dev.	Mean (Gr 2)	St.dev.	Total mean	St.dev.
Youngs modulus, E	[Gpa]	71.14	8.06	76.90	4.20	74.02	1.93
Poissons ratio, ν	[-]	0.26	0.04	0.24	0.02	0.25	0.01
Density, ρ	[kg/m^3]	2700.9	6.08	2700	0	2700.45	3.04
Sonic velocity, Vp	[m/s]	6534.08	86.12	6436	88	6485.04	0.94
UCS	[Mpa]	87.14	5.29	99.4	8.7	93.27	1.705
Fracture angle, β	(°)	20	1.0	23	4.6	21.50	1.8
Basic friction angle, ϕ_b	(°)	34.7	2.4	30.1	1.5	32.40	0.45
PLI Diametric, Is50	[MPa]	4.21	1.54	3.80	0.63	4.01	0.455
PLI Axial, Is50	[MPa]	3.94	1.32	3.64	0.72	3.79	0.3
Tensile strength, σ_t,*	[MPa]	10.16	1.51	10.54	1.41	10.35	0.05
Flakiness value, f	[-]	1.28	-	1.36	-	1.32	0.04
Brittleness value, S20	[-]	50.7	3.7	53.0	2.5	51.84	0.62
Surface hardness, SJ	[mm/10]	80.9	1.8	81.0	1.9	80.95	0.05
Abrasion, AV	[-]	0.5	0	0.75	0.5	0.63	0.25
Abrasion, AVS	[-]	0.5	0	1	0	0.75	0

* This is the Uniaxial Tensile Strength

Table 3.2.2 gives the drillability indices for the limestone determined from drillability tests in the NTNU/SINTEF laboratory. The results indicate a good drillability and low abrasivity for the limestone due to the high drilling rate index (DRI), and the equally low bit wear index (BWI). The cutter life index (CLI) is an estimate of the expected lifetime for the cutting discs in a TBM, not relevant for this thesis. Rock of good drillability and low wear capacity is beneficial for rock excavation and they seldom represents any risk with regards to costs (Bruland, 1998).

Table 3.2.2 – Drillability indices determined from drillability testing (Pedersen et al., 2013).

Compaction index	DRI	BWI	CLI
2	62	10	97.9

[2] Group 1: Anja Hammernes Pedersen, Siri Todnem, Magni Vestad, Susanne Myhre
Group 2: Margrete Langåker, Inger Lise Sollie, Christine Langås

Chapter 4

Theory

4.1 Stresses

The stability of underground excavations depends on the rock mass strength and the stresses induced in the rock. The induced stresses will be a function of the excavations shape and the preexisting in-situ stresses. The magnitude of these preexisting in-situ stresses will vary widely depending on the geological history of the rock mass. Hoek (2007) recommends that measurements of the actual in-situ stresses be performed, as theoretical predictions of these are considered unreliable for excavation design.

Simple gravitational loading produces a vertical stress equal to the weight of the overlying material as expressed in the following equation:

$$\sigma_v = \rho \cdot g \cdot z = \gamma \cdot z \tag{4.1.1}$$

where

$\sigma_v =$ vertical induced stress (Pa).
$\gamma =$ unit weight of the overlying rock (N/m^3).
$z =$ depth below the surface (m).

The horizontal stresses at some depth, z, below the surface are much more difficult to estimate than the vertical stresses. The ratio of the average horizontal stress to vertical stress is typically denoted by the letter k such that:

$$\sigma_h = k \cdot \sigma_v = k \cdot \gamma \cdot z \tag{4.1.2}$$

According toTerzaghi and Richart (1952) a gravitationally loaded rock mass where

no strain is permitted during formation of the overlying strata the value of k is independent of depth and given by:

$$k = \frac{\nu}{1 - \nu} \tag{4.1.3}$$

where

ν = Poisson's ratio

This relationship was widely used in the early days of rock mechanics, but it proved quite inaccurate and has been replaced with a more realistic relationship (Hoek, 2007):

$$k = 0.25 + 7E_h \left(0.001 + \frac{1}{z}\right) \tag{4.1.4}$$

where

k = ratio of horizontal to vertical stresses.
E_h = average deformation modulus of the upper part of the earth's crust measured in a horizontal direction (GPa). This direction of measurement is particularly important, especially in layered sedimentary rocks, in which the deformation modulus may be differerent in the different directions.
z = depth below the surface (m).

Equation 4.1.4 is known as Sheorey's equation (Sheorey, 1994) and gives the ratio of horizontal to vertical stresses, k, for different deformation moduli E_h. At shallow depths the model predicts a high ratio, but it decreases with increasing depth (z).

Results of in-situ stress measurements in underground mines have demonstrated that the horizontal stress can be greater than the vertical stress due to active or residual tectonic stress. Furthermore, horizontal stress is rarely equal in all directions underlining the importance of thorough stress measurements when planning an underground design. According to Call (1992), in the absence of in-situ stress measurements or other indications of a high horizontal stress, it is most reasonable to assume that the horizontal stress is equal to the vertical stress.

Influence of Topography

Figure 4.1.1 shows how horizontal stresses are influenced by the topography. It is evident that underneath valleys there will always be a high stress concentration, especially if there are geological stresses across the valley. This principle applies even if there is only gravitational stresses present. On a regional basis, the geological stresses tend to adapt to the topography in a similar matter. As indicated by the figure, both stress released "noses" and stress concentrations in depressions occur in the horizontal plane.

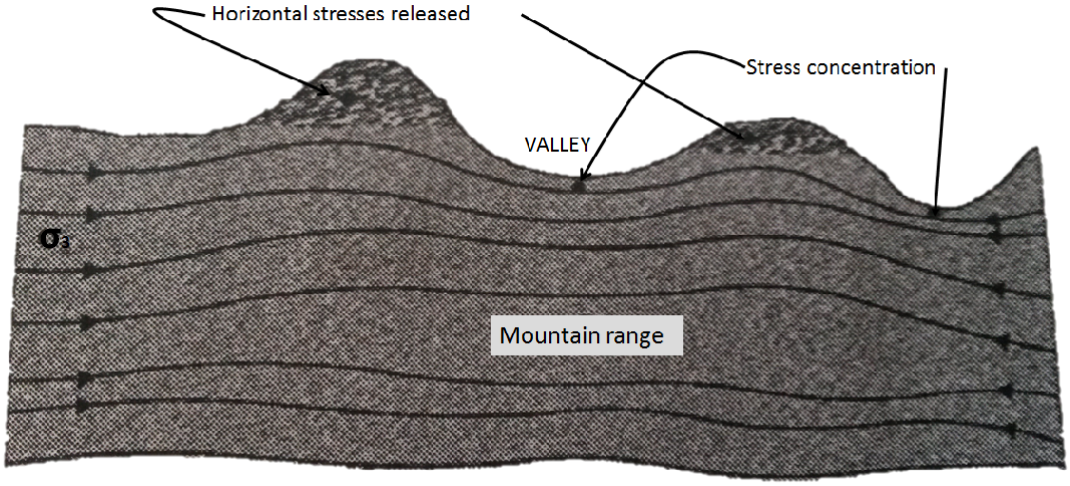

Figure 4.1.1 – Horizontal section showing regional influence of topography, adapted from Myrvang (2001).

Stress Analysis

As soon as a cavern or opening is made in a rock, the original stress field is altered. Theoretically speaking there will be a change in the stresses in every point that is in close proximity to the opening. The stresses absorbed by the removed mass needs to be redistributed to the remaining masses.

When opening a room, the stresses tend to follow the contours of the opening as seen in figure 4.1.2. A higher stress intensity is reached in the areas close to point A, which means that the tangential stress is increased and there is a stress concentration on the sides. In point B on the other hand, tensile stresses are induced. The tangential tensile stress is approximately equal to the original stress situation, independent of the openings shape. The compressive stress concentration is however dependent of the width to height ratio of the opening, and increases correspondingly. See figure 4.1.3 for an illustration of stress distribution at various width to height ratios.

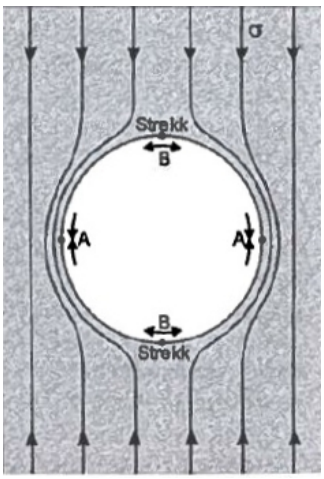

Figure 4.1.2 – Stress distribution around a circular opening (Myrvang, 2001).

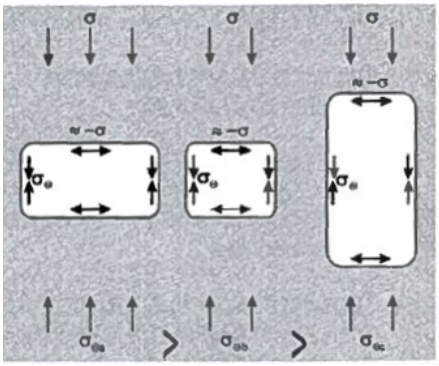

Figure 4.1.3 – Stress distribution at different width to height ratio (Myrvang, 2001).

Room Orientation

When determining the orientation of the longitudinal axis of a shallow underground excavation a simple rosette plot is useful. The idea is to orient the room according to the bisection line of the largest angle of intersection between the two major joint directions (Nilsen and Broch, 2001).

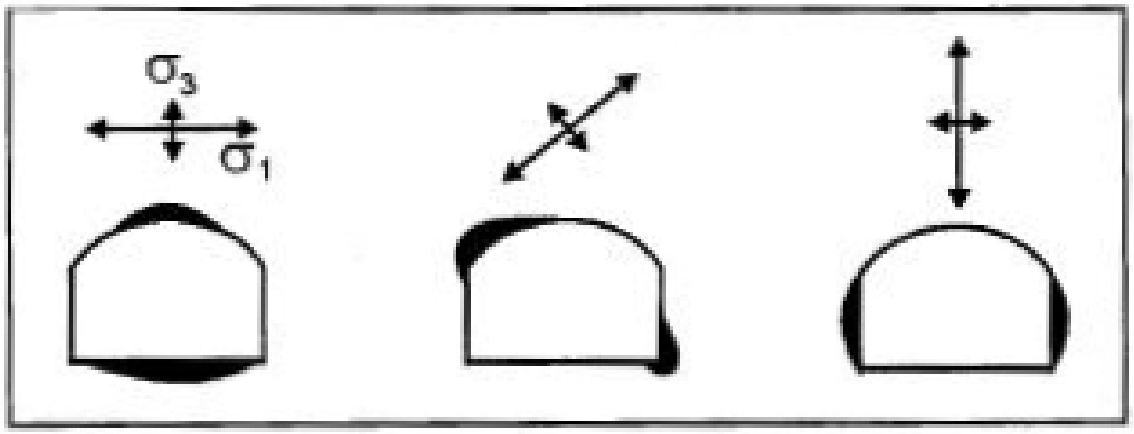

Figure 4.1.4 – The shaded areas illustrates where rock pressure problems might occur in excavations with varying orientation of the major principal stress, σ_1 (Selmer-Olsen and Broch, 1977).

Regarding excavations at greater depths, the rock stresses play a more central role. The formation of new cracks, rock burst and spalling occurs where the direction of the major principal stress is tangent to the excavation's periphery. See figure 4.1.4. In order to get the best possible room orientation it is necessary to make the tangent

surface as small as possible. Normally, the best orientation is achieved when the longitudinal axis of the excavation forms an angle of 15-35° to the direction of the major principal stress (Nilsen and Broch, 2001).

4.1.1 Strength Criterion

Hoek-Brown Failure Criterion

The Generalized Hoek-Brown criterion is an empirically derived criterion that establishes the strength of rock in terms of major and minor principal stresses. The criterion predicts strength envelopes in agreement with values determined from laboratory triaxial tests of intact rock, and from observed failures in jointed rock masses (Hoek et al., 2002; Rockscience Inc., 2012).

This non-linear criterion relates the major and minor effective principal stresses ($\sigma_1^{'} \, and \, \sigma_3^{'}$) according to the following equation:

$$\sigma_1^{'} = \sigma_3^{'} + \sigma_{ci} \left(m_b \frac{\sigma_3^{'}}{\sigma_{ci}} + s \right)^a \tag{4.1.5}$$

where

$\sigma_1^{'} \, and \, \sigma_3^{'} =$	Axial (major) and confining (minor) effective principal stresses.
$\sigma_{ci} =$	The uniaxial compressive strength (UCS) of the intact rock material.
$m_b =$	Reduced value (for the rock mass) of the material constant m_i (for the intact rock)
$s \, and \, a =$	Constants which depend upon the characteristics of the rock mass.

According to Hoek et al. (2002), it is in many cases almost impossible to carry out triaxial tests on rock masses at the necessary scale to obtain direct values of the parameters in the Generalized Hoek-Brown equation. In their latest research, some practical means of estimating the material constants m_b, s and a have been given:

$$m_b = m_i \exp\left(\frac{GSI - 100}{28 - 14D}\right) \tag{4.1.6}$$

$$s = \exp\left(\frac{GSI - 100}{9 - 3D}\right) \tag{4.1.7}$$

$$a = \frac{1}{2} + \frac{1}{6}\left(e^{-GSI/15} - e^{-20/3}\right) \tag{4.1.8}$$

where

$GSI =$ Geological Strength Index, that relates the failure criterion to geological observations in the field.

$m_i =$ Material constant for intact rock.

$D =$ Disturbance factor. It depends on the degree of disturbance the rock mass has been subject to by blast damage and/or stress relaxation. It varies from 0 for undisturbed in situ rock masses to 1 for very disturbed rock masses.

4.2 Underground Mining

Underground mining refers to various underground mining techniques used to excavate minerals from a known deposit or ore. The intention is that the carbonate deposit in Tromsdalen is to be mined with a mining method called sublevel stoping. In the subsequent section, the basic principles of this method are presented.

4.2.1 Terminology

A brief vocabulary of technical terms used in the mining field is listed below:

Adit Primary horizontal or near horizontal opening from the surface by which a mine is entered and dewatered.

Crosscut Tertiary horizontal opening, often connecting drifts, entries or rooms.

Crown Pillars Horizontal pillars that separate levels or stopes.

Decline Secondary inclined opening, driven downwards to connect levels, sometimes on the dip of a deposit.

Dilution Reduction of ore grade due to mixing of ore with barren rock.

Drifts Primary or secondary horizontal or near horizontal opening. Not connected to the surface.

Ore Pass Sub-vertical chutes for movement of ore.

Raise Secondary or tertiary vertical or near vertical opening, driven upward from one level to another.

Ramp Secondary or tertiary inclined opening, driven to connect levels, usually in a downward direction, and used for haulage (wheeled transport). The gradient should not exceed 10 to 15% if it is used for ore transport. If it is not used for ore, the gradient can be up to 25%.

Rib Pillars Vertical pillars separating the stopes, supports the hanging wall.

Shaft Primary vertical or near vertical opening, connecting the surface with underground workings.

Sill Pillars Horizontal pillars that divide the orebody into multiple mining horizons.

Slot Narrow vertical or inclined opening excavated in the deposit at the end of a stope to provide a bench face.

Stope Large exploitation opening, usually inclined or vertical, but may also be horizontal. They may be backfilled with cement or waste material.

Sublevel Secondary or intermediate level between main levels or horizons. Used to drill the ore for blasting, but can also be used for transport.

4.2.2 Sublevel Stoping

In General

> *Sublevel stoping, also known as blasthole or longhole stoping, is an open stoping, high production, bulk mining method applicable to large, steeply dipping, regular ore bodies having competent ore and rock that require little or no support.* Haycocks and Aelick, 1992

There are several variations of sublevel stoping described in the literature, but common for all of them is the use of gravitational ore flow from end point of production sublevel drifts to drawpoints. Typically, the dip of the deposit must be at least 50°, i.e. greater than the angle of repose of broken material, so that material transport to drawpoints occur by gravity. However, if the deposit is massive, stopes with vertical walls will be created and the overall dip of the deposit is immaterial (Haycocks and Aelick, 1992; Bullock, 2001).

Mine development starts with infrastructure such as adits, ramps or shafts for accessing the ore. Additionally, drilling drifts, declines to sublevels, crosscuts and transportation drifts must be in place before the stoping can commence (Bullock, 2001; Villaescusa, 2014).

Figure 4.2.1 shows a typical layout for the *sublevel open stoping* method. In this case, the principles of downward fan drilling is illustrated. There may be one or multiple drill drifts on each sublevel, and fans of holes may be drilled downwards as illustrated, upwards, or in full rings. An alternative is to drill parallel holes from the sublevels, *longhole drilling*, this is illustrated in figure 4.2.2 (Hamrin, 2001; Haycocks and Aelick, 1992).

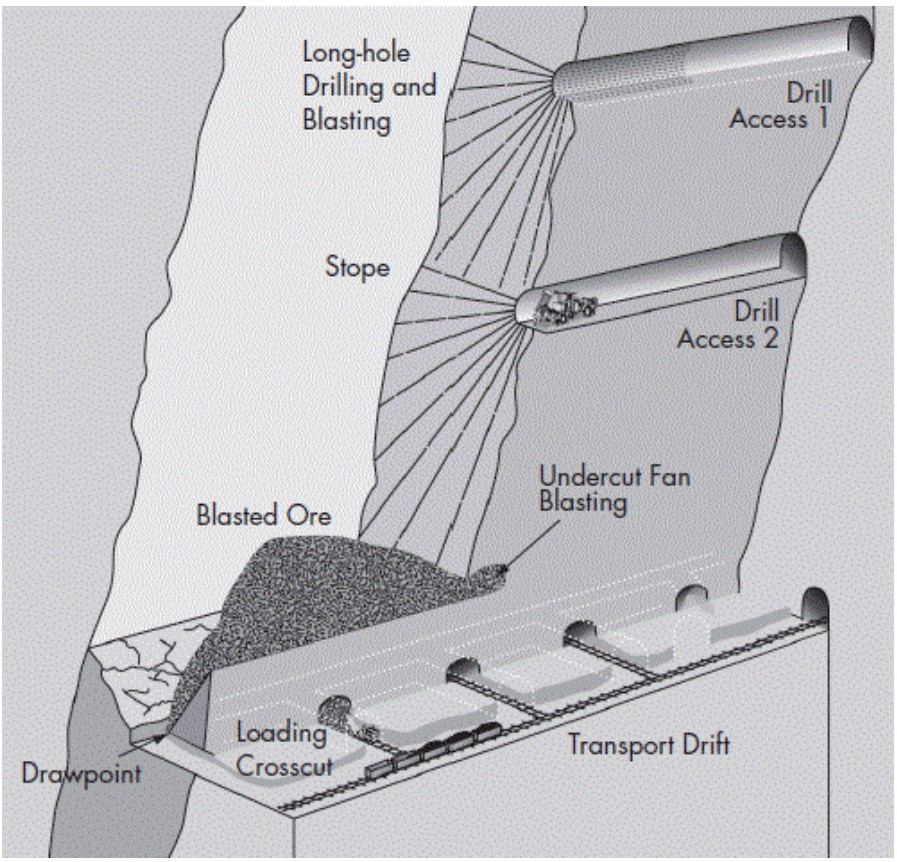

Figure 4.2.1 – Sublevel open stoping with fan drilling, after Hamrin (2001).

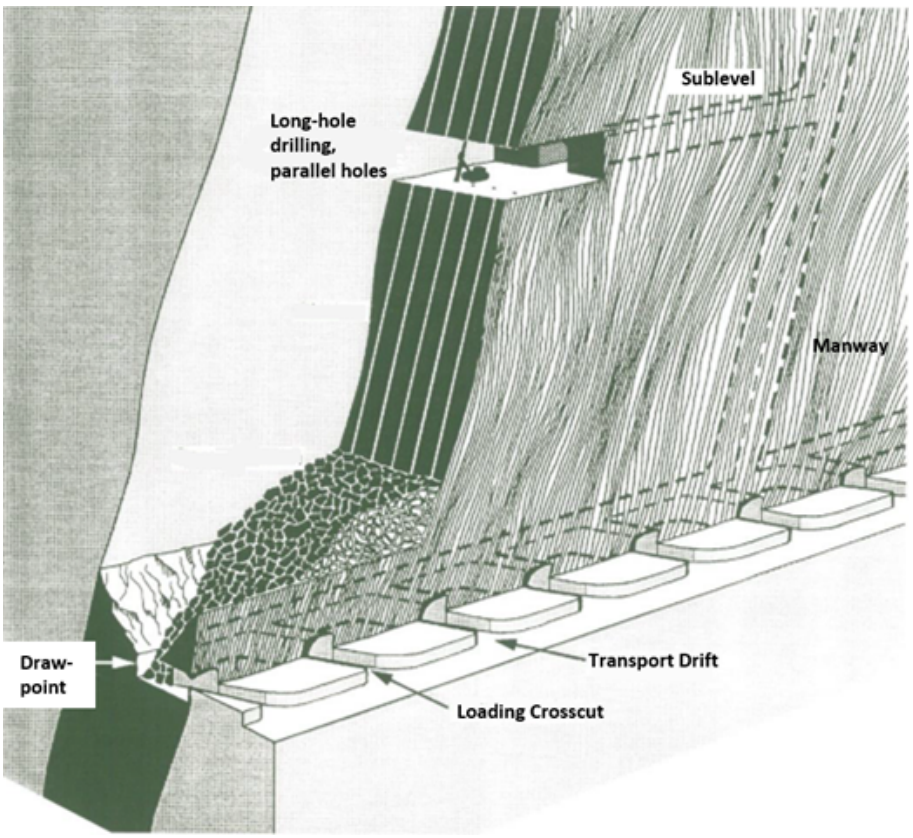

Figure 4.2.2 – Longhole parallel drilling, from Haycocks and Aelick (1992).

As previously mentioned there are several varieties of sublevel stoping and a third option is that of *cut and fill stoping* where the ore is removed in horizontal slices (Hamrin, 2001). Figure 4.2.3 illustrates horizontal drilling. A Norwegian mine used horizontal slicing for extraction of ore, see section 4.3.6 regarding Lefdal Olivine. However, they used horizontal slicing in combination with the *room and panel* method (Sollid and Kristiansen, 2014).

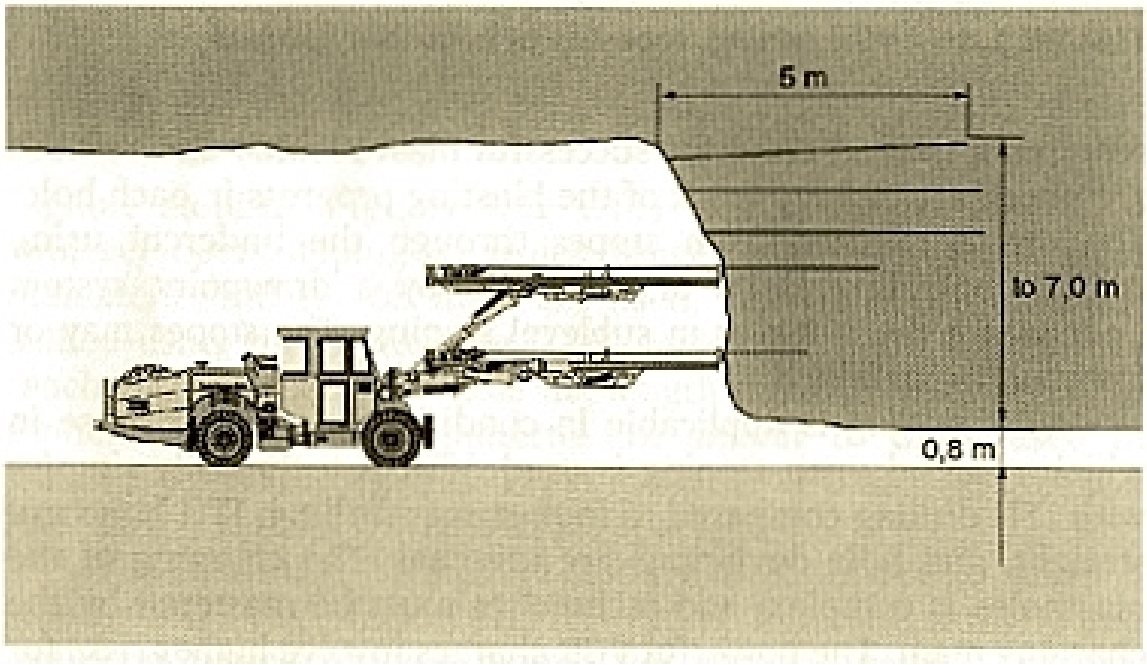

Figure 4.2.3 – Horizontal drilling (Hamrin, 2001).

Moreover, there is a special variant of sublevel stoping called *vertical crater retreat*. This method uses crater blasting and the ore is excavated upwards in horizontal slices. However, this method involves a higher risk for damaging the surrounding rock than sublevel open stoping. For a steep dike like deposit, *shrinkage stoping* is an option. This method requires little investment because of the simple development, but it is not a very effective method and it is not suitable for mechanization (Villaescusa, 2014; Haycocks and Aelick, 1992).

Stable Design

According to Haycocks and Aelick (1992) the stopes are typically contained by crown pillars that protects the levels above, rib pillars, and sill pillars in which the ore haulage system is cut. Sublevel stoping is generally more efficient with large stope dimensions. The stability of the country rock is usually the limiting factor for the design, therefore extensive rock mechanical investigations and monitoring is crucial.

Large open stopes can serve to concentrate high horizontal stresses and cause severe deterioration in development openings that are in close proximity to the stopes. Table 4.2.1 contains some examples of basic dimensions for stope design.

Table 4.2.1 – Sublevel Stoping Basic Dimensions, from Haycocks and Aelick (1992).

		Stope Dimensions [m]					
Mine	Ore Body	Width	Length	Height	Sublevel	Pillars [m]	Haulage Interval [m]
Kidd Creek	Massive metal sulfide	24	30	91	30	21-30	121
Torman	Massive limestone	45-50	100-150	100	15-50	45-50	-
Rio Tinto	Massive sulfide	20	20-50	40-72	40-72	12	53-84
Mt. Isa	Bedded sulfide	25-50	30	125-250	20	25	175-300
Burra Burra	Massive sulfide	12	100	50	13	13	60
Luanshya	Bedded sulfide	12	12	35	11	5-10	50-70

Backfilling

Sublevel stoping is a very development intensive mining method, but most of the cost is compensated by the fact that much of the development is done in ore. Backfilling of the stopes is an alternative if it is desirable to make the most of the ore body. Backfilling allows for future recovery of support pillars, and recovery of pillars permits up to 90% recovery of the ore. Backfilling further minimizes the occurrence of subsidence (surface deformations) and allows for redistribution of stresses created during the lifespan of the mine. Backfilling is also known to minimize the occurrence of rock bursting. Typically, backfill includes uncemented rock and sandfill, cemented rock fill, cemented hydraulic tailings fill, high-density tailings or alluvial fill. The downside of backfilling is that is reduces productivity and increase the costs, especially if there is nothing to fill the stopes with except from cement (Haycocks and Aelick, 1992; Tatiya, 2013; Villaescusa, 2014).

Economy

Economically speaking, sublevel stoping is a low-cost mining method with a high production rate. The key to minimize the costs lies in mechanization of the operation. Creating large openings and using the largest possible equipment in terms of production capacity. The use of large-diameter drilling machines can reduce the development compared to smaller-diameter longhole drills that have limiting lengths (less than 30 m) restricted by drilling accuracy. In addition, Haycocks and Aelick (1992) states that sublevel stoping frequently is selected as the primary underground method when surface mining no longer is economical.

Figure 4.2.4 shows a breakdown of mining costs for a typical operation. It is evident from the figure that development accounts for almost one-third of the total mining costs.

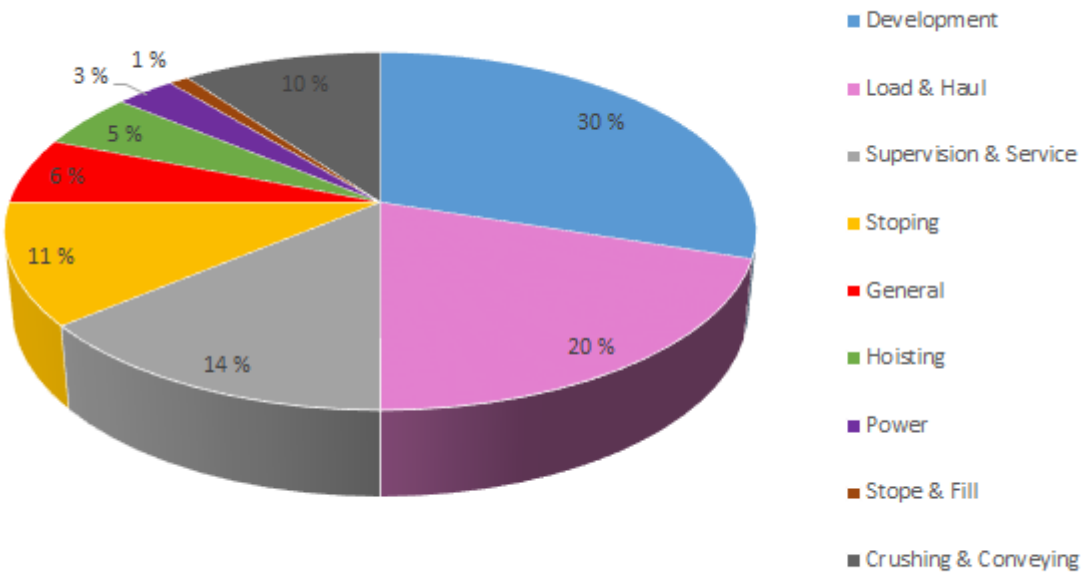

Figure 4.2.4 – Cost distribution for a typical sublevel stope, modified after Lawrence (1982); Haycocks and Aelick (1992).

Advantages of Sublevel Stoping

- Favourable for massive deposits with a dip $> 35°$.
- The method is safe, both drilling and loading takes place in drifts or drilling slices that easily can be scaled and supported.
- Easily ventilated.
- High productivity and efficiency.
- Easy to mechanize and can use large equipment.
- The early development can be done in ore rather than in waste.
- Drilling, blasting and loading can be done independently. This flexibility gives an effective utilization of the equipment.

- Large scale blasting lowers costs.
- Reasonable to high recovery, pillars left in place can be removed once adjacent stopes have been backfilled
- Low Dilution. (Haycocks and Aelick, 1992; Ellefmo, 2013a)

Disadvantages of Sublevel Stoping

- Extensive development before a stope can be in production.
- Initial recovery is usually 35-50%.
- Not a highly selective mining method, but a certain quality control will occur in the stope during loading.
- Relatively high ore loss and dilution if the ore/waste rock boundary is irregular.
- Borehole deviation will increase with increasing borehole length. This could lead to increased ore loss, dilution and limited control of blasting.
- Narrow ore bodies (< 6m wide) often have higher costs because there will be lower production for each blast.
- Fumes can leak back into stopes if secondary blasting is required. (Haycocks and Aelick, 1992; Ellefmo, 2013a; McIsaac, 2006)

4.3 Mine Design & Layout

Mine planning is an engineering process that encompasses all the major technical functions undertaken in sublevel stoping, with the key performance indicators being safety, dilution control, recovery, productivity, and mining cost. Mine planning provides the means for the safe, efficient, continuous, and economic recovery of ore while considering the life of mine issues and their implications for short-term planning and design. It also helps to maintain the long-term security of production, while ensuring satisfactory economic return. Trout, 1997

4.3.1 Stope Design

Mine planning prepares and evaluates the future stope design and the operating strategies. During this process, factors such as ore reserve estimation, overall sequences of extraction, dimensioning of regional pillars and sublevel intervals, design of haulage systems, fill and ventilation is determined. Villaescusa (1998) recommends that the mine-planning process be an interaction between geology, mine planning, rock mechanics and operating personnel (see figure 4.3.1).

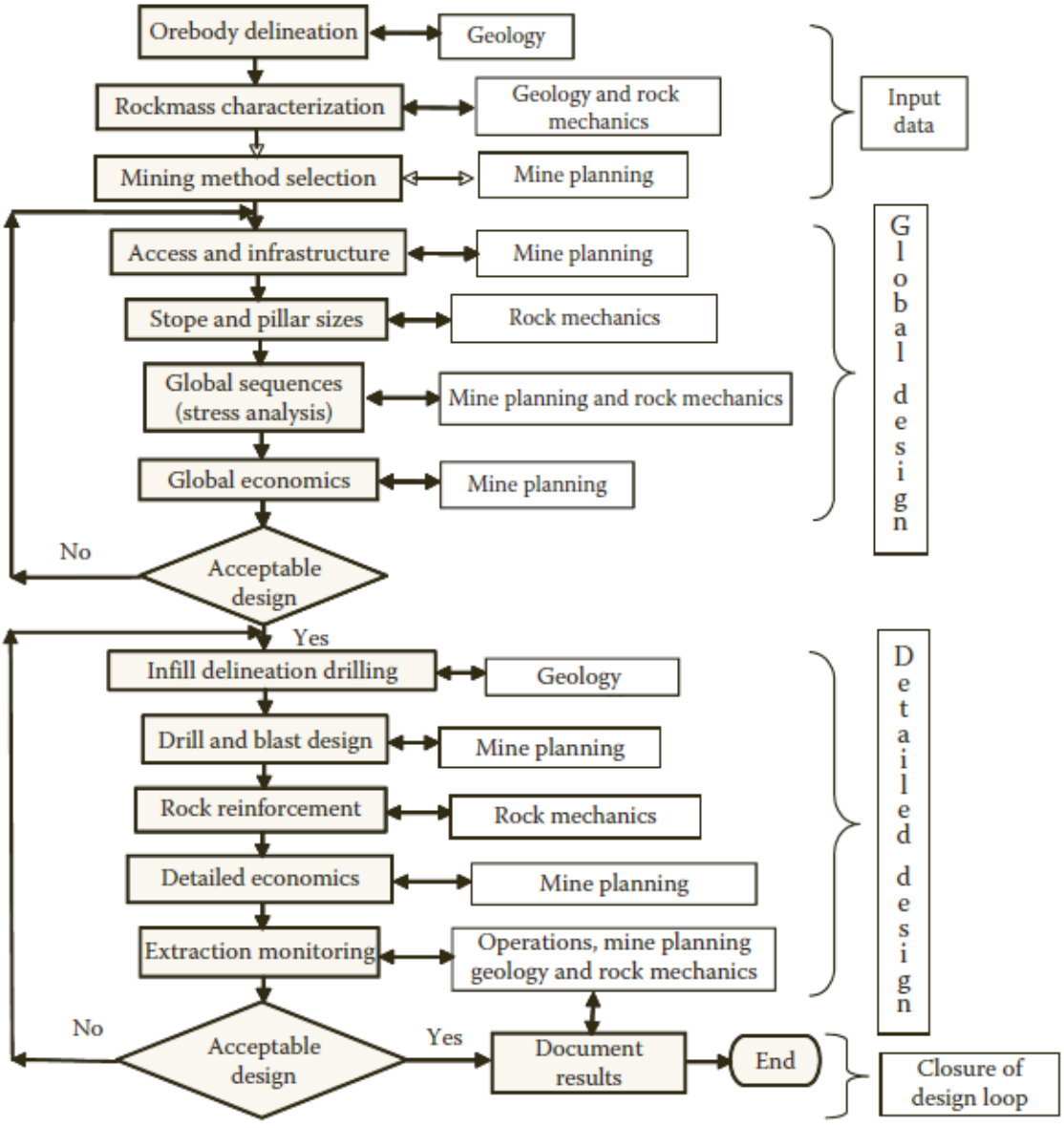

Figure 4.3.1 – Flowchart of mine-planning process, from Villaescusa (1998).

The key stages in the stope planning process are shown in table 4.3.1, where the orebody delineation and rock mass characterization constitute the basic inputs. They

require an early determination of rock mass properties on a block scale, followed by a selection of mining method and an estimation of likely loading conditions from the stoping sequences. Both global and detailed design stages are needed. Whilst global design problems are relevant and applicable within entire areas of a mine, detailed design problems are applicable to the extraction of individual stopes. In order to close the design loop a monitoring and back analysis strategy is required.

Table 4.3.1 – Key stages within a Stope Planning and Design Process, from Villaescusa (2014).

	Stope Design Process Stages	
Basic Input	**Control of Ground Behaviour**	**Closure of the Design Loop**
Orebody delineation	Stope block design	Monitoring
Rock mass characterization	Detailed stope design	Back analysis
Mining method selection		Documentation

4.3.1.1 Design Checklist

A number of issues needs to be considered during stope design. Villaescusa (2014) lists some of the most important factors:

- Location, orientation, and strength properties of large-scale geological structures
- Size of existing development and suitability for available drilling rig
- Additional development requirements, size, shape and gradient
- Ground support requirements for development and stope walls
- Equipment needs for development including drilling, mucking, charging and ground support
- Water drainage
- Tramming distances and alternate ore and waste passes
- Emergency escape routes during development and production
- Drill drive layout, blasthole design and firing sequence
- Drawpoint brow location and ground support requirements

- Ventilation requirements during development and stope production
- Bomb bays for storage of oversized rocks and secondary blasting
- Explosive types for development and production blasting
- Location, size and orientation of pillars
- Overall rock mass stability of the area prior to, during and after stope extraction
- Detailed scheduling of stope developments and production blasting (and filling)
- Cost comparison of alternative design
- Continuing stope performance monitoring during extraction
- Undertaking stope performance review after stope extraction

4.3.1.2 Span Determination

A stope span is defined as the minimum dimension of a stope wall (Villaescusa, 2014). Hutchinson and Diederichs (1996) related Bieniawski's (1989) RMR system to stope span. Figure 4.3.2 presents the maximum stable unsupported stope span as a function of the RMR value. For a temporary mine opening such as a 10 m-wide drill drive in downhole bench stoping with a required stand-up time of less than 5 years, it is visible from figure 4.3.2 that a rock mass with RMR_{89} of 80 or greater, the drill drive may not need systematic cablebolt reinforcement, only bolts and possibly mesh for personnel safety. Nevertheless, it is recommended to use ground support for all sublevel stope access infrastructure, even in hard rock masses. This is due to the fact that stress path effects and localized effect of large-scale structures likely to form wedges are not considered when using the RMR_{89} method. Further limitations when using the RMR_{89} values is that is does not consider the induced stresses. Supplementary illustrations are found in Appendix B on page 139.

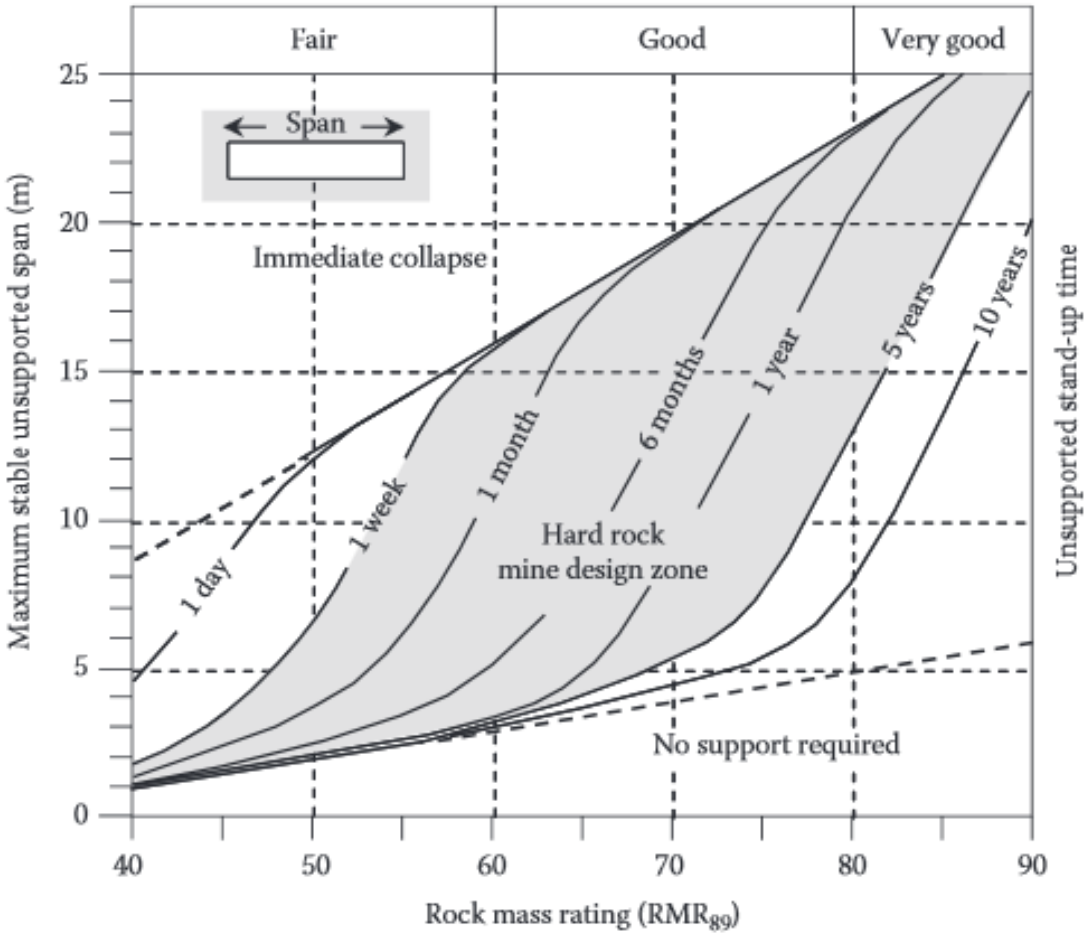

Figure 4.3.2 – RMR_{89} stand-up time guidelines, from Hutchinson and Diederichs (1996).

Table 4.3.2 – Excavation support ratio, from Barton (1988)

Type of excavation	**Number of cases**	**ESR (Approx.)**
Temporary mine openings	2	3-5
Permanent mine openings: lowpressure water tunnels; pilot tunnels; drifts and headings for large openings	83	1.6
Storage caverns; water treatment plants; minor road and railway tunnels; surge chambers; access tunnels	25	1.3
Power stations; major road and railway tunnels; civil defense chambers-, portals; intersections	79	1
Underground nuclear power stations; railway stations; sports and public facilities, factories	2	0.8

Hutchinson and Diederichs (1996) also related the Tunnel Quality Index System (Q - system) to span design. Figure 4.3.3 provides guidelines for no-support limits in order of decreasing reliability, related to Barton's original ESR values. The ESR factor is used by Barton to allow for varying degrees of instability based upon excavation

service life and use. The actual excavation span is divided by the ESR value to find the equivalent span for use in figure 4.3.3. Values for excavation support ratios (ESR) are given in table 4.3.2.

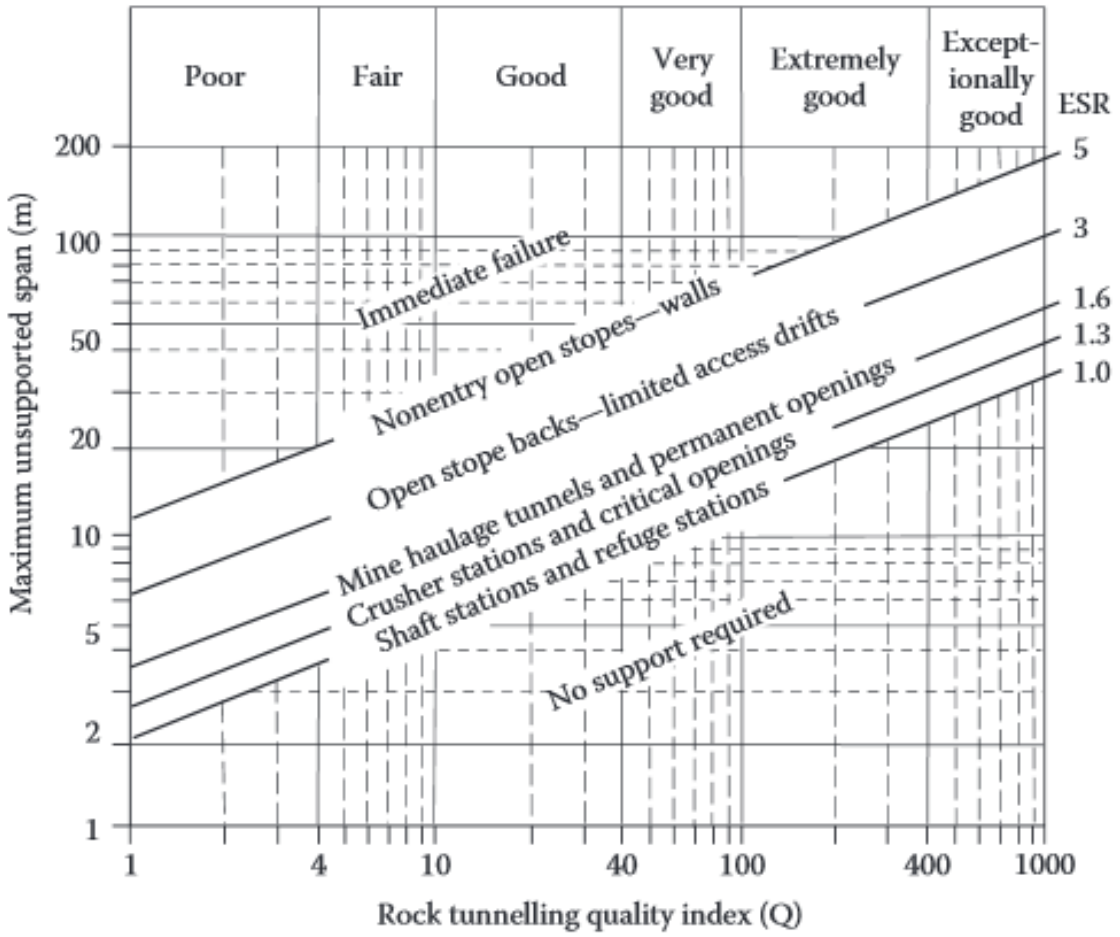

Figure 4.3.3 – Q-system, no-support span limits for underground mine openings, from Hutchinson and Diederichs (1996).

Hutchinson and Diederichs (1996) notes that the recommended ESR value for temporary mine openings is extremely limited, it is only based on two case studies. They therefore suggest using an ESR value of maximum 3, unless local experience validates a higher value. Nevertheless, the direct use of Q for open span design is not very common within the mining industry.

4.3.2 Mine Access

According to Bullock (2001), an adit or drift entry is the most economical approach to a new mine when the minable material is higher than the surface elevation. Most of the limestone and dolomite mines throughout the Missouri-Mississippi River Basin used this type of development. The exposed rock was opened with horizontal or near horizontal adits into the mountainsides. When the minable material reaches a depth below the surrounding terrain, a slope (decline) or shaft must be developed.

The adits, declines and shafts can be viewed as a network providing access to designated areas of the orebody. This network is a means of transportation and handling of the ore, and finding an efficient layout for such a network is a difficult design problem (Brazil et al., 2008).

4.3.3 Road Dimensioning

A key design consideration when planning a mine is that the roads and declines must be navigable by trucks and other mining equipment. The quality of haul roads have a profound impact on underground machine performance and a small improvement or change in this area can have a huge impact on the total cycle time. The three key factors in design of underground haul roads are according to Caterpillar Global Mining (2010): material quality, design and maintenance.

NTNU Department of Civil and Transport Engineering (2008) states that in order to achieve a satisfying transport capacity, the following requirements for the roads must be sustained:

- Proper road surface
- Sufficient road width
- Well adapted grades
- Geometrical design of the road
- Safety precautions

Technical Properties of Road

The condition of the road is decisive for which speeds can be used for safe and sound transport, which again influences the transport capacity. A poor roadway will result in unreasonable wear on the transport material (NTNU Department of Civil and Transport Engineering, 2008).

Caterpillar Global Mining (2010) urge that the grade of the roads and declines should be smooth and constant, with the rolling resistance kept to a minimum. Rolling resistance affects the productivity in such manner that it does not allow equipment to travel at its optimum speed for maximum productivity. Table 4.3.3 below shows the correlation between increase in tire penetration and increase in rolling resistance.

Table 4.3.3 – Rolling resistance in correlation to tire penetration, from Caterpillar Global Mining (2010).

Rolling Resistance	
Hard, well-maintained road	1.5%
Well-maintained road with flex	3%
25 mm/1 in tire penetration	4%
50 mm/2 in tire penetration	5%
100 mm/4 in tire penetration	8%
200 mm/8 in tire penetration	14%

Geometrical Design

The minimum radius of a curve in the road is limited to the turning radius of the vehicles in use. A small curve radius will result in low speeds and a low transport capacity. The same holds for the choice of road width. The road should be built wide enough so that two vehicles can meet without much delay. If this is not possible, pullovers should be built at intervals matching the cycle time of the vehicles. Table 4.3.4 below lists the dimensions and turning radius of the equipment currently in use in the open pit today. In addition, there are some underground machines listed for comparison.

Table 4.3.4 – Equipment dimensions and turning radius.

Equipment	Open pit	Belted	Length	Height	Width	Turning radius inner	Turning Radius outer	Steering angle
CAT 990 H	x		13.00	8.60	4.00	10.35	10.70	35
CAT 775 F	x		10.40	4.50	5.30	11.75	-	31
Komatsu HD 605-7R	x		9.40	4.40	5.30	8.50	-	39
SmartRig ROC F9C	x	x	11.30	3.80	2.50	11.30	-	-
Atlas Copco EMT50			11.82	3.50	3.70	5.10	11.25	45
Boltec LC			14.20	5.00	2.50[1]	4.75	7.50	45
Sandvik DS510-C			15.20	9.60[2]	3.50	5.15	8.50	35

[1] Without bolt rack
[2] Sandvik DS510-C with BH40 bolting head

Tannant and Regensburg (2001) claims that for straight sections the following equation can be used to determine the minimum road width:

$$W = (1.5L + 0.5) \cdot X \tag{4.3.1}$$

where

W = road width
L = number of lanes
X = vehicle width

For curved roads, the design is more complicated as more factors are taken into consideration. In order to enable vehicles to safely negotiate around curves at a given speed, the mining engineer must take into account factors such as front and rear overhang of the vehicle, stopping distance and the minimum turning radius for the vehicle.

Monenco (1989) gives the following equations for determining the minimum road width of a two-lane curved road:

$$W = 2\left(U + F_A + F_B + Z\right) + C \tag{4.3.2}$$

$$C = Z = \left(U + F_A + F_B + Z\right)/2 \tag{4.3.3}$$

where

U = Track width of vehicle (center - to - center tires)
F_A = Width of front overhang
F_B = Width of rear overhang
C = Total lateral clearance
Z = Extra width allowance due to difficulty of driving on curves

The illustration in figure 4.3.4 shows the different input variables for equations 4.3.2 and 4.3.3.

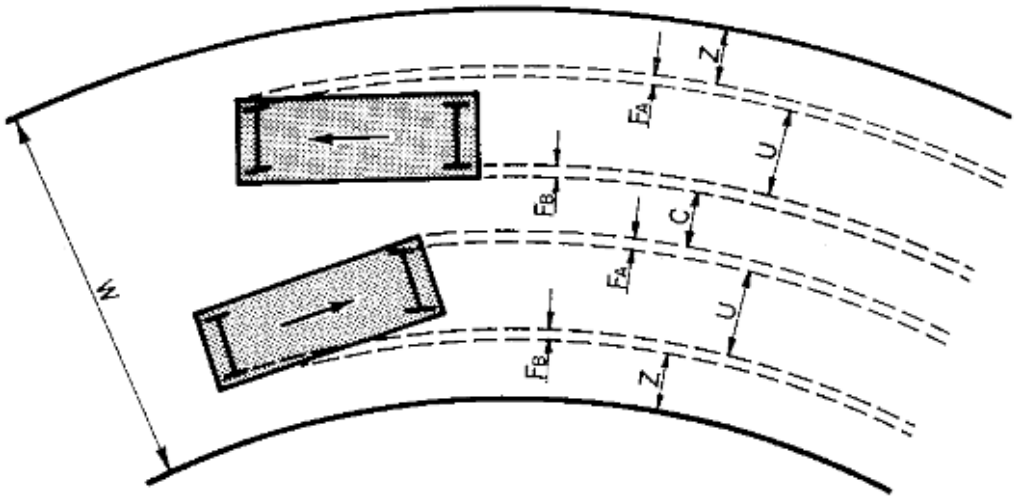

Figure 4.3.4 – Two-lane curved road (Monenco, 1989).

Ascending Grades

Practically, the road gradient is normally set at 10 % - 12.5 % (i.e. 1:10 to 1:8). According to the technical specifications of the transport vehicles, the road grade can be up to 20 % - 25 %. However, this is intended for runaway lanes in open pit mines. Norwegian underground mines have commonly used a gradient of 1:12 (8.3 %) for their declines. See section 4.3.6 for more information. Furthermore, increasing the length of the road to reduce the gradient is unprofitable seen from a capacity point of view (NTNU Department of Civil and Transport Engineering, 2008).

4.3.4 Ventilation

The main objective of mine ventilation is to provide suitable quality and quantity of air to maintain a safe and healthy environment in which workers can work. This applies to all working areas and transportation ways in the underground mine. A mine ventilation system includes fans, airways, control devices to direct or restrict airflow, cooling and filtering air and systems for monitoring air quality and quantity. It is important to reduce, dilute or extract the concentration of any airborne contaminants or gases to meet the air quality and safety standards. (Safe Work Australia, 2011; Brake, 2007).

Hazards that are controlled by ventilation include oxygen content, toxic and asphyxiant gases, flammable gases, airborne dust, fumes, products of combustion, humidity, temperature and naturally occurring radioactive materials.

Workers in mines and quarries need to be extra careful of dust and fine particles containing respirable crystalline silica (RCS). If workers are overexposed to RCS they can develop a lung disease called silicosis. RCS may also cause chronic obstructive pulmonary disease (COPD). The Tromsdal Limestone has a very low content of silica, see table 3.1.1, but nonetheless, it is important to take precautions (Sherson, 2002).

The amount of air required for dilution control depends on the strength of the contaminant source and the effectiveness of other control measures such as water for dust suppression or conditioning for the exhaust gas. In mechanized mines with diesel-powered equipment the exhaust gas dilution is used to determine the minimum ventilation requirements. Normally, the amount of air required ranges between 0.03 and 0.06 m^3/s per kW of rated power at the point of operation. The minimum dilution limit is determined by the carbon dioxide emissions, which is proportional to the engine power (Howes, 2011).

According to Howes (2011), the general relationship for determining the ventilation design criteria for a mine is:

$$Mine\,quantity = \alpha t + \beta \tag{4.3.4}$$

where

$t =$ the annual production rate in million tonnes per annum (Mtpa)
$\alpha =$ variable air quantity factor directly related to production rate
$\beta =$ the constant air quantity required to ventilate the mine infrastructure such as the ore handling system

Typical values of α are given in table 4.3.5.

Table 4.3.5 – Design air quantity factors (Howes, 2011).

Mining method	**α (air quantity factor $m^3/s/Mtpa$)**
Block-caving	50
Room-and-pillar	75
Sublevel caving	120
Open stoping:	
large $>$ 0.5 Mtpa	160
small $<$ 0.5 Mtpa	240
Mechanized cut-and-fill	320
Non-mechanized mining	400

The air quantity constant β depends on the ore handling system, and to some extent the overall mine production rate. In mines where rock is transported through a decline using diesel powered truck haulage or there is no crushing of the mined rock, a suitable value of β is 50 m^3/s. This value doubles if crushers are placed underground and skip hoisting is installed (Howes, 2011).

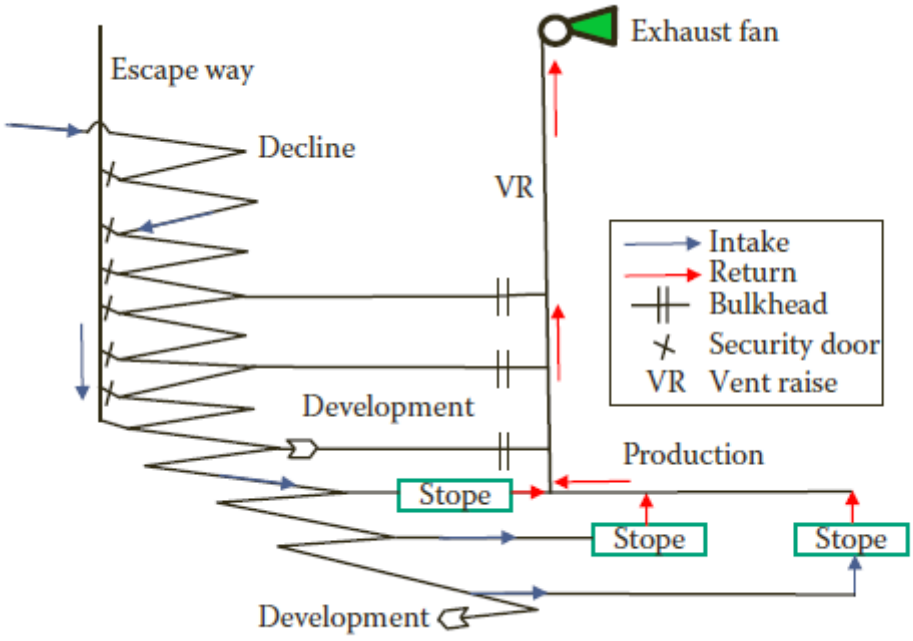

Figure 4.3.5 – Schematic of primary ventilation, Konkola deep mining project, Zambia. (Villaescusa, 2014)

Due to the difficulty of designing efficient structures in three dimensions and the combinations of choices for operational constraints, it can be a good idea to illustrate the ventilation solution in two dimensions first. Figure 4.3.5 shows the schematic

of a primary ventilation network from a deep mining project in Konkola, Zambia (Villaescusa, 2014).

4.3.5 Rock Support

> *Keeping disturbance to natural ground settings to a minimum could be considered as directly proportional to cost reduction and minimizing problems encountered during ground excavation and mining. Tatiya 2013*

Support Necessity

Proper selection of support is vital to mines and excavations. It determines the safety of work, ore production cost, losses and dilution, intensity of mining and productivity of the mine. The stress equilibrium state of a rock is disturbed by the mining operations. A stress field commonly called rock pressure develops around the workings, and acts upon the surrounding rock, pillars and supports (see also section 4.1 and figure 4.1.2).

Factors that contribute to the determination of rock pressure are:

- The stressed state of rock mass and the mechanical properties of the rock.
- The shape, dimensions and location of the excavation.
- The duration of the exposure of the rock excavation.
- The depth of the excavation. (Tatiya, 2013)

Natural Support

According to Tatiya (2013), use of in-situ rock to support the mine is the best way of designing a support system wherever feasible. For this to work, rock mechanical tests must be performed in order to evaluarte the structural properties of the rock. If the rock is to support in an effective manner it cannot be allowed to loosen. This requires a careful blasting and selection of properly shaped openings.

Pillars form a near-rigid type of support, and in sublevel stoping they are used to

maintain stability between the stopes. Typically, pillar support can be classified in three categories based upon their purpose and arrangement:

- *Protective pillars:* Are required to preclude caving of shafts or particular structure.
- *Level pillars:* Are pillars left above and under the workings of main horizons of the levels in order to support these. Both crown pillars and sill pillars belong to this category.
- *Rib/block/side pillar:* These are pillars left between two adjacent stopes or blocks.

Rock Bolting

The use of rock bolts in underground mines have increased rapidly since they first were used in 1918 in the underground mines of Poland (Franklin and Dusseault, 1989; Tatiya, 2013). Today, all types of mines, caverns and tunnels have an extensive use of rock bolts for support. Bolts can be used as permanent support for supporting the roof and sides of main roadways, roadway junctions and wide chambers. In stoping areas, bolts are used to support brows of drawpoints and other openings that require immediate and temporary support.

The number of bolts per square meter is called the bolt density. This, and the spacing between the rows of roof bolts, and within a row, can be calculated using the equations from Biron and Arioglu (1983):

$$Length\,of\,rock\,bolt\ (l) = Thickness\,of\,immediate\,roof + 0.5 \tag{4.3.5}$$

$$Number\,of\,bolts,\ m \geq (L\,h\,c\,\gamma)\,/R \tag{4.3.6}$$

$$Allowable\,axial\,force,\ r \geq \left(0.785\,d^2\,\sigma_a\right)/n \tag{4.3.7}$$

$$Bolt\,density\ (m_0) = m/\,(L\,c) \tag{4.3.8}$$

$$Bolt\,spacing\ (b) = L/m \tag{4.3.9}$$

Where

$h =$ Thickness of immediate roof $[m]$.
$l =$ Length of rock bolt $[m]$.
$m =$ Number of rock bolts.
$L =$ Gallery width $[m]$.
$c =$ Distance between rows of bolts $[m]$.
$\gamma =$ Immediate roof rock density $[t/m^3]$.
$n =$ Factor of safety.
$\sigma_a =$ Yielding strength of steel $[t/m^2]$.
$d =$ Diameter of bolt, $[m]$.
$R =$ Allowable axial force $[tonnes]$.

Typically, the bolt length varies with the conditions of the rock mass. Bolts tend to be delivered in standard lengths from the factory, and for practical reasons the lengths are usually related to the drill rod lengths i.e. 1.60 m, 2.0 m, 2.40 m etc. (Myrvang, 2001). With systematic bolting, the bolt lengths are adjusted in accordance to the span of the rock caverns. This is based on the impression that the influence from the rock cavern itself into the rock mass is dependent on the dimensions of the cavern. An illustration of systematic bolting pattern is displayed in figure 4.3.6. In Norway, the empirical IFF-formula[1] is often used as a rule of thumb for calculating the bolt length for systematic bolting:

$$Boltlength\, L = 1.40 + 0.184B \tag{4.3.10}$$

where

$B =$ span

Other means of support are wooden support, steel support such as shields, steel sets, steel arches and rigid arches, concrete support such as concrete lining and arches, shotcrete and reinforced shotcrete. Some mines also use filling as a mean of support. Filling has almost 100% ability to support the overlaying load without yielding Myrvang (2001); Tatiya (2013).

[1] IFF: Practical Handbook in rock bolting, Praktisk Håndbok i fjellbolting, Oslo 1973.

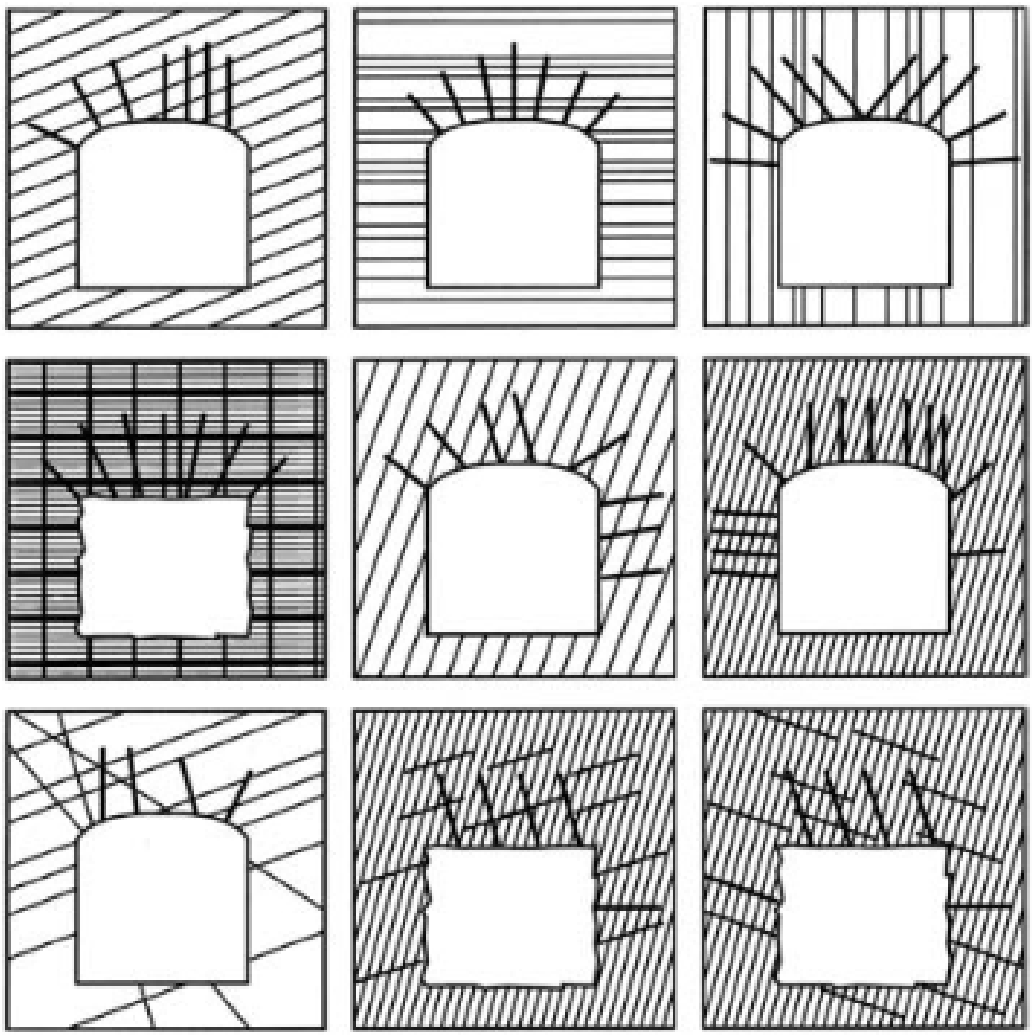

Figure 4.3.6 – Systematic bolting in jointed rock, after Choquet (1991).

4.3.6 Examples from the Industry

Stjernøy Nepheline

Since the 1960's North Cape Minerals, now Sibelco Nordic, have extracted nepheline syenite on a small island called Stjernøy in the Alta fjord. The deposit mainly consist of nepheline and feldspar, with some dark mineral contaminants such as biotite, hornblende and pyroxene. There are also some small occurrences of hematite, magnetite and titanite.

Up to approximately year 2000, the company had an underground operation with

sublevel stoping. This gave enormous rooms with a width of 25 metres, length 50 metres and heights up to 400 metres. The Access to the different levels of the mine is though a spiral-adit (inclination 1:12 and 1:10) which today exits at the top of the mountain "Nabbaren". The adit (tunnel) now functions as the access for the open pit at the top of the mountain, where the production takes place only during the summer months. The crusher is located underground below the old stopes, and the crushed rock is transported on a conveyor belt to the beneficiation plant. See figure 4.3.7 for a model of the mine (Sollid and Kristiansen, 2014).

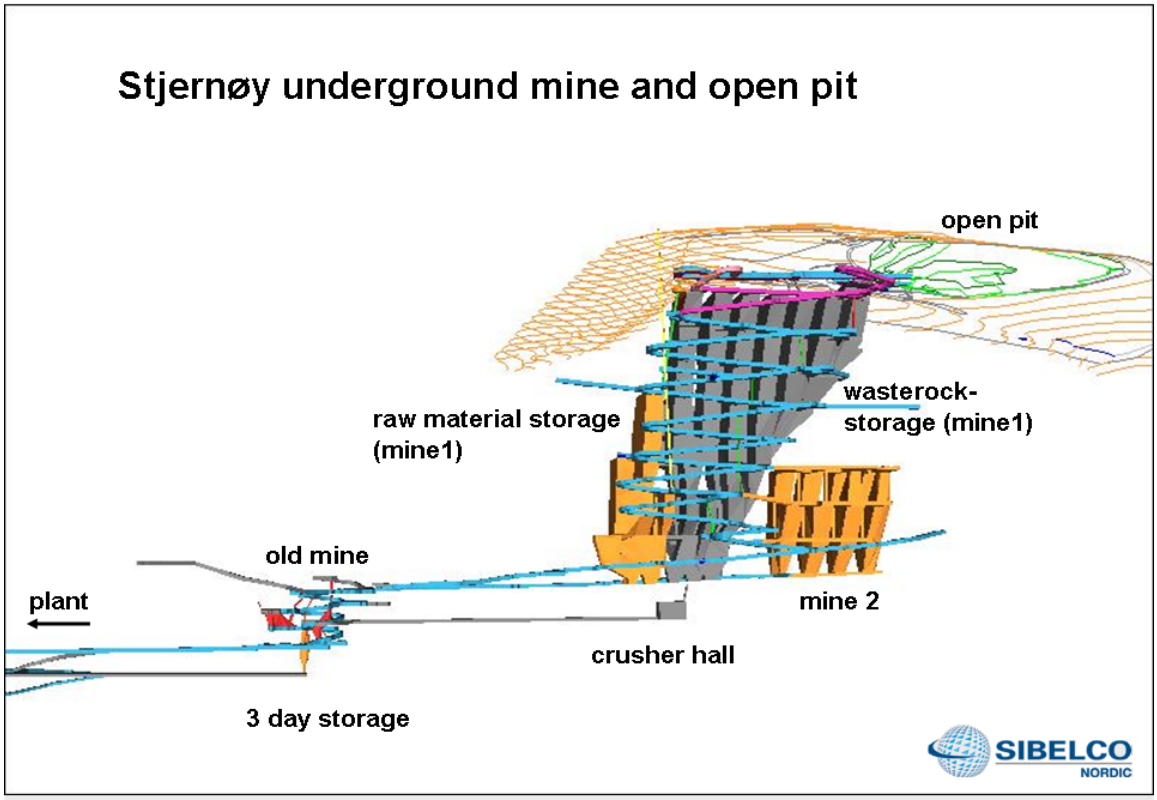

Figure 4.3.7 – Model of the sublevel stoping mine and open pit at Stjernøy (Sollid and Kristiansen, 2014).

The drilling drifts were excavated with a traditional tunnel rig (Ø = 51 mm), horizontal drilling, and subsequently expanded to the required stope width. Furthermore, the stopes were benched down using a custom-made surface drill rig with boreholes up to 40 meters long. As an example, in mine 2, a stope-panel of roughly 25x90 m were excavated with a 40 m intermediate bench/slice. Vertical holes were drilled towards an opening-shaft of 4x4 meters, and eventually the entire slice was blasted. Production blasts of 30 000 tonnes was normal.

The mountain on Stjernøya is of a particularly good quality that makes it possible to excavate large caverns with little rock support. The stress situation is favourable and

standard systematic bolting was applied to the stopes and roads. A few locations required shotcrete and/or steel mesh.

The ventilation system in the mine is unique due to all the openings into the mined stopes. Depending on the time of the year, the fresh air enters the tunnel at sea level; passes through the entire mine and exits at the top, or the other way around. In order to control the ventilation, gates and fans for forced ventilation have been installed (Sollid and Kristiansen, 2014).

Lefdal Olivine

The olivine deposit in Lefdal have been under operation since 1971. However, the production stopped when the financial crisis started in 2009 and the current owner, Sibelco Nordic, has had a production rest since. The high-density olivine was mined using a room and panel production method, leaving 18-meter high rooms that were 13 meters wide and 120-130 meters long. This was said to be the largest olivine mine in the world, with 120 000 m^2 divided into 75 chambers (Ulvedal, 2003).

During production, olivine was extracted using a traditional tunnel rig, i.e. drilling horizontal boreholes. Initially, a "standard" tunnel of 13 x 8.5 m was excavated before it was benched down, with horizontal drill holes (Ø=51 mm), to reach the full height of 18 meters. The transport drifts in the mine were 11x8.5 m. Lefdal olivine mine started with 15 m horizontal pillars between the sublevels, and decreased these to 12 m after a while, based on rock stress measurements.

Rock support in the hanging wall was conducted by scaling, manual bar scaling and then bolting with fully grouted rockbolts. Shotcrete was only used in rare occasions where extra support was necessary. Rock stress measurements have revealed relatively high, but favourable, horizontal rock stresses in the mine. There are no registered incidents of breakouts or rock burst.

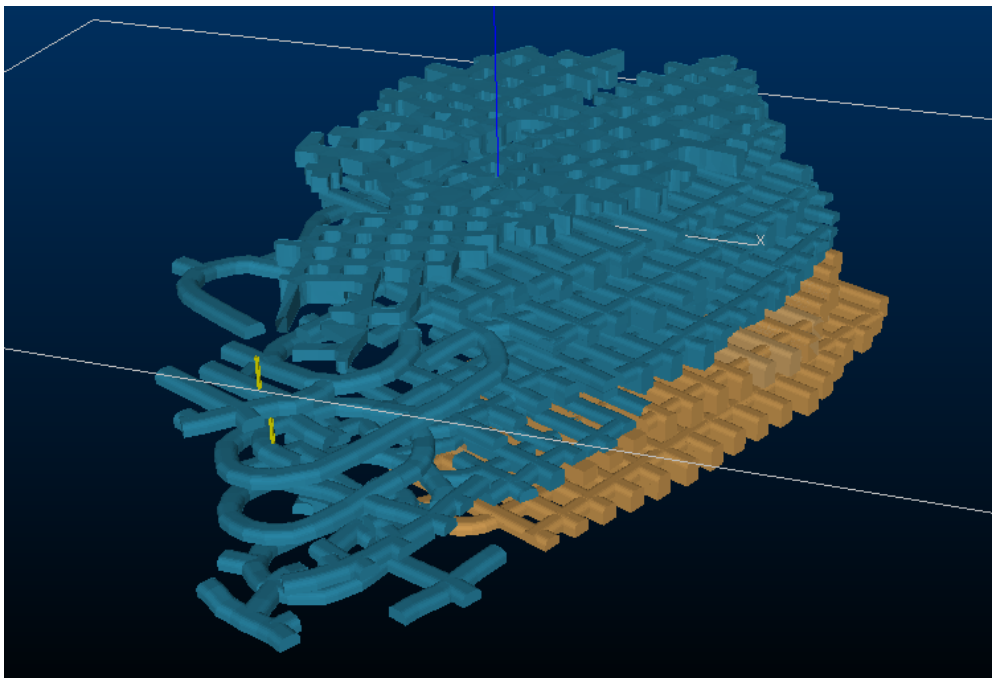

Figure 4.3.8 – Lefdal mine layout and infrastructure (Sollid and Kristiansen, 2014).

The mine access is at sea level and declines in a spiral (14x8.5 m) with a gradient of 1:12, almost a 100 meters below the sea. Every production drift was excavated with a slight inclination of 1:80 in order to drain out the water. This water was collected in a water basin located near the spiral and eventually pumped to the surface. In the middle of the spiral there is a ventilation shaft. This shaft had fans at each operating level with forced ventilation from the shaft to the faces. A 1.20 m vent duct was utilised. The ventilation shaft also worked as an emergency exit for the workers. See figure 4.3.8 for an illustration of the infrastructure in the mine (Sollid and Kristiansen, 2014).

Fana Underground Quarry

"Fana Stein AS" and "Fana Stein & Gjenvinning AS" are two companies outside the town of Bergen that has a combined mining concept. They run an underground aggregate quarry with a co-use of the fully excavated stopes: aggregate out – waste in. "Fana Stein AS" runs the mine production and "Fana Stein & Gjenvinning AS" is responsible for filling the stopes with recycled material.

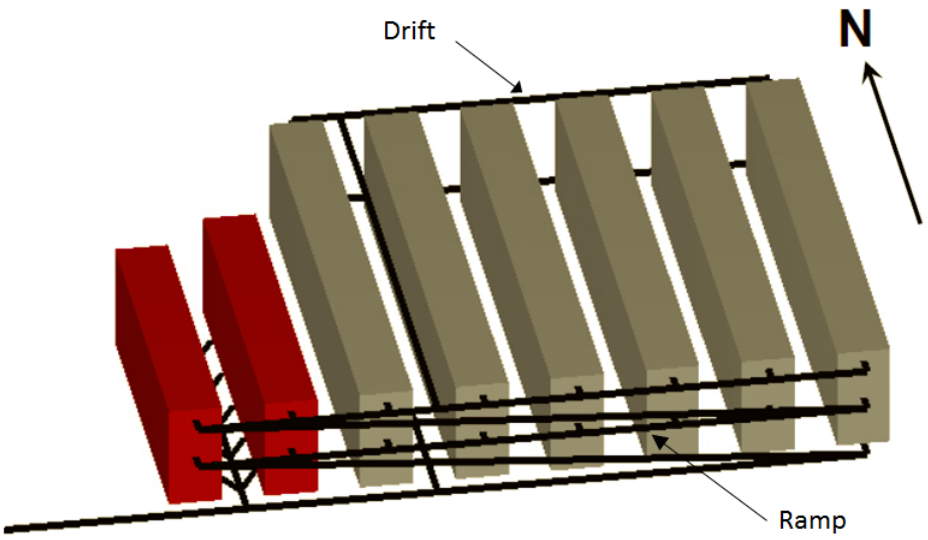

Figure 4.3.9 – Stope layout at Fana Stein & Gjenvinning. The red stopes are mined out and backfilled with waste. Modified after Ellefmo (2013b).

The rock, good quality gabbro, is mined with a sublevel open stoping production method and the company extract between 350 000 to 400 000 tonnes per year. Due to the small overburden, rock stress measurements reveals a low stress situation in the rock. Nevertheless, the stope roofs are fully reinforced with systematic bolting, and shotcrete is applied where needed. The sidewalls are not reinforced during loading, however loading and rock support is combined if required. The low stress situation allows the company to orientate the stopes transversely to the crushed zones in the area.

The stopes are benched down in 2-4 steps before full height is reached. Vertical blast holes (Ø = 76 mm) are drilled for the benching operation with up to 20-meter high benches. The finished stopes are 55 meters high, 25 meters wide and 160-200 meters long. The loading and transport access is at the end walls of each stope, both sub- and bottom levels (see figure 4.3.9). In total, there are three loading levels per stope. An intermediate bench is created with a ramp from the lower level, and a decline behind the drilling rig. For the final benches it is necessary to make a road up to the benches for each drill and blast cycle, this is illustrated in figure 4.3.10. Fana Stein have found that it is not necessary with drilling drifts as they use a drill rig with depth measurements. Furthermore, their experience suggests that drilling rigs do not need a perfectly planar foundation in order to achieve a god result. Their drilling principle is similar to that of open pit mining (Nødtvedt, 2014).

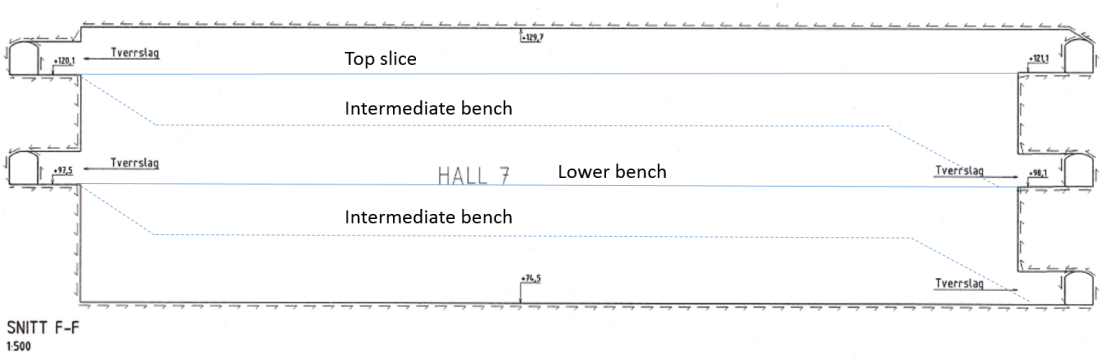

Figure 4.3.10 – Stope layout at Fana Stein AS, modified from Nødtvedt (2014). For a complementary illustration, see Appendix D on page 157.

For practical reasons the bench height cannot exceed 20 m, this makes scaling difficult. Particularly the transition zone between the benches require a lot of scaling. The drill holes are not fully loaded and this makes it even more important to reach the bench edge. Scaling is performed with a scaling rig equipped with a bucket in the front, this gives the workers more control before the next blasting sequence.

The mine access has a gradient of approximately 1:7. The drifts have a gradient of 1:100. In figure 4.3.11, a vertical section shows the complete mine layout with the mine access at 60 masl, the crushing plant, ramps and stopes.

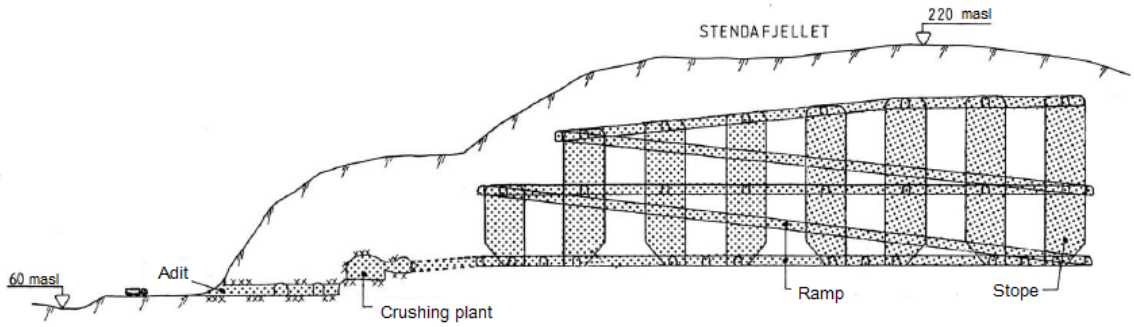

Figure 4.3.11 – Section through the mine (Nødtvedt, 2009).

Regarding ventilation, the company has solved this by installing fans and vent ducts inside the mine. The forced ventilation gives a total of 100-110 m^3/sec. There is also an emergency shaft for security reasons (Nødtvedt, 2014).

Norcem Brevik

Norcem AS is the only cement producer in Norway, and the factory in Brevik produces roughly 1.2 million tonnes of cement every year. Norcem Brevik is located in Porsgrunn municipality, south of Oslo and has about 180 employees.

Norcem extracts limestone with a room & pillar benching method as shown in figure 4.3.12. They use a traditional tunnel rig ($\emptyset = 48\,mm$) to drill vertical holes (downwards) and bench down in two levels, each bench being approximately 7.5 meters high. This leaves a total room height of 15-16 meters. The horizontal pillar between the levels are 8 meters thick and the vertical pillars are roughly 14x14 m. However, the top slice is opened with a wedge cut to minimize the blasting damage. This means that the blastholes are drilled at an angle to the face in a uniform wedge formation so that the axis of symmetry is at the centre line of the face. From the initial blast, the cut displaces a wedge of rock out of the face. In subsequent blasts, this wedge is widened to the full width.

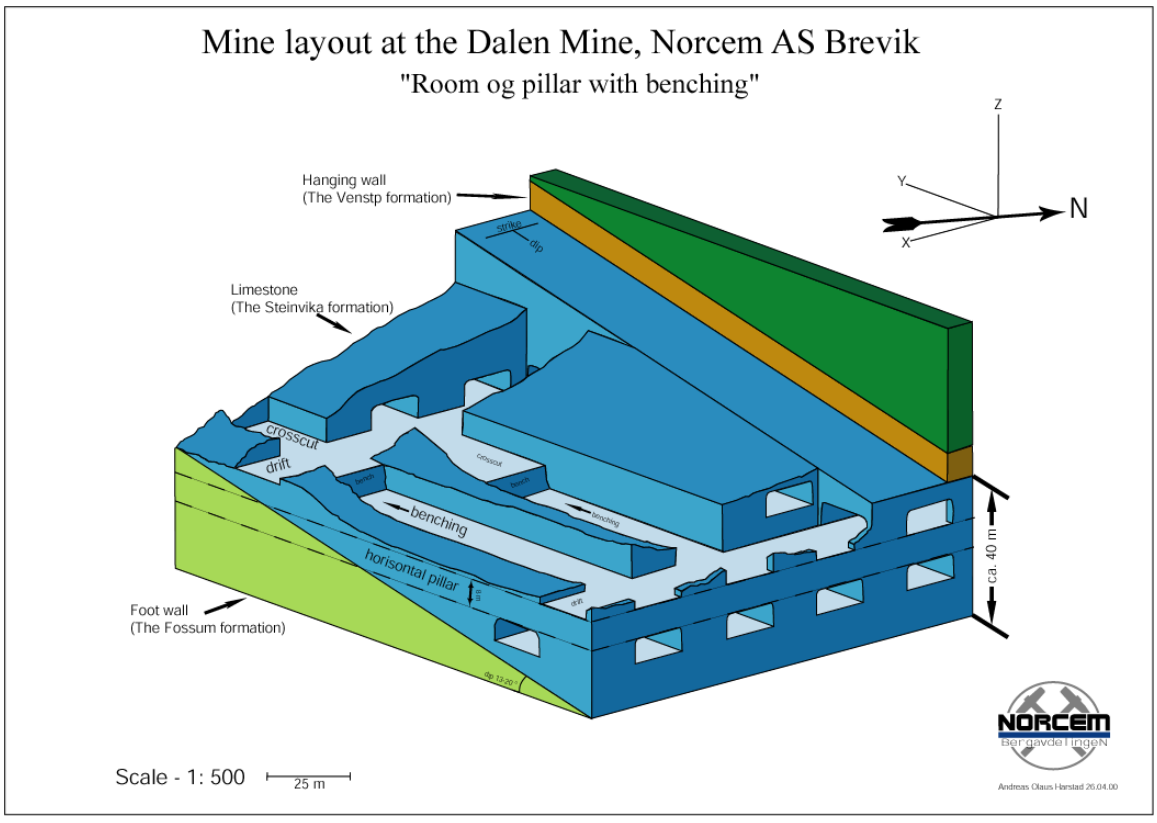

Figure 4.3.12 – Schematic of the Room & Pillar mine in Brevik (Kaasa, 2014).

Chapter 5

Methodology

5.1 Empirical and Analytical Methods

According to Swart and Handley (2005), empirical design could be defined as experienced-based application of known performance levels. This includes lab work, rock mass classification and engineering judgement based on experience. It is believed that empirical design of stope spans is the most dominant design approach today. However, this method ought to be used in conjunction with observational methods and analytical studies to formulate an overall stope design compatible with the design objective and site geology.

In order to evaluate the stability of the stope spans, geotechnical classification systems are useful. Swart and Handley (2005) suggests four different systems that can be used for evaluating the stability:

- The RMR system developed by Bieniawski (1989).
- The Q-system, developed by Barton et al. (1980).
- The MRMR system, developed by Laubscher (1977). This is a modification of the RMR system.
- The modified stability graph method, using the modified stability number, N', originally developed by Mathews et al. (1981).

Alternatively, analytical methods include techniques such as closed form solutions, numerical methods and structural analysis. The aim is to create conceptual models that are able to reproduce the behaviour and response of the stope panel. Numerical

methods are very effective because they enable comparative assessment of the stope stability for various input parameters. A suitable failure criterion should be selected to model the expected failure mechanism and mode of failure. To obtain the best stope design it is recommended to use more than one analytical method. Swart and Handley (2005) suggests the following methods:

- Elastic and Voussoir beam analyses.
- Kinematic analyses.
- Probabilistic analyses.
- Numerical analyses.

In this thesis, both empirical and analytical methods have been used in the attempt to determine a suitable mine design and layout. The subsequent sections will elaborate this further.

5.2 Surface Mapping

Outcrop mapping is a fundamental type of data collection and a key input for kinematic analysis and numerical design analysis. It allows you to collect important information about the deposit prior to mining and after mining has commenced. According to Read and Stacey (2009), it is important to be well prepared. This includes determining roughly what is relevant to the task at hand, setting the appropriate scale of the mapping, preparing field logging sheets, deciding the level of data to be recorded and selecting the right mapping tools.

5.2.1 Mapping of joint sets

Joint sets in Tromsdalen were mapped in coherence with RQD measurements, RMR rating and determination of the Q-value. The location for each mapping site was registered on a GPS and transferred to a map, see figure E.0.4. The mapping was concentrated on the sout side of the open pit because this is where the future underground mine will be located. The following geotechnical features were registered during field mapping in the fall of 2013:

Orientation	Spacing of discontinuities
Infill (gouge)	Persistence of discontinuities
Aperture	Groundwater inflow
Roughness	JRC
Weathering	GSI

In figure 5.2.1 the typical geotechnical features of a joint is illustrated. Not all of these features were mapped during fieldwork in Tromsdalen. For further information on how the mapping of the different characteristics are registered, see tables in Appendix A. The result of the surface mapping is presented in table 6.1.1 on page 73.

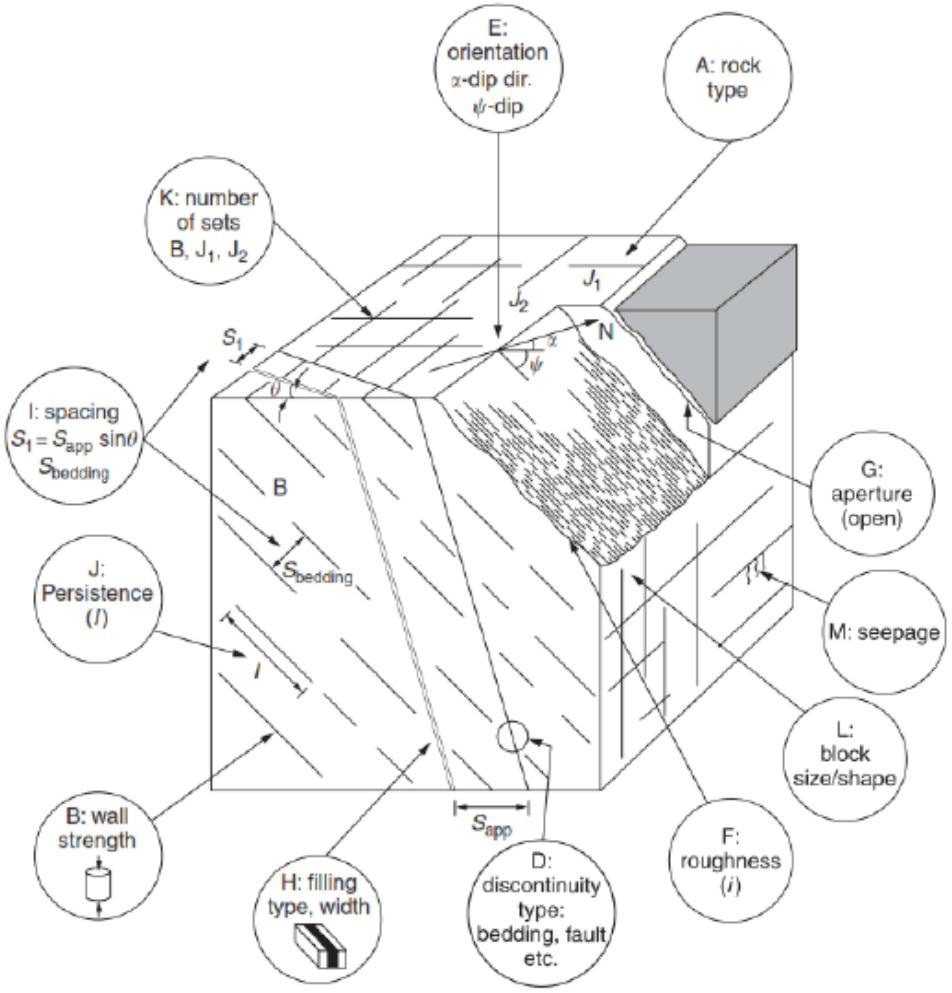

Figure 5.2.1 – Typical geotechnical features of a joint (Wyllie and Mah, 1981).

During mapping in an open pit mine some caution must be used, not all fractures should be mapped. Blasting will always affect a mine face and enhances or creates many of the observed fractures. In many cases, underground mining included, it is very difficult to decide if specific joints would have been present in the rock before blasting (Read and Stacey, 2009).

In order to make mapping possible, certain general guidelines should be followed:

- Fractures that have a very irregular surface (non-planar) and are not continuous are probably blast induced.
- Fractures that appear to radiate out from blast holes are also suspicious.
- Fractures with a rust, clay or mineral coating, or infilling are most likely joints.

5.2.2 Geological Strength Index (GSI)

The Geological Strength index (GSI) was introduced by Hoek in 1994, and later developed by Hoek et al. (1995) and Hoek & Brown (1998). It provides a system for estimating the reduction in rock mass strength for different geological conditions identified through field observations. Based upon visual impression of the rock mass structure and the surface conditions of the rock discontinuities, it is possible to estimate a GSI value from the contours given in the table in figure A.1.2 on page 134.

5.2.2.1 Limitations

A practical problem that arises when estimating GSI in the field is related to blasting and blast damage. The difference in appearance of a rock face excavated by controlled blasting and a rock face that has been damaged by bulk blasting is considerable. If possible, the estimation of the GSI value should be based on an undamaged rock face.

5.2.3 Determination of RQD

One of the most common methods for classifying the extent of jointing in a given rock mass is Rock Quality Designation. Although RQD logging is normally performed on drilled cores, it can also be done in the field as line mapping. In this case, a measured length of 1 m was marked with a measuring tape, and the length between each joint was registered. All lengths larger than 10 cm are summed and divided by the total length (approximately 1 m). When determining RQD in the field this way, it is important to separate the actual joints from blast-induced fractures.

Hoek (2007) presents a good illustration of the practical application of RQD logging, this can be seen in figure A.2.1 on page 136. Table 5.2.1 shows how RQD relates to rock mass quality. For more information, see section 5.2.4.1 on the next page.

Table 5.2.1 – Classification table of RQD index.

RQD	Rock mass quality
< 25%	Very poor
25-50%	Poor
50-75%	Fair
75-90%	Good
90-100%	Excellent

5.2.4 Q-system

The Q-system is a system developed by NGI between 1971 and 1974 and can be used for classification of rock masses around an underground opening as well as for field mapping. It is a classification system for rock masses with respect to stability of underground openings. The Q-value for a rock mass can be calculated based on six estimated rock mass parameters. The calculated Q-value then gives a description of the rock mass stability of an underground opening in jointed rock masses. High Q-values indicates good stability and low values are consistent with poor stability. The different Q-values are related to various types of permanent rock support through a schematic support chart (see figure A.1.1 on page 133), where type and quantity of rock support may be found. Hence, the Q-system can be used as a guideline in rock support design decisions and as documentation of rock mass quality .

The Q-value is most precise when mapped for underground openings. Results of calculated Q-values from field mapping, core logging and borehole investigations must be handled with care (NGI, 2013). See table 6.1.2 on page 75 for Q-values from surface mapping in Tromsdalen.

5.2.4.1 Parameters

The Q-value is calculated from the following equation:

$$Q = \frac{RQD}{J_n} \cdot \frac{J_r}{J_a} \cdot \frac{J_W}{SRF} \tag{5.2.1}$$

where:

RQD Degree of jointing (Rock Quality Designation)

J_n Number of joint sets

J_r Joint roughness number

J_a Joint alteration number

J_w Joint water reduction factor

SRF Stress Reduction Factor

According to Barton et al. (1974), a combination of the six parameters express the three main factors which describe the stability in underground openings:

$\frac{RQD}{J_n}$ Degree of jointing (or block size)

$\frac{J_r}{J_a}$ Joint friction (inter-block shear strength)

$\frac{J_w}{SRF}$ Active stress

Rock Quality Designation (RQD)

RQD was developed by Deere (1963) to provide a quantitative estimate of rock mass quality from logging of drill cores. It is defined as the percentage of intact core pieces longer than 10 cm in the total length of core. The core should be at least NW size (54.7 mm) (Hoek, 2007). The procedure for estimating RQD is shown in equation 5.2.2:

$$RQD = \frac{\sum \text{Length of core pieces} > 10\,\text{cm length}}{\text{Total length of core}} \cdot 100\% \tag{5.2.2}$$

R QD will be a percentage between 0 and 100, see list in table A.1.5 on page 132.

Joint set number ($\mathbf{J_n}$)

Shape and size of blocks in the rock mass is dependent on the joint geometry. Normally there are 2-4 joint sets in within a certain location. The handbook from NGI (2013) states that: *"if more than one joint belonging to a joint set appears in the underground opening, it has an effect on the stability and should be regarded as a joint set".* The joint set number is determined after the list in table A.1.5.

Joint roughness number ($\mathbf{J_r}$)

The joint friction depends on the nature of the joint wall surfaces. They can be undulating, planar, rough or smooth. The joint roughness number describes these conditions of the joint surface and is estimated from the list in table A.1.5 and figure A.3.1 on page 137.

Joint alteration number ($\mathbf{J_a}$)

The joint infill is also significant to the joint friction. When evaluating joint infill there are mainly two factors of importance: thickness and strength. These factors depend on the mineral composition, see list in table A.1.5 for how to determine the alteration value.

Joint water reduction factor ($\mathbf{J_w}$)

If water is present in the joints, it may have softened or washed out the mineral infill and thereby reduced the friction on the joint planes. Water pressure may also reduce the normal stress on the joint walls and cause blocks to shear more easily. The factor is determined by observation after list in table A.1.5. The lowest Jw values (Jw <0.2) represents large stability problems.

Stress Reduction Factor (SRF)

Generally, the SRF describes the relation between stress and rock strength around an underground opening. Both stresses and rock mass strength are measurable, and the SRF can then be calculated from the relation between the uniaxial compression strength and major principal stress, or the relation between the maximum tangential stress and UCS in massive rock. During planning of an underground excavation, SRF can be stipulated or estimated from the overburden and topographic features or based upon general experiences from the same geological and geographical region (see table A.1.5 for how to determine the SRF value).

5.2.4.2 Correlation between RMR and Q-value

$$\mathrm{RMR} = 9 \ln \mathrm{Q}' + 44 \tag{5.2.3}$$

where Q' reflects the rock mass strength, the J_w/SRF term is set to unity (Seedsman, 2011).

5.2.4.3 Limitations

The Q-system is mainly based on case studies of underground excavations in Norway and the majority of these are derived from hard, jointed rocks. There are only a few examples for weak rocks with few or no joints. For evaluation of support in such types of rocks, other methods of investigation should be considered utilized in addition to the Q-system. In squeezing rock or very weak rock (Q<1) it is essential to combine application of the Q-system with deformation measurements and numerical simulations (NGI, 2013).

5.2.5 Rock Mass Rating (RMR)

The RMR is a geomechanical classification system first developed by Bieniawski (1973) and later developed and modified by Bieniawski in 1989. The Rock Mass Rating system is presented in table A.1.6, giving the ratings for each parameter. The overall basic RMR is the sum of all the individual rates found in the table, including the adjustment for the discontinuity orientation. RMR takes values between 0 and 100 with an accuracy of plus/minus five. See table 5.2.2 for a rock mass classification.

Table 5.2.2 – Rock Mass Classification Bieniawski (1989).

RMR	Rock mass class
81-100	Very Good
61-80	Good
41-60	Fair
21-40	Poor
< 20	Very Poor

The following six parameters were used in classification of the rock mass by the RMR system:

1. Uniaxial compressive strength of rock material
2. Rock Quality Designation (RQD)
3. Spacing of discontinuities
4. Condition of discontinuities
5. Groundwater conditions
6. Orientation of discontinuities

The results from RMR classification is found in table 6.1.3 on page 75.

5.2.5.1 Correlation between GSI and RMR

$$GSI = RMR_{89} - 5 \tag{5.2.4}$$

5.2.5.2 Limitations

The RMR value is not factual data in respect to the engineering geology of a rock mass, it includes a significant degree of interpretation and relate to a particular structure at a particular depth. Furthermore, the stress parameters are not taken into account (Pells and Bertuzzi, 2011; Hoek, 2007).

5.3 Analytical Software

In order to analyse the situation in Tromsdalen the author has made use of analytical software. The following section gives a brief description of these software's and their purpose for this thesis.

5.3.1 Phase^2

Phase^2 8.0 (latest version) is a powerful 2-dimensional elasto-plastic finite element stress analysis program for underground or surface excavations in rock or soil. It can be used to solve a wide range of mining, geotechnical and civil engineering problems (Rocscience, 2014; Trinh et al., 2010).

Lack of data input on rock mass properties is a major obstacle often encountered in numerical modeling of geotechnical structures and excavations. If engineers cannot obtain or estimate geotechnical parameters, numerical analysis programs are greatly limited. RocData[1] provides analysis tools and data that assists the engineers when determining rock material properties.

5.3.1.1 Input Parameters

Most of the rock mass properties for the Tromsdalen Limestone have been determined from laboratory testing, see table 3.2.1 on page 21, and from fieldwork, see section 5.2 and Section 6.1. The rest of the necessary input parameters needed for the numerical modelling was determined with the help of RocData and from field investigations performed by Saellegg 2005. From the map in figure 2.3.1 it is clear that there are three lithologies in Tromsdalen: Limestone, Greenschist and Phyllite. However, mapping and core drilling also show a layer of white marble. This is believed to have the same dip as the carbonate deposit, see figure **5.3.4 on page 69**. In table 5.3.1 the input parameters for the analysis in *Phase*^{2} are displayed, for further details about the complete rock analysis for all lithologies used in the model see Appendix C.1.

In this analysis of the carbonate underground mine, the Generalized Hoek-Brown failure criterion has been used for a plastic material, i.e. the material can yield. The

[1] RocData is a versatile toolkit for the analysis of rock and soil strength data, and the determination of strength envelopes and other physical parameters

residual strength is = 0, thus defining a brittle material.

Table 5.3.1 – Input parameters for the analytical method

Limestone		**White marble**		**Greenschist**		**Phyllite**		
Rock Mass Properties		Rock Mass Properties		Rock Mass Properties		Rock Mass Properties		
γ	0.027	γ	0.0279	γ	0.0299	γ	0.0267	$[MN/m^3]$
υ	0.25	υ	0.26	υ	0.20	υ	0.17	
E_{rm}	26.5	E_{rm}	70.2	E_{rm}	38.6	E_{rm}	5.6	$[GPa]$
Hoek-Brown Classification		Hoek-Brown Classification		Hoek-Brown Classification		Hoek-Brown Classification		
σ_{ci}	94	σ_{ci}	110.9	σ_{ci}	219	σ_{ci}	51	$[MPa]$
GSI	55	GSI	77	GSI	63	GSI	45	
m_i	12	m_i	9	m_i	10	m_i	7	
D	0.1	D	0	D	0	D	0	
E_i	74	E_i	83.2	E_i	65.7	E_i	24.9	$[GPa]$
Hoek-Brown Criterion		Hoek-Brown Criterion		Hoek-Brown Criterion		Hoek-Brown Criterion		
mb	2.210	mb	3.958	mb	2.668	mb	0.982	
s	0.0057	s	0.0776	s	0.0164	s	0.0022	
a	0.504	a	0.501	a	0.502	a	0.508	

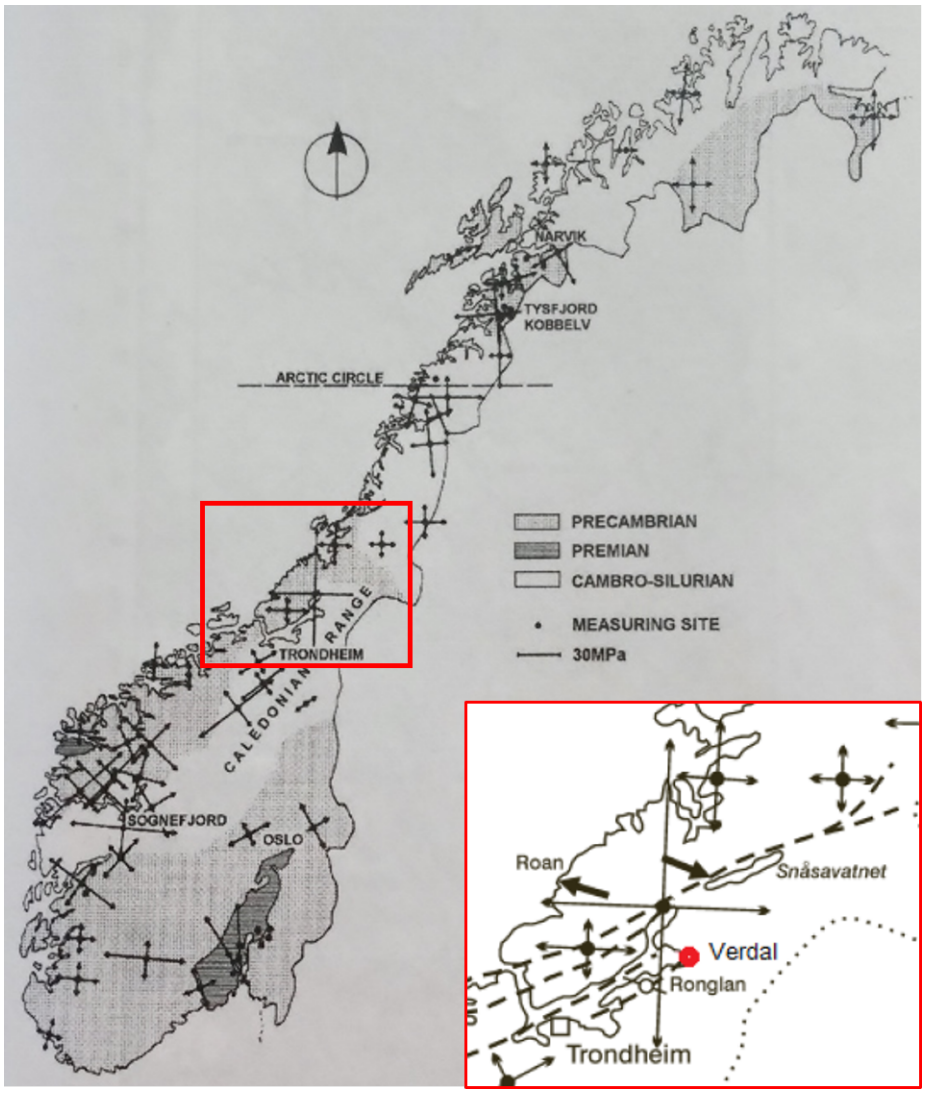

Figure 5.3.1 – Horizontal stress map of Norway (Myrvang, 2001).

The horizontal stress map of Norway (Myrvang, 2001) was intended for assistance in estimating the possible horizontal stresses in Tromsdalen, see figure 5.3.1. However, after consulting with Myrvang (2014) it is evident that these stress measurements are not suitable for estimating horizontal stresses in Tromsdalen as they are measured at great depths and under various geological conditions. Based on similar conditions from other locations in Norway, Myrvang suggests a constant horizontal stress of 5 MPa in Tromsdalen. Both the total stress ratio (σ_H/σ_V) in plane and the total stress ratio out of plane is set equal to one ($k = 1$). Due to time constraint, the author has not looked into the stress situation for $k = 2$. For further information about the settings for $Phase^2$, the reader is referred to the online user manual from Rocscience.

5.3.1.2 Cross-Sections

Two cross-sections have been modelled and analysed with $Phase^2$, to determine the stope span, stope length, pillar width, and how much deformation that can be expected from this mining method. Figure 5.3.2 displays where the cross-sections are made in relation to the future open pit border. Figures 5.3.3 and 5.3.4 show section A-A' and section B-B' respectively. For design parameters used in the numerical modelling the reader is referred to table 6.1.4 on page 76. Cross-section A-A' has five stope levels with four stopes on each level. Section B-B' is also illustrated with five stope levels.

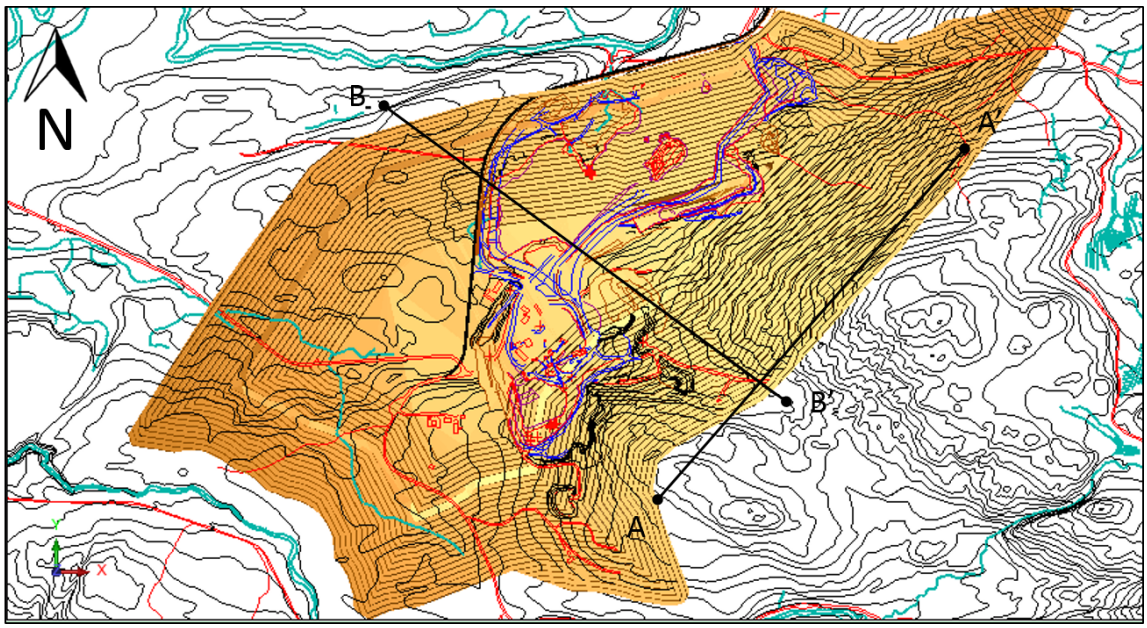

Figure 5.3.2 – Approximate location of analysed cross-sections. Profile A-A' is a cross-section through the future mine, and profile B-B' is a cross-section through the open pit and the future mine. (Map from Surpac, geological model by courtesy of Ruiz, 2014)

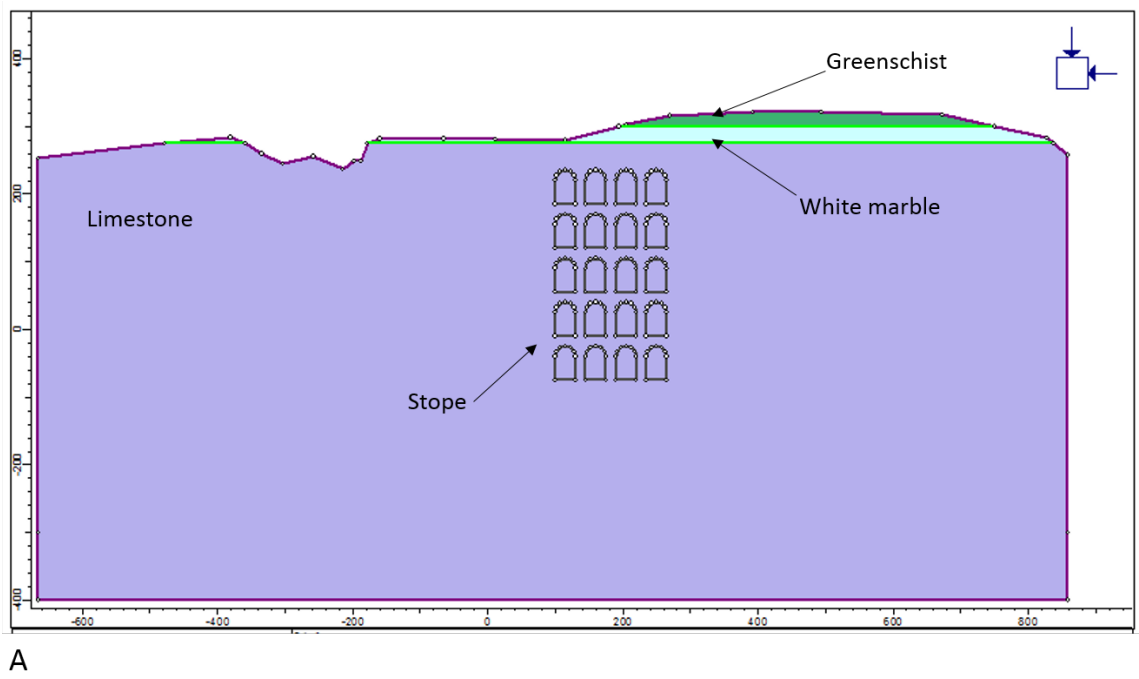

Figure 5.3.3 – Cross-section A-A' through the future underground mine. The stopes are not excavated at this point. (Scale 1:6000)

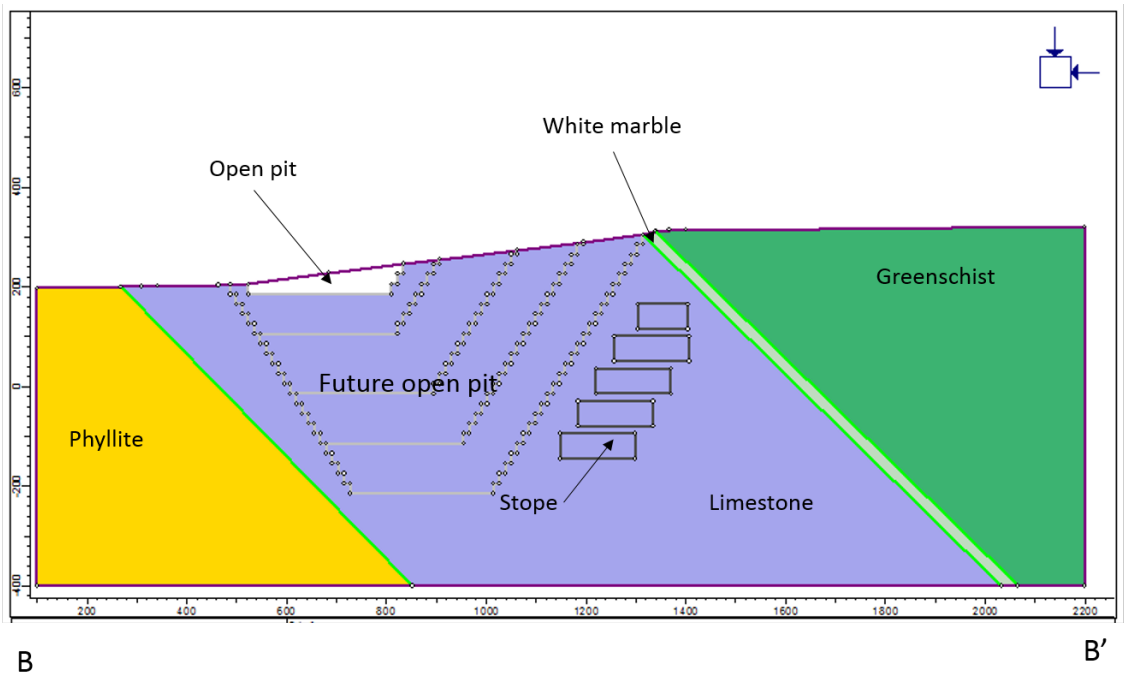

Figure 5.3.4 – Section B-B' through the mine. The current open pit is excavated (white). The possible future open pit is displayed in several excavation stages, these are assumed. The stopes are not excavated at this point. (Scale 1:8000)

Limitations to the model

- The water table and rock support is not implemented in the numerical analysis of the stopes and pillars. Nor are joints, due to the size of the model. Adding joints made the program crash.

- The rock boundaries are estimates based on the current existing borehole data. These are not sufficient to create an accurate model.

- This is a simplified model. Adits, drifts and ramps have not been considered in this model.

- The author experienced "beam" effect problems with cross-section B-B'. A two-dimensional model of the stopes looking at the longitudinal axis can be seen as a "beam" fixed at both ends and under self-gravity loading. The longer the "beam", the more this will deform at the middle. In three dimensions the stope walls would reduce this effect, especially for a rock of good quality (Trinh and Broch, 2008). Trinh and Broch (2008) suggests to simulate a cross-section perpendicular to the longitudinal axis (cross-section A-A' in this case) to find the maximum deformation in the roof, and then assign this value as a limit to the section looking at the longitudinal axis. This is also what the author has done for cross-section B-B'.

5.3.2 FLAC3D

FLAC3D is a numerical modelling code for advanced geotechnical analysis of soil, rock, and structural support in three dimensions. This program is used in analysis, testing, and design by geotechnical, civil and mining engineers. FLAC3D makes use of an explicit finite difference formulation that can model complex behaviours that normally might not be suited for FEM codes. This is typically problems that consist of several stages, large displacements and strains, non-linear material behaviour and unstable systems. Even cases of yield/failure over large areas or total collapse can be simulated (Itasca Consulting Group, Inc., An Itasca International Company, 2014). The advantage of three-dimensional analyses is that they provide clear indications of stress concentrations and of the influence of three-dimensional geometry. But, the definition of the input parameters and interpretation of the results of these models would stretch the capabilities of all but the most experienced modellers (Hoek, 2007).

5.3.3 Unwedge

Unwedge 3.0 is a simple 3D stability analysis and visualization program for underground excavations in hard rock that contains intersecting structural discontinuities. The program quickly calculates the safety factor for potentially unstable wedges, and rock support requirements can easily be implemented in the model (Rocscience, 2007).

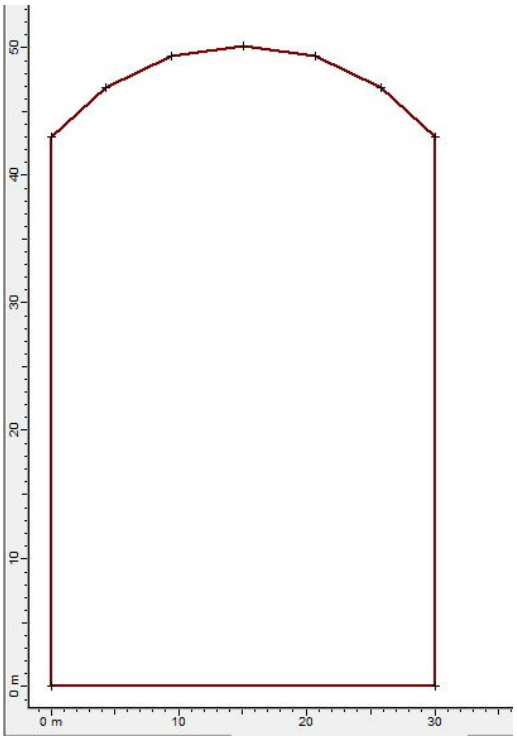

Figure 5.3.5 – Opening section from *Unwedge 3.0.*

In the wedge analysis for this thesis, the three most prominent joint orientations from Tromsdalen have been used when examining for possible wedge failures in the stopes. The stope cross-section is 30x50 m, see figure 5.3.5. Joint orientations originates from mapping conducted by the author during the fall of 2013, for further information about the mapping the reader is referred to the previous section (5.2 Surface mapping) and table 6.1.1 on page 73. The result is a vertical cross-section perpendicular to the axis of the stope. Standardised project settings have been used for the wedge computations, for further information the reader is recommended to visit the Rocscience webpage. The stopes are designed with rounded roofs based on simple rock mechanical principles regarding stability. Rectangular openings will have stress concentrations in the roof corners. For further readings on this topic see Hoek (2007).

The author has used a Factor of Safety of 1.5 for the wedge analysis. The Factor of Safety (FS) of a structure is commonly defined as $F = C/D$ and failure is assumed to occur when FS is less than 1. Where, C = Capacity of the element (strength or resisting force), and D = demand (stress or disturbing force) (Hoek et al., 1995).

Limitations

- Unwedge should be used to analyse wedge failure around excavations constructed in hard rock, where discontinuities are persistent, and where stress induced failure does not occur.
- It is assumed that displacements take place at the discontinuities, and that the wedges move as rigid bodies with no internal deformation or cracking.
- All of the discontinuity surfaces are assumed to be perfectly planar
- The underground excavation is assumed to have a constant cross section along its axis.(Rocscience, 2007)

5.3.4 GEOVIA Surpac™

GEOVIA Surpac™ is a mine planning software, supporting both open pit and underground operations. The software delivers powerful 3D graphics and workflow automation, and it has a comprehensive tool package including drillhole data management, geological modelling, block modelling, geostatistics, resource estimation and more. Surpac addresses the requirements of the geologist, surveyor and mining engineer, and the software is suitable for any commodity, orebody and mining method.

In this thesis, Surpac have been used for illustrational purposes. Index maps are created to show the geological model of the carbonate deposit, borehole locations, and general topography of Tromsdalen. Furthermore, a simple illustration of the underground mine layout is created with Surpac based on the results from both the empirical and analytical methods. The result is presented in section 6.2.5 on page 100.

Chapter 6

Results

6.1 Empirical Data

Data from surface mapping performed by the author during the fall of 2013 is presented in the tables below. The outcome of the laboratory work can be found in Chapter 3, table 3.2.1.

6.1.1 Discontinuites

The surface mapping resulted in 78 measured discontinuity orientations, revealing two distinct discontinuity sets. In table 6.1.1 below, the outcome of the empirical survey is summarized. The orientation of the joint is that of the most pronounced joint set at the site. For an index map of the locations the reader is referred to Appendix E, figure E.0.4.

Table 6.1.1 – Rock mass description of mapped joints in Tromsdalen (Pedersen, 2013).

Loc	**Type**	**Dip/dip dir**	**Infill**	**Aperture [mm]**	**Roughness**
1	Joint	88/050 NE	Soft mineral, paper like	0.1-0.25	rough
2	Joint	70/120 NE	Soil and other minerals	0.5-2.5	rough
4	Joint	78/333 NW	white mineral	< 4	rough
5	Joint	88/050 NE	Soft mineral, paper like	0.1-0.25	rough
6	Joint	20/050 NE	white + pink mineral *	< 4	rough
7	joint	54/250 SW	Soft mineral, paper like	< 4	rough
9	joint	40/326 NW	Soil and vegetation	10-100	rough

* White marble with pink manganese contamination, 3 cm infill.

Loc	Spacing [mm]	Persistence [m]	Water	Weathering	JRC	GSI
1	60-600	0-3	Dry	SW	16-18	60-70
2	200-600	1-3	Dry	SW	12-14	50-60
4	200-600	0-3	Dry	SW	12-14	50-60
5	60-600	0-3	Dry	SW	16-18	60-70
6	200-600	3-10	Dry	SW	14-16	45-60
7	200-600	0-3	Dry	SW	14-17	45-61
9	>2000-6000	3-10	Dry	SW	12-14	60-70

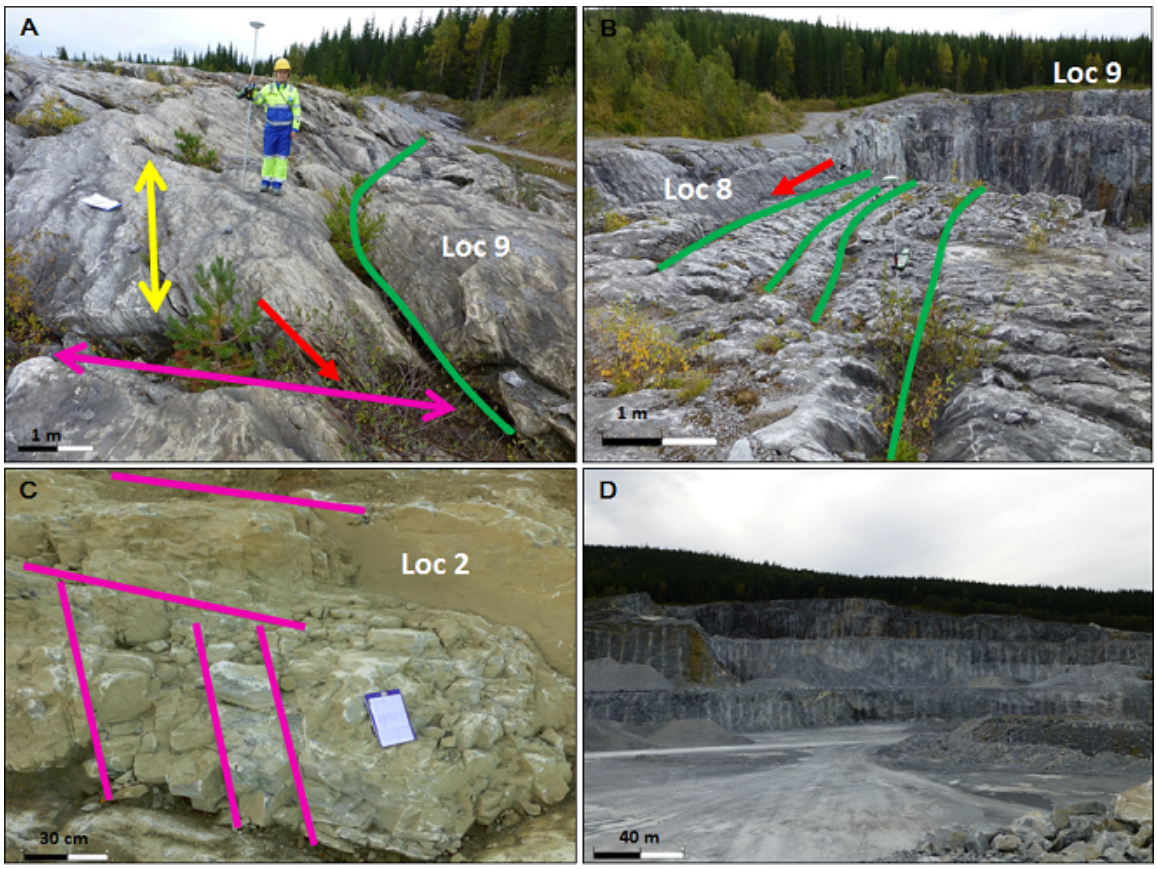

Figure 6.1.1 – Mapping of discontinuities. A: Field observations at location 9. The yellow arrow indicates the direction of the foliation, the green line illustrates how the foliation appears in the outcrop, the red arrow shows the dip of the deposit, and the purple arrow indicates the secondary joint system. B: Visible foliation at location 8. The green lines illustrate how the foliation appear in the outcrop, the red arrow shows the dip of the limestone deposit. C: Joint sets at location 2. The two main joint sets are indicated with purple, the smaller joints in between are caused by blasting. D: An overview photo of the open pit taken from location 10, looking from north to south (Photos: Author).

6.1.2 Q-system

Table 6.1.2 – Q-rating of Tromsdalen Limstone (Pedersen, 2013).

	RQD	**Jn**	**Jr**	**Ja**	**Jw**	**SRF**	**Q-value**	**Quality**	**RMR_Q**
Loc 1	84.6	6	3	1	1	2.5	16.92	Good	78
Loc 3	68.3	6	3	1	1	2.5	13.65	Good	68
Loc 4	64.7	6	3	1	1	1	32.35	Good	75
Loc 5	64.4	6	3	1	1	1	32.22	Good	75
Loc 6	58.4	6	3	6	1	1	4.87	Fair	58
Loc 7	58.9	6	3	2	1	1	14.72	Good	68
Mean	66.6	6	3	2	1	1.5	19.1	Good	69

6.1.3 RMR

Table 6.1.3 – Rock Mass Rating of Tromsdalen Limstone (Pedersen, 2013).

	Strength	**RQD**	**Spacing of discontinuities**	**Condition of discontinuities**	**Groundwater**	**RMR_{89}**	**GSI_{RMR}**
Loc 1	8	17	19	18	10	64	59
Loc 3	8	13	20	19	10	59	54
Loc 4	8	13	19	18	10	58	53
Loc 5	8	13	19	18	10	60	55
Loc 6	8	13	15	14	10	54	49
Loc 7	8	13	8	21	10	60	55
Mean	8	13.7	8.7	18.8	10	59.2	54.2

6.1.4 Design Parameters

The design parameters found in table 6.1.4 are determined based on experiences from other underground mines in Norway, see section 4.3.6, criteria from Verdalskalk AS (see section 2.6), and suggestions made by the author. The subsequent sections give supplementary information.

Table 6.1.4 – Suggested design parameters.

Design	Dimension
Top slice	30x10m
Drifts	10.6x10m (min road width x height)
Stope length	100 -150 m
Stope width	30 m
Stope height	50 m (total, including top slice)
Crown pillar	15 m
Distance from stope to access point	50 m
Overburden	50 m (minimum)
Rib pillar (vertical)	15 m
Adit, drift inclination	1:12 m (1:10) (1:7)
Ramp inclination	1:12 m (1:10)
Stope inclination	1:100 m (1:80)
Turning radius, min	11.75 m

6.1.5 Suggested Stope Layout

In this section the author presents some possible stope layouts for the future underground mine in Tromsdalen. The open pit wall is illustrated with adits and transportation levels (load and haul) to show how the stope is accessed from the open pit. Nonetheless, in reality, the adit will be connected to drifts and ramps much like the illustration in figure 4.3.9.

6.1.5.1 Method 1

Method 1 illustrated in figure 6.1.2 requires only one drilling drift, the top slice. The stope is drilled with conventional bench drilling, vertical boreholes, and the blasted ore is loaded from a sublevel. Before drilling and blasting can commence, an opening slot needs to be made in the correct end of the stope to allow for the blasted rock to expand. Bench I is drilled and blasted first, and the bench floor created from this blasting will be the drilling level for the second bench. An opening slot is drilled in the other end of the stope, and loading takes place from the bottom of the stope. In figure 6.1.3 the mining direction of the stope is illustrated together with the order of the development (numbering).

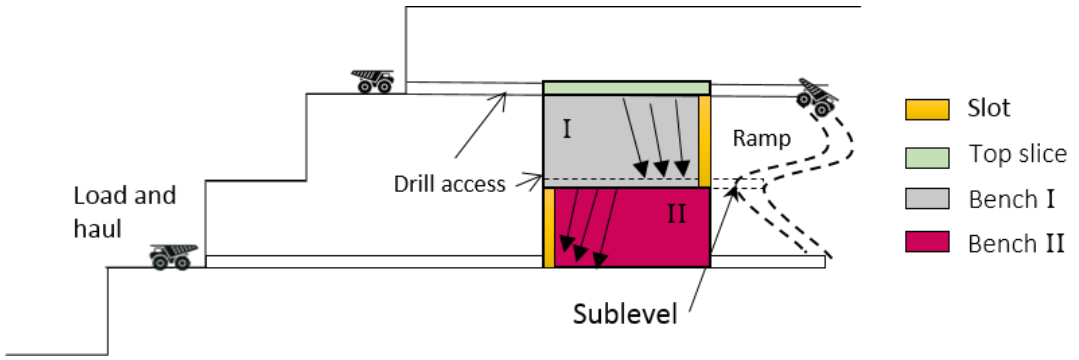

Figure 6.1.2 – Method 1, stope layout.

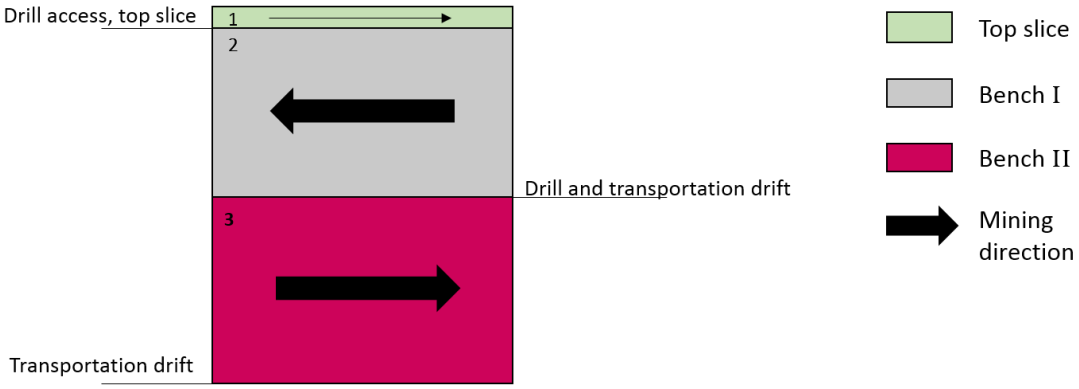

Figure 6.1.3 – Stope excavation.

Another option for method 1 is to use longhole drilling. In this case, the full height of the stope is drilled from a top slice. The opening slot is only needed on one side of the stope, and the blasted ore is loaded from the bottom of the stope. In order to ease the loading and minimize wear on the equipment, a transportation drift can be made in the bottom of the stope.

6.1.5.2 Method 2

Method 2 illustrated in figure 6.1.4 requires three drifts; a top slice, a drilling and transportation drift mid stope, and a transportation drift in the bottom level of the stope. Bench I is drilled vertically down to the drilling drift mid stope, blasted and then loaded from the sublevel. The next bench is drilled vertically down from the drift mid stope and to the bottom drift. Loading of Bench II takes place on the lower drift. Furthermore, opening slots are required in the same manner as for method 1. The stope illustration in figure 6.1.5 shows the mining direction and the development order for drifts and benches.

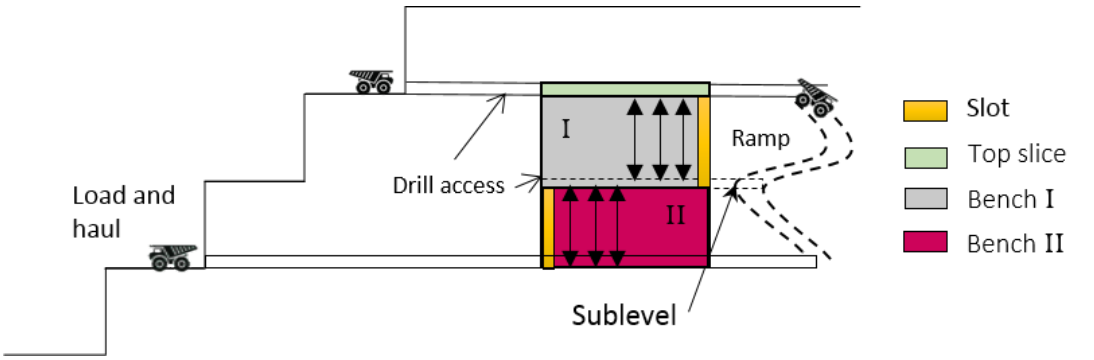

Figure 6.1.4 – Method 2, stope layout.

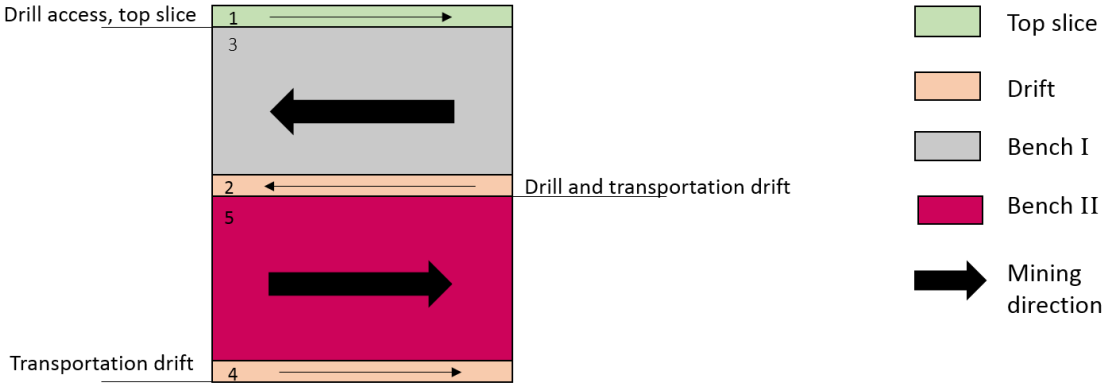

Figure 6.1.5 – Stope excavation

A second possibility exists for method 2 that requires one less drilling drift, and vertical upward holes. Bench I will be drilled from the top slice (downwards), and bench II will be drilled from the lower drift and upwards, hence arrows both ways in the figure (6.1.4).

6.1.5.3 Method 3

Method 3 is illustrated in figure 6.1.6. This excavation type requires only one drilling drift, and the two benches are blasted almost simultaneously. Mining of the lower bench has to be slightly ahead of the upper bench in order for the blasted ore to have somewhere to fall/expand, illustrated with the blue line in the figure. From the drilling drift, bench II is drilled upwards and bench I is drilled downwards. Only one opening slot is required for the stope, and one loading access. In figure 6.1.7 the stope layout is presented with arrows indicating the mining direction.

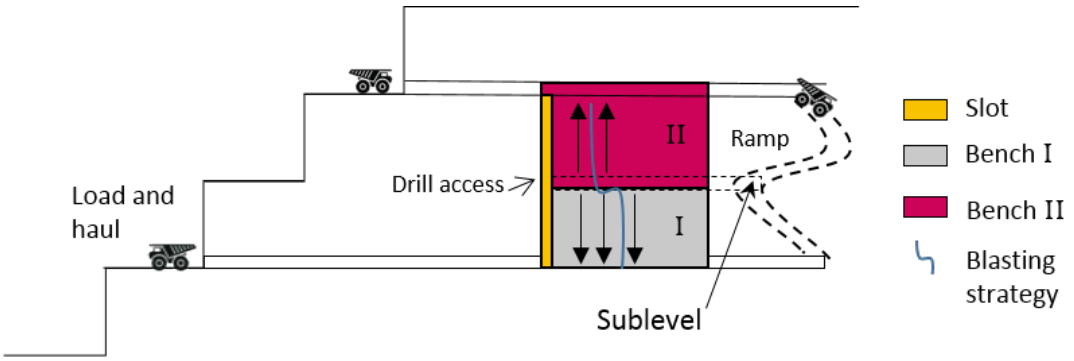

Figure 6.1.6 – Method 3, stope layout.

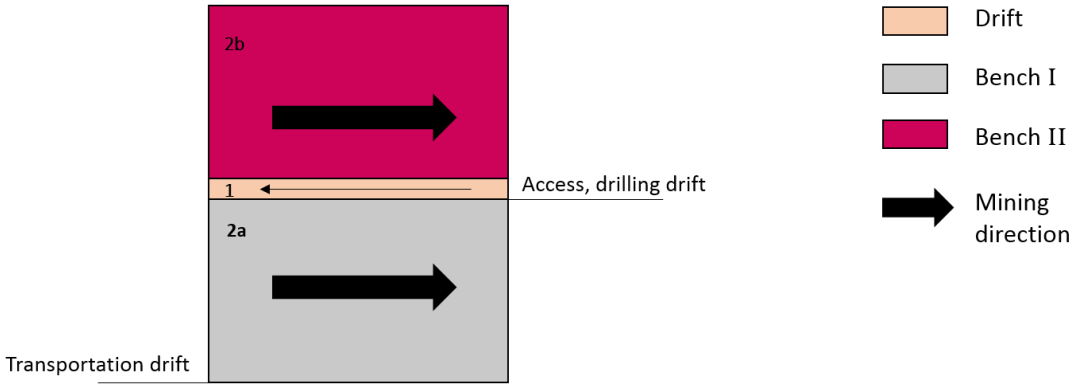

Figure 6.1.7 – Stope excavation.

Automated loading is recommended for safety reasons in all three illustrated examples.

6.1.6 Road Dimensions and Turning Radius

In an attempt to recommend the road width for the mine infrastructure, equations 4.3.1 and 4.3.2 in section 4.3.3 have been used, together with experiences from underground mines in Norway. A suggestion for the turning radius for a one-lane road-curve is displayed in figure 6.1.8. Table 6.1.5 below lists some estimated road widths.

Table 6.1.5 – Suggestions for road dimensions.

	One-lane Road		Two-lane Road	
	Straight	Curved	Straight	Curved
Width	10.6 m	12.9 m	18.6 m	21.7 m

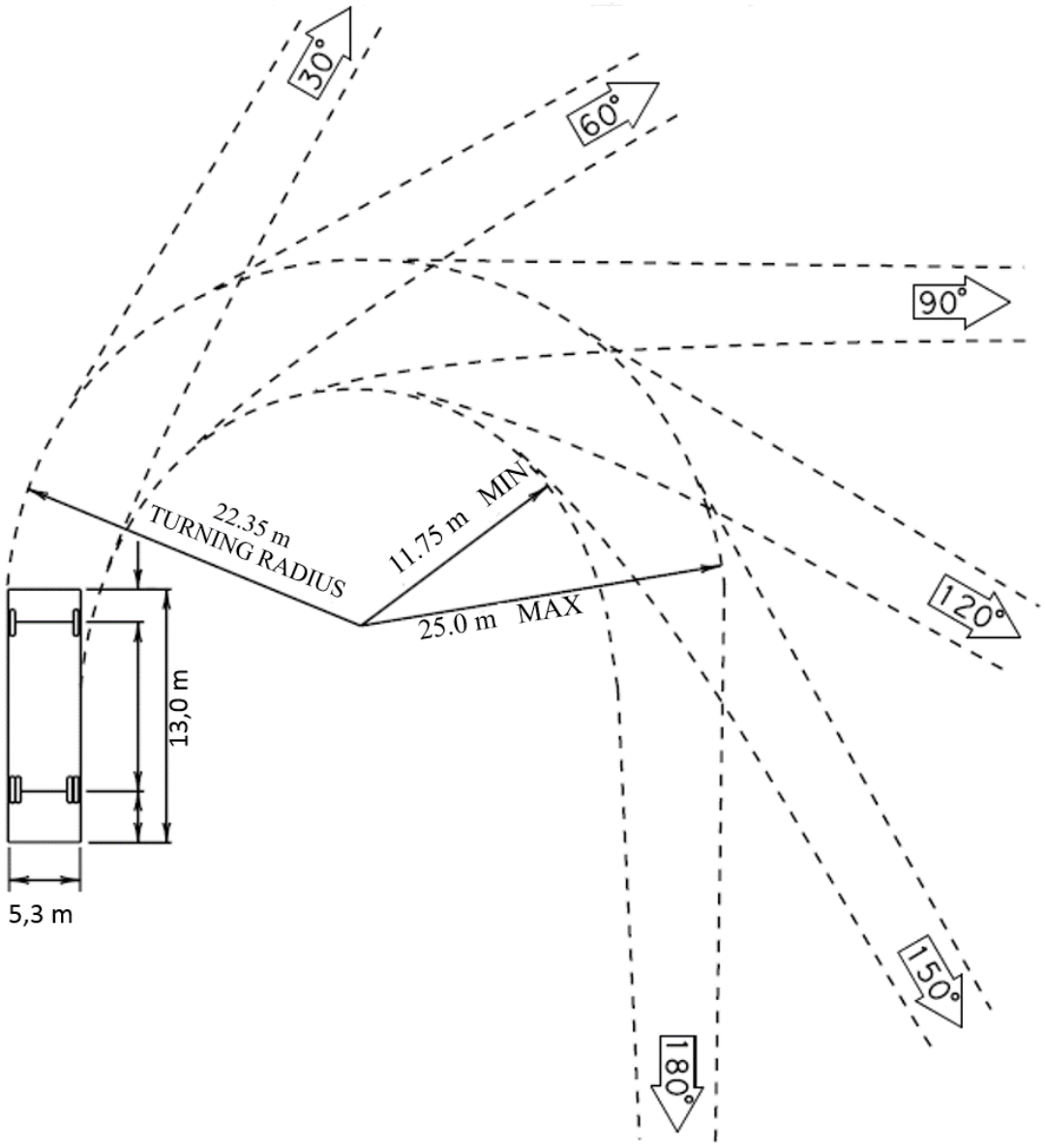

Figure 6.1.8 – Turning radius based on the largest equipment currently operating in the open pit mine. Note, not to scale. Modified after Mark and Marek (2013).

6.1.7 Ventilation

Figure 6.1.9 is a schematic of a possible ventilation solution in Tromsdalen.

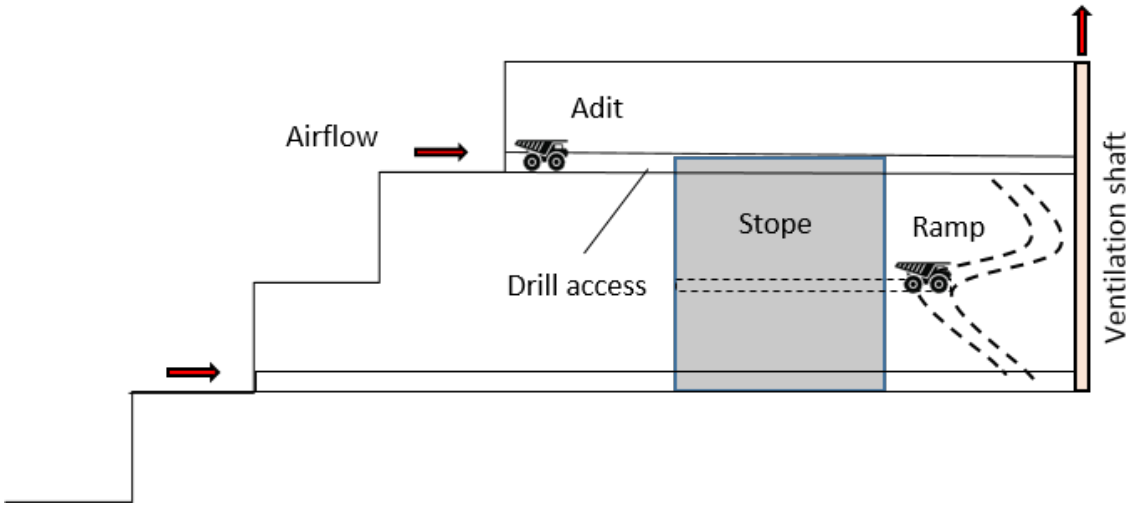

Figure 6.1.9 – Main access and mine ventilation. The adit represents the main access to the deposit and the main intake of air to the mine. The ventilation shaft functions as an exhaust vent. Vertical section.

6.2 Analytical Models

In the following subsections, the reader will find the results from the stope and pillar analysis, the stope orientation in relation to the open pit and a small wedge analysis of possible wedge failure due to the joint orientations.

For input parameters in the numerical analysis: see table 5.3.1 on page 67 and table 6.1.4 on page 76. The design dimensions used in the $Phase^2$ models are illustrated in figures 6.2.1 and 6.2.2 on the following page.

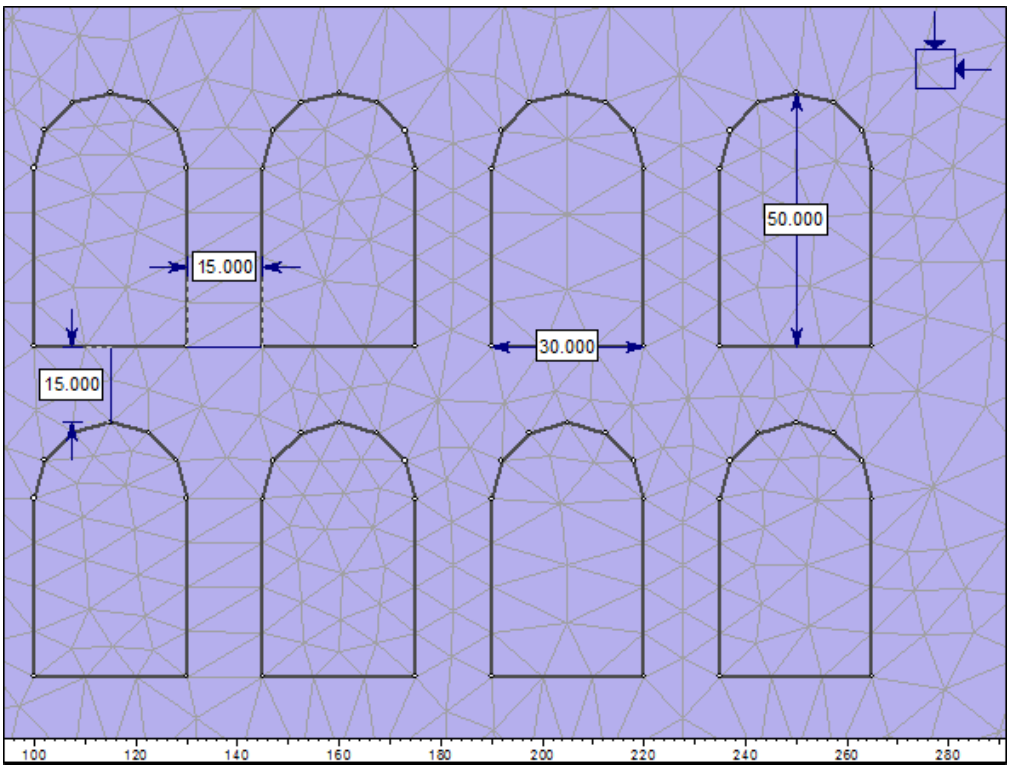

Figure 6.2.1 – Dimensions of cross-section A-A'.

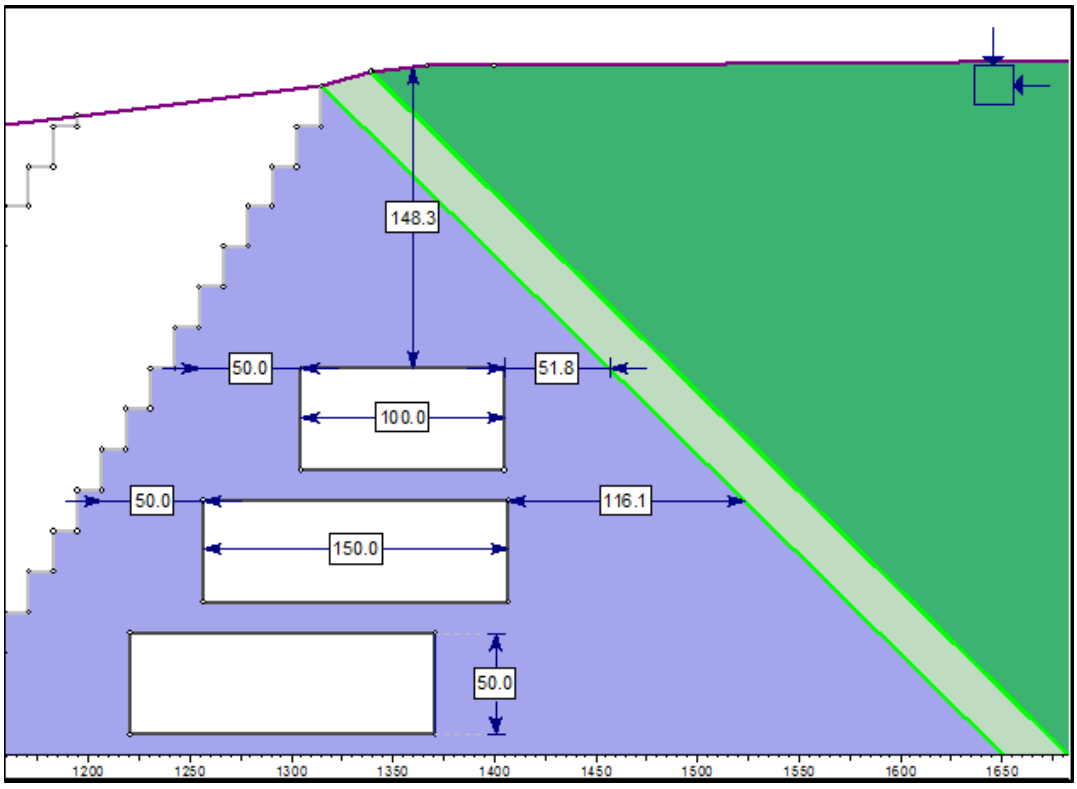

Figure 6.2.2 – dimensions of cross-section B-B'.

6.2.1 Cross-Section A-A'

Sigma 1

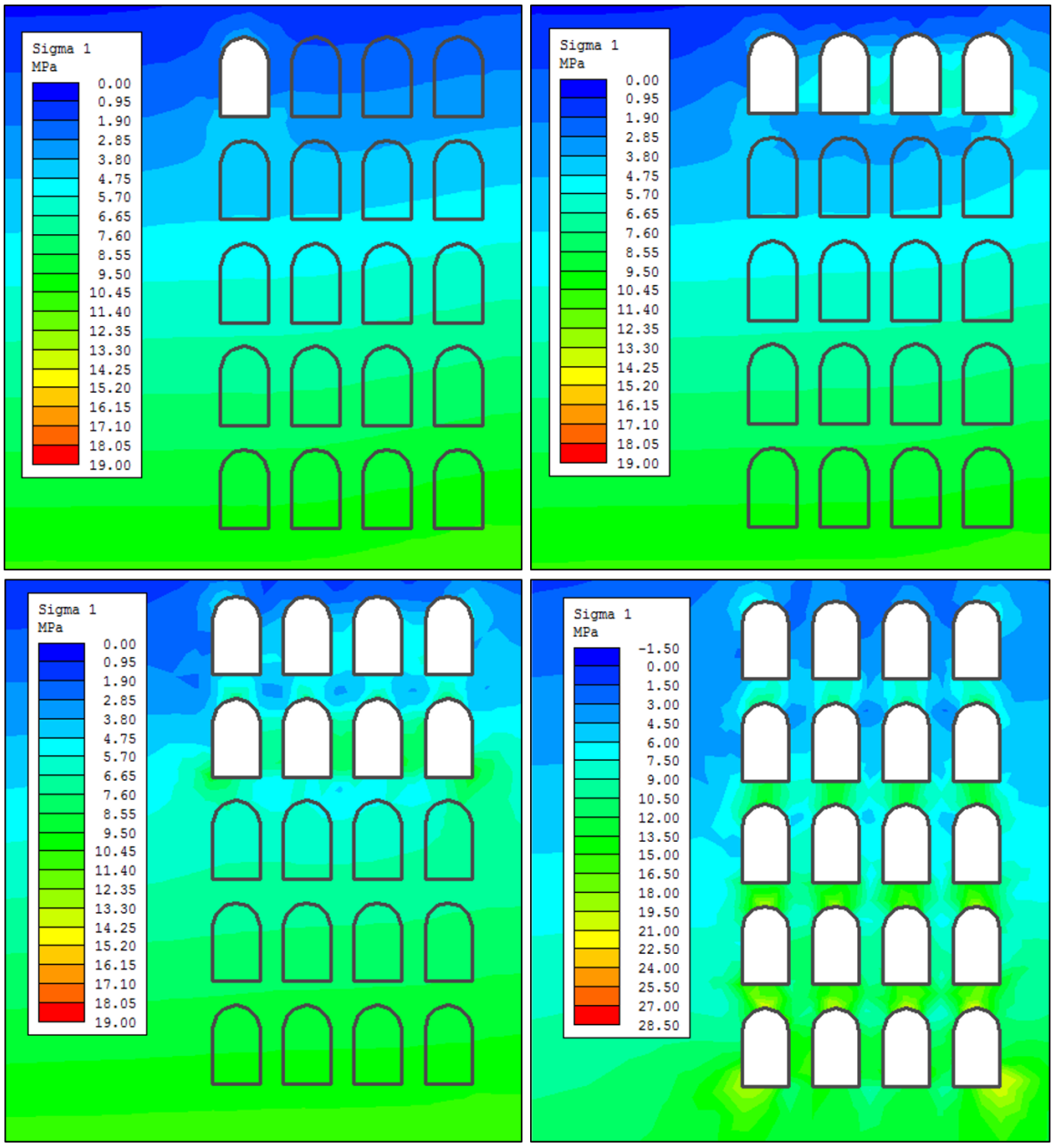

Figure 6.2.3 – Stress distribution of σ_1 after stope excavation.

From figure 6.2.3 it is evident that there are stress concentrations directly above and below the excavated stopes, as well as a stress concentration in the corner points for the lowermost stopes, see also figure 6.2.6 on page 85. Sigma 1 is generally higher in the crown pillars then in the rib pillars. For further illustrations see figures in Appendix C.3 on page 148.

Stress Trajectories

It is evident from the stress trajectories in figures 6.2.5, 6.2.6 and 6.2.7 that there is only vertical stress in the rib pillars and mostly horizontal stress in the crown pillars. The pillar stress is increasing with the increasing depth. The figures further illustrates how the stress is redistributed around the excavated openings. For comparison, a close-up of an unexcavated stope is illustrated in figure 6.2.4.

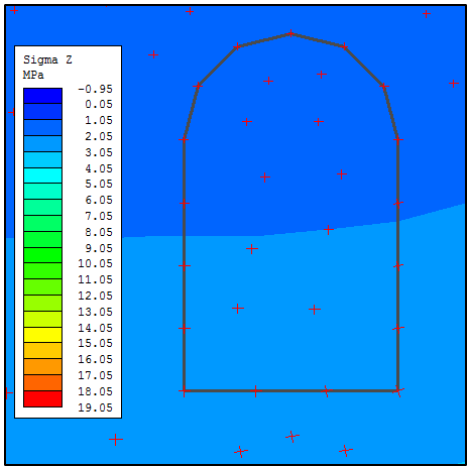

Figure 6.2.4 – Stress trajectories around the first stope on level one, before excavation.

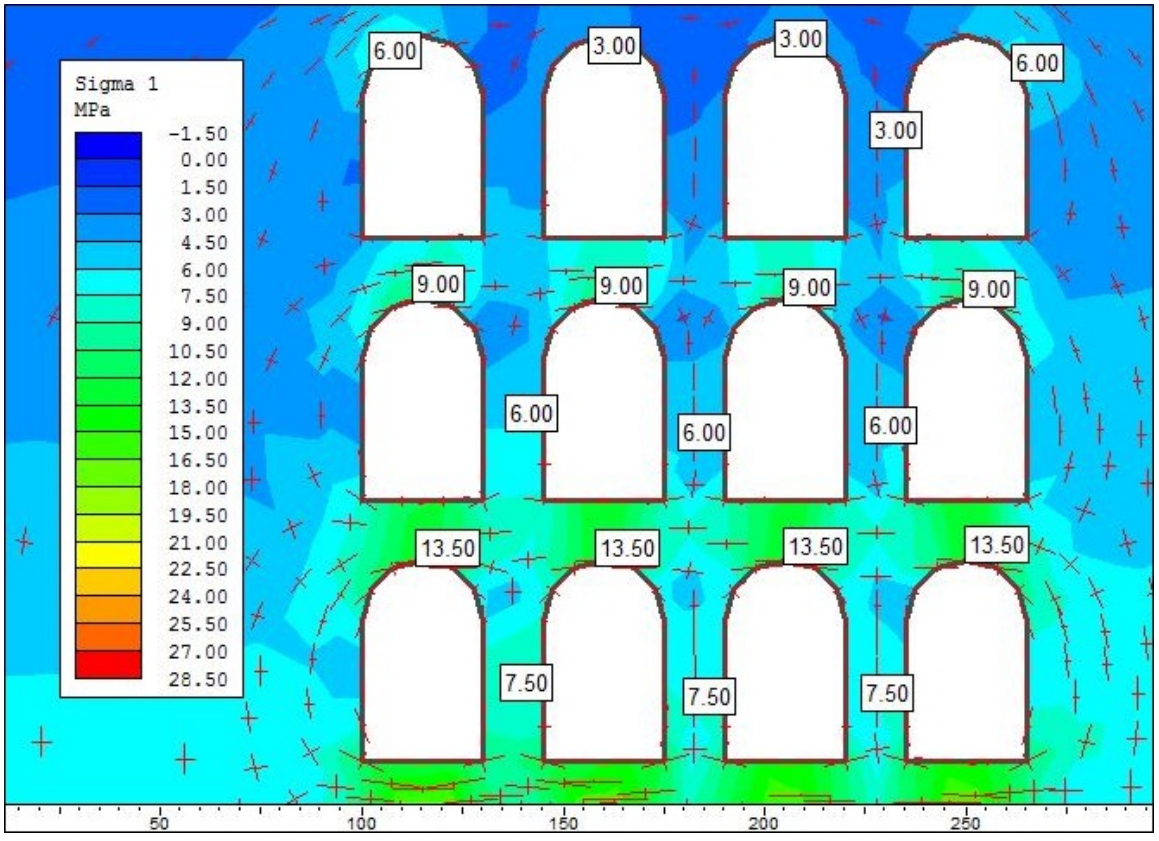

Figure 6.2.5 – Stress trajectories, levels 1,2 and 3. The labelled contours gives the stress value for that particular area.

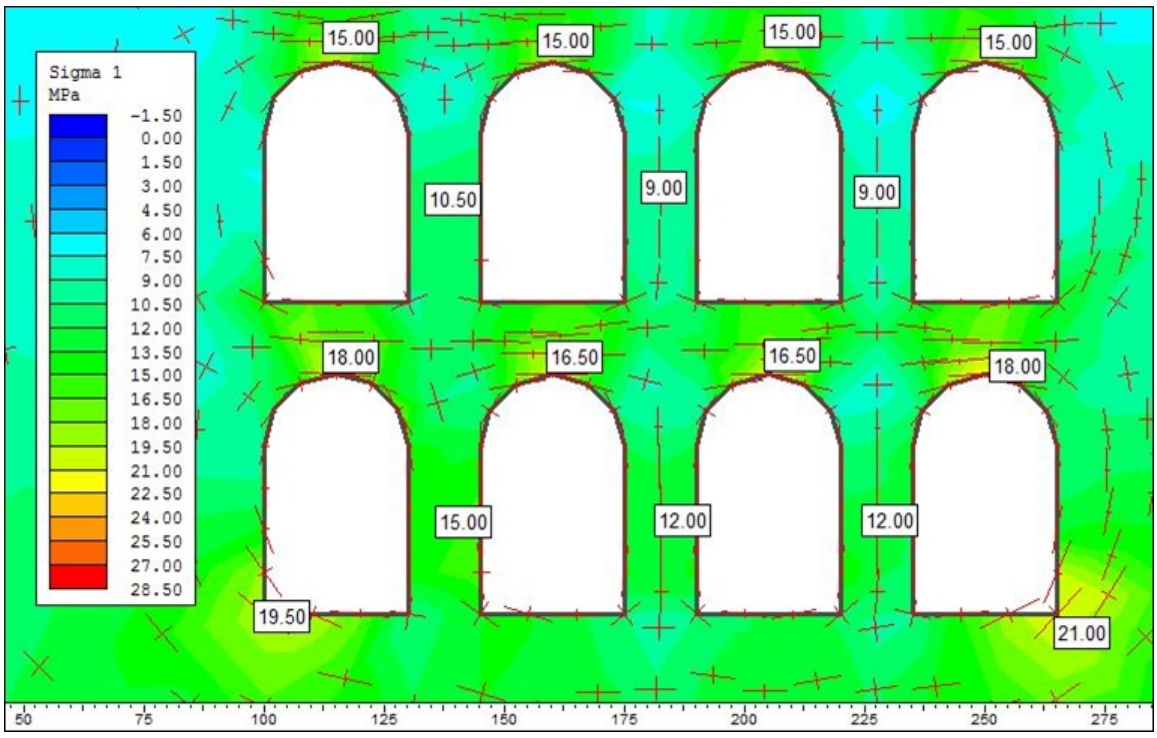

Figure 6.2.6 – Stress trajectories, levels 4 and 5. The labelled contours gives the stress value for that particular area.

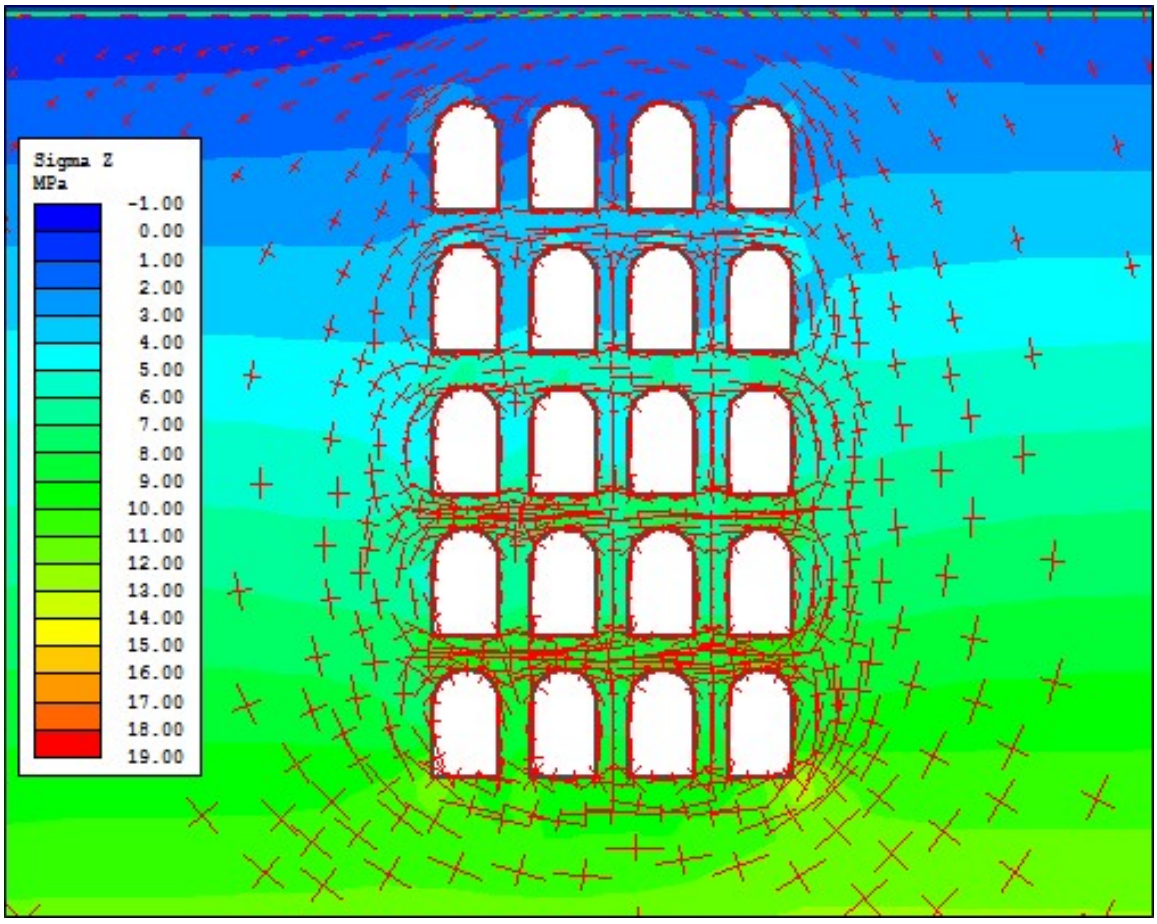

Figure 6.2.7 – Stress trajectories around all stopes overlaid sigma Z (σ_z).

Sigma 3

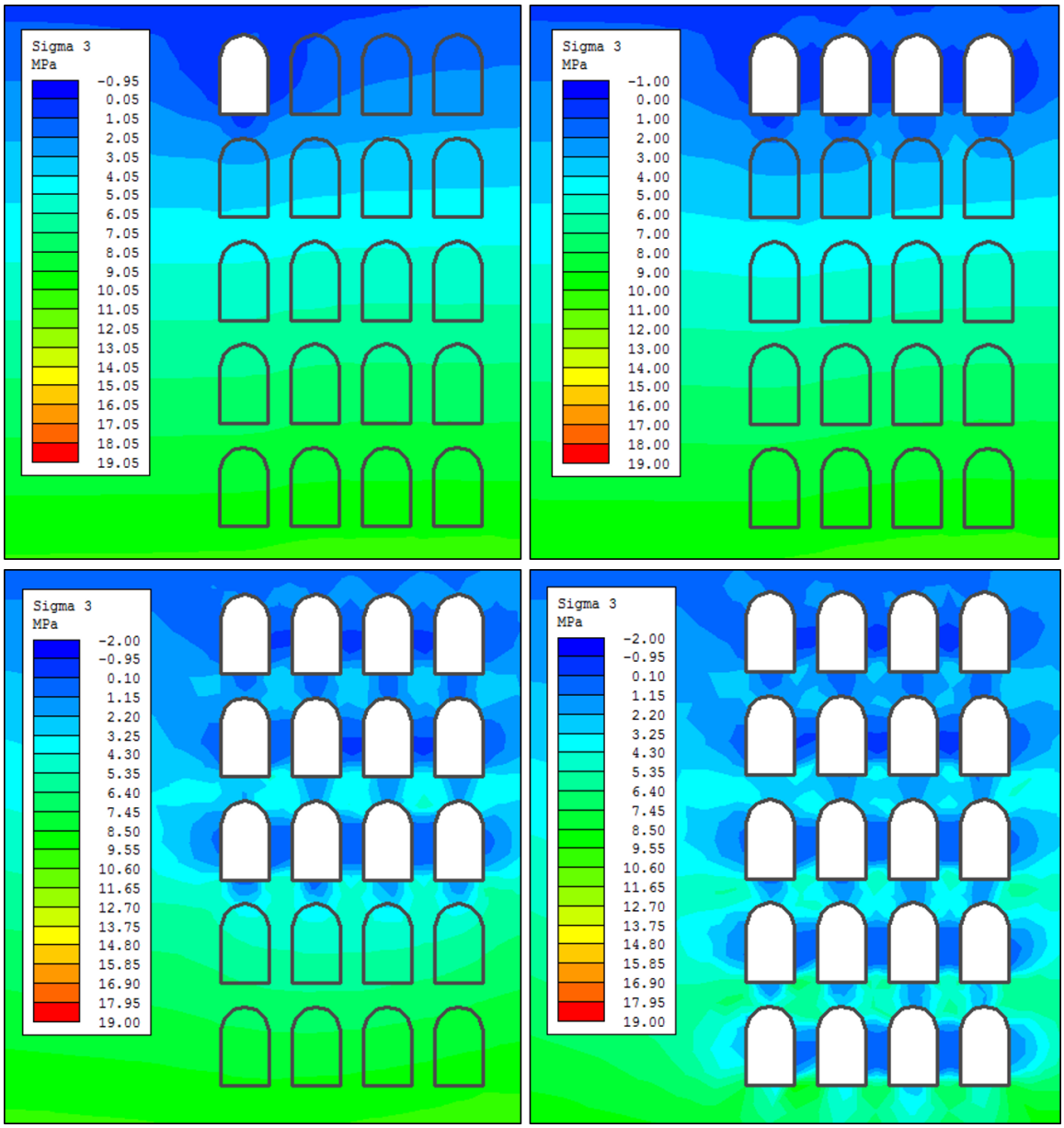

Figure 6.2.8 – Stress distribution of σ_3 after stope excavation.

Figure 6.2.8 illustrates the stress distribution of sigma 3 after stope excavation. The primary stope, and stope levels one, three and five are shown in this figure. For illustrations of the other stope levels see figure C.3.4 on page 149. It is evident from the illustrations that the minor principal stress (sigma 3) is decreasing in the rib pillars as the excavation propagates. The stress distribution before the stope excavation is shown in figure C.3.3 on page 149.

Yielded Solid Elements

Figures 6.2.9 and 6.2.10 demonstrates the yielded solid elements in the model, overlaid the sigma 3 stress distribution. The first stope level does hardly have any failed elements. In the second level there is both shear and tension failure of the rib pillars to the right. For all the other stope levels there is failure in all rib pillars. There is also evidence of failure in the crown pillars between levels one and two, levels three and four, and levels four and five. A segment showing all the failed elements in the stopes can be found in figure C.3.5 on page 150.

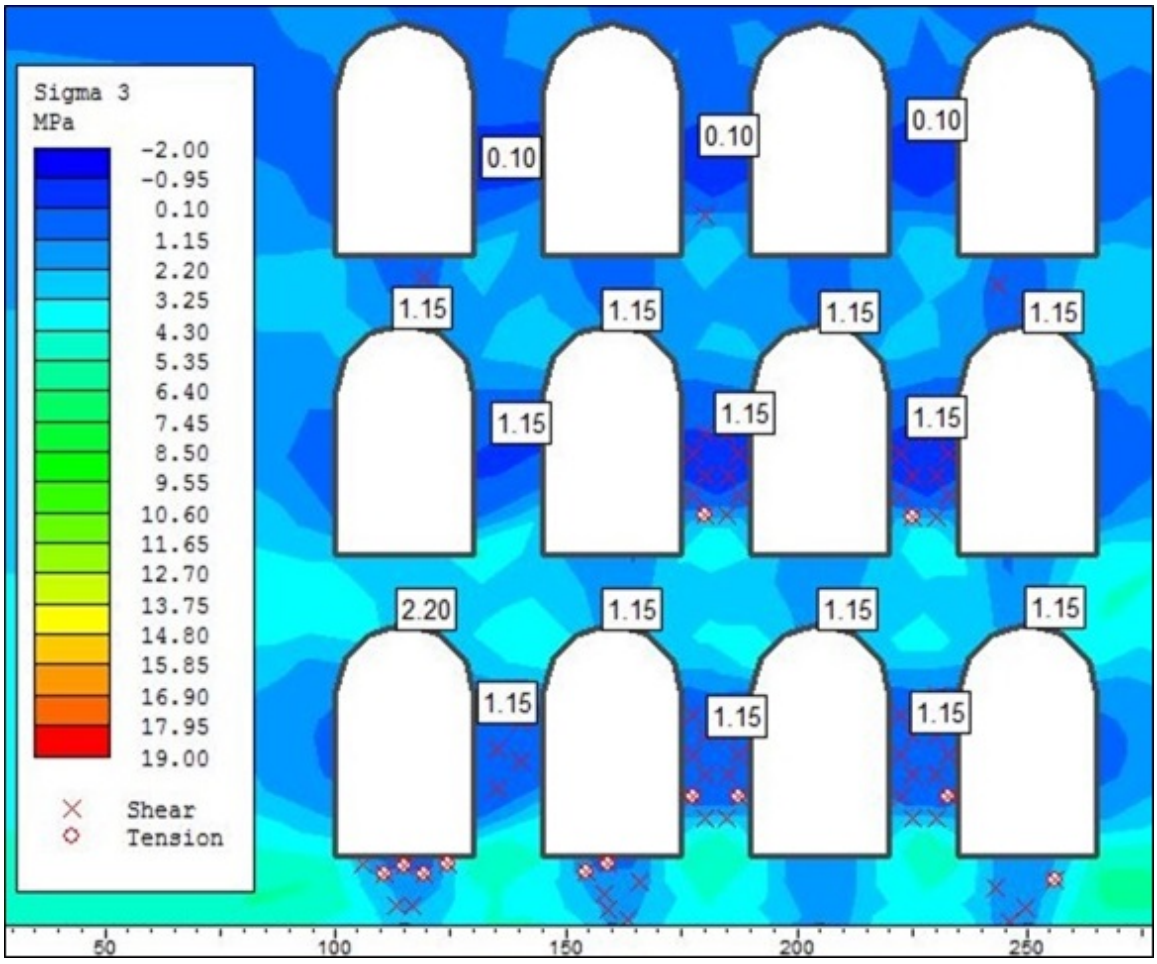

Figure 6.2.9 – Yielded solid elements, levels 1, 2 and 3.

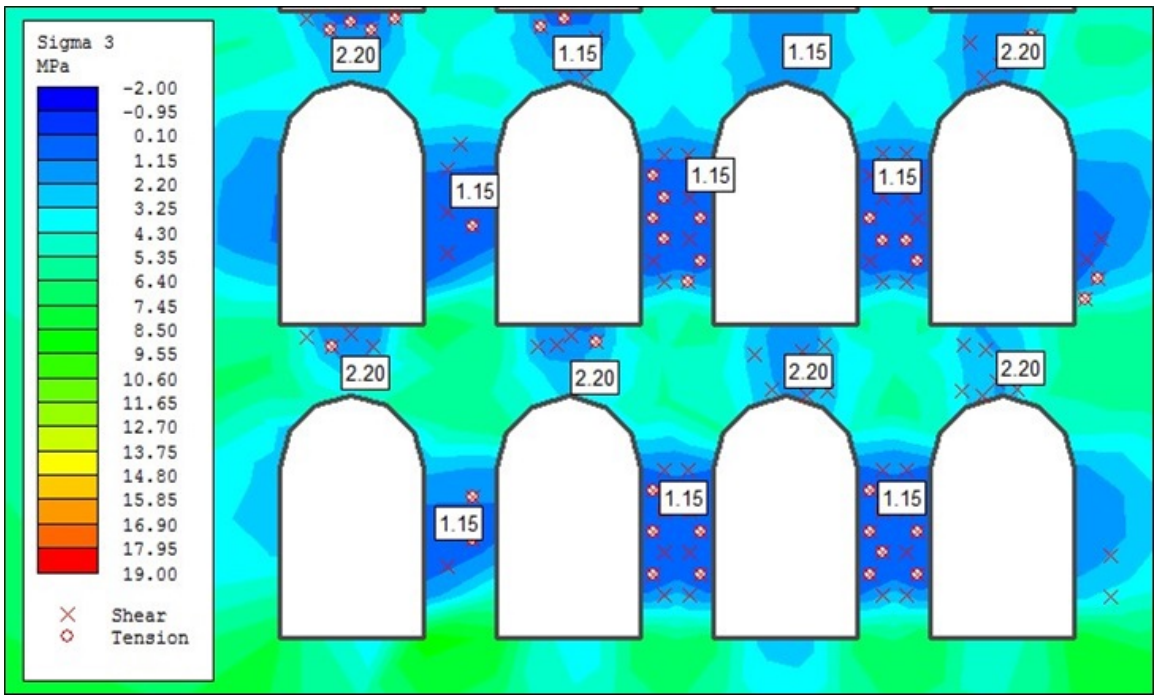

Figure 6.2.10 – Yielded solid elements, levels 4 and 5.

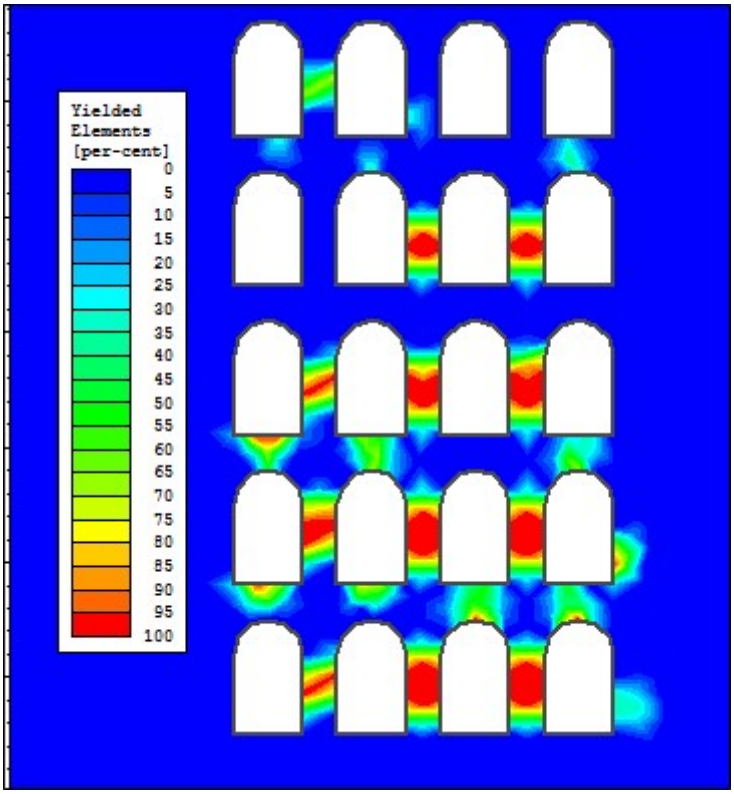

Figure 6.2.11 – Yielded elements, percent of failure.

Figure 6.2.11 illustrates the percent of failure of the rock elements in the model. From this figure it is evident that all rib pillars from level three and down have 100%

failure. The crown pillars between levels three and four, and levels four and five is in a worse state than the rest of the crown pillars.

Displacements

Figure 6.2.12 illustrates the total displacement within the rock mass after the stopes are excavated. Not all levels of excavation are illustrated, but the main trend is evident. For further illustrations see figure C.3.6 on page 150. The highest displacements are found in the outer edges of the stopes. The displacements increase successively with the depth and the maximum displacement is 0.032 meter.

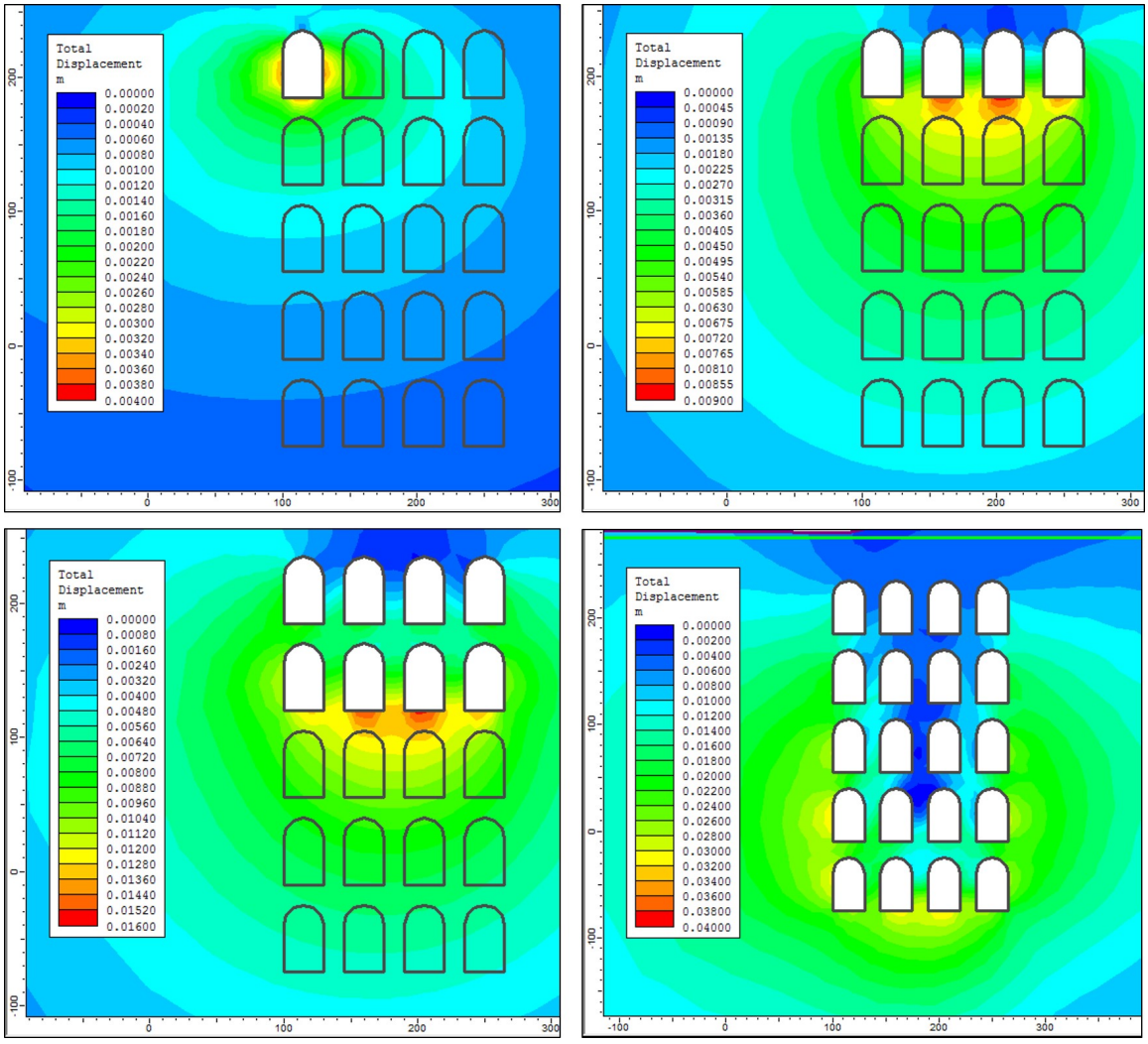

Figure 6.2.12 – Toal displacement in stopes after excavation.

6.2.2 Cross-Section B-B'

Sigma 1

From the illustrations in figure 6.2.13 it is evident that the major principal stress increases in both ends of the stope as soon as they are opened. However, when the next stope level is excavated, the stress is reduced in the same area. Towards the open pit wall the stress approaches zero, meanwhile in the back of the stope (towards the white marble) the stress only decrease slightly.

For supplementary illustrations on the stress distribution, the reader is referred to the figures in Appendix C.3.1 on page 151.

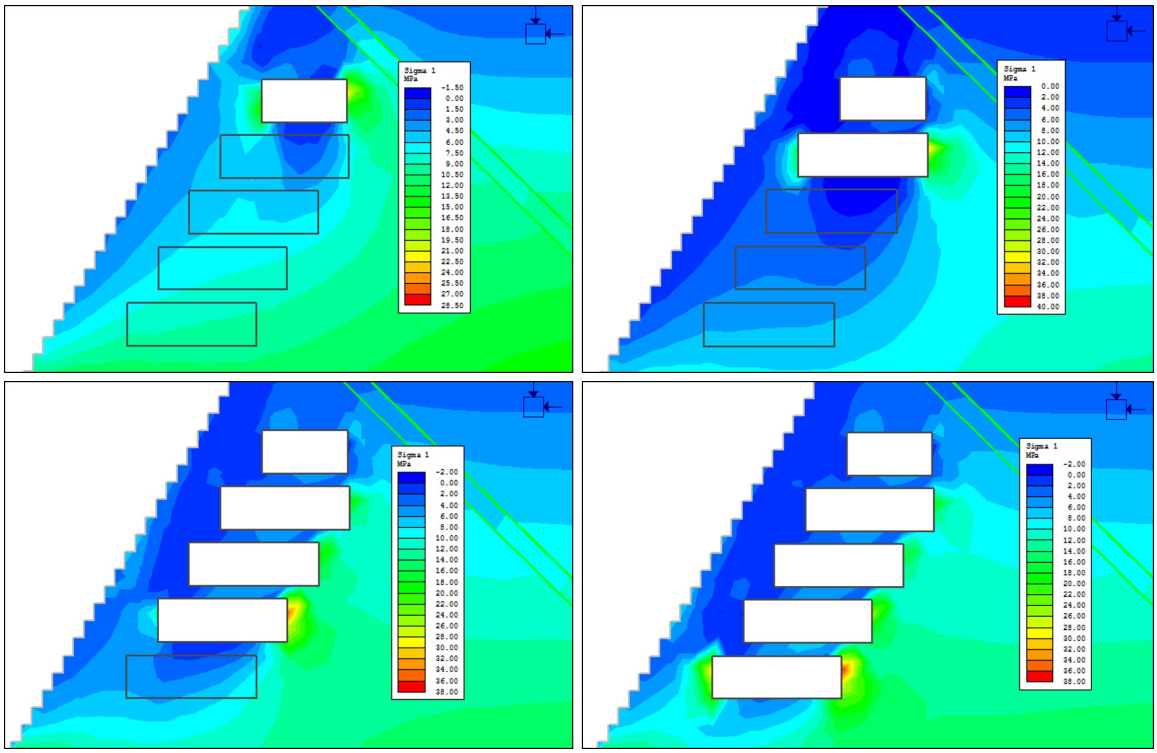

Figure 6.2.13 – Stress distribution - sigma 1.

Stress Trajectories

The stress trajectories indicate that there are only horizontal stresses in the crown pillars. Close to the open pit wall, the horizontal stress is released and there is mostly vertical stress in this area, see figure 6.2.14. The section presented in figure 6.2.15 is a close-up of stope level 5. It is obvious that the stresses are redistributed and follows the contours of the excavated opening.

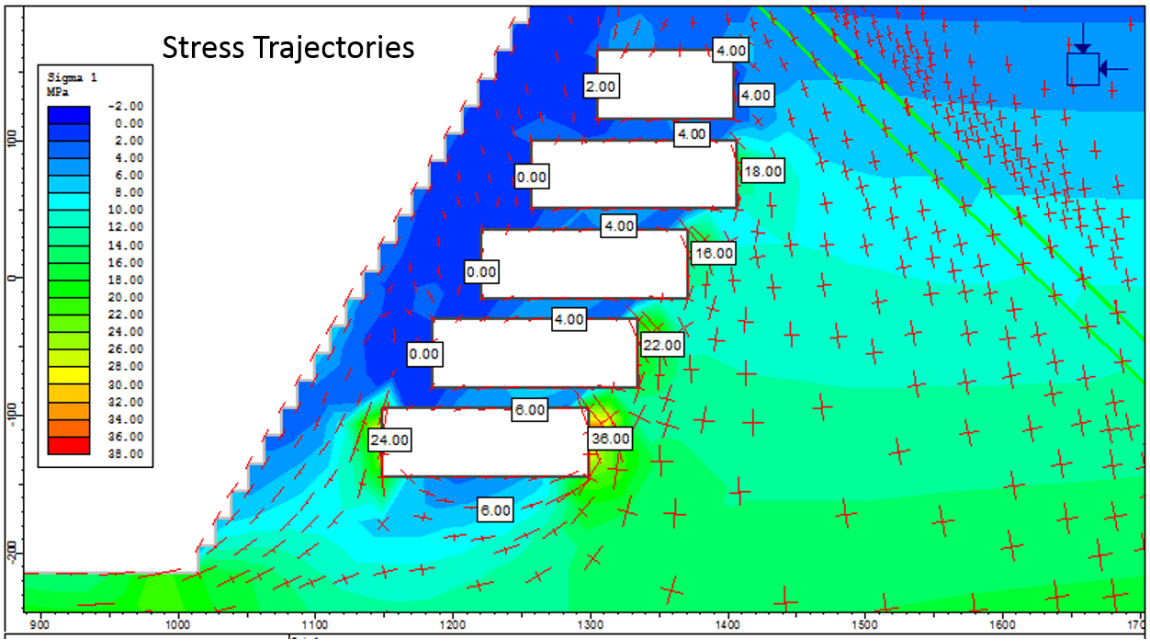

Figure 6.2.14 – Stress trajectories - all stope levels are excavated.

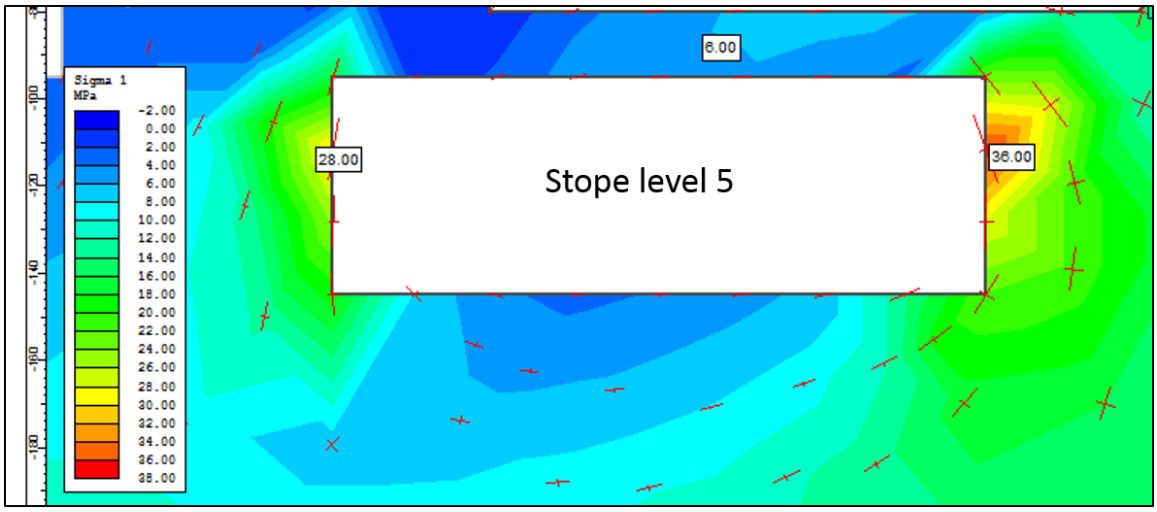

Figure 6.2.15 – Stress trajectories, a close-up of stope level five.

In figure 6.2.16 the stresses seem to follow the contours of the large open pit boundary. However, around the two excavated stopes the stresses appear to follow the stope

boundary. A supplementary illustration is found on page 152.

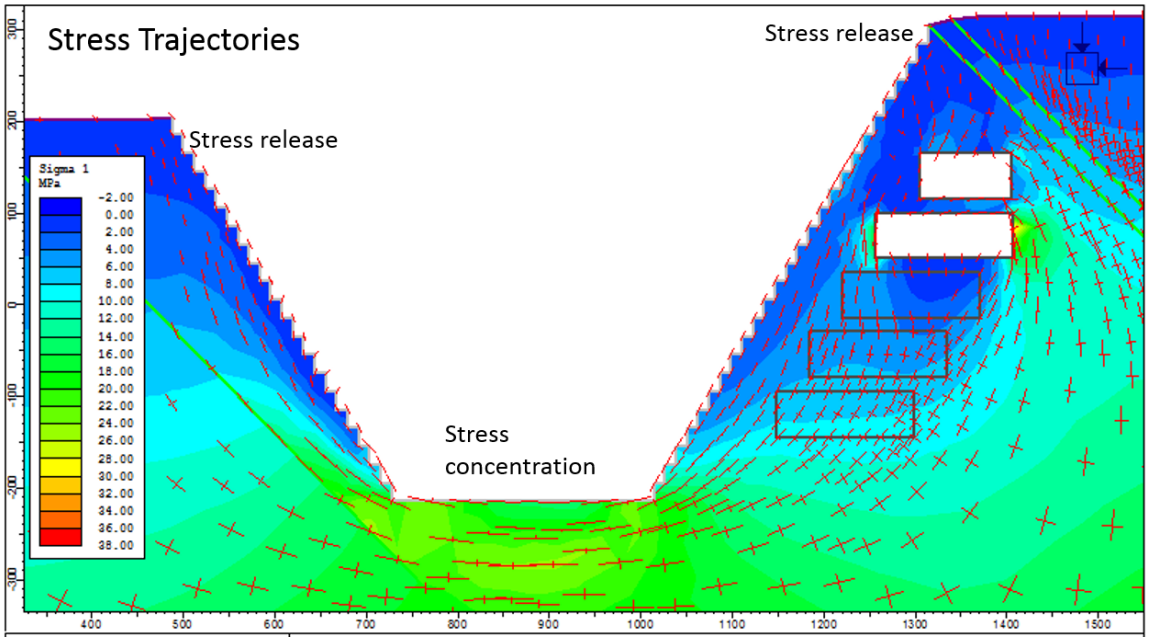

Figure 6.2.16 – Stress trajectories - open pit and stopes. Stope levels one and two are excavated.

Sigma 3

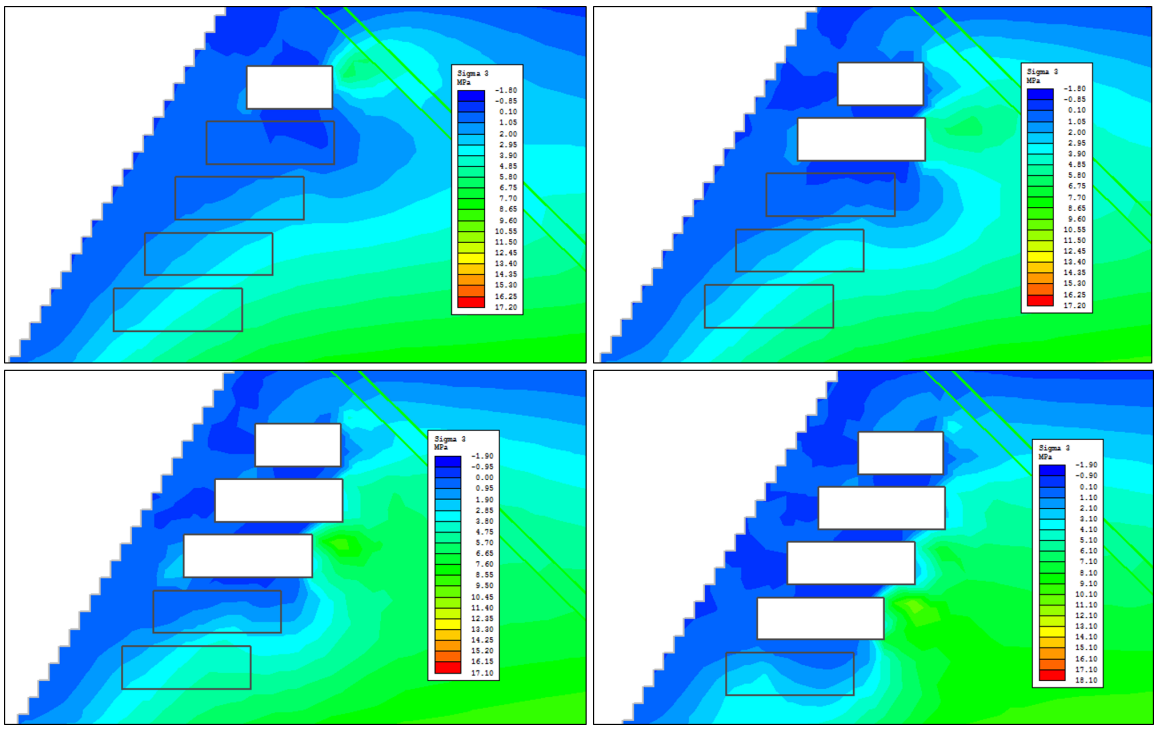

Figure 6.2.17 – Stress distribution - sigma 3

The minor principal stress appears to decrease with the propagating stope excavation both in the crown pillars and in front of the stopes (towards the open pit wall), see figure 6.2.17 on the preceding page. Similar to the major principal stress there is an increase in the stress field in the back of the stopes immediately after excavation. This phenomenon is shifted downwards with the excavation.

For illustrations of the full model with the open pit excavations, see Appendix C.3.1 on page 153.

Yielded Elements

From figure 6.2.18 it is clear that there are yielded elements between all stopes and along the entire open pit wall, in front of the stopes. There is both shear and tension failure. Figure C.3.14 on page 154 displays shear failure in the bottom of the large open pit. There is also a zone of both shear and tension failure in the top right of the model, in the area above the stopes.

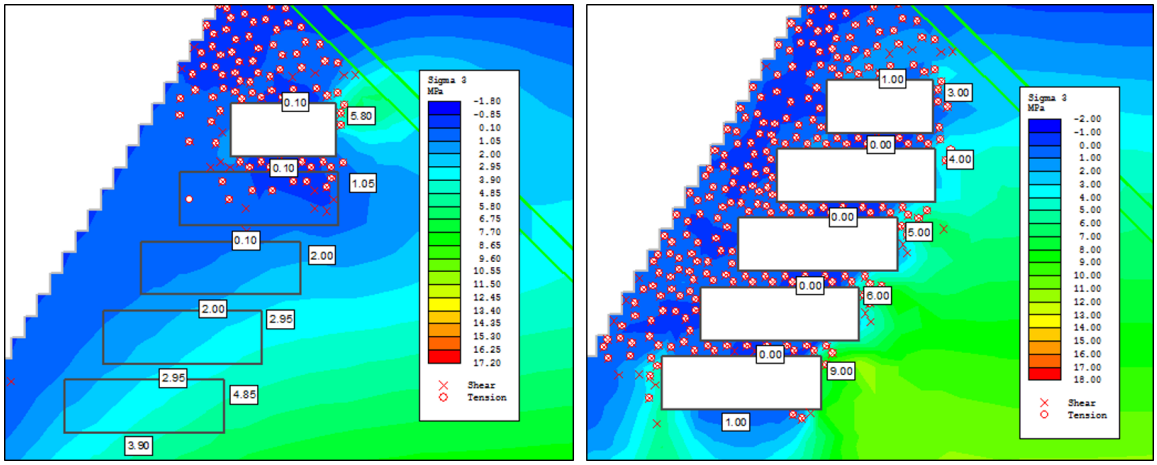

Figure 6.2.18 – Yielded solid elements, stope excavation.

Figure 6.2.19 on the following page illustrates the yielded elements in percent of failure. From this figure it appears that the entire open pit wall on the south side has a 100% collapse. The bottom of the open pit also has 100% failure.

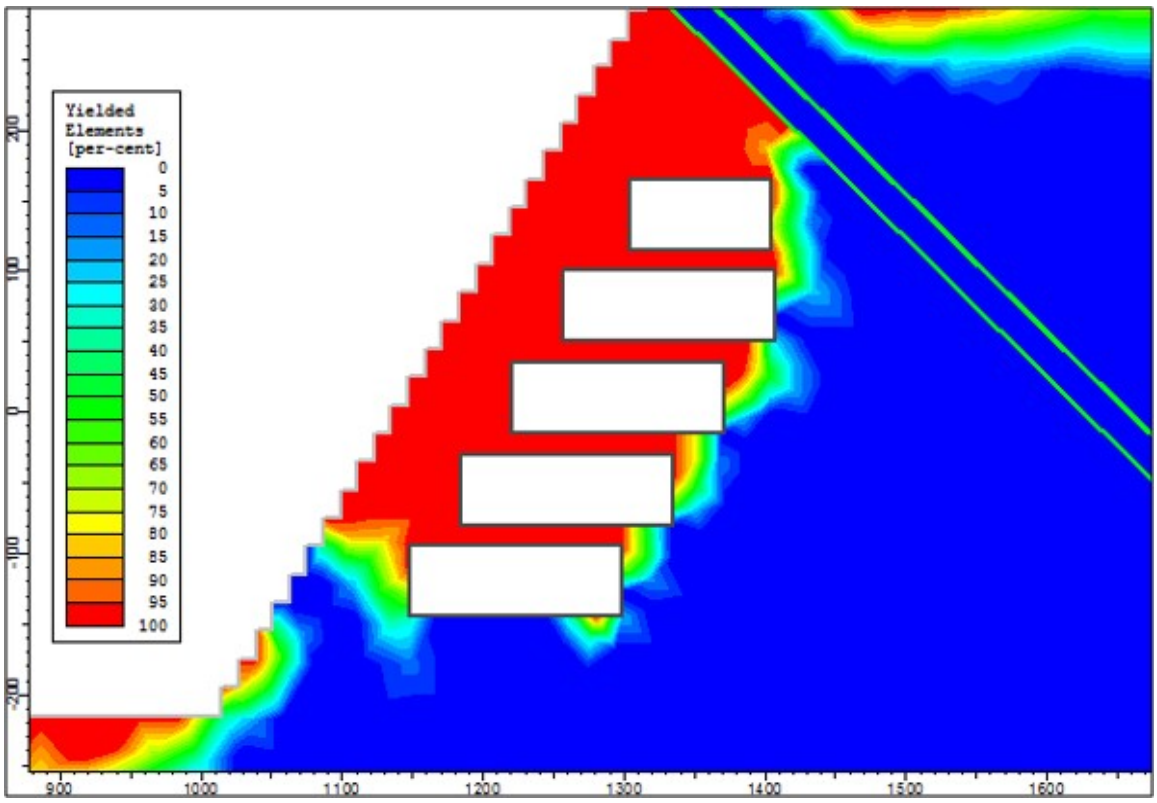

Figure 6.2.19 – Yielded elements - percent of failure.

Displacements

The following figures 6.2.20, 6.2.21 and 6.2.22 illustrates the total displacement found in the numerical modelling of cross-section B-B'. This shows displacements of up to 12 cm on the south side of the open pit. The largest displacement is however on the north side of the open pit, with 36 cm deformation, see figure C.3.16 on page 155.

The maximum total displacement ($\delta = 32\,mm$) from the analysis of cross-section A-A' is assigned as a limiting value for cross-section B-B'. This is illustrated in figure C.3.15 on page 155.

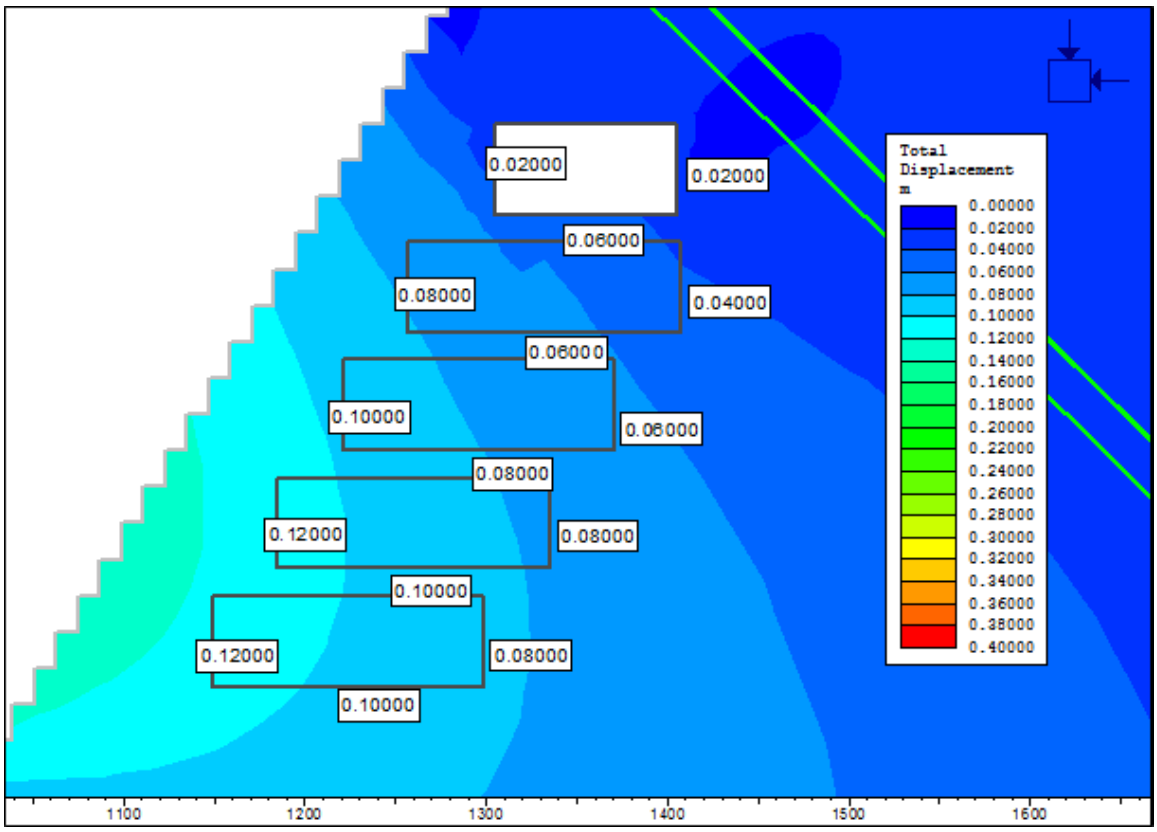

Figure 6.2.20 – Total displacement, with contour labels. Top stope is excavated.

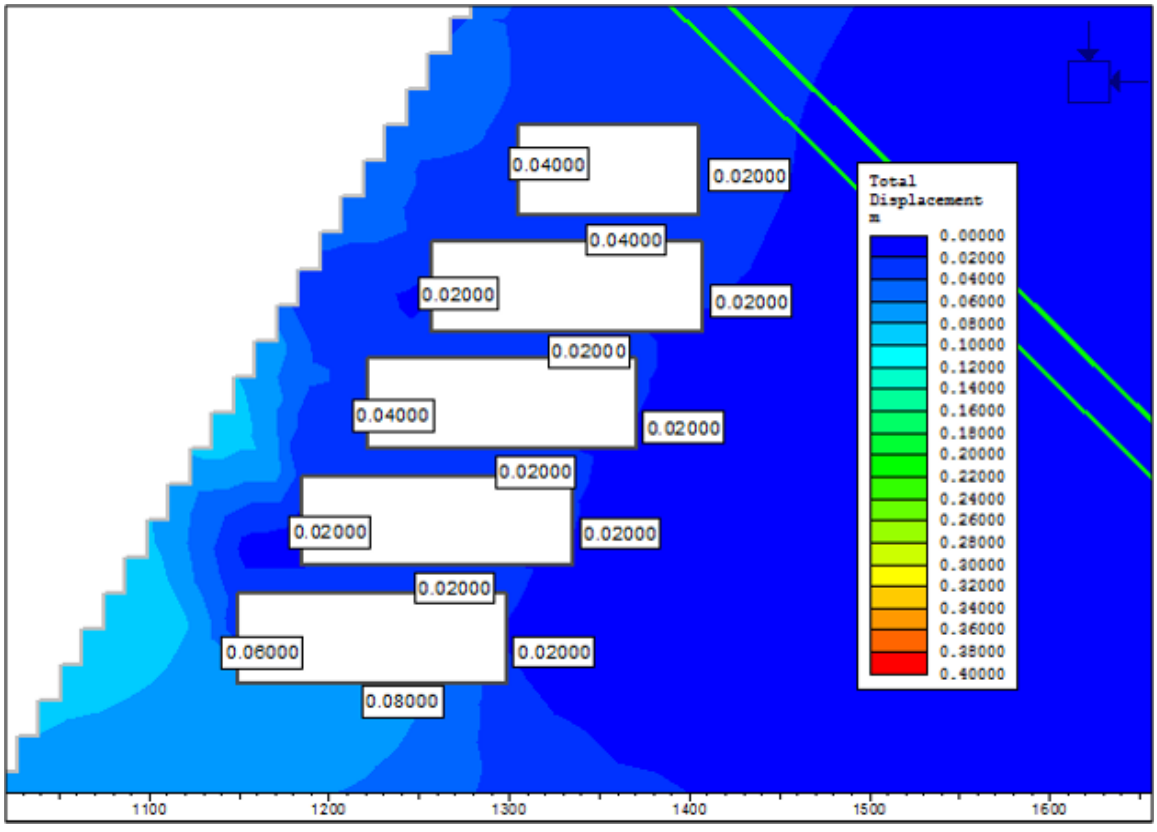

Figure 6.2.21 – Total displacement, with contour labels. All stopes are excavated.

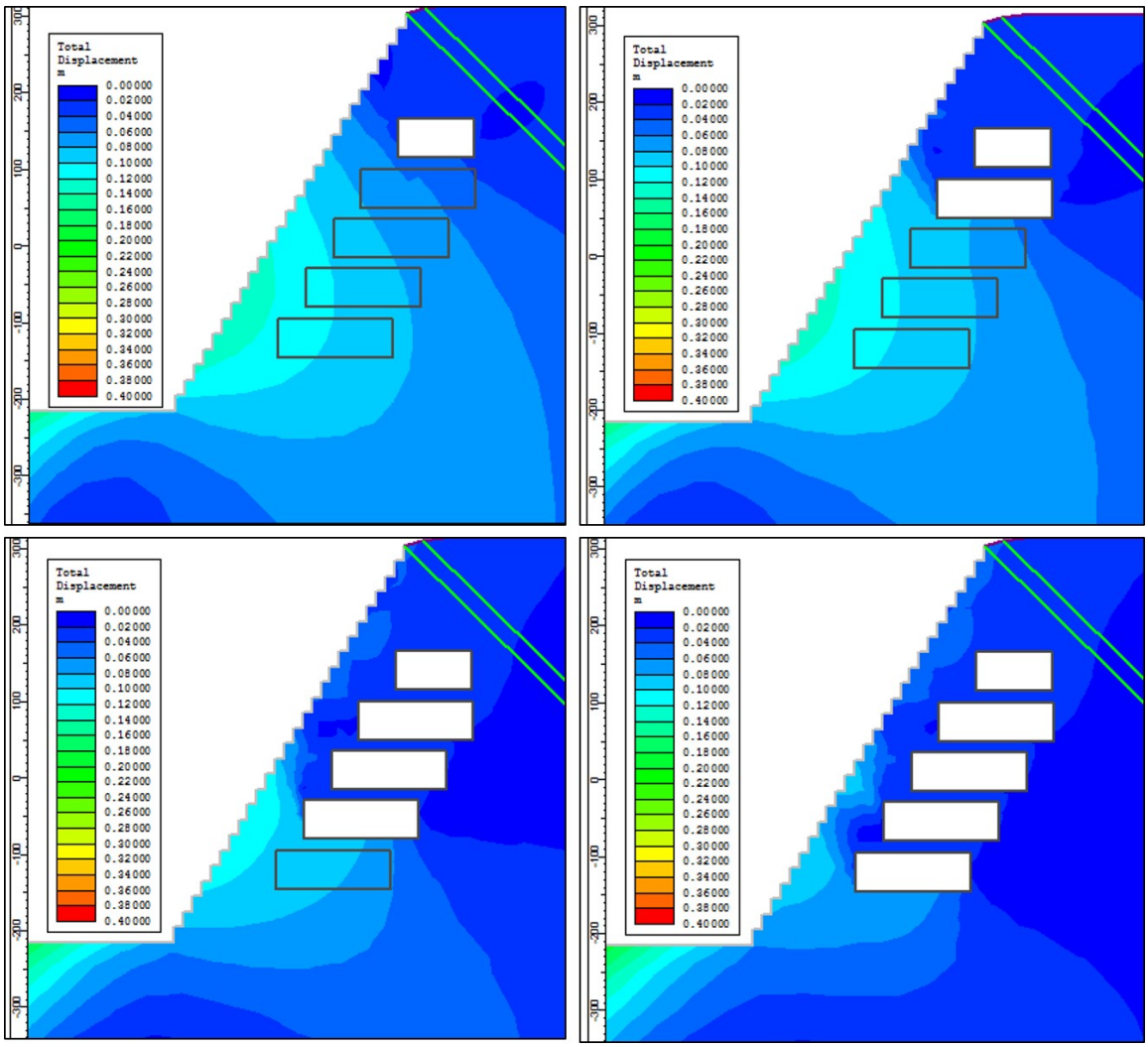

Figure 6.2.22 – Total displacement.

6.2.3 Stope Orientation

Figures 6.2.23 and 6.2.24 on the next page presents the most favourable orientation of the stopes with regards to the joint orientation in the area. The dip direction is approximately 298° NW. The joint mapping was, as previously mentioned, conducted during fieldwork in the fall of 2013.

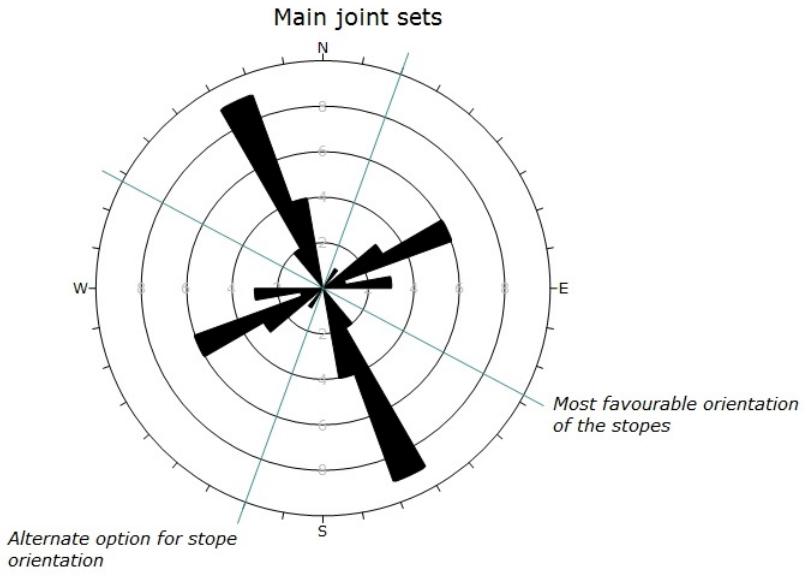

Figure 6.2.23 – Rosette plot of the main joint sets in Tromsdalen, modified after Pedersen (2013).

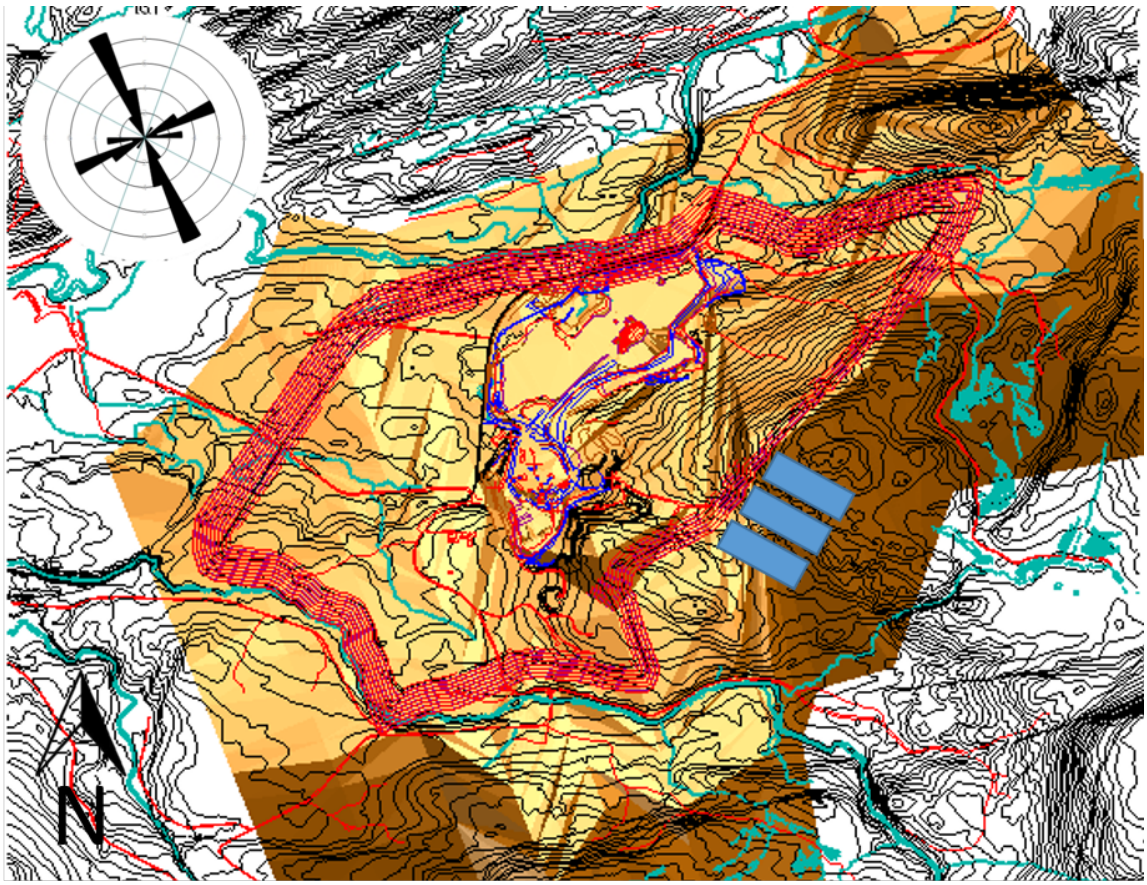

Figure 6.2.24 – Stope orientation based on the joint orientations seen in the rosette plot. The blue rectangles represents the stopes and how they are oriented according to the open pit and the joint sets. The red lines represents the future open pit border. Note, the stopes are not to scale. Their size is only for illustrational purposes. (Map from Surpac)

6.2.4 Wedge analysis

Figure 6.2.25 displays a rosette plot, the three great circles represents the three most profound joint orientations in Tromsdalen. The stope orientation is determined from the rosette plot in figure 6.2.23, with a dip direction of approximately 298° NW.

Figures 6.2.26 and 6.2.27 shows the perspective and front view of the wedges found in the stope.

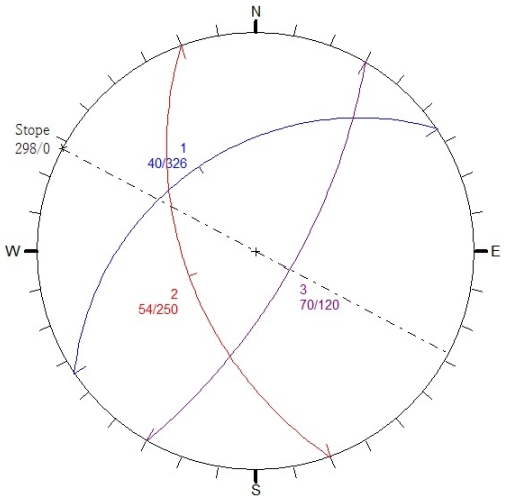

Figure 6.2.25 – Stereoplot from *Unwedge* showing three joints and the stope orientation.

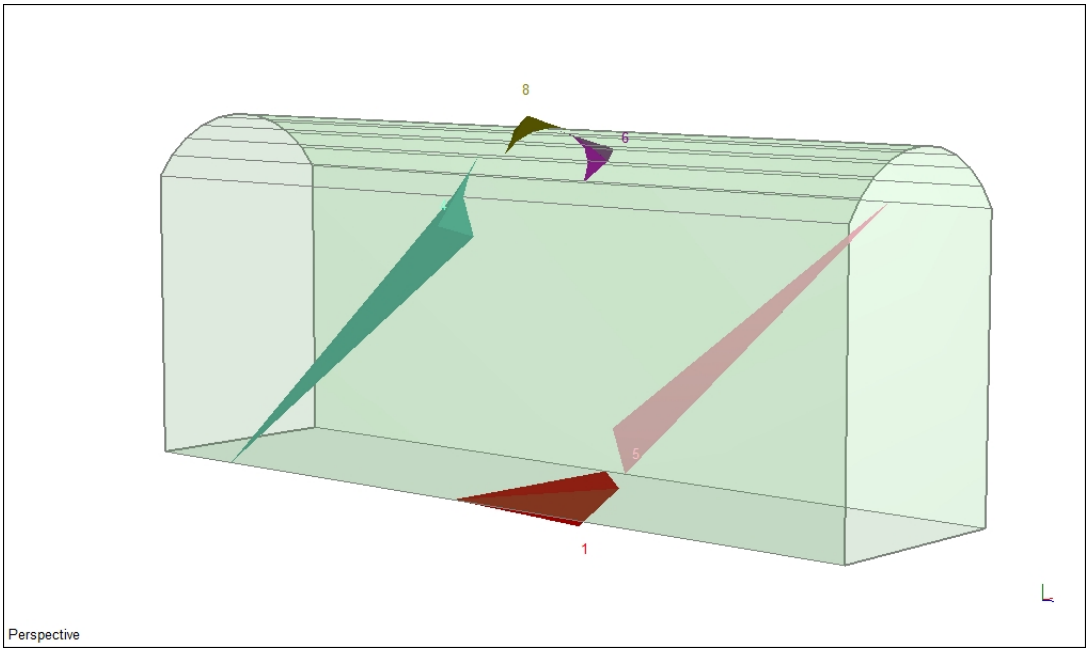

Figure 6.2.26 – Perspective view of the wedges. Note, the stope length cannot be defined in this program.

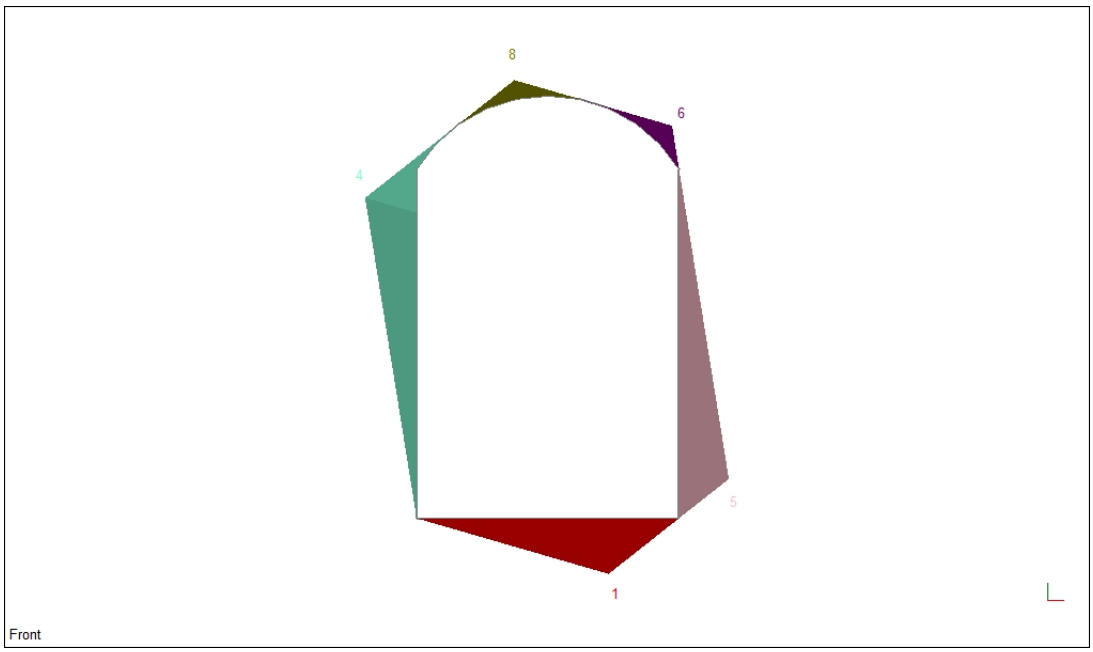

Figure 6.2.27 – Front view of wedges in the stope.

The wedge information from the analysis is listed below. It shows two unstable wedges; roof wedge (6) and roof wedge (8). The three other wedges are stable, with a factor of safety greater than the design factor of safety.

Floor wedge [1]
FS: stable
Volume: 330.657 m3
Weight: 892.773 tonnes
Support Pressure: 0.00 tonnes/m2

Upper Left wedge [4]
FS: 1.464
Volume: 437.518 m3
Weight: 1181.299 tonnes
Support Pressure: 0.00 tonnes/m2

Lower Right wedge [5]
FS: 2.351
Volume: 421.966 m3
Weight: 1139.309 tonnes
Support Pressure: 0.00 tonnes/m2

Roof wedge [6]
FS: 1.015
Volume: 11.603 m3
Weight: 31.327 tonnes
Support Pressure: 0.55 tonnes/m2

Roof wedge [8]
FS: 0.000
Volume: 20.285 m3
Weight: 54.770 tonnes
Support Pressure: 2.70 tonnes/m2

6.2.5 Surpac Models

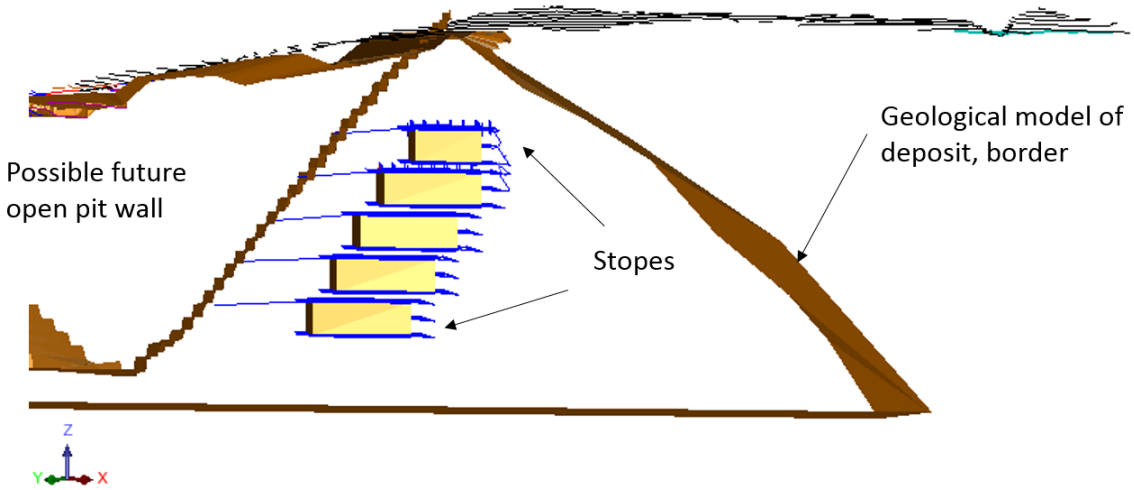

Figure 6.2.28 – Vertical section illustrating a potential layout of the future stopes.

In figure 6.2.28 a vertical section of the potential stope layout is illustrated. The blue colour indicate adits, drifts and ramps. The stopes are seen in relation to the possible future open pit wall, the topography and the deposit. Note that the top stope is 100 m long, while the rest of the stopes are 150 m long. This vertical section has the same location as cross-section B-B', see figure 5.3.2.

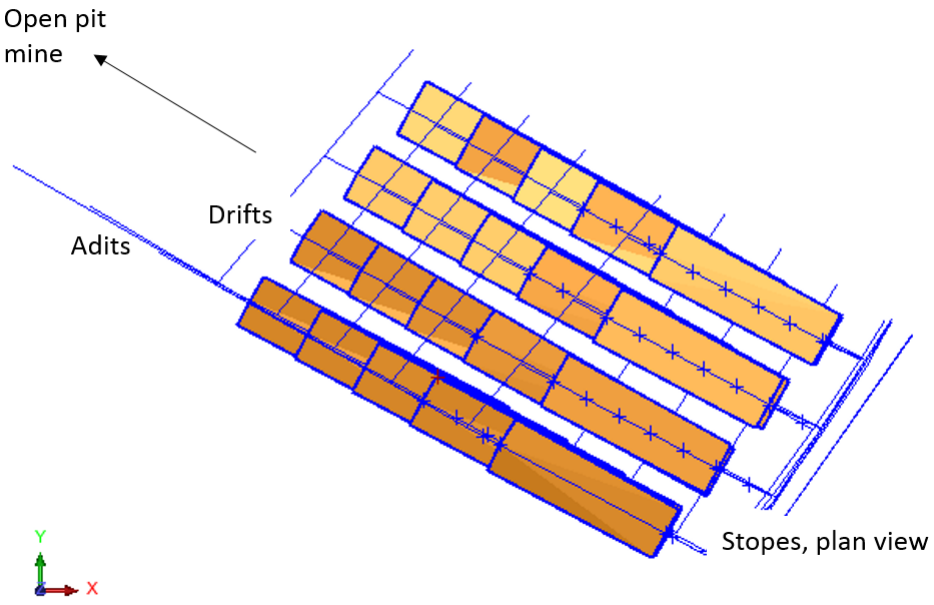

Figure 6.2.29 – Plan view of stopes.

Figure 6.2.29 illustrate the stopes seen in plan view. Figures 6.2.30 and 6.2.31 illustrate the side view and front view of the stopes, respectively. The drifts and adits are drawn with a gradient of 1:12, the ramps have a gradient of 1:7. The stope inclination is 1:100. The stopes are oriented according to the most favourable stope orientation found in the previous illustrations, 298 ° NW. The drifts are oriented parallel to the open pit wall.

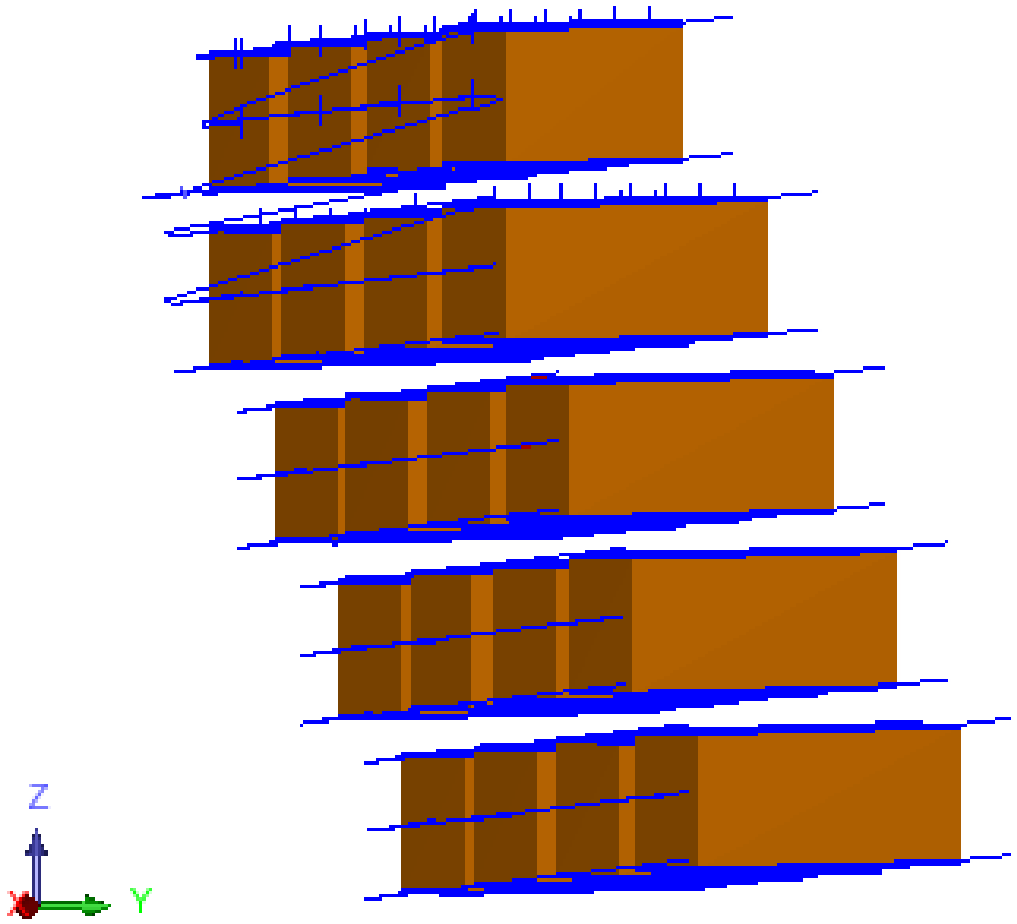

Figure 6.2.30 – Side view of the stopes, as seen from the backside of the stopes.Ramps are illustrated on the top stope.

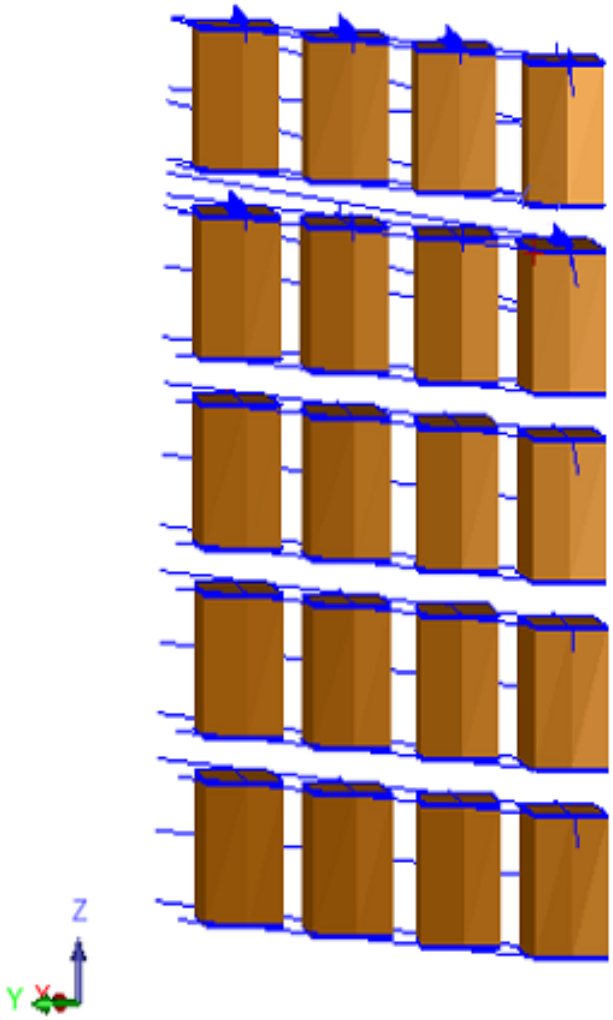

Figure 6.2.31 – Front view of stopes, as seen from the open pit mine.

Chapter 7

Discussions

7.1 Dimensioning and Design

From the design checklist on page 37, it is evident that a number of issues needs to be addressed concerning stope design. Nonetheless, not all of the listed items have been considered in this thesis because this is a preliminary study were the stope excavation not have started, so some factors are impossible to account for. In this chapter, the author will discuss the alternatives of the stope layout, findings of the numerical modelling of the stopes, stope orientation and span, mapping of discontinuities, road dimensions and gradient, ventilation, and support requirements.

7.2 Stope Layout

There are many ways of drilling a stope: horizontal drilling, vertical drilling both upwards and downwards, large-hole drilling and longhole drilling. The figures presented in section 6.1.5 illustrates some variations of vertical drilling and an option for longhole drilling.

Although horizontal drilling and "flat" benching is a more practical alternative because the same drill jumbo can be used for both topheading and drilling flat bench holds, it is not presented as an option for stope excavation in Tromsdalen.

There is a desire from the company to utilize the same equipment both in the open pit and in the underground mine. Verdalskalk AS currently use a surface drill rig, see table 4.3.4 on page 43. This rig can drill horizontal holes, but it is not suited

for development drilling due to the weight of the boom. For the development of the mine access, transportation and drilling drifts, the author would recommend development drill jumbos. A multi-boom drill jumbo offers efficiency, lower overall cost and occupational health and safety factors (Tatiya, 2013).

Regarding flat benching, this is normally reserved for benches with lower heights than those planned for the Tromsdalen underground mine. Lefdal Olivine mine (see page 52) used horizontal drilling and flat benching. However, their total room height was 18 m and the bench height was 8.5 m. The stopes in Tromsdalen will most likely have a total height of 50 m, which means that the benches will be 15 m or higher, depending on how the stopes are mined.

If the author is to meet the criteria from the company, the most suitable drilling method for this project is Method 1 with longhole drilling, see page 77. This gives a cost efficient operation, possibilities for automation, and the open pit equipment can be utilized underground. However, the risk of borehole deviation increase with longhole drilling, and the stope walls will be unsecured during loading. Automated loading is recommended for safety reasons, but to further improve the loading conditions a drift can be created in the bottom of the stope. This leaves a smoother surface that will reduce the wear on the vehicles. Fana Stein AS use a similar excavation method, except they do not use longhole drilling.

Method 2 on page 77 illustrates both vertical upwards and downwards drilling. Compared to the previous method, this stope layout inevitably requires higher development costs because it requires 2-3 access/drilling drifts in the stope. Regardless of whether drilling is done upwards or downwards the bench height is decreased with Method 2, which decrease the possibility for borehole deviation. The use of drilling drifts provides a better working foundation for the vehicles.

Both Methods 1 and 2 require rock support in the roof if the stopes are to be a safe work environment. Scaling of the sidewalls and automated loading is also recommended for safety reasons.

Method 3, illustrated on page 78, is the most cost effective in terms of development and rock support. If loading is automated, the need for rock support is very low. Where rock support is required, scaling and bolting can be done for up to 20 m high benches (based on experiences from Fana Stein AS).

The author considers Method 3 to be an equally good layout option as Method 1. Both layout suggestions requires maximum two drifts, and automated loading reduce

the need for rock support. However, Method 3 requires both upwards and downwards drilling.

One option that is possible for all three of the above-mentioned methods is to use large-diameter blastholes. According to Villaescusa (2014), this will actually decrease the specific drilling cost (NOK per cubic meter of blasted rock), and improve the drilling accuracy. However, large-hole drilling has the potential to create more damage to the surroundings than other drilling techniques due to the increased explosive concentration. Additionally, the rock fragmentation is affected due to larger quantities of fines per blast. A further disadvantage is the difficulty of charging large-diameter upholes.

Generally, the drilling cost will be kept to a minimum due to the extremely low abrasion values for the Tromsdalen Limestone. Laboratory tests conclude that wear on the drilling bits are very low, and the rock drillability is good. See test results in tables 3.2.1 and 3.2.2 on page 21.

7.2.1 Limitations

In the evaluation of the drilling method the author has not looked into the details of the drillhole pattern, the explosive types, or the initiation sequences. Emergency escape routes during development and production are not considered, nor is the explosive types for development and production blasting.

7.3 Stope and Pillar Design

The author has created two cross-sections of the carbonate deposit in Tromsdalen. Table 6.1.4 on page 76 founds the basis for the design dimensions used in the cross-sections. These design parameters were determined based on experiences from underground mines in Norway, criteria from the company, and the authors own estimations. The author has conducted a numerical analysis of the stope design parameters in the abovementioned table. The results are presented in section 6.2 on page 81.

Analysis of Section A-A'

Cross-section A-A' is analysed for a 50 m high, and 30 m wide stope with 15 m horizontal and vertical pillars. Due to lack of stress measurements in the area the author has tested a stress ratio of $k = 1$, based on consultations with Myrvang (2014).

It is apparent from the analysis of the major principal stress that there are stress concentrations in the roof and floor of the stopes, and the stress increase with the propagation of the stope excavations. Seen in connection with the minor principal stress, where the stress decrease as the excavation continues to the next level, this phenomenon can be explained by the theory of stress redistribution. When the stopes are opened, the minor principal stress approaches zero because the stress here is released. The major principal stress increases due to redistribution of the original stress field, see Stress Analysis on page 25. This stress distribution is very similar to the rock stress problem illustrated in figure 4.1.4 on page 26, where a large major principal stress causes problems in the roof and floor. The increase of the major principal stress in the corner points of the two lowermost stopes is also explained by the stress redistribution, see section 4.1 on page 25. The illustrated stress trajectories corresponds well with the demonstrated problems in figure 4.1.4.

Further investigations reveals failure in both rib pillars and crown pillars. There is mainly shear failure, but in some rib pillars and below the bottom stope level there is both shear and tension failure. The failure of the pillars is clearly illustrated in figure 6.2.11 on page 88, where the percent of failure is indicated. The rock mass will have a shear failure when the major principal stress exceeds the uniaxial compressive strength of the rock mass ($\sigma_1 \geqslant \sigma_{cm}$). Tensile failure occurs when the minor principal stress exceeds the tensile strength of the rock mass ($\sigma_3 \geqslant \sigma_t$). In this case $\sigma_{cm} = 6.93$ Mpa and $\sigma_t = 0.24$ Mpa (estimated by RocData).

The total deformation of the stopes are displayed in figure 6.2.12 on page 89. The location of the displacements corresponds well with the stress concentrations and the orientation of the stresses. The maximum total displacement (δ) from cross-section A-A' is 0.032 m. This displacement was used as a limiting value for cross-section B-B' to compensate for the "beam" effect (see page 70). Although Trinh and Broch (2008) suggests using the roof displacement as a limit, the author has chosen to use the maximum total displacement, found in the floor of the stopes. This is due to low deformation values in the first place, and the fact that the maximum displacement in the roof was approximately equal to that of the floor (difference of 0.004 m). Even

though the deformations are quite small, the analysis shows severe failure in most rib pillars, indicating the need of substantial rock support.

Analysis of Section B-B'

Cross-section B-B' is analysed for 50 m high, and 100-150 meter long stopes, with 15 m crown pillars. Stress analysis reveals large stress concentrations of the major principal stress in the front and back end of the stope when this is opened. See figure 6.2.13 on page 90. When the next stope level is excavated the stresses are reduced. In the area close to the open pit wall the stress approaches zero, whilst in the back end of the stope facing the white marble, the stress is only slightly reduced from the previous state. A similar pattern is visible for the minor principal stress.

When the large open pit is excavated, the horizontal stresses are released and therefore there are no horizontal stresses acting on the open pit wall. This situation is illustrated with stress trajectories in figure 6.2.14 and 6.2.16. Also evident from these figures is the concentration of horizontal stresses in the bottom of the large open pit. This event corresponds well with the theory about topographic influence presented in section 4.1.

When looking into the stability of the open pit wall, the findings illustrated on page 93 show severe failure along the entire wall zone in front of the stopes. Both shear and tensile failure are predicted. The entire wall does in fact have 100% failure. The author believes that this instability is largely due to the excavation of the future open pit. The deformations in the rock mass made by the stope excavation is small compared to the deformations created by the open pit. The largest displacement within the stopes are 0.08 m, and the displacement in the same area made by the open pit excavation is 0.12 m. A general rule of thumb states that deformations up to 1% of the stope dimension are considered acceptable. If the deformation exceeds 2%, the situation is unstable (Nilsen, 2014). This means that the stopes in Tromsdalen can have a deformation of 0.30 m and still be considered stable. The results of the numerical analysis however, demonstrates failure in both rib pillars and crown pillars, and the south side of the open pit wall.

It is a criterion from Verdalskalk AS that surface damage is avoided to the greatest possible extent. The analysis of cross-section B-B' reveals a large percentage of yielded elements in the subsurface area above the stopes, mainly caused by the excavation of the open pit mine.

Based on these observations it is reasonable to assume that the stability of the future open pit affects the overall stability of the stopes. Further investigation is recommended regarding the design of the future open pit, especially regarding the overall slope angle. Furthermore, the stope height should be considered in conjunction with the bench height of the open pit.

The reader should take notice of the starting level of section A-A', which is at 230 m.a.s.l. This is one stope level higher than the model of cross-section B-B', which is located at 165 m.a.s.l. The reason for doing this was to investigate how high the access point of the stopes could be. After creating section B-B', it was obvious that due to the wanted stope lengths, it would not be beneficial nor possible to have stopes at this level. These stopes would be too close to the white marble dipping in the same degree as the limestone (see figure 5.3.4 on page 69). Furthermore, there is little tolerance regarding overburden if the stopes are accessed at 230 m.a.s.l. Conversely, the preliminary model of the stopes created in *Surpac* appears to have a larger distance to the rock boundary than the model created in $Phase^2$, see illustration on page 100. This is largely due to the inaccuracy of the boundary conditions of the numerical model in $Phase^2$.

If the geological model of the limestone deposit is accurate, it could be debated whether the stopes can be longer than 150 m. The general rule of thumb states that the minimum distance from the stope excavation to a rock boundary should be no less than the thickness of this rock layer (Myrvang, 2014). The thickness of the white marble is estimated to be 20-30 m. From the illustration in figure 6.2.28, it is evident that there is at least 140 m to the rock boundary from the back end of the top stope. This distance increase gradually as the excavation moves downwards.

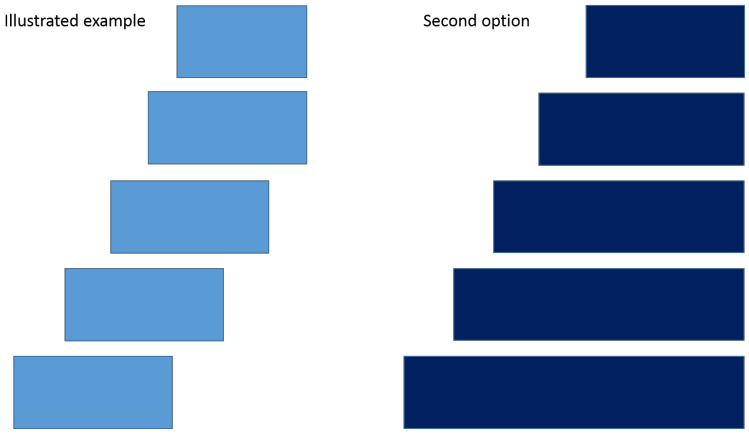

Figure 7.3.1 – Examples of stope design regarding length.

If the stability of the rock holds, the stopes could be extended in the back end towards

the marble. This could make the ramp development easier. The currently illustrated example forces the ramps to use a bigger area for development, and the stopes will be aligned at an angle in both ends. The second option allows the ramps to be developed in a more concentrated area. Figure 7.3.1 shows the difference between the two options. It is not clear how the stress field would react if the second option were used, but it is reasonable to assume that it would not drastically change the situation. However, the extension of the stope lengths should be seen in conjunction with an increase of the pillar thickness. The suggested pillar thickness of 15 m is not stable under the modelled conditions.

Limitations to the Model

Why are the results of the numerical analysis giving such devastating results for the stope dimensions in this situation? One explanation could be the very fact that *Phase*^{2} is a two-dimensional simulation tool, and this is a three-dimensional problem.

The 2D numerical analysis is considered conservative compared to a 3D simulation, and one might expect lower deformations from 3D simulations. The solution of the "beam" effect explained in section 6.2 on page 70 is in accordance with this assumption. Trinh and Broch (2008) explains how the deformations of the beam (or stope) is reduced by the support of the walls. The author has not carried out any three-dimensional simulations in this thesis due to the capabilities and time this requires.

The simulations in *Phase*^{2} are all considered for a stress field with $k = 1$. The intention was to evaluate the stress situation for both $k = 1$ and $k = 2$, due to the lack of stress measurement in Tromsdalen. The idea was that this would give a better understanding of how different stress situations would affect the stope excavations. Based on experience from underground excavations, it is evident that high horizontal stresses normal to the stope axis will give technical problems. High stress concentrations in the roof and floor tend to cause spalling or rock burst (Dahle et al., 2006). The analysis in *Phase*^{2} shows stress concentrations in both the roof and floor of cross-section A-A', consistent with rock burst and spalling problems. Cross-section B-B' shows elevated stresses in both ends of the stope. This is consistent with the major principal stress oriented normal to the stope roof. Further investigations regarding this subject is required when the actual in-situ stress field is known.

The models in *Phase*^{2} show a simplified situation of the situation. As previously mentioned, drifts and adits have not been considered for the analyses. The stress redistribution is expected to be slightly different when drifts are made in connection with the stopes. This field requires more work.

The input parameters used in the numerical analysis could be a source of error. Most of the rock mechanical properties for the lithologies have been determined by RocData and cannot be trusted blindly. The rock boundaries found in the models are determined based on information given by the geologist in Verdalskalk AS. The geologist states that these are mere estimations based on borehole information, which is insufficient in this case, and surface mapping of the outcrop (Ruiz, 2014).

Lastly, the author feels obligated to mention the stability issues in the bottom of the open pit, and on the north side of the wall. This is however not the focus of this thesis, and will not be discussed further.

Stope Span

The stope width tested in the numerical modelling was 30 meters, the stress results are commented in the previous section. Equally important is the relation of the RMR and Q-values to stope span made by Hutchinson and Diederichs (1996); Bieniawski (1989).

From field mapping the author has estimated an RMR value of 59 for the limestone, which correlates fair to good rock quality. The Q-value of the limestone concludes a good rock quality, with an average rating of 19. When these ratings are compared to the guidelines found in Section 4.3.1.2 and in Appendix B, it is obvious that a stope span of 30 m requires RMR $>$ 70 to avoid immediate collapse. The equivalent Q-value needs to be greater than 10.

Based on the results from tables 6.1.2 and 6.1.3 on page 75, the RMR rating is too low to be stable and the stopes will have an immediate collapse. The Q-value is sufficient for nonentry open stopes.

It can be debated whether the ratings are too uncertain to be taken into consideration. The mean RMR rating estimated from the Q-value (see table 6.1.2) is close to 70, this creates further questions of how accurate the field investigations have been, and how the author has evaluated the joints compared to other rock engineers. Rock support appears to be inevitable, but with a favourable design this could be kept to

a minimum. The most likely rock support for this mining project is the use of rock bolts. There are a number of different rock bolts on the marked, but the author has not investigated which bolt type that is most suitable. This requires supplementary investigation and time that the author does not have.

7.4 Stope Orientation

When the orientation of the longitudinal axis of the stopes are to be determined, both joint orientations and rock stresses play a central role.

7.4.1 Stresses

Application and knowledge about rock stress in a mining area is of great importance when planning and evaluating a (new) mine design (Dahle et al., 2006). As previously mentioned, the stress field in Tromsdalen is not measured, which makes it difficult to assess the situation in the area. Based on the literature it can be assumed that the major principal stress is normal to the direction of foliation. However, this is pure speculation and this alone cannot found the basis for the stope orientation. In order to determine a suitable stope orientation in Tromsdalen, the author has examined the orientation of discontinuities in the open pit mine.

Generally, the consequence of positioning the stopes in an unfavourable orientation could be severe. High stress concentrations in combination with a stope oriented normal to the major principal stress could cause rock burst or spalling, or worse: total collapse. The horizontal stresses play a major role in the stability of excavations and it is vital to have correct information about these. In order to get the best possible stope orientation it is normally best to have the longitudinal axis of the excavation form an angle of 15-35° to the direction of the major principal stress (Nilsen and Broch, 2001).

7.4.2 Discontinuities

The illustrations on page 97, as well as the stereoplot in figure 6.2.25, indicate the stope orientation for the future stopes. The most favourable stope orientation is

found to be approximately 298° NW. This is the bisection line of the largest angle of intersection between the two major joint directions.

After the stope orientation was determined, the author performed a small wedge analysis of the proposed stope orientation in relation to the three most profound joint orientations from field mapping, see section 6.2.4 on page 98. The results show two unstable wedges in need of rock support. The estimated required support pressure for the unstable wedges are 0.55 $tonnes/m^2$ and 2.70 $tonnes/m^2$, see page 99 . While this is true, the reader should remember that this is a preliminary analysis of one possible joint combination. A minor change in the joint dip and dip direction could give a completely different result.

Due to time constraint and the scope of this thesis, the author has not conducted multiple wedge analyses. It is however worth mentioning that the joint orientation varies with the foliation of the deposit, and a joint combination: 45/335, 54/245 and 70/120 reduces the side wedges to a minimum. Based on this knowledge it is evident that this field requires further investigation.

Limitations

The mapped discontinuities could be affected by the authors' ability to separate blast induced fractures from joints. Furthermore, the design Factor of Safety used in the wedge analysis is 1.5. This is a value sufficient for a permanent excavation, and a lower Factor of Safety might give a different result. A Factor of Safety of 1.3 for instance is adequate for a temporary mine opening (Hoek et al., 1995).

The joint properties such as the friction angle will also affect the analysis in *Unwedge*. A small friction angle leaves more room for wedge sliding, and a high friction angle results in a more stable condition for the wedges. In this analysis the residual friction angle was set to 32°, based on estimations from RocData. However, the basic friction angle found from testing in laboratory is 34°, and Hoek (2007) states that this is approximately equal to the residual friction angle. If this is true, the wedge stability would be further strengthened.

Additional work is required regarding wedge analysis. The stress situation might further influence the stability of the analysed wedges. Rock support appears to be inevitable, but with a favourable design this could be kept to a minimum.

7.5 Mine Access

Finding an efficient layout for the mine access is a difficult design problem, and the limited borehole data does not make it easier. The geometrical model of the carbonate deposit is as of today incomplete. Additional boreholes ought to be drilled to reveal the quality and thickness of the entire deposit.

In the future, if the company can expand their customers to include the cement industry, almost all of the deposit can be produced, and the location of the mine access is not of great significance. If however there are mostly PCC customers (buying quicklime for PCC production), it is crucial to know the location of the A quality limestone. This will be decisive for a profitable access to the deposit (Ruiz, 2014).

Based on this knowledge, the author finds it difficult to recommend a suitable access point for the future underground mine. However, for the illustrations and models displayed in this thesis the author has chosen an access in close proximity to an already existing road.

7.6 Road Dimensions and Inclination

A normal practice in Norway is to have road widths of 5 to 10 meters in underground mines. This however depends on two things, the stability of the rock mass and the excavation costs. The rock mass properties determines how big a span can be opened. The costs are directly dependant on the type of rock the roads and ramps are made in. Generally, the infrastructure is made in waste rock, which constitutes a pure cost for the operation. In Tromsdalen, the limestone deposit is so massive that it allows the roads to be as wide as possible, within reasonable safety requirements. The overall road width must account for the vehicle width, ditches for water drainage and prospective curves.

Based on equations from the literature, see section 4.3.3, the author has come up with some suggestions for road widths in the underground mine. The road is dimensioned for the largest vehicle currently operating in the open pit mine, and the results can be found in table 6.1.5 on page 79. The author has looked into both one-lane and two-lane road widths for the underground project.

In brief, the stability of the rock mass is the limiting factor for the road dimensions. This will determine whether a two-lane road is possible, or if the company has to

have a one-lane road. The advantage of a two-lane road is that traffic can run both ways and the vehicles does not have to stop for oncoming traffic. This is time saving and increases the efficiency of production. It will costs more to create a wider road. A one-lane road will require pullovers/meeting points that match the cycle time of the vehicles in order to avoid delays. The initial costs might be lower, but the lower efficiency and workflow might have economic consequences.

The minimum curve radius is limited by the inner turning radius of the vehicles used in the mine. If the curve radius is small, this will result in lowered speed and transport capacity. The turning radius for the largest vehicle currently operating in the open pit, based on inner turning radius, can be found in figure 6.1.8 on page 80. The Cat 775F, mine truck, has an inner turning radius of 11.75 meters. Compared to an underground machine, the Cat 775F requires a much larger turning radius. An electric mine truck such as the EMT50 from Atlas Copco requires half the turning radius, see illustration in figure D.0.1 on page 158. If the company choose to use underground equipment in the mine, with smaller dimensions and turning radius, this could reduce their development costs.

Regarding inclination of the ramps, adits and drifts, the author has conducted a literature study of commonly used ascending grades from already existing underground mines in Norway. The results are found in table 6.1.4 on page 76. The common denominator seems to be a gradient of 1:12 m for adits, drifts and ramps. However, some use a higher gradient depending on the situation. Fana Stein AS use a gradient of 1:7 m for their adit, and Sibelco Nordic, Stjernøy, varies the gradient of the adit between 1:10 and 1:12 m. For the stope inclination it appears that a gradient somewhere between 1:80 and 1:100 is acceptable. The author suggests that a gradient of 1:12 m is used as a starting point for the roads, and that the stopes have a gradient of 1:100. However, it is difficult to decide a design gradient for the infrastructure, this largely depend on the equipment. The equipment used in Verdalskalk AS today can manage a gradient of 1:7, but the equipment going to be used in the future underground mine is yet to be determined.

7.7 Ventilation

The illustration found in figure 6.1.9 gives a schematic view of a possible solution to the ventilation of the mine. This shows how the main access can function as the air intake. The idea is that air flows into the mine from the access points in the open pit wall and exits through a ventilation shaft inside the mine. This requires installation

of an exhaust fan in the ventilation shaft to aid in the process of removing toxic gases from blasting and transportation, see also the schematic of the primary ventilation in Konkola deep mine (figure 4.3.5). This project makes use of security doors in order to better control the airflow in the underground mine.

Ventilation design requires a lot of planning from the engineers to meet the air quality and safety standards. A problem to assess in the ventilation design from figure 6.1.9 is if a fire starts in the lower adit/drift. This will fill the stope with smoke and dangerous gases, and the workers will need a safe escape route or a rescue container. Furthermore, installation of security doors will give the miners a better control of the ventilation in the mine by stopping the air supply.

The amount of air required for the future underground mine in Tromsdalen is calculated based on equation 4.3.4 on page 45. This gives a mine quantity of 290 m^3/s for the new mine. The air quantity factor for a large open stoping mine is used (>0.5 Mtpa), and the air quantity constant is assumed to be 50 m^3/s for diesel-powered transport on declines. The annual production rate in million tonnes is assumed equal to 1.5 Mtpa (annual production rate is based on information from Mork, 2014).

For comparison, Fana Stein AS use forced ventilation in the mine with a total of 100-110m^3/s. The equation estimates the required air to be 134 m^3/s for a small sublevel stoping mine with an annual production rate of 0.3-0.4 Mtpa. This is not too far from what they actually use (a difference of 24 m^3/s), so it is reasonable to assume that the estimated air quantity for Tromsdalen underground mine lies somewhere around 290 ± 25 m^3/s.

Further work on the ventilation design is required, and the choice of equipment will be a decisive factor.

Chapter 8

Conclusions

8.1 Final Mine Design

Based on the results presented in this thesis it is evident that the author does not have sufficient information to recommend a viable design for the mine. However, some suggestions can be made:

- Both Method 1 and 3 are recommended as possible layout options. They both require maximum two drifts, and automated loading reduce the need for rock support.

- According to the preliminary results of wedge analyses, it appears that the major stability issue lays in the possibility of wedge failure due to the orientation of the main joint sets.

- The stope dimensions (100-150x30x50m) are suggested tested with increased pillar thickness. Although the deformations are within the stability limits, the results show tensile and shear failure in both rib pillars and crown pillars for the tested thickness (15 m). It is evident that substantial rock support is required.

- The stability of the rock mass greatly influence the road dimensions in the underground mine. For this reason, the author does not conclude with any road dimensions, but the calculated values in table 6.1.5 can be used as a guideline.

- The minimum turning radius is suggested to 11.75 m, dimensioned after the largest vehicle currently operating in the open pit mine.

- The most favourable stope orientation is found to be roughly 298° NW. This

is based on mapping of discontinuities in Tromsdalen. Although this appears to be the best orientation of the stopes, it should be verified by in-situ rock stresses.

- Some guidelines to the gradient of the stopes, drifts, ramps and adits have been made based on experiences from other underground mines in Norway. The stopes are suggested to have an inclination of 1:100, and the adits, drifts and ramps are suggested to have an inclination of 1:12. This however largely depends on the equipment intended for the mine.

- Ventilation design requires a lot of planning to meet the air quality and safety standards. It is estimated that the underground mine in Tromsdalen will have a required air quantity of $290 \pm 25\, m^3/s$.

- The stope illustrations in section 6.2.5 on page 100 are preliminary illustrations of how a system of stopes might look like.

- The extent of the rock support cannot be determined at this stage.

8.2 Further Investigations

- Before a final design of the stopes are determined, it is recommended to view the stope dimensions in conjunction with the bench height of the open pit. These ought to be adjusted to each other to accommodate the development of the mine access. The design parameters in table 6.1.4 can be used as a starting point for further investigations.

- At the moment the geological model has some shortcomings. Due to insufficient borehole information, the model cannot be considered a proven reserve, but rather an indicated mineral resource. Supplementary diamond boreholes are required to map the full extent of the deposit.

- Stress measurements must be conducted prior to any underground production in Tromsdalen. The company is advised to excavate a test drift with the intention of measuring the stress field and to monitor the deformations due to the stress redistribution.

- As a preliminary test, hydraulic fracturing can be done. This is a stress measuring technique that does not require a test drift.

- A more extensive field mapping of the jointing and rock mass quality might give a better image of how the rock behaves in different areas of the mine. In addition, a separation of the area into sections can give an indication of where one might expect to find rock of poorer quality during excavation.

- The stability of the large open pit is subject to further investigations. The analysis in $Phase^2$ indicates failure both in the bottom of the open pit and on the north side of the wall.

- Further analyses of possible wedge failures are necessary to establish a good image of the stability issues in the mine.

- A 3D analysis of the situation is recommended to get a more correct evaluation of the situation. The 2D numerical simulation in $Phase^2$ is considered to be conservative. FLAC3D described on page 70 is a suitable tool for this purpose.

Bibliography

Barton, N., 1988. Rock Classification Systems for Engineering Purposes: ASTM Special Technical Publication 984. ASTM International, Philadelphia, Ch. Rock mass classification and tunnel reinforcement selection using the Q-system, pp. 59–88. 39

Barton, N., Lien, R., Lunde, J., 1974. Engineering classification of rock masses for the design of tunnel support. Rock Mech. (4) (6), 189–239. 62

Barton, N., Løser, F., Lien, R., Lunde, J., 1980. Application of q-system in design decisions concerning dimensions and appropriate support for underground installations. In: ISRM International Symposium-Rockstore 80. 57

Bieniawski, Z., 1973. Engineering classification of jointed rock masses. Trans S. Afr. Inst. Civ. Engrs 15, 335–344. 64

Bieniawski, Z. T., 1989. Engineering Rock Mass Classifications: A Complete Manual for Engineers and Geologists in Mining, Civil, and Petroleum Engineering. John Wiley & Sons. 57, 64, 110, 135, 141

Biron, C., Arioglu, E., 1983. Design of supports in mines. John Wiley & Sons. 48

Brake, R., 2007. Mine ventilation 1 - introduction. Online course. URL `http://www.edumine.com/courses/online-courses/mine-ventilation-1-introduction/` 44

Brazil, M., Grossman, P., Lee, D., Rubinstein, J., Thomas, D., Wormald, N., 2008. Mining Technology. Vol. 117. Ch. Decline design in underground mines using constrained path optimisation, pp. 93–99. 41

Bruland, A., 1998. Hard rock tunnel boring: Drillability test methods. Project report 13A-98, NTNU Trondheim. 21

Bullock, R., 2001. Underground Mining Methods, Engineering Fundamentals and International Case Studies. SME, Ch. 2 and 3, pp. 15–48. 30, 41

Call, R., 1992. Slope stability. In SME Mining Engineering Handbook., 2nd Edition. Littleton, CO:SME. 24

Caterpillar Global Mining, 2010. Improving efficiency underground: A challange worth tackling. Viewpoint, Perspectives on Modern Mining 7. 41, 42

Choquet, P., 1991. Rock Bolting Practical Guide. Minister of Supply and Services Canada. 50

Dahle, H., Larsen, T., Myrvang, A., 2006. Horizontal rock stresses - a key factor in mine design. Vol. 2. Mine Planning and Equipment Selection - Cardu, Ciccu, Lovera & Michelotti (eds), pp. 1363–1368. 13, 109, 111

Deer, W., Howie, R., Zussman, J., 1992. An Introduction to The Rock - Forming Minerals. Pearson Education Limited. 17

Deere, D. U., 1963. Technical description of rock cores for engineering purposes. Felsmechanic und Ingenieurgeologie 1, 16–22. 62

Ellefmo, S. L., 2013a. Underground mining, Lecture in subject TGB4245 Mining Engineering. 35

Ellefmo, S. L., 2013b. Underground Quarrying In Bergen Norway, an Alternative Method of Mining Rock, Lecturenotes in subject TGB4245 Mining Engineering. 54

Franklin, J., Dusseault, M., 1989. Rock engineering. McGraw-Hill, New York, 556. 48

Gautneb, H., 2012. Kommunedelplan Tromsdalen, Verdal. Oversikt over geologiske forhold, marked og produksjon av kalkstein. Tech. rep., NGU, Norges geologiske undersøkelse. 6, 7

Halvorsen, E., Tuttle, K., 2013. Konsekvensutredning for Tromsdalen kalksteindagbrudd, Konsekvenser for grunnvann. "Impact Study". Unpublished, Norconsult. 15

Hamrin, H., 2001. Underground Mining Methods: Engineering Fundamentals and International Case Studies. Littleton, CO:SME, Ch. Underground mining methods and applications, pp. 3–14. 30, 31, 32

Hast, N., 1958. The measurements of rock stress in mines. Sveriges geologiska undersökning, Publication 52-3, Stockholm. 12

Haycocks, C., Aelick, R., 1992. SME Mining Engineering Handbook - Sublevel stoping. Vol. 2. Society for Mining, Metallurgy and Exploration, Inc., Ch. 18.4, pp. 1717–1731. 30, 31, 32, 33, 34, 35

Hoek, E., 1994. Strength of rock and rock masses. ISRM News J. 2, 4–16. 60

Hoek, E., 2007. Practical Rock Engineering. 23, 24, 60, 62, 65, 70, 71, 112, 134, 136

Hoek, E., Brown, E., 1998. Practical estimates of rock mass strength. Int J Rock Mech Min Sci 34, 1165–1186. 60

Hoek, E., Carranza-Torres, C., Corkum, B., 2002. Hoek-Brown Failure Criterion - 2002 Edition. Rockscience. 27

Hoek, E., Kaiser, P., Bawden, W., 1995. Support of underground excavations in hard rock. Funding by Mining Research Directorate and Universities Research Incentive Fund. 60, 72, 112

Howes, M., 2011. Ventilation and cooling in underground mines. Mining and Quarrying 74. 45, 46

Hutchinson, D., Diederichs, M., 1996. Cablebolting in underground mines. Bitech Publishers, Richmond, British Colombia, Canada. 38, 39, 40, 110

Itasca Consulting Group, Inc., An Itasca International Company, 2014. URL `http://www.itascacg.com/software/flac3d` 70

Kaasa, T., May 2014. Personal communication. Norcem Brevik, Norcem AS. 56

Korneliussen, A., 2009. Karbonatforekomster (carbonate deposits). Foredrag NGU 5 - 6. februar (Lecture NGU February 5-6). 7

Laubscher, D., 1977. Geomechanics classification of jointed rock masses - mining applications. Trans. Instn. Min. Metall 86, 1–8. 57

Lawrence, B., 1982. Considerations for Sublevel Open Stoping, Underground Mining Methods Handbook. SME-AIME, New York, Ch. 2.2.2, pp. 364–366. 34

Mark, A., Marek, P., December 11. 2013. Roadway design manual.

URL http://onlinemanuals.txdot.gov/txdotmanuals/rdw/minimum_designs_truck_bus_turns.htm 80

Marshak, S., 2008. Earth: Portrait of a Planet, 3rd Edition. Norton. 17

Mathews, K., Hoek, E., Wyllie, D., Stewart, S., 1981. Prediction of stable excavtion for mining at depth below 1000 m in hard rock. DSS Serial No. OSQ80-00081, DSS File No. 17SQ.23440-0-9020, Dept. Energy, Mines and Resources. 57

McIsaac, G., 2006. Mine 244: Underground mining. Kingston: The R.M Buchan Department of Mining, Queens University. 35

Møller, T., May 2013. Regulated maps of Tromsdalen. Innherred samkommune, "Innherred municipality".
URL http://www.verdal.kommune.no/Politikk/Kommunestyret-2011-2015/17062013/4313-Kommunedelplan-Tromsdalen/ 15, 162

Monenco, 1989. Design manual for surface mine haul roads. Tech. rep., Draft report by Monenco Consultants Limited, Calgary, Alberta. 43, 44

Mork, H., May 2014. Personal communication, Verdalskalk AS. 6, 11, 12, 14, 115

Myrvang, A., 2001. TGB4210 Bergmekanikk, "Rock Mechanics". Tapir akademiske forlag, Norwegian. 25, 26, 49, 67, 68

Myrvang, A., 2013. Personal communication, November 19, 2013. 13

Myrvang, A., May 2014. Personal communication. 68, 106, 108

Nødtvedt, I., March 2009. Quarrying underground, Fana Stein & Gjenvinning AS, Presentation. 55

Nødtvedt, I., May 2014. Personal communication. 54, 55

NGI, 2013. Using the Q-system. Rock mass classification and support design. 61, 63, 64, 132, 133, 137

Nilsen, B., May 2014. Personal conversation. 107

Nilsen, B., Broch, E., 2001. Ingeniørgeologi-Berg Grunnkurskompendium (Engineering Geology Compendium). Institutt for geologi og bergteknikk (Department of Geology and Mineral Resources Engineering), Norwegian. 26, 27, 111

Nixon, J., Pauley, S. P., 2014. Geological Survey Program - Missouri Limestone. URL http://www.dnr.mo.gov/geology/geosrv/imac/limestone.htm 18

NTNU Department of Civil and Transport Engineering, 2008. Report 12e-08 rock quarrying transport. Tech. rep., NTNU. 41, 42, 44

Pakalnis, R., July 7-10 2002. Empirical design methods - ubc geomechanics an update. In: R. Hammah, W. Bawden, J. C., Telesnicki, M. (Eds.), Mining and Tunneling Innovation and Opportunity, Proceedings of the 5th North American Rock Mech Symp & 17th Tunneling Association of Canada Conference. University of Toronto, Toronto, Ontario, Canada, pp. 203–210. 140

Pedersen, A. H., 2013. Assessment of Underground Mining in Tromsdalen. Project report, NTNU. iii, 1, 2, 15, 19, 73, 75, 97

Pedersen, A. H., Todnem, S., Vestad, M., Myhre, S., Langåker, M., Sollie, I. L., Langås, C., 2013. Results from testing in laboratory in subject TGB4505 Engineering Geological Laboratory Methods, NTNU/SINTEF Laboratory. 15, 21

Pells, P., Bertuzzi, R., 2011. Limitations of rock mass classification systems for tunnel support designs. Pells Sullivan Meynink Pty Ltd. 65

Ramberg, I. B., Bryhni, I., Nøttvedt, A. (Eds.), 2007. The Making of a Land: Geology of Norway. Norsk Geologisk Forening (NGF), Norwegian Geological Association. 7

Read, J., Stacey, P., 2009. Guidelines for open pit slope design. Collingwood: CSRO Publ. 58, 59

Roberts, D., Myrvang, A., 2004. Contemporary stress orientation features in bedrocks, Trøndelag, central Norway, and some regional implications. NGU Bulletin 442, 53–63. 12, 13

Rockscience Inc., 2012. Generalized Hoek-Brown Criterion. URL http://www.rocscience.com/ 27

Rocscience, October 12 2007. Underground wedge stability analysis. URL https://www.rocscience.com/products/10/Unwedge 71, 72

Rocscience, 2014. Phase2 - excavation and support design. URL http://www.rocscience.com/products/3/Phase2 66

Ruiz, J. R., June 2014. Personal communication. Geologist, Verdalskalk AS. 5, 8, 9, 10, 13, 20, 68, 110, 113

Safe Work Australia, July 2011. Ventilation of underground mines, code of practice. Draft, Work Health and Safety Act. 44

Seedsman, R., 2011. SME Mining Engineering Handbook, 3rd Edition. Vol. 1. Society for Mining, Metallurgy and Exploration, Inc., Ch. 8.4 Rock Mechanics, pp. 527–549. 64

Sellæg, T., 2005. Engineering geological issues with the establishment of a transport tunnel, Tromsdal -Ørin. Project report, NTNU. 15

Sellæg, T., 2006. Feasibility study for tunnel transport Ørin - Tromsdalen. Master thesis, NTNU. 15

Selmer-Olsen, R., Broch, E., 1977. General design procedure for underground openings in Norway. Bergman: Storage in excavated Rock Caverns, Pergamon Press, Oxford, 219–227. 26

Sheorey, P., 1994. A theory for in situ stresses in isotropic and transversely isotropic rock. Int. J. Rock Mech. Min. Sci. & Geomech. Abstr. 1, 23–34. 24

Sherson, D., 2002. Silicosis in the twenty first century. Occup Environ Med 59, 721–722. 45

Skjerlie, F., Gausdal, O., 1961. Diamantboringer Tromsdalen kalksteinsforekomst. NGU rapport 300B. Tech. rep. 15

Skjerlie, F., Tan, T., 1961. Geologiske undersøkelser Tromsdalen kalksteinsforekomst. NGU rapport 300b. Tech. rep. 15

Sollid, O., Kristiansen, R., April 2014. Personal communication, Sibelco Nordic. 32, 51, 52, 53

Sverdrup, T., 1966. Geologiske undersøkelse av Tromsdalen, Nord-Trøndelag fylke. NGU rapport 725. Tech. rep. 15

Svinndal, S., Vassbotn, S., 1969. Teknisk rapport over diamantboringer ved Tromsdalen Kalkfelt Verdal. NGU rapport 804A. Tech. rep. 15

Swart, A., Handley, M., 2005. The design of stable stope spans for shallow mining

operations. The Journal of The South African Institute of Mining and Metallurgy 105, 275–286. 57, 58

Tannant, D. D., Regensburg, B., 2001. Guidelines for mine haul road design. School of Mining and Petroleum Engineering, Department of Civil and Environmental Engineering, University of Alberta. 43

Tatiya, R. R., 2013. Surface and Underground Excavations, Methods, Techniques and Equipment, 2nd Edition. CRC Press. 33, 47, 48, 49, 104

Terzaghi, K., Richart, F., 1952. Stresses in rock about cavities. Geotechnique 3, 57–90. 23

Thomas-Lepine, C., 2012. Rock bolts - improved design and possibilities. Civil and Environmental Engineering (2 year), NTNU. 15

Trinh, Q., Broch, E., 2008. Tunnel Cave-in - Convergence Confinement and 2D Analyses. Australian Centre for Geomechanics, Perth. 70, 106, 109

Trinh, Q., Broch, E., Lu, M., 2010. 2D versus 3D modelling for tunneling at a weakness zone. Taylor and Francis Group, LondonRock Engineering in Difficult Ground Conditions - Soft Rocks and Karst. 66

Trout, P., 1997. Formulation and application of new underground mine scheduling models. Ph.D. thesis, The University of Queensland, Brisbane, Queensland, Australia. 35

Ulvedal, T., April 2003. "I verdas største olivingruve". Bergens Tidende, Newspaper. URL `http://www.bt.no/nyheter/lokalt/I-verdas-storste-olivingruve-2416920.html` 52

Verdalskalk AS, March 2013a. Kalkindustrien i Verdal. Informasjon om utviklingsplaner. 9, 163

Verdalskalk AS, 2013b. Mapping of the contact between marble and phyllite and tracing of major joints. 15

Villaescusa, E., October 5-9 1998. Geotechnical design for dilution control in underground mining. In: Singhal, R. (Ed.), Proceedings of the Seventh International Symposium on Mine Planning & Equipment Selection. Balkema, Rotterdam, the Netherlands, pp. 141–149. 36

Villaescusa, E., 2014. Geotechnical Design for Sublevel Open Stoping. CRC Press. 30, 32, 33, 37, 38, 46, 47, 105, 141

Wiktionary, 2013.
URL `http://en.wiktionary.org/wiki/rhombohedral` 19

Wyllie, D. C., Mah, C. W., 1981. Rock Slope Engineering, 4th Edition. 59, 130, 131

Appendix A

Collection of Data

A.1 Classification Schemes

A.1.1 Field Descriptions

Table A.1.1 – Persistence of discontinuities (Wyllie and Mah, 1981).

Description	**Persistence [m]**
Very Low Persistence	< 1
Low Persistence	1 - 3
Medium Persistence	3 - 10
High Persistence	10 - 20
Very High Persistence	> 20

Table A.1.2 – Aperture of discontinuity surfaces (Wyllie and Mah, 1981).

Term	**Aperture [mm]**	**Description**
Very Tight	0.1	
Tight	0.1 - 0.25	*Closed features*
Partly Open	0.25 - 0.5	
Open	0.5 - 2.5	
Moderately Wide	2.5- 10	*Gapped features*
Wide	> 10	
Very Wide	10 - 100	
Extremely Wide	100 -1000	*Open features*
Cavernous	> 1000	

Table A.1.3 – Spacing of discontinuities (Wyllie and Mah, 1981).

Term	**Spacing [mm]**
Extremely Close	< 20
Very Close	20- 60
Close	60 - 200
Medium	200 - 600
Wide	600 - 2000
Very Wide	$>$ 2000 - 6000
Extremely Wide	$>$6000

Table A.1.4 – Effect of weathering on fresh rock, (Wyllie and Mah, 1981).

Term	**Symbol**	**Description**
Fresh Rock	FR	No visible signs of weathering; perhaps slight discolouration on major discontinuity surfaces.
Slightly Weathered	SW	Partial (<5 %) staining or discolouration of rock substance, usually by limonite. colour and texture of fresh rock is recognizable. No discernible effect on the strength properties of the parent rock type; but all the rock material may be discoloured by weathering and may be somewhat weaker externally than in its fresh condition.
Moderately Weathered	MW	Less than half of the rock material is decomposed and/or disintegrated to a soil. Fresh or discoloured rock is present either as a continuous framework or as corestones.
Highly Weathered	HW	Limonite staining or bleaching affects all rock substance and other signs of chemical or physical decomposition are evident. More than half of the rock material is decomposed and/or disintegrated to a soil. Fresh or discoloured rock is present either as a discontinuous framework or as corestones.
Completely Weathered	CW	Rock has soil properties, i.e. it can be remoulded and classified according to the USCS 1, although texture of the original rock can still be recognized. All rock material is decomposed and/or disintegrated to soil. The original mass structure is still largely intact.
Residual Soil	RS	All rock material is converted to soil. The mass structure and material fabric are destroyed. There is a large change in volume, but the soil has not been significantly transported.

A.1.2 Q-system

Table A.1.5 – Input parameters to the Q-system, after NGI (2013).

Rock quality designation (RQD)

Very poor	RQD = 0 - 25%
Poor	25 - 50
Fair	50 - 75
Good	75 - 90
Excellent	90 - 100
Notes:	
(i) Where RQD is reported or measured as < 10 (including 0), a nominal value of 10 is used to evaluate Q	
(ii) RQD intervals of 5, i.e. 100, 95, 90, etc. are sufficiently accurate	

Joint set number (Jn)

Massive, no or few joints	Jn = 0.5 - 1
One joint set	2
One joint set plus random	3
Two joint sets	4
Two joint sets plus random	6
Three joint sets	9
Three joint sets plus random	12
Four or more joint sets, heavily jointed, "sugar-cube", etc.	15
Crushed rock, earthlike	20
Notes: *(i) For tunnel intersections, use (3.0 x Jn); (ii) For portals, use (2.0 x Jn)*	

Desciption and ratings for the parameter Jr *(joint roughness number)*

a) Rock-wall contact, b) rock-wall contact before 10 cm shear	
Discontinuous joints	Jr = 4
Rough or irregular, undulating	3
Smooth, undulating	2
Slickensided, undulating	1.5
Rough or irregular, planar	1.5
Smooth, planar	1.0
Slickensided, planar	0.5
Note*: i) Descriptions refer to small scale features, and intermediate scale features, in that order*	

c) No rock-wall contact when sheared	
Zone containing clay minerals thick enough to prevent rock-wall contact	Jr = 1.0
Sandy, gravelly or crushed zone thick enough to prevent rock-wall contact	1.0
Notes:	
i) Add 1.0 if the mean spacing of the relevant joint set is greater than 3 m	
ii) Jr = 0.5 can be used for planar, slickensided joints having lineations, provided the lineations are oreintated for minimum strength	

Descriptions and ratings for the parameter Ja *(joint alteration number)*

Contact between joint walls	**JOINT WALL CHARACTER**		**Condition**	***Wall contact***
	CLEAN JOINTS	Healed or welded joints:	filling of quartz, epidote, etc.	Ja = 0,75
		Fresh joint walls:	no coating or filling, except from staining (rust)	1
		Slightly altered joint walls:	non-softening mineral coatings, clay-free particles, etc.	2
	COATING OR THIN FILLING	Friction materials:	sand, silt calcite, etc. (non-softening)	3
		Cohesive materials:	clay, chlorite, talc, etc. (softening)	4

Partly or no wall contact	**FILLING OF:**	**Type**	***Partly wall contact*** *Thin filling (< 5 mm)*	***No wall contact*** *Thick filling*
	Friction materials	sand, silt calcite, etc. (non-softening)	Ja = 4	Ja = 8
	Hard cohesive materials	compacted filling of clay, chlorite, talc, etc.	6	5 - 10
	Soft cohesive materials	medium to low overconsolidated clay, chlorite, talc, etc.	8	12
	Swelling clay materials	filling material exhibits swelling properties	8 - 12	13 - 20

Description and ratings for the parameter Jw *(joint water reduction factor)*

Dry excavations or minor inflow, i.e. < 5 l/min locally	p_w < 1 kg/cm^2	Jw = 1
Medium inflow or pressure, occasional outwash of joint fillings	1 - 2.5	0.66
Large inflow or high pressure in competent rock with unfilled joints	2.5 - 10	0.5
Large inflow or high pressure, considerable outwash of joint fillings	2.5 - 10	0.3
Exceptionally high inflow or water pressure at blasting, decaying with time	> 10	0.2 - 0.1
Exceptionally high inflow or water pressure continuing without noticeable decay	> 10	0.1 - 0.05
Note: *(i) The last four factors are crude estimates. Increase Jw if drainage measures are installed*		
(ii) Special problems caused by ice formation are not considered		

Description and ratings for parameter SRF *(stress reduction factor)*

A. Weakness zones intersecting excavation	Multiple weakness zones with clay or chemically disintegrated rock, very loose surrounding rock (any depth)			SRF = 10
	Single weakness zones containing clay or chemically disintegrated rock (depth of excavation < 50 m)			5
	Single weakness zones containing clay or chemically disintegrated rock (depth of excavation > 50 m)			2.5
	Multiple shear zones in competent rock (clay-free), loose surrounding rock (any depth)			7.5
	Single shear zones in competent rock (clay-free), loose surrounding rock (depth of excavation < 50 m)			5
	Single shear zones in competent rock (clay-free), loose surrounding rock (depth of excavation > 50 m)			2.5
	Loose, open joints, heavily jointed or "sugar-cube", etc. (any depth)			5
Note: *(i)*	*Reduce these valued of SRF by 25 - 50% if the relevant shear zones only influence, but do not intersect the excavation*		σ_c / σ_1	σ_θ / σ_c
B. Competent rock, rock stress problems	Low stress, near surface, open joints		> 200	< 0.01	2.5
	Medium stress, favourable stress condition		200 - 10	0.01 - 0.3	1
	High stress, very tight structure. Usually favourable to stability, may be except for walls		10 - 5	0.3 - 0.4	0.5 - 2
	Moderate slabbing after > 1 hour in massive rock		5 - 3	0.5 - 0.65	5 - 50
	Slabbing and rock burst after a few minutes in massive rock		3 - 2	0.65 - 1	50 - 200
	Heavy rock burst (strain burst) and immediate dynamic deformation in massive rock		< 2	> 1	200 - 400
Notes: *(ii)*	*For strongly anisotropic stress field (if measured): when 5 < σ_1/σ_3 <10, reduce σ_c to 0.75 σ_c. When $\sigma 1/\sigma 3$ > 10, reduce σ_c to 0.5 σ_c*				
(iii)	*Few case records available where depth of crown below surface is less than span width. Suggest SRF increase from 2.5 to 5 for low stress cases*			σ_θ / σ_c	
C. Squeezing rock	*Plastic flow of incompetent rock under the influence of high pressure*	Mild squeezing rock pressure		1 - 5	5 - 10
		Heavy squeezing rock pressure		> 5	10 - 20
D. Swelling rock	*Chemical swelling activity depending on presence of water*	Mild swelling rock pressure			5 - 10
		Heavy swelling rock pressure			10 - 15

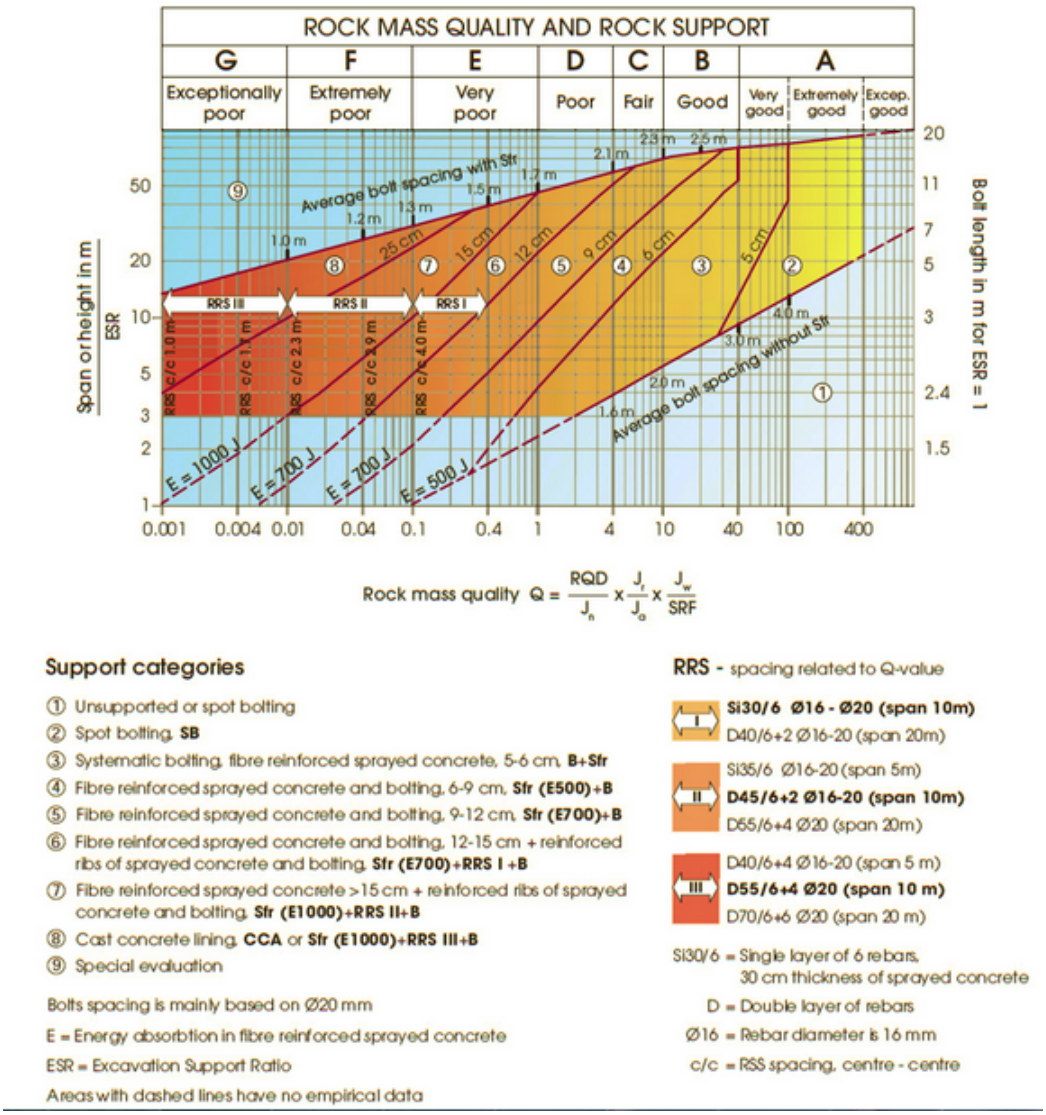

Support categories

① Unsupported or spot bolting
② Spot bolting, **SB**
③ Systematic bolting, fibre reinforced sprayed concrete, 5-6 cm, **B+Sfr**
④ Fibre reinforced sprayed concrete and bolting, 6-9 cm, **Sfr (E500)+B**
⑤ Fibre reinforced sprayed concrete and bolting, 9-12 cm, **Sfr (E700)+B**
⑥ Fibre reinforced sprayed concrete and bolting, 12-15 cm + reinforced ribs of sprayed concrete and bolting, **Sfr (E700)+RRS I +B**
⑦ Fibre reinforced sprayed concrete >15 cm + reinforced ribs of sprayed concrete and bolting, **Sfr (E1000)+RRS II+B**
⑧ Cast concrete lining, **CCA** or **Sfr (E1000)+RRS III+B**
⑨ Special evaluation

Bolts spacing is mainly based on Ø20 mm
E = Energy absorbtion in fibre reinforced sprayed concrete
ESR = Excavation Support Ratio
Areas with dashed lines have no empirical data

RRS - spacing related to Q-value

I
Si30/6 Ø16 - Ø20 (span 10m)
D40/6+2 Ø16-20 (span 20m)

II
Si35/6 Ø16-20 (span 5m)
D45/6+2 Ø16-20 (span 10m)
D55/6+4 Ø20 (span 20m)

III
D40/6+4 Ø16-20 (span 5 m)
D55/6+4 Ø20 (span 10 m)
D70/6+6 Ø20 (span 20 m)

Si30/6 = Single layer of 6 rebars, 30 cm thickness of sprayed concrete
D = Double layer of rebars
Ø16 = Rebar diameter is 16 mm
c/c = RSS spacing, centre - centre

Figure A.1.1 – Rock support chart from NGI, 2013.

A.1.3 GSI

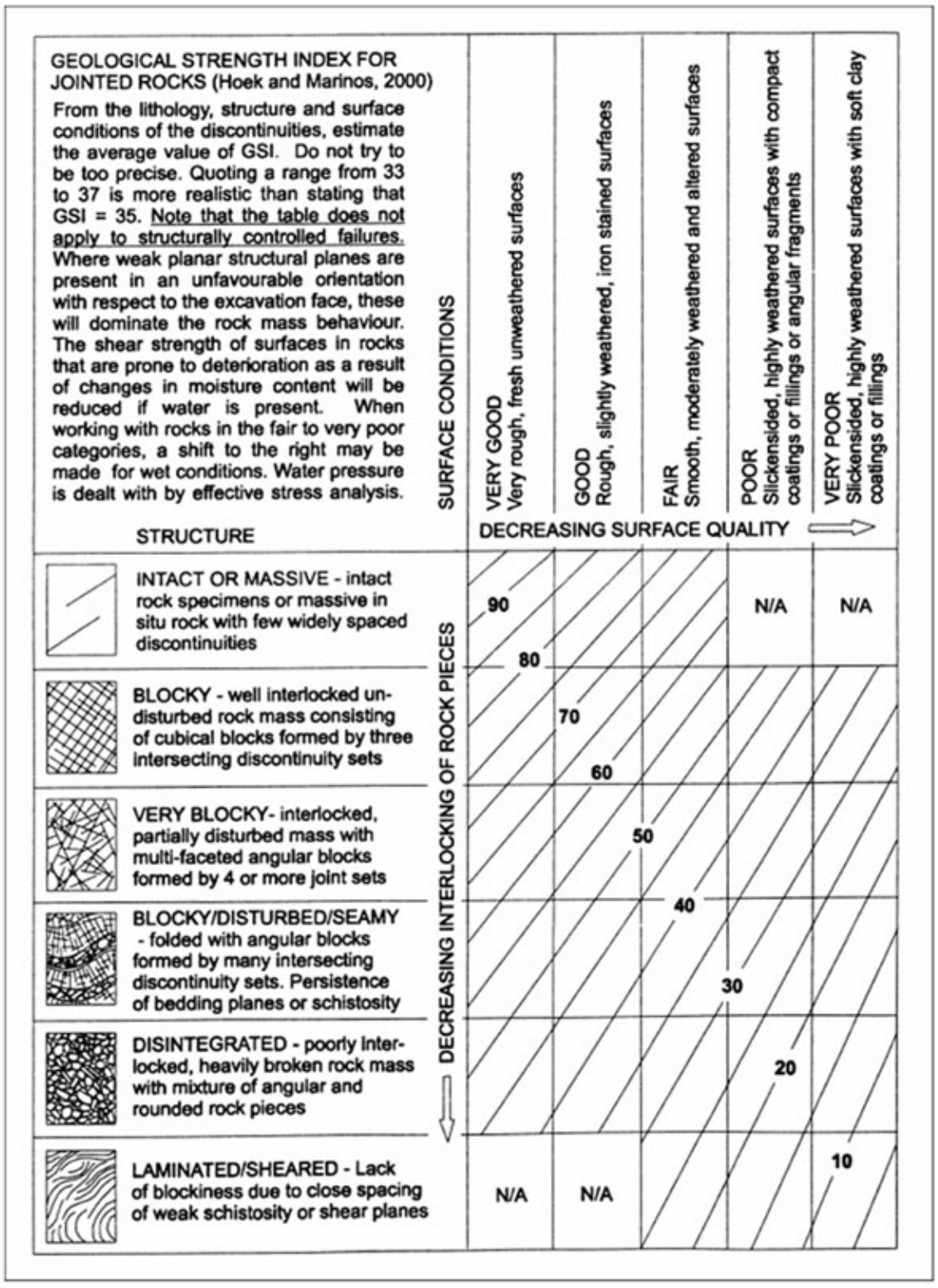

Figure A.1.2 – Estimation of Geological Strength Index, from Hoek (2007).

A.1.4 RMR

Table A.1.6 – Rock mass classification RMR system, after Bieniawski (1989).

(a) Five basic rock mass classification parameters and their ratings									
1. Strength of intact rock material	Point load strength index (MPa)	> 10	4 – 10	2 – 4	1 – 2				
	Uniaxial compressive strength (MPa)	> 250	100 – 250	50 – 100	25 – 50	5 – 25	1 – 5	< 1
	Rating	*15*	*12*	*7*	*4*	*2*	*1*	*0*
2. RQD (%)		90 – 100	75 – 90	50 – 75	25 – 50	< 25		
	Rating	*20*	*17*	*13*	*8*	*3*		
3. Joint spacing (m)		> 2	0.6 – 2	0.2 – 0.6	0.06 – 0.2	< 0.06		
	Rating	*20*	*15*	*10*	*8*	*5*		
4. Condition of joints		not continuous, very rough surfaces, unweathered, no separation	slightly rough surfaces, slightly weathered, separation <1 mm	slightly rough surfaces, highly weathered, separation <1 mm	continuous, slickensided surfaces, or gouge <5 mm thick, or separation 1–5 mm	continuous joints, soft gouge >5 mm thick, or separation >5 mm		
	Rating	*30*	*25*	*20*	*10*	*0*		
5. Groundwater	inflow per 10 m tunnel length (l /min), or	none	< 10	10 – 25	25 – 125	> 125		
	joint water pressure/major in situ stress, or	0	0 – 0.1	0.1 – 0.2	0.2 – 0.5	> 0.5		
	general conditions at excavation surface	completely dry	damp	wet	dripping	flowing		
	Rating	*15*	*10*	*7*	*4*	*0*		

(b) Rating adjustment for joint orientations						
Strike and dip orientation of joints		very favourable	favourable	fair	unfavourable	very unfavourable
Rating	tunnels	0	– 2	– 5	– 10	– 12
	foundations	0	– 2	– 7	– 15	– 25
	slopes	0	– 5	– 25	– 50	– 60

(c) Effects of joint orientation in tunnelling						
Strike perpendicular to tunnel axis				Strike parallel to tunnel axis		Dip 0° – 20°
Drive with dip		Drive against dip				
Dip 45° – 90° very favourable	Dip 20° – 45° favourable	Dip 45° – 90° fair	Dip 20° – 45° unfavourable	Dip 45° – 90° very unfavourable	Dip 20° – 45° fair	irrespective of strike fair

A.2 Rock Quality Designation

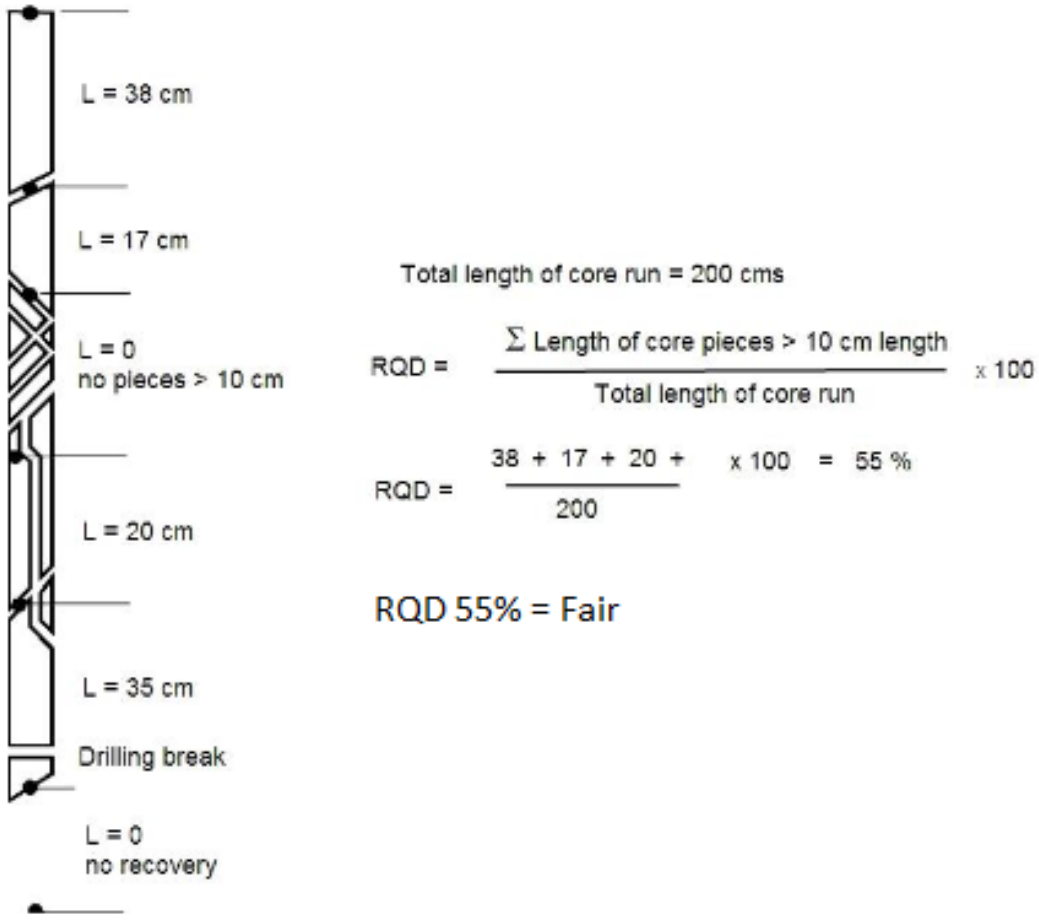

Figure A.2.1 – The procedure for determining RQD, (Hoek, 2007).

A.3 Joint Roughness

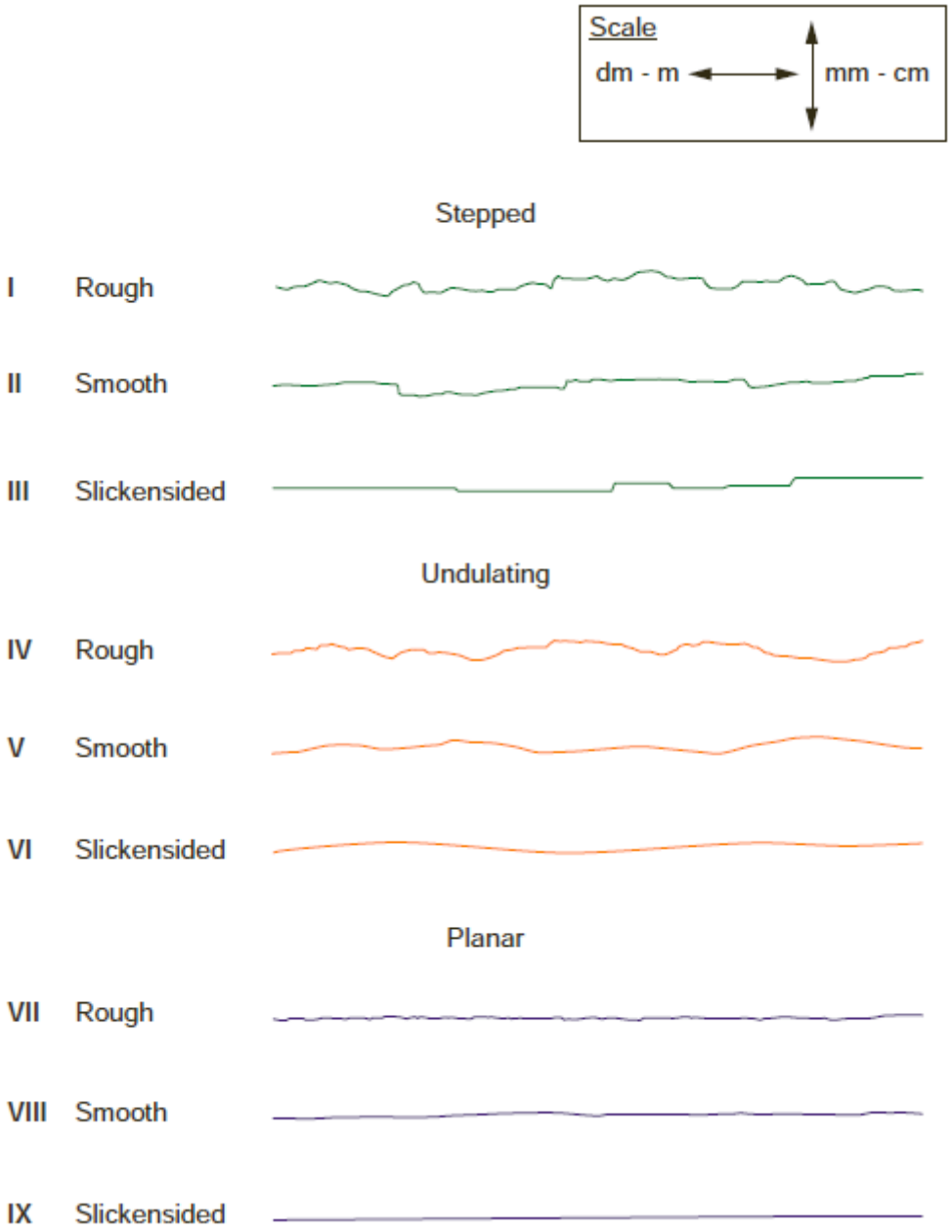

Figure A.3.1 – Joint roughness number, from NGI (2013).

Appendix B

Empirical Data

Span and Pillar Design

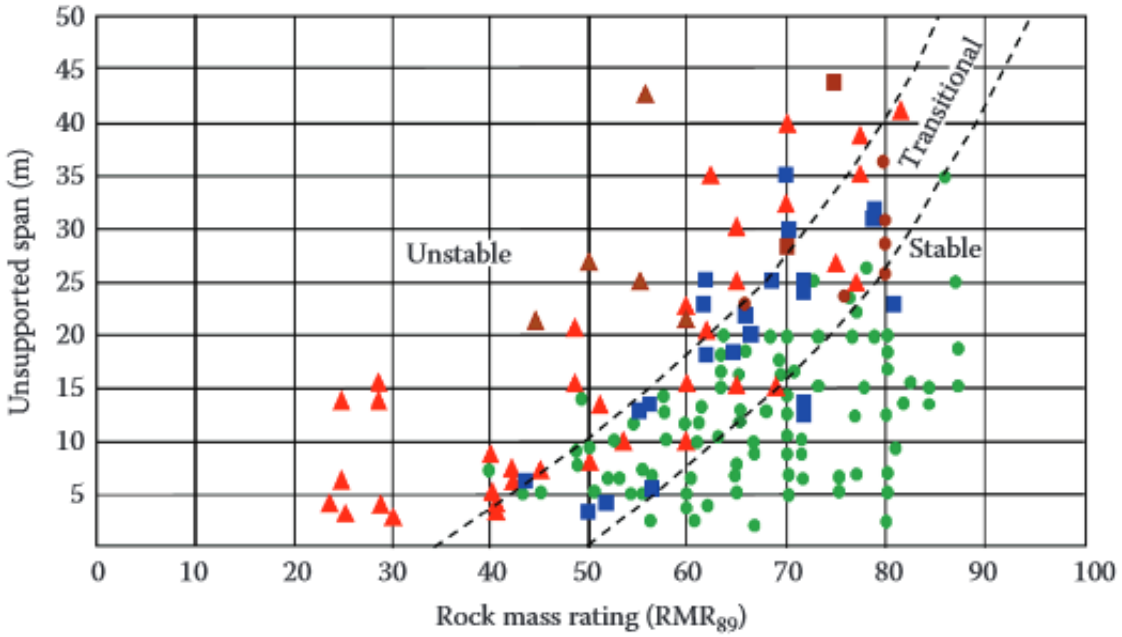

Figure B.0.1 – Span design for open stoping using the RMR_{89} method. The circles represents stable spans (depths of failure below 2 m), square symbols represents transitional spans (depths of failure ranging from 2 to 4 m), and triangles represents unstable spans (depth of failure exceeding 4 m) (Pakalnis, 2002).

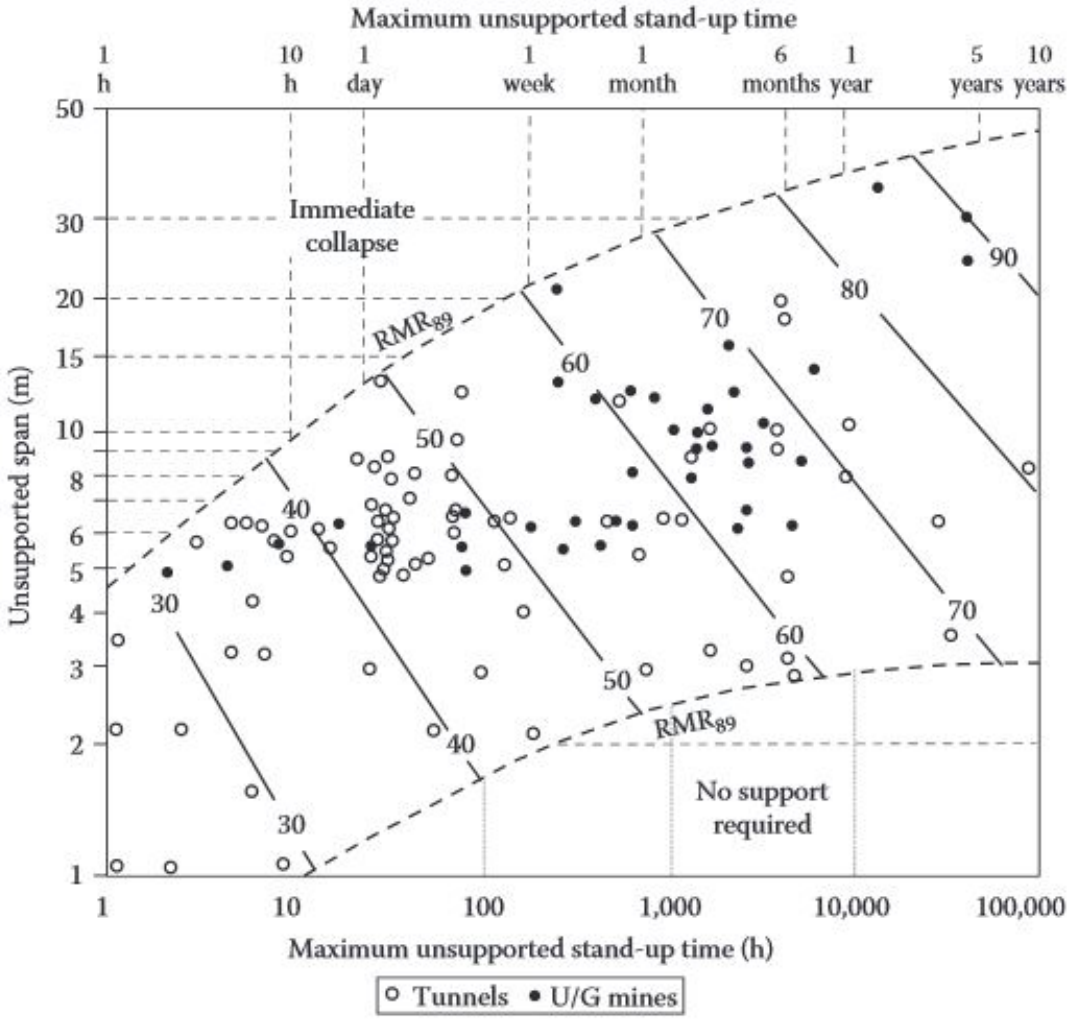

Figure B.0.2 – Unsupported tunnel and underground mine limits (Bieniawski, 1989; Villaescusa, 2014).

Appendix C

Analytical Data

C.1 Rock Analysis

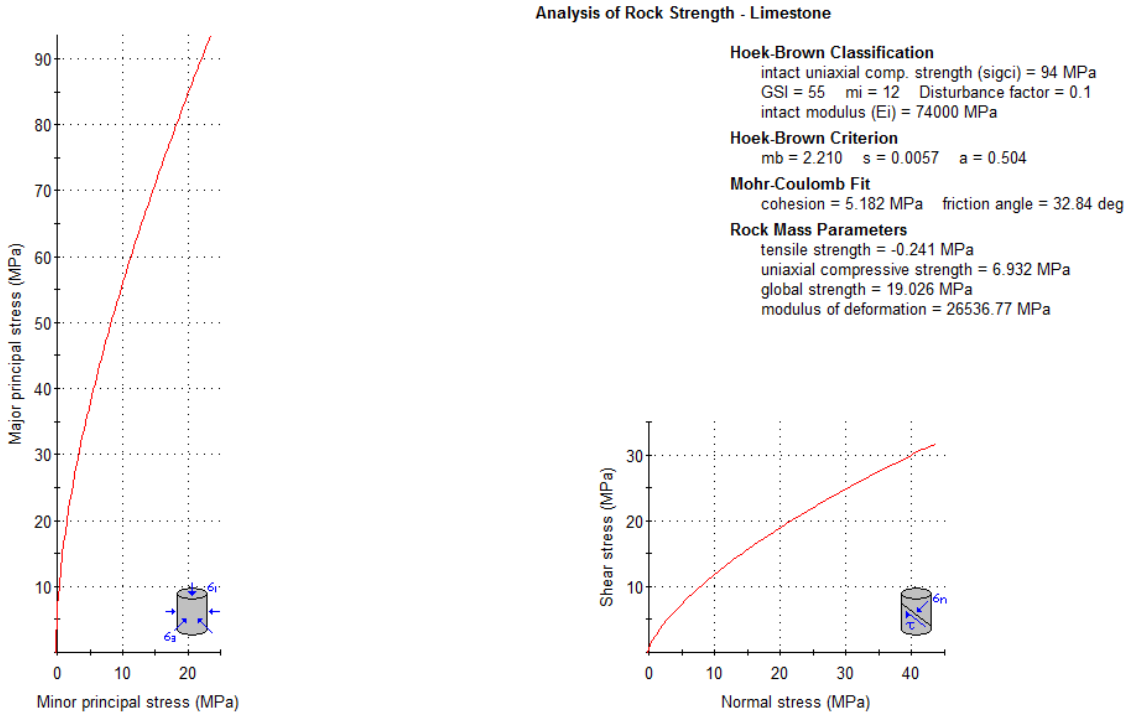

Figure C.1.1 – Analysis of rock strength for Limestone from *RocData*.

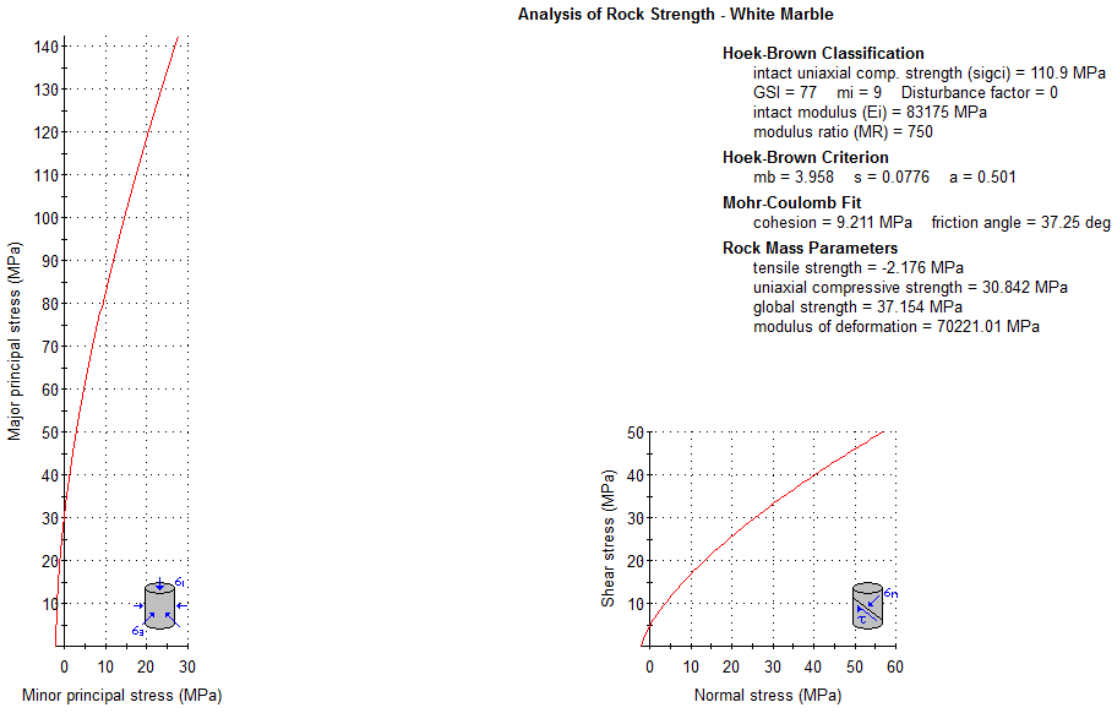

Figure C.1.2 – Analysis of rock strength for White Marble from *RocData*.

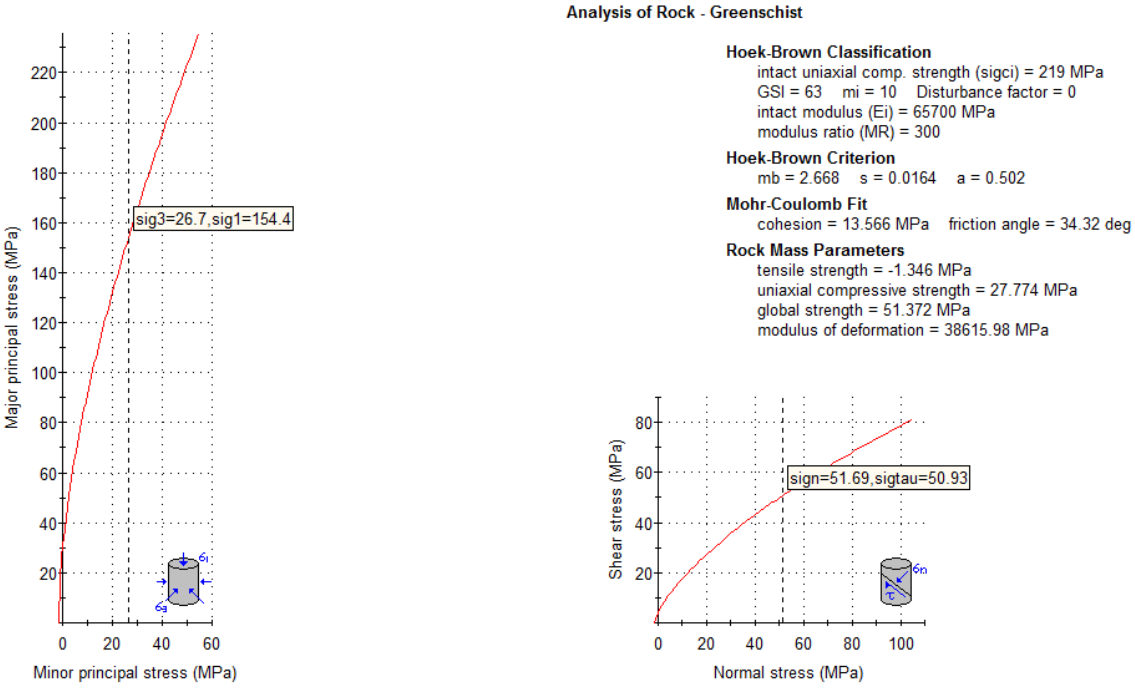

Figure C.1.3 – Analysis of rock strength for Greenschist from *RocData*.

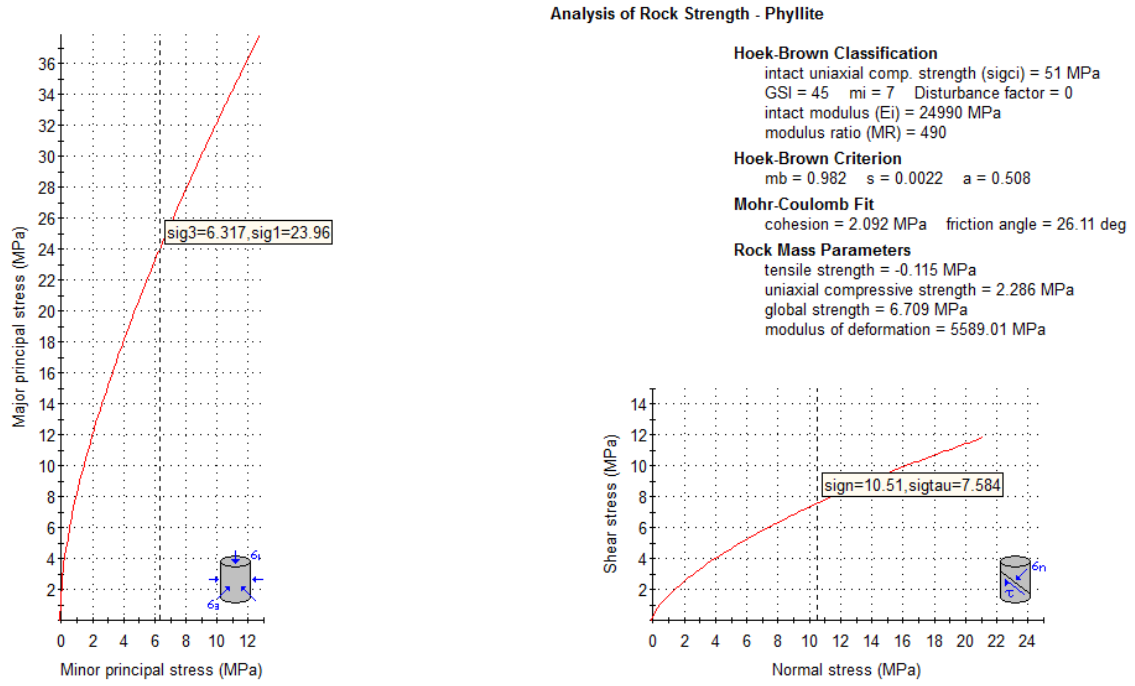

Figure C.1.4 – Analysis of rock strength for Phyllite from *RocData*.

C.2 Material Properties

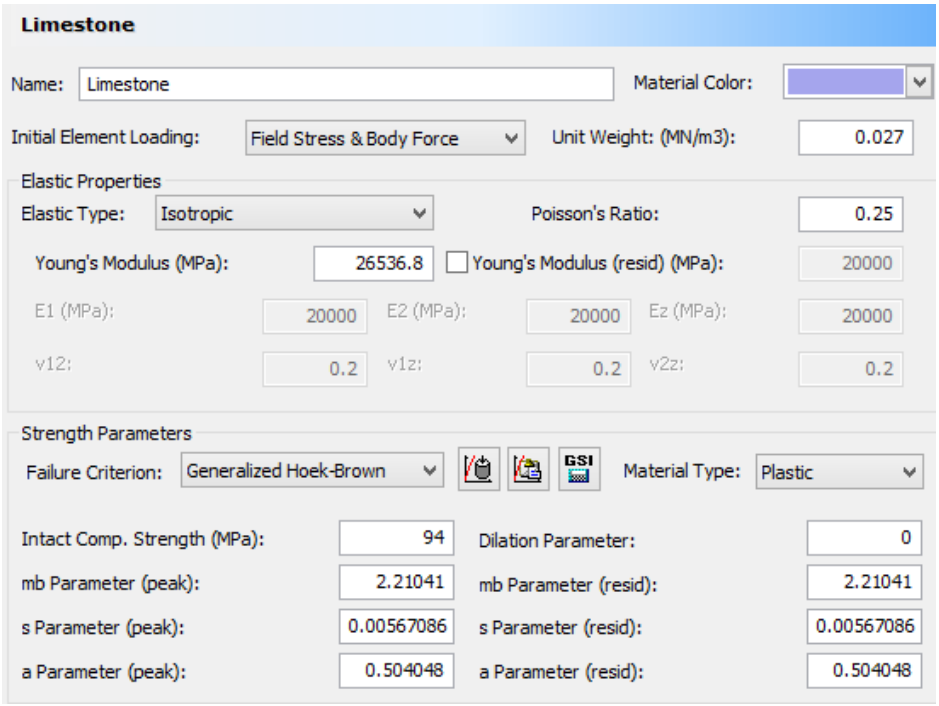

Figure C.2.1 – Material properties for Limestone from *Phase*^{2}.

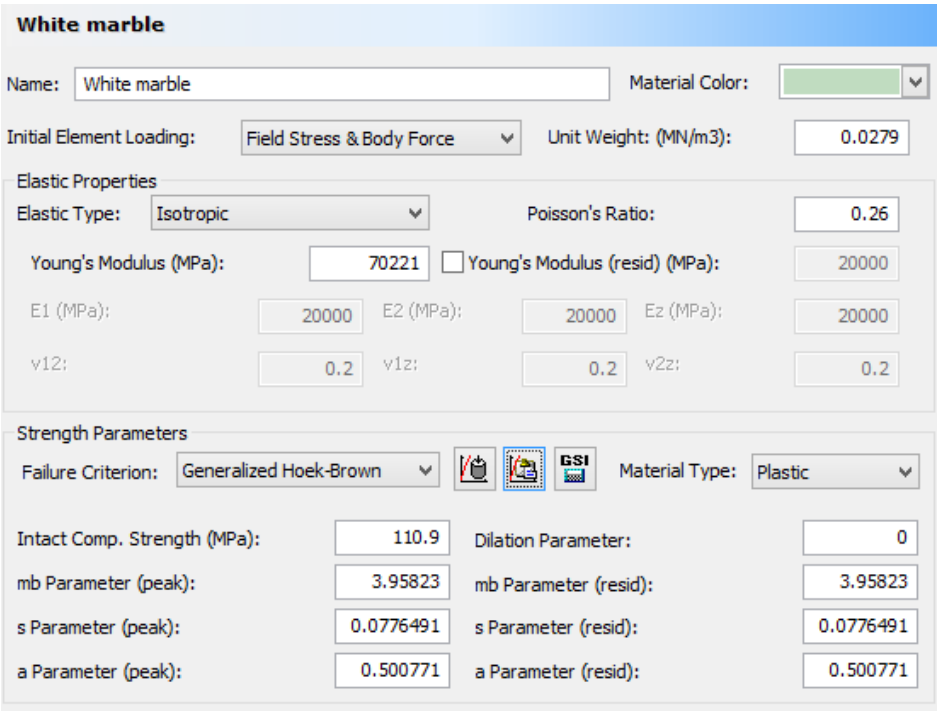

Figure C.2.2 – Material properties for White Marble from *Phase*^{2}.

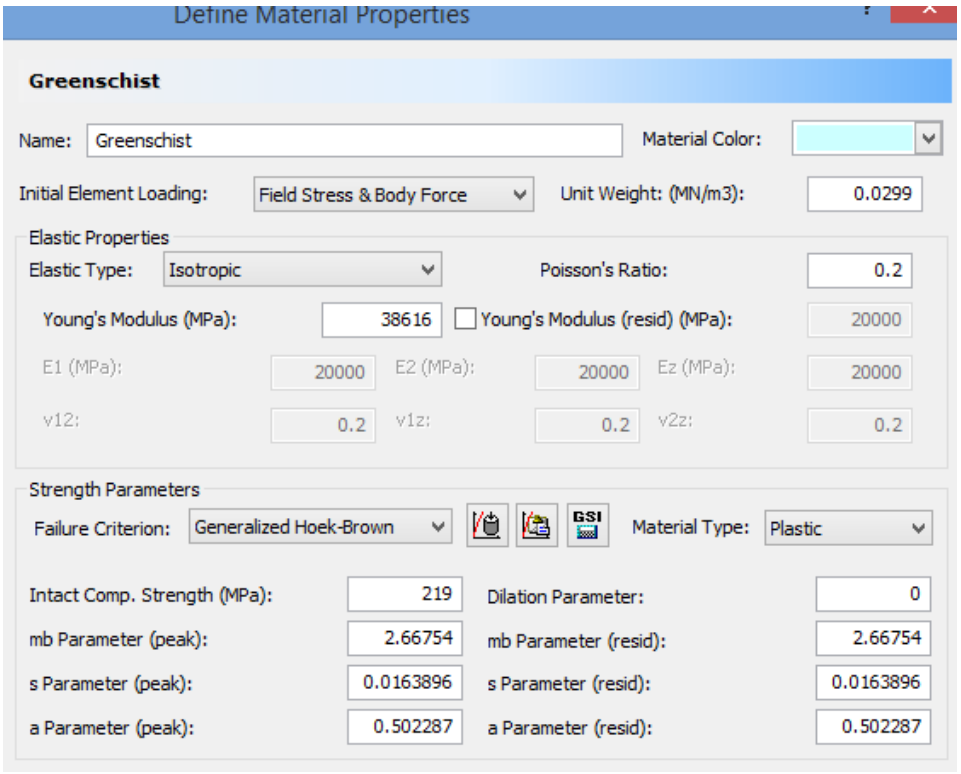

Figure C.2.3 – Material properties for Greenschist from *Phase*^{2}.

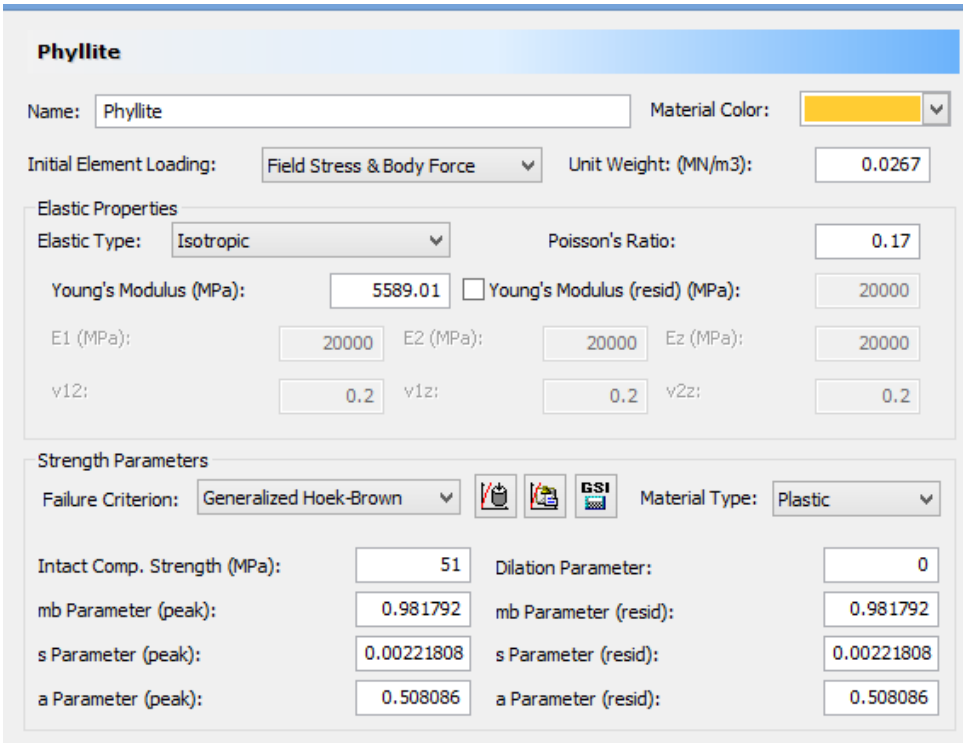

Figure C.2.4 – Material properties for Phyllite from *Phase*^{2}.

C.3 Models

C.3.0.1 Cross-Section A-A'

Sigma 1

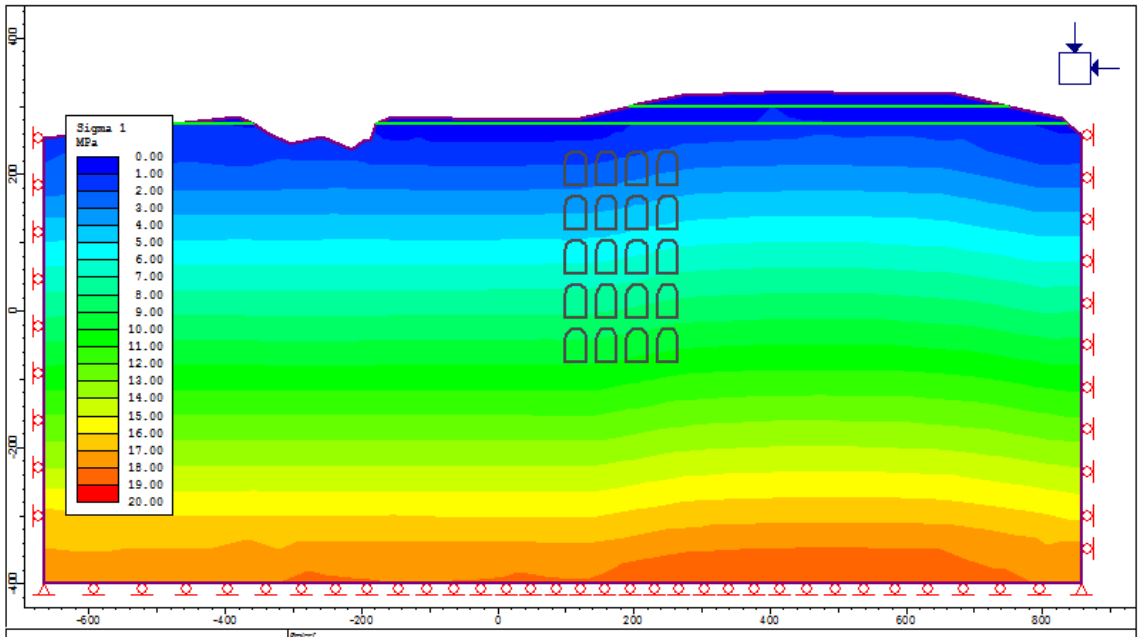

Figure C.3.1 – Stress distribution of σ_1 before stope excavation. (scale 1:6000)

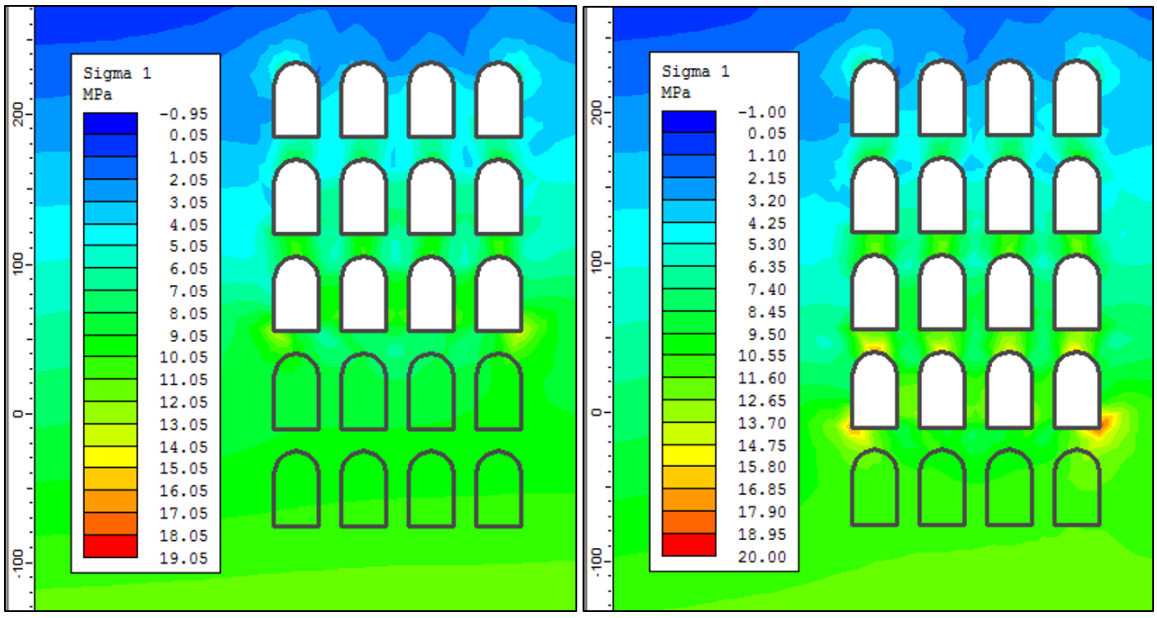

Figure C.3.2 – Stress distribution of $\sigma_1$after stope excavation. Stope levels 3 and 4.

Sigma 3

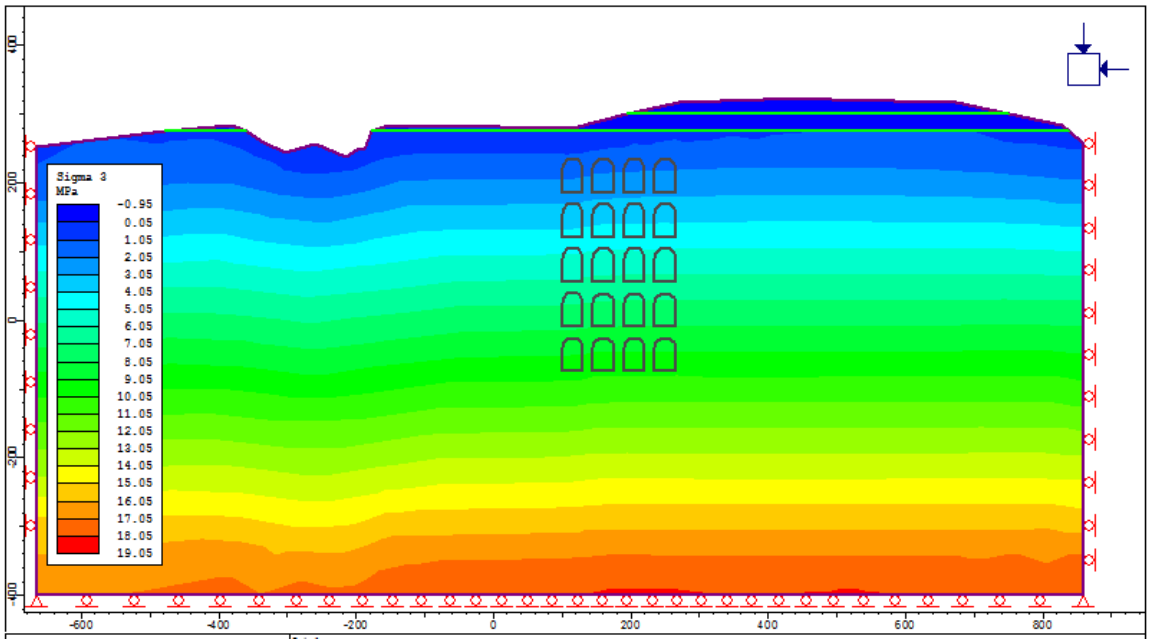

Figure C.3.3 – Stress distribution of σ_3 before stope excavation. (scale 1:6000)

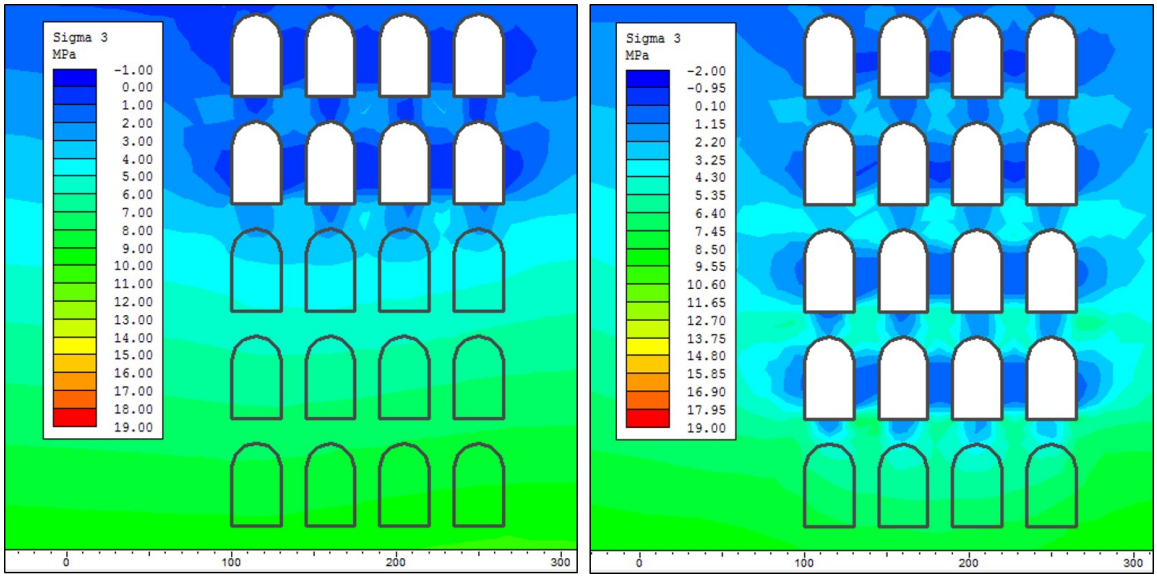

Figure C.3.4 – Stress distribution of σ_3 for stope levels two and four.

Yielded Elements

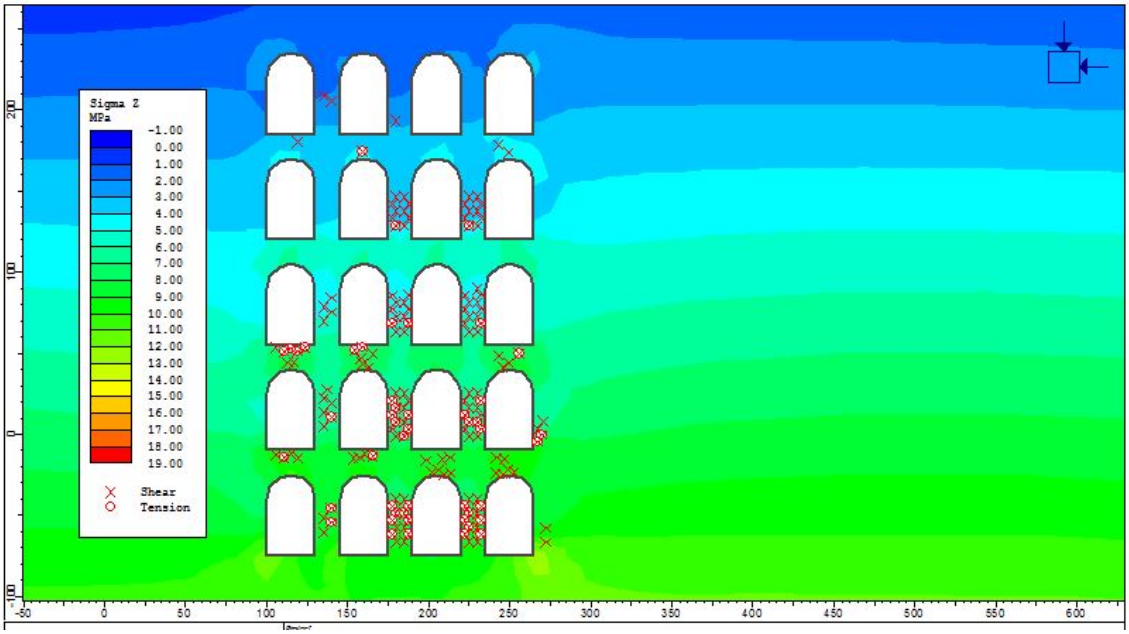

Figure C.3.5 – Yielded elements overlaid σ_z. (scale 1:2500)

Displacements

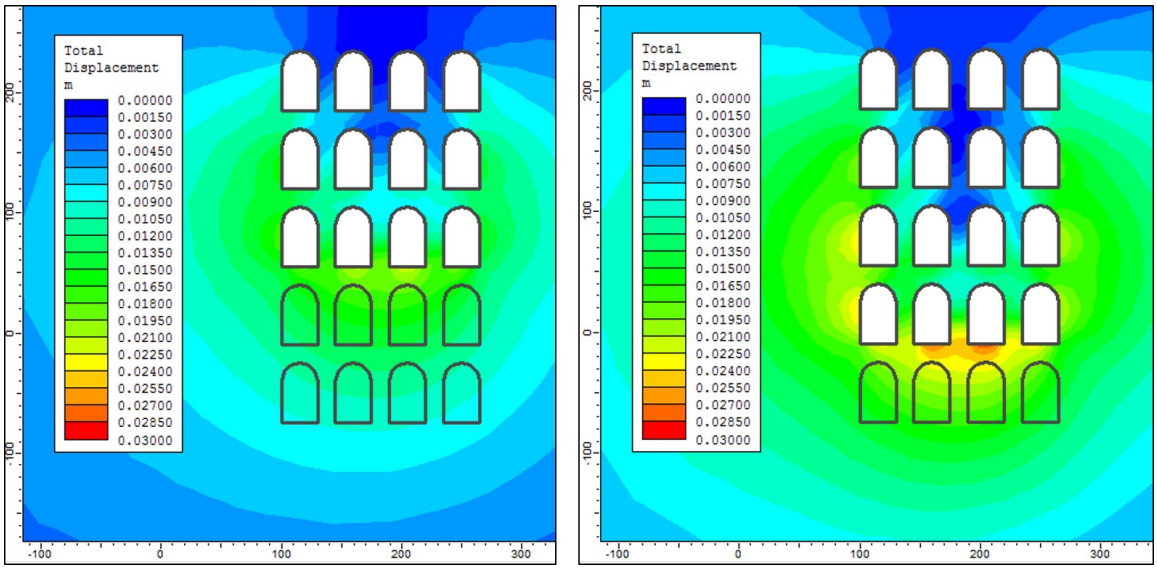

Figure C.3.6 – Total displacement after stope excavation of levels three and four.

C.3.1 Cross-Section B-B'

Sigma 1

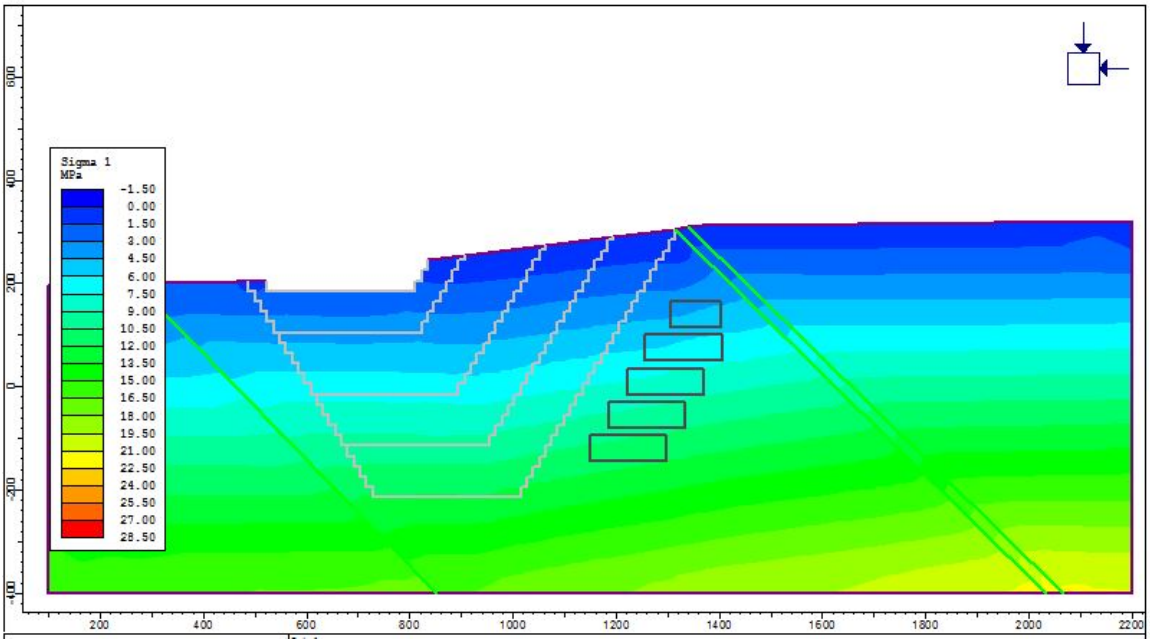

Figure C.3.7 – Stress distribution of σ_1, the current open pit is excavated. (scale 1:8000)

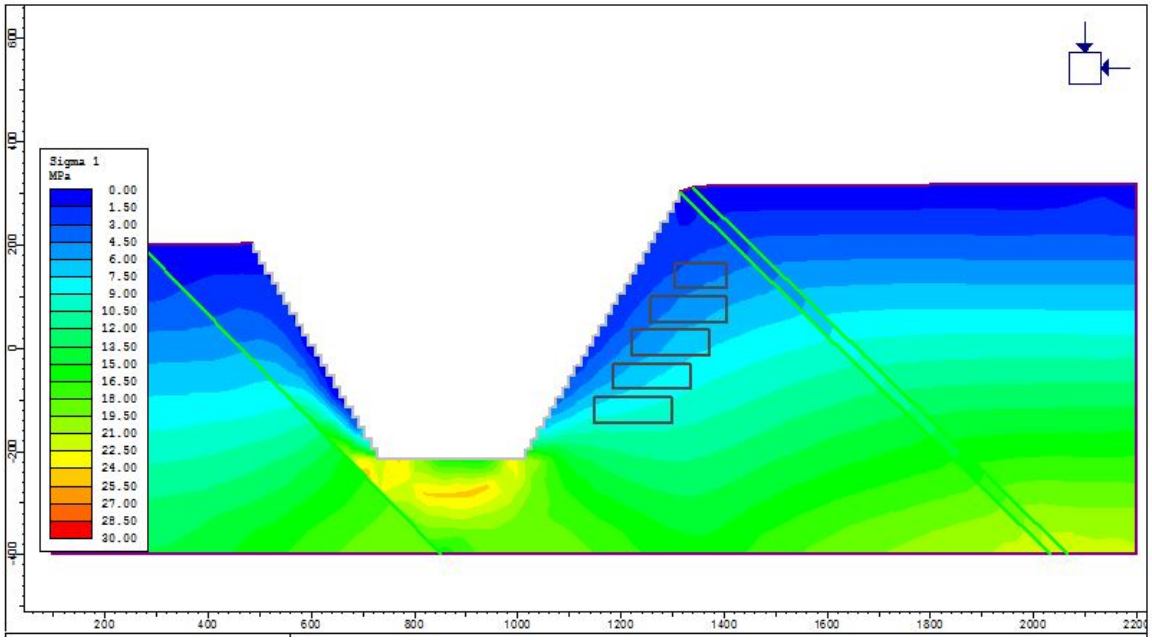

Figure C.3.8 – Stress distribution of σ_1, the future open pit is excavated. (scale 1:8000)

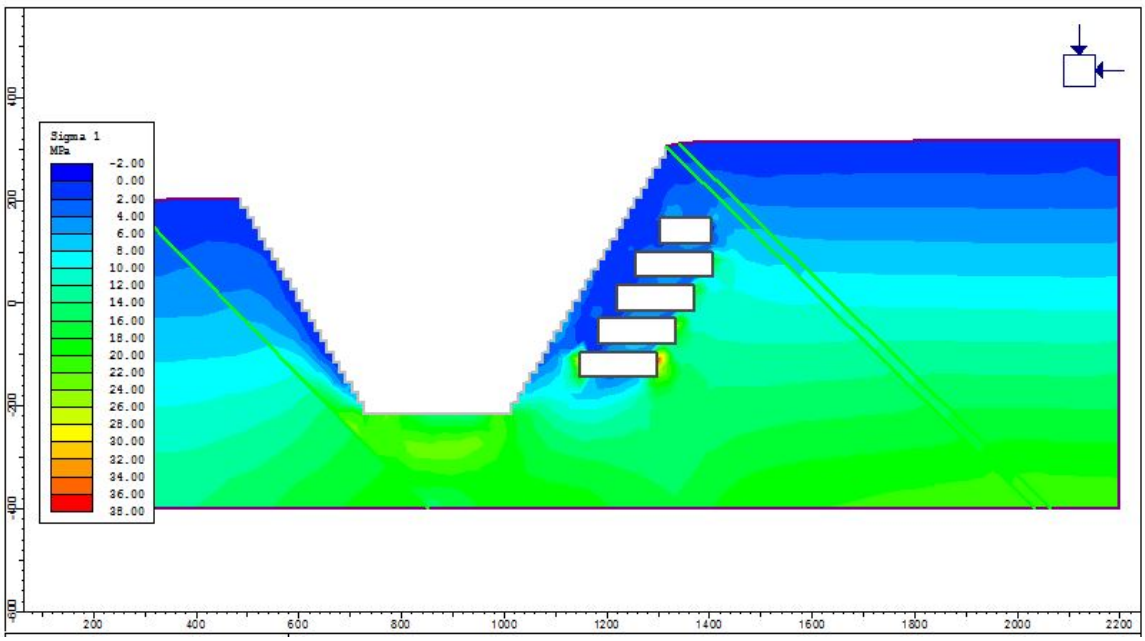

Figure C.3.9 – Stress distribution of σ_1, all stope levels are excavated. (scale 1:8000)

Stress Trajectories

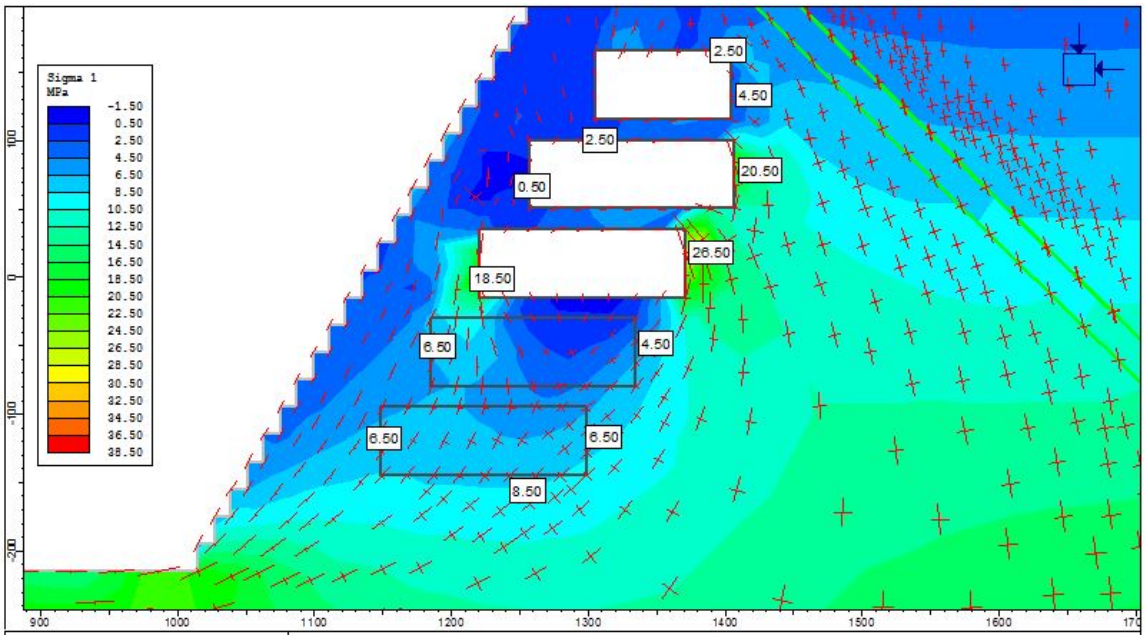

Figure C.3.10 – Stress trajectories - three stope levels excavated. (scale 1:3000)

Sigma 3

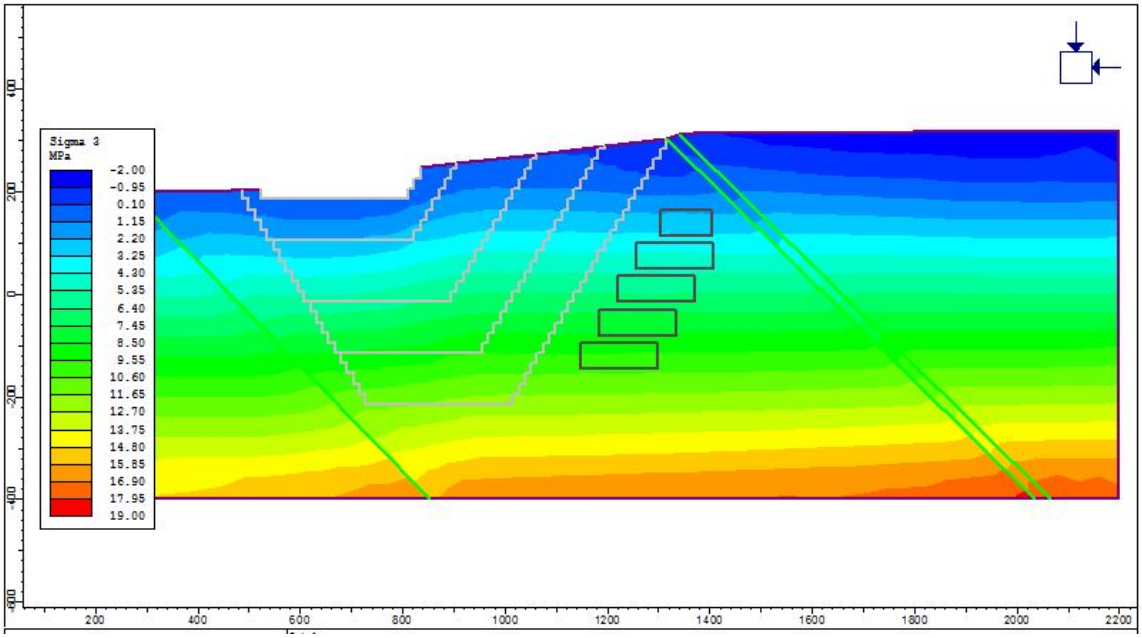

Figure C.3.11 – Stress distribution of σ_3, current open pit is excavated. (scale 1:8000)

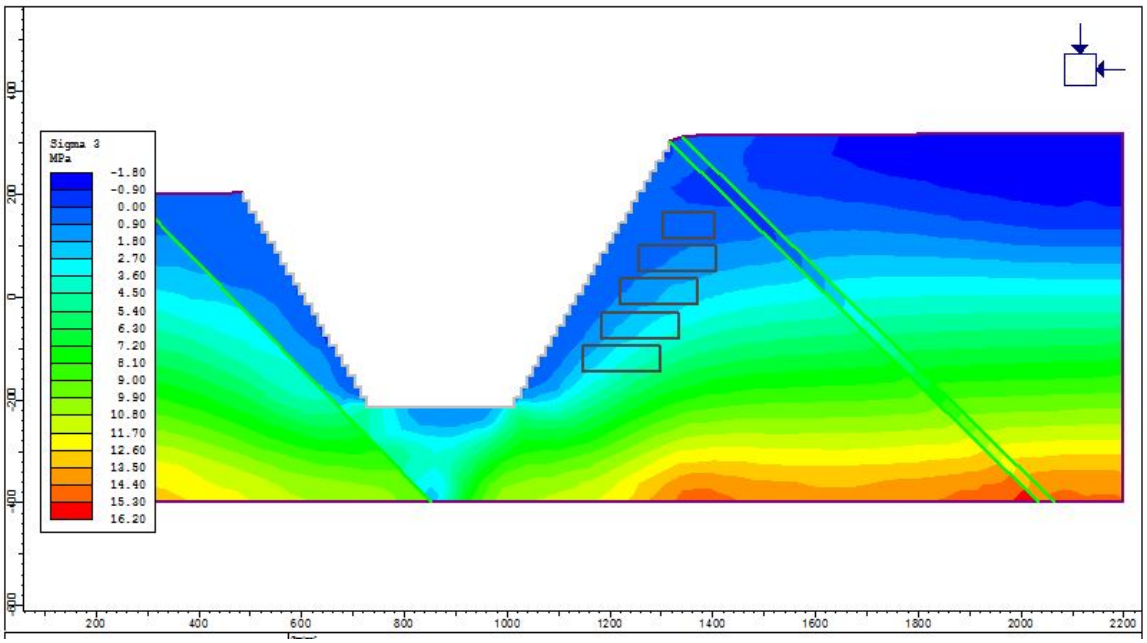

Figure C.3.12 – Stress distribution of σ_3, future open pit is excavated. (scale 1:8000)

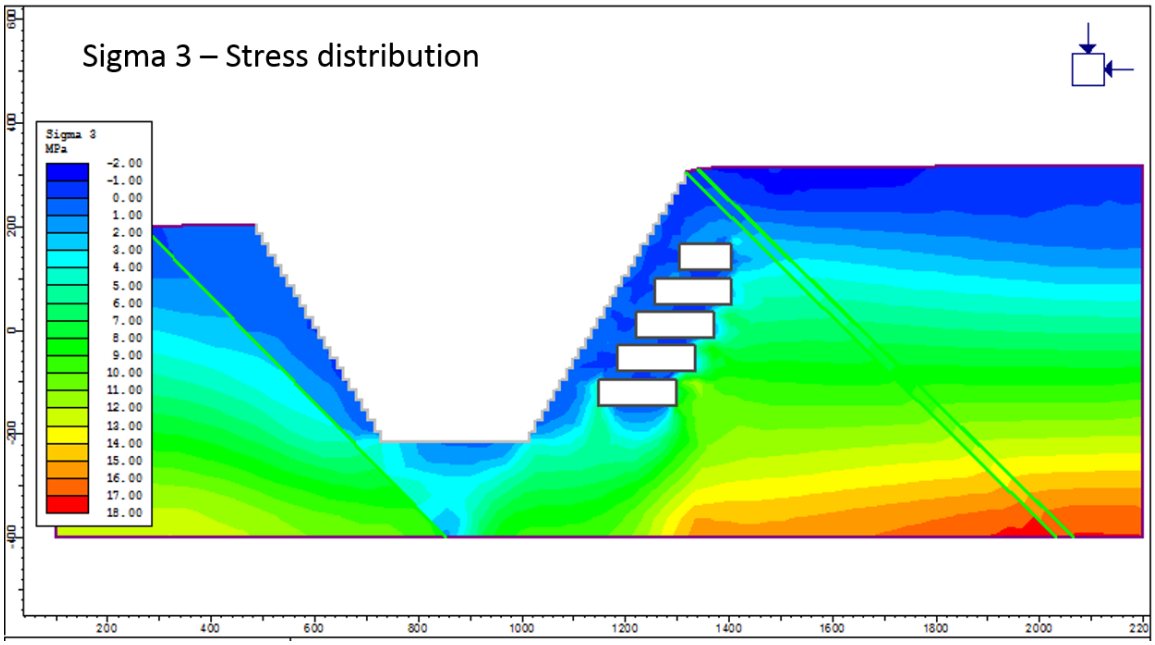

Figure C.3.13 – Stress distribution of sσ_3, all stope levels are excavated. (scale 1:8000)

Yielded Elements

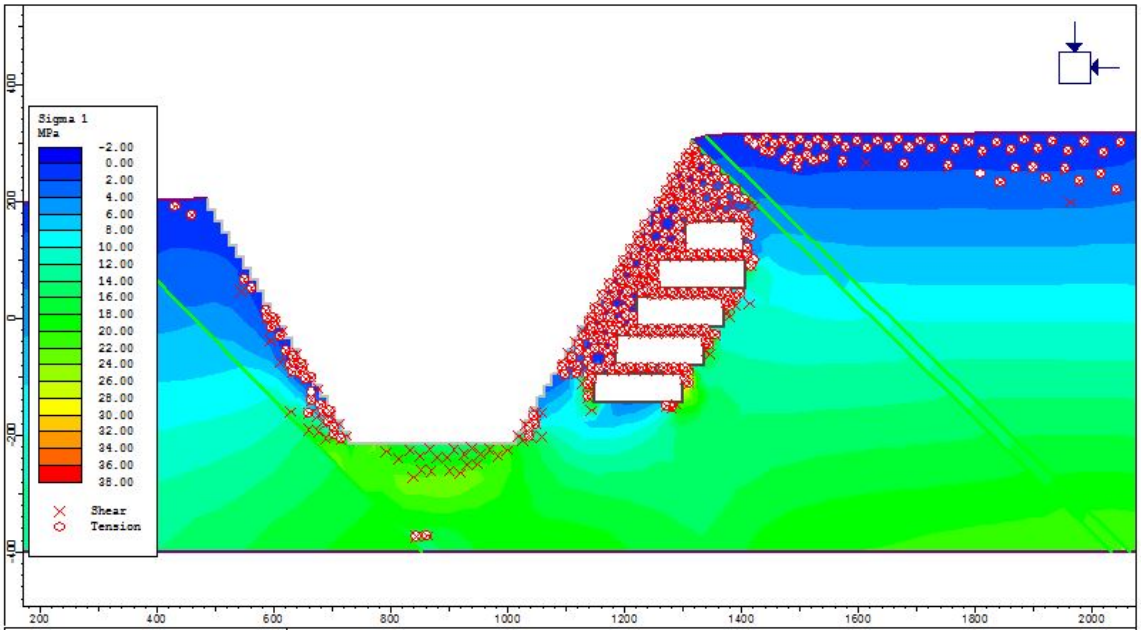

Figure C.3.14 – Yielded solid elements along the open pit wall, around the stopes, and in the area close to the topography. (scale 1:7000)

Displacements

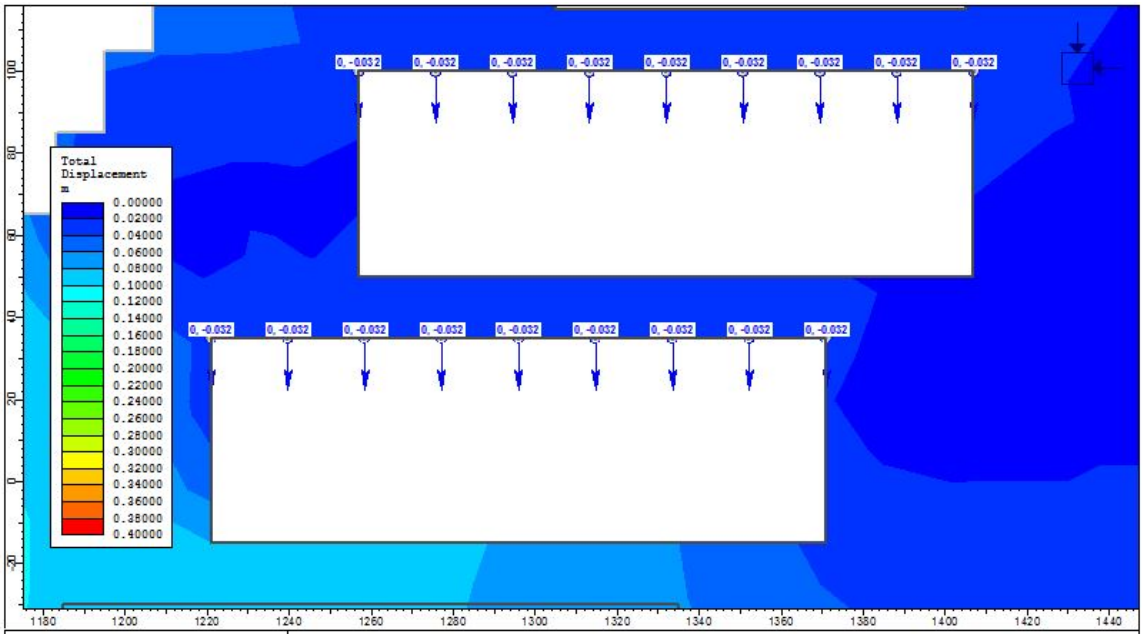

Figure C.3.15 – Given vertical displacement, based on maximum total displacement from cross-section A-A'. (scale 1:1000)

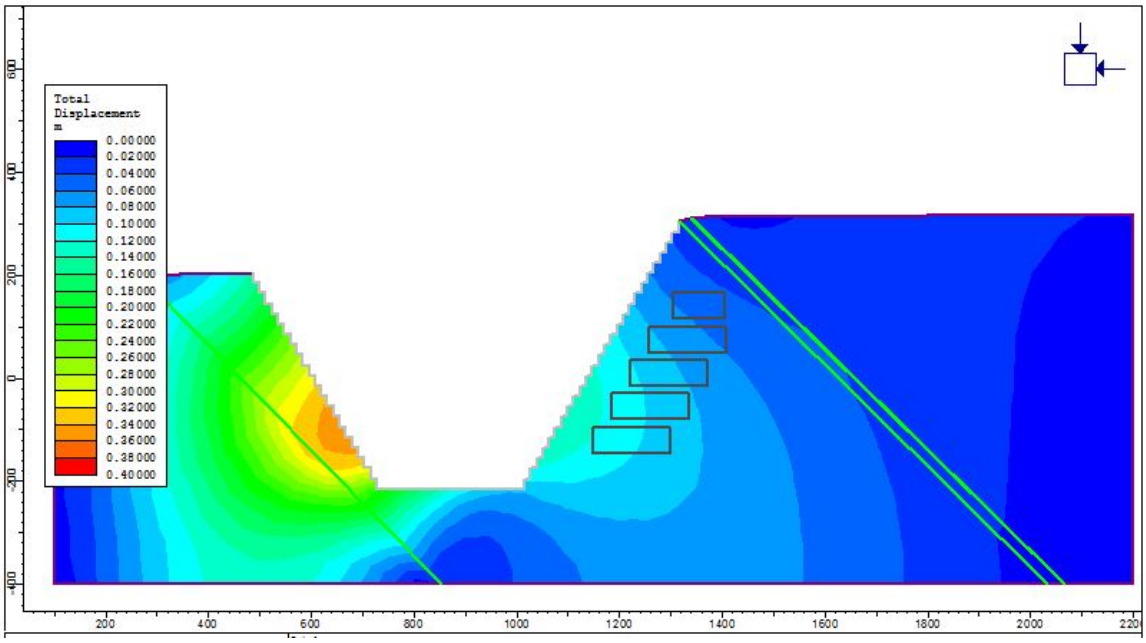

Figure C.3.16 – Total displacement of the future open pit. (scale 1:8000)

Appendix D

Illustrations

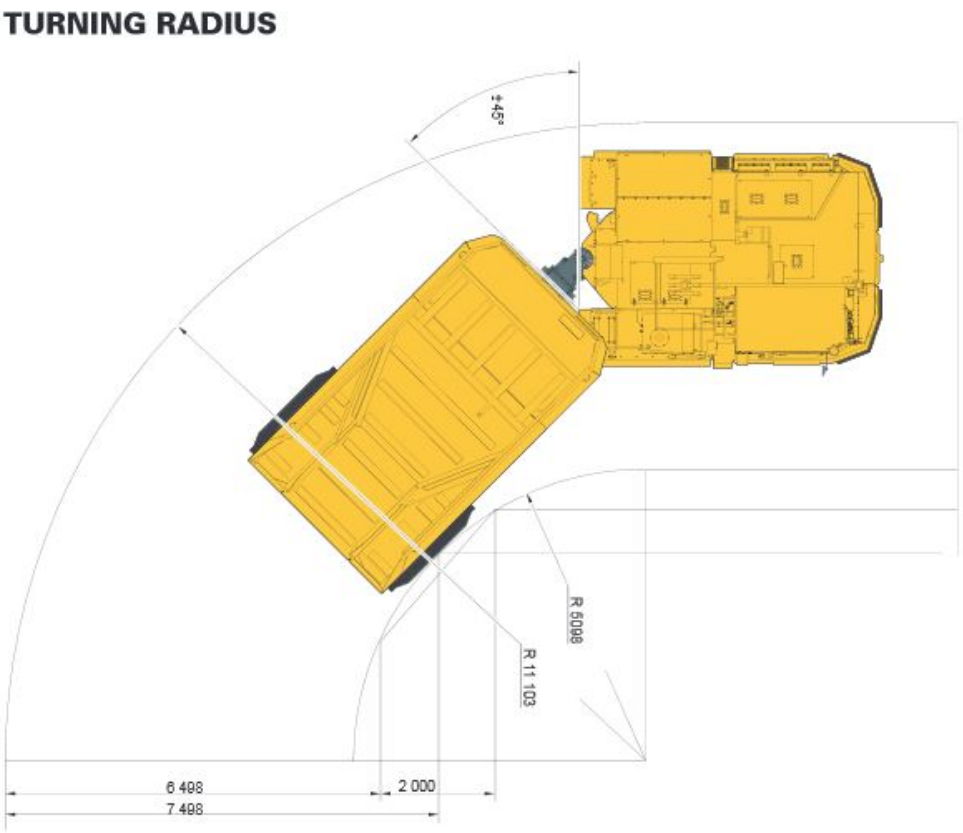

Figure D.0.1 – Turning radius for Atlas Copco EMT50, Electric Minetruck.

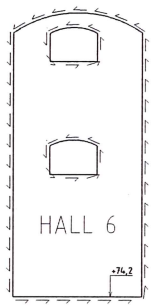

SNITT H-H
1:500

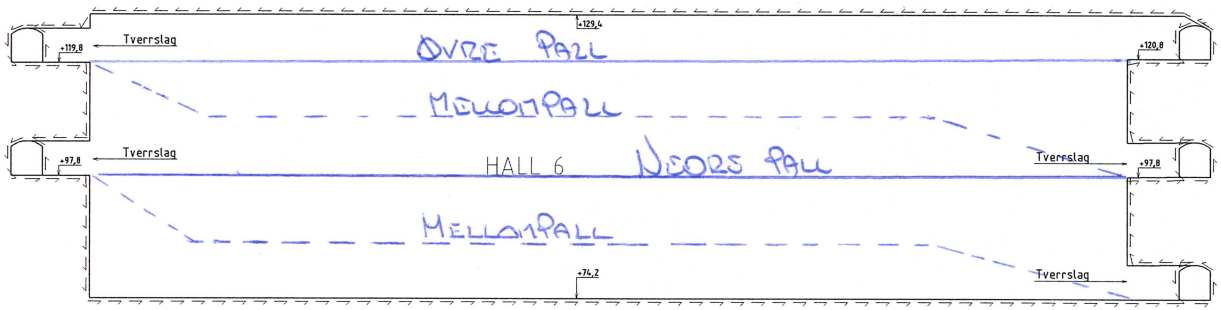

SNITT E-E
1:500

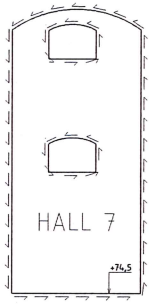

SNITT I-I
1:500

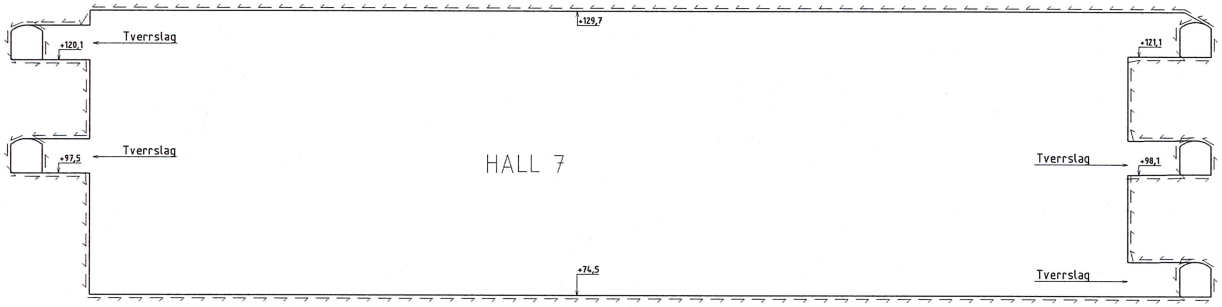

SNITT F-F
1:500

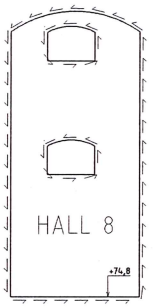

SNITT J-J
1:500

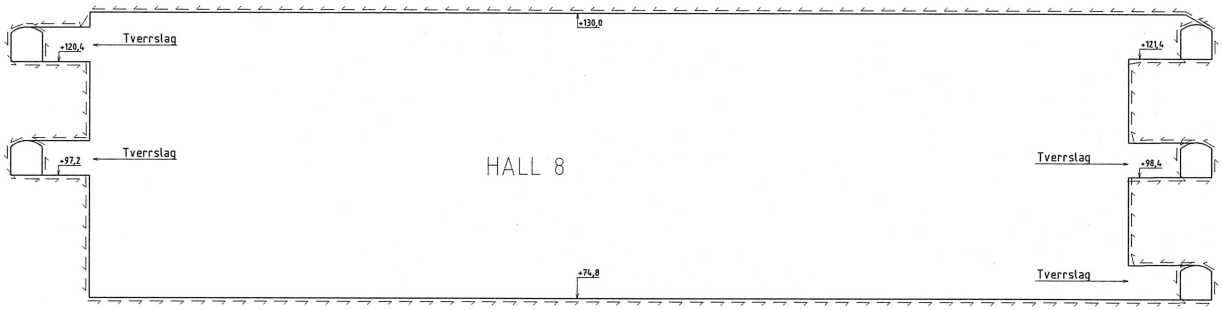

SNITT G-G
1:500

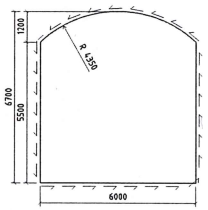

TYPISK SNITT TUNNEL
1:100

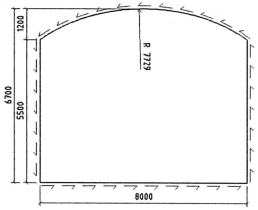

SNITT TVERRSLAG
1:100

1:500 0 10 20 30 40 50m

Tegningstittel	Tegningsnr	Rev
SNITT	006	1

BEMERKNINGER

HENVISNINGER

1. FOR KOORDINATER, SE KOORDINATLISTE SIDE 001
2. SE OGSÅ TEGNING 002, NIVÅ 60-70, PLAN
3. SE OGSÅ TEGNING 003, NIVÅ 90-100, PLAN
3. SE OGSÅ TEGNING 004, NIVÅ 110-130, PLAN
3. SE OGSÅ TEGNING 005, SNITT

ARBEIDSTEGNING

Rev.	Beskrivelse	Dato	Utarb.	Kontr.	Godkj.
1	Snitt	07.10.2009	Kjl	FSA	FSA

FANA STEIN AS

STENDAFJELLET HALLER

SNITT
E-E til J-J

Original format A1 | Fag GEO | Tegningens fagnavn Modell 2D | Undertegnts fagnavn | Målestokk 1:500

MULTICONSULT

MULTICONSULT AS
BERGEN
Nesttunbrekka 95
5221 Nesttun
Tlf: 55 62 37 00
Fax: 55 62 37 01

Dato 07.10.2009 | Utarbeidet Kjl | Kontrollert FSA | Godkjent FSA

Oppdragsnr 610548 | Tegningsnr 006 | Rev 1

Appendix E

Maps

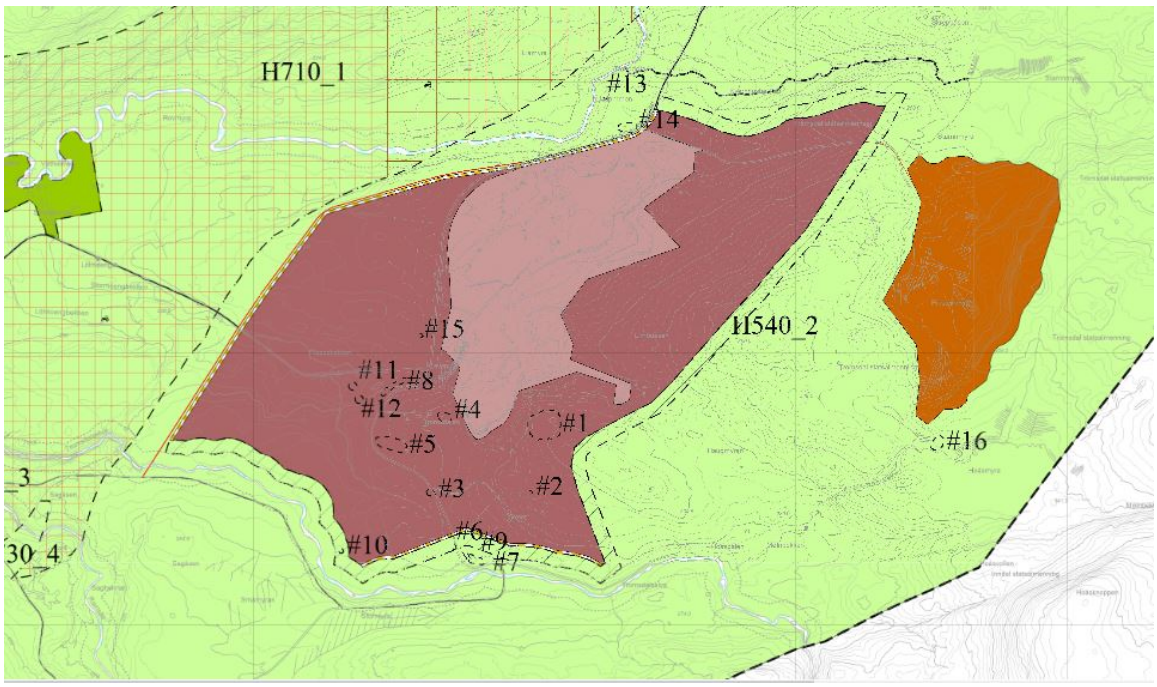

Figure E.0.1 – Regulated area for surface mining, as of 29.05.2013 (Møller, 2013).

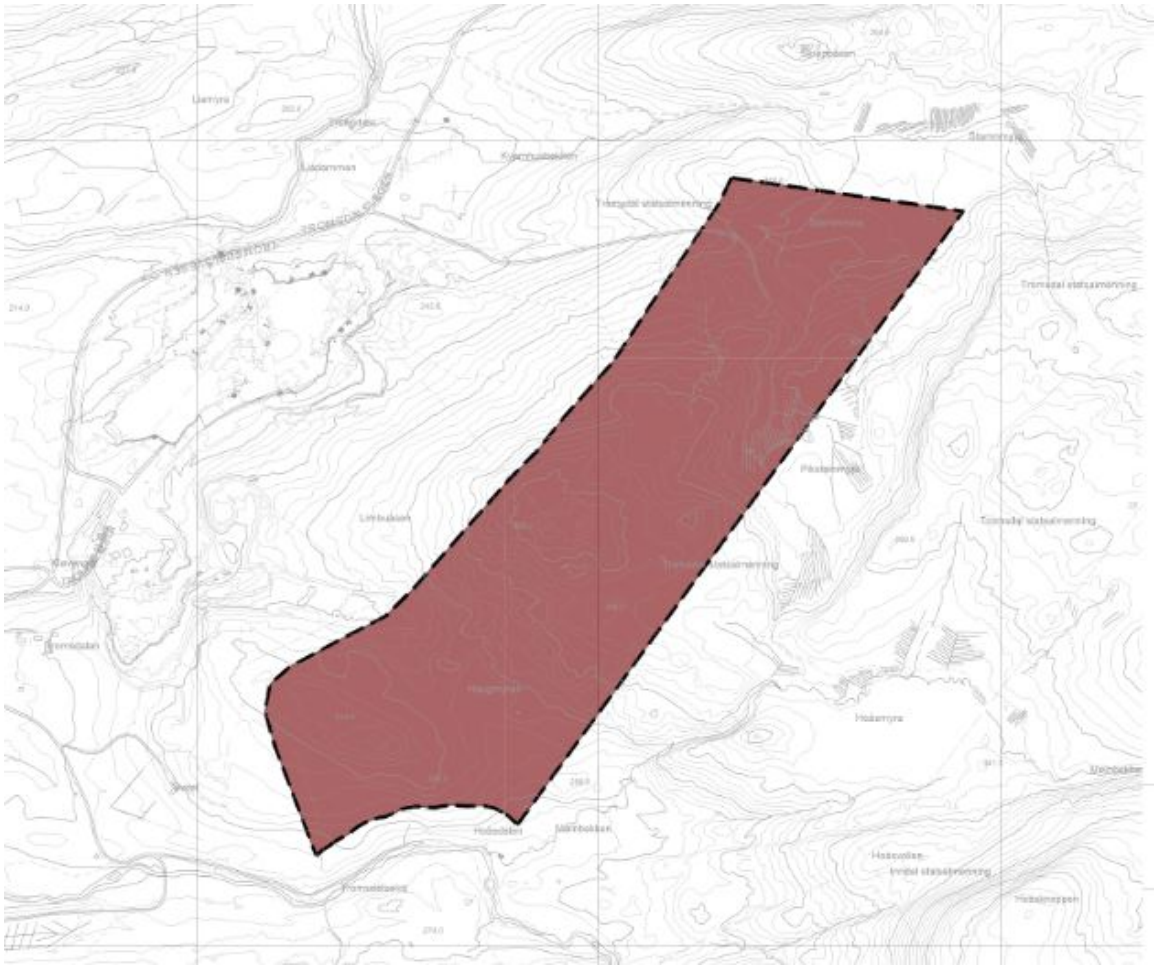

Figure E.0.2 – Regulated area for underground mining, as of 29.05.2013 (Møller, 2013).

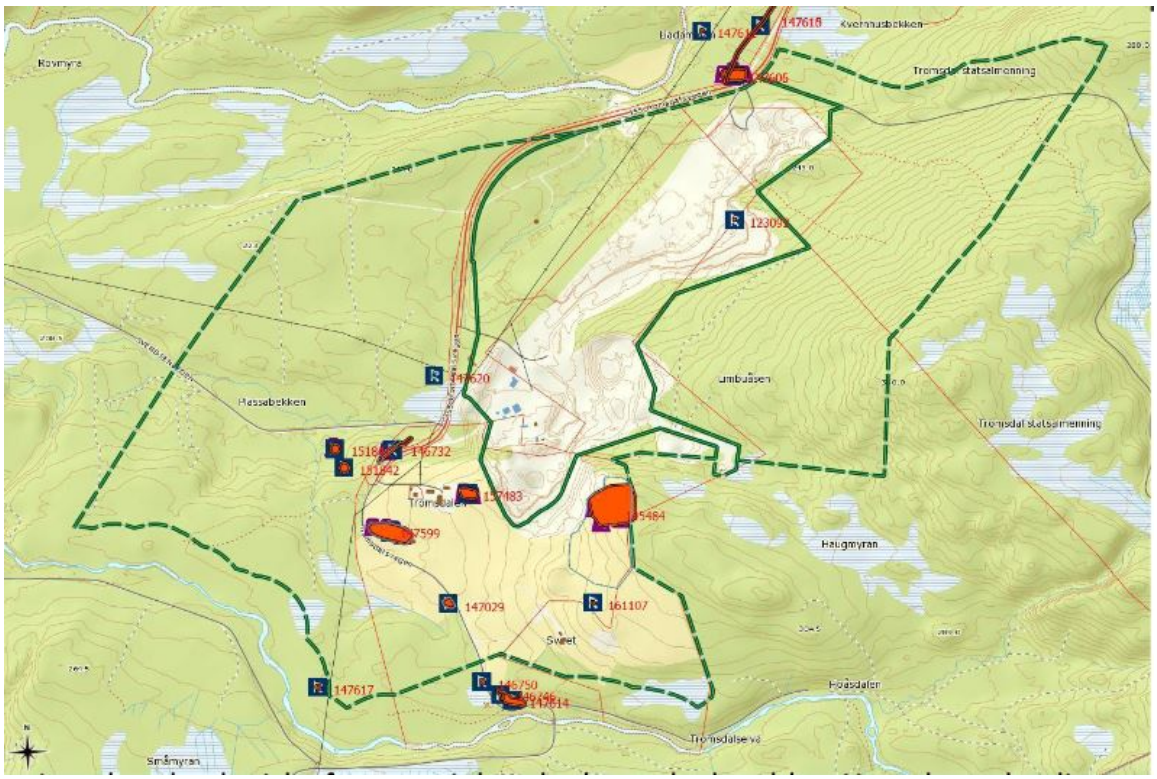

Figure E.0.3 – Map showing the current open pit and the border for the future open pit (Verdalskalk AS, 2013a).

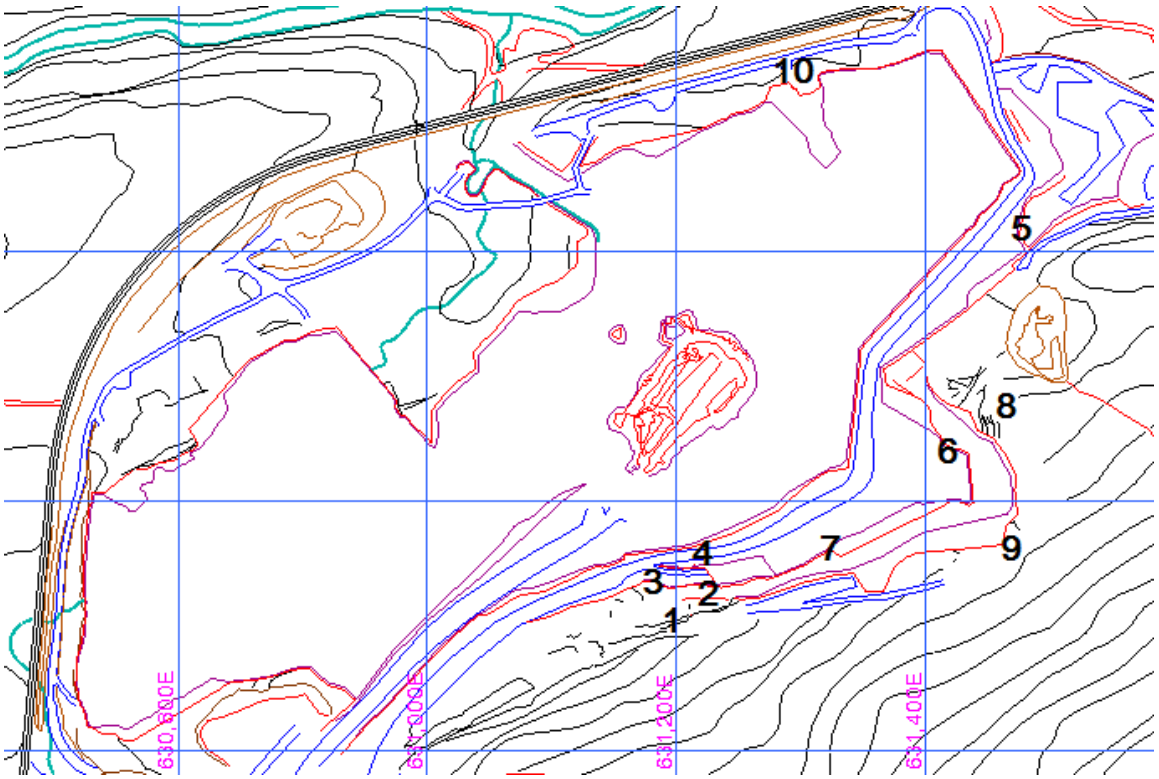

Figure E.0.4 – Index map showing the localities where surface mapping was conducted. (Map from Surpac)